PETROMINERALOGICAL AND GEOCHEMICAL CHARACTERIZATION OF REHATIKHOL FORMATION, CHHATTISGARH SUPERGROUP IN SINGHORA PROTOBASIN TO DECIPHER CONTROLS OF URANIUM AND FLUORITE MINERALIZATION IN PARTS OF MAHASAMUND DISTRICT, CHHATTISGARH AND BARGARH DISTRICT, ODISHA

by

ROHIT KUMAR SAINI

ENGG1G201801001

Bhabha Atomic Research Centre, Mumbai

A thesis submitted to the
Board of Studies in Engineering Sciences

In partial fulfillment of requirements

for the Degree of

MASTER OF TECHNOLOGY

of

HOMI BHABHA NATIONAL INSTITUTE

February, 2021

Homi Bhabha National Institute

Recommendations of the Thesis Examining Committee

As members of the Thesis examining Committee, we recommend that the thesis prepared by **Rohit Kumar Saini** entitled "Petromineralogical and Geochemical Characterization of Rehatikhol Formation, Chhattisgarh Supergroup in Singhora Protobasin to decipher controls of uranium and fluorite mineralization in parts of Mahasamund district Chhatisgarh and Bargarh district, Odisha" be accepted as fulfilling the thesis requirement for the Degree of Master of Technology.

	Name	Signature
Member-1	Dr. D. K. Sinha	DKSinha
Member-2	Dr. T. S. Sunil Kumar	TSSunilkumar
Member-3	Dr. Navin Goyal	
Member-4	Dr. Pranesh Sengupta$	P. Sengupta
Member-5	Dr. A. Rama Raju	
Technical advisor	S. K. Das	
Examiner	Prof. A.M. Pophare $	A pophare
Guide & Convener	Dr. Ajay Kumar	A Kumar
Chairman	Prof. Vivekanand Kain$	

$ Participated through video conferencing

Final approval and acceptance of this thesis is contingent upon the candidate's submission of the final copies of the thesis to HBNI.

I hereby certify that I have read this thesis prepared under my direction and recommend that it may be accepted as fulfilling the thesis requirement.

(Dr. Ajay Kumar)
Guide

Date: 15-02-2021

Place: Hyderabad

DECLARATION

I, hereby declare that the investigation presented in the thesis has been carried out by me. The work is original and has not been submitted earlier as a whole or in part for a degree / diploma at this or any other Institution / University.

रोहित कु. सैनी

(Rohit Kumar Saini)

DEDICATION

This thesis is dedicated to my mother and father, who nurtured and educated me through their hardship of life. They have taught me the best kind of knowledge to never give up and to make full efforts honestly in any kind of work. They have encouraged and supported me to overcome every difficult stage of my life.

ACKNOWLEDGEMENTS

First of all, I am deeply grateful to my project guide Dr. Ajay Kumar, Adjunct Professor, HBNI and technical adviser Shri. S.K. Dash, Incharge, Chhattisgarh Basin Investigations for their valuable guidance, advice and encouragement throughout the course of this work. Next, I would also like to extend sincere thanks to Shri P.K. Gupta, Incharge, Nandgaon- Khairagarh Basin Investigations for his valuable suggestions and constant support in every stage of this project.

I would like to express my sincere thanks to Chancellor, Vice-Chancellor, HBNI and Dean, HBNI and all the competent authorities of HBNI for providing the opportunity to pursue the M. Tech. degree. I am thankful to Chairman, M. Tech. Standing Committee, Monitoring Committee and all members for their suggestions made during different meetings. I would like to express special thanks to Dr. D. K. Sinha, Director, AMD, for providing kind permission to pursue this project and his valuable suggestions for designing the structure of this course.

I express my gratefulness towards Shri Sandeep Hamilton, Additional Director (OP-I), Shri B. Saravanan, Additional Director (OP-II), Dr. T.S. Sunil Kumar, Additional Director (R & D), Shri Arjun Panda, Regional Director, AMD/CR (central region, Nagpur) and Shri V.K. Srivastava, Deputy Regional Director, AMD/CR for their constant encouragement and support. I extend my sincere thanks to Dr. A. Rama Raju, Incharge, BARC Training School and Dr. S. K. Srivastava, Retired Head, BARC Training School, AMD, Hyderabad.

I would like to thank Dr. (Mrs.) A. Latha, Dr. V. Madakkaruppam and Shri Prakash Bediya of AMD/CR for their support at different stages of this project. I express my gratitude towards Shri Manu Thandra, Incharge Physics Lab, Dr. V. Padma Subashini, Incharge Chemistry Lab, AMD/CR, and officers of Laboratories, AMD/CR for their support in sample analysis. Lastly, I would like to thank all my senior colleagues and staff of AMD who have helped me to carry out this project successful at different stages either directly or indirectly. I am very grateful to my parents and family members who supported all through and made me able to pursue this project.

CONTENTS

SYNOPSIS

Several uranium anomalies were reported earlier in different litho-units in the environs of Singhora proto-basin of Chhattisgarh Basin by both Central and Eastern Regions, reflecting it as an important geological domain to look for unconformity related and/or structurally controlled uranium mineralisation. Uranium anomalies were reported both in the basement Sambalpur granites (Structure controlled at Dongripali, Dulapali, Amapali, Paraskol areas), proximal to unconformity of Chandrapur sediments & associated with granitic basement (Damdama - altered and fractured granite with values upto 0.430% U_3O_8) and in various lithounits of Rehatikhol Formation (Juba-Banjhapali, fluorite at Chiwarakuta) etc. Some of the anomalies were probed by sub-surface exploration (Dulapali- Dongripali fracture in altered basement Sambalpur granite with borehole intercept of 0.081% eU_3O_8 X 1.90m and beta-gamma values in the range of 0.017-0.25% U_3O_8), Damdama and more importantly at Juba-Banjhapali (associated with pyrite bearing fractured feldspathic arenite of basal sediments of Rehatikhol Formation of Singhora Group sediments, with borehole core beta gamma values in the range of 0.012-0.079% U_3O_8) etc.

Though sub-surface exploration was discontinued in the area due to lack of correlatability & low grade/thickness, but it was established that the reactivation of basement fractures have a dominant role in uranium remobilization and enrichment in suitable locales. Study area of this project i.e. Chiwarakuta- Rehatikhol- Malaikhaman- Dongar Raksha sector lies just south of above mentioned earlier explored Juba-Banjhapali area, has been taken to look for similar potential for uranium, polymetallic sulphides and fluorite mineralisation. The present project was designed to study the petromineralogical and geochemical characteristics of basement rock and Rehatikhol Formation mainly to decipher possible controls of U and fluorite mineralisation. A total 55 sq km area has been mapped and surveyed radiometrically on 1:10000 scale and attempt has been made to describe the lithostructural disposition by various cross sections and geological map. The integration of field observations, geological mapping, petrominerological and geochemical studies enabled the author to characterise the basement rocks and Rehatikhol Formation exposed in the study area. Present study resulted in classification of Rehatikhol Formation into 5 lithounits and their petromineralogical and geochemical characterisation to decipher provenance, tectonic setting, paleoweathering and paleoclimatic conditions of Rehatikhol Formation. Paleocurrent analysis revealed average NW paleocurrent direction of Rehatikhol arenites. Alluvial fan to marginal marine depositional environment has been deciphered based on the field studies. NE, WNW, NW and ~N-S are important dominant structural grains that has been identified in the study area and their mutual relationship of reactivation has been established as N-S is oldest, affected by NE-SW (younger) and NW-SE, often silicified is youngest. Although NW is oldest structural grain in the area.

Basement Sambalpur granitoids of Chhibarra, Murmuri and Muchbal- Banabira are characterised as biotite tonalite and biotite granodioritic composition by petromineralogical studies. Detailed characterisation of Rehatikhol Formation has been carried out for all defined Members. Significant variation has been established in grain size, roundness, sorting and overall feldspar content in sandstones of different member. Some bipyramydal and euhedral quartz grains has been observed in feldspathic arenite Member and ferruginous sandstone indicating acidic volcanic origin. Based on the modal analysis, classification diagrams for Rehatikhol sandstone indicate their feldspathic to subfeldspathic arenite composition. Present study deciphered mainly plutonic acidic provenance, passive margin tectonic setting, semi-arid to semi humid paleoclimate for Rehatikhol Formation. These interpretations are well corroborated by geochemical studies. Basement granite and other important intrusive rocks has been also characterised. Significant interpretation has been made about radio elemental distribution, uranium, sulphides and fluorite mineralisation by the present study.

LIST OF FIGURES

LIST OF TABLES

LIST OF PROBABLE PUBLICATIONS

- Petromineralogy and geochemistry of Rehatikhol Formation of Chhattisgarh Super Group: Implications on provenance, paleo-weathering and tectonic setting.
- Uranium, sulphides and fluorite mineralization in Rehatikhol Formation of Chhattisgarh Super Group and in its environs in parts of Mahasamund district, Chhattisgarh and Bargarh district, Odisha.

CHAPTER 1
INTRODUCTION

1.1 AIMS AND OBJECTIVES

Singhora Protobasin that forms lowermost part of Chhattisgarh basin, is a promising geological domain where several uranium anomalies have been reported in different litho units during early 90's in different phases of exploration (Sinha and Hansoti, 1995; Misra and Rao, 1995). Uranium exploration in Singhora Protobasin during past decades has proven its potential as uranium province for unconformity related and fracture controlled mineralisation. Detailed radiometric investigation followed by sub-surface exploration at Juba, Dongripali, Dulapali, Amapali, Paraskol and Damdama areas resulted in location of radioactivity either in Singhora sediments or within basement rocks and hence have proved the uranium potentiality of the geological domain. Further exploration including drilling led to establish uranium mineralization in reactivated basement faults/fracture. Proper geochemical and petrological characterisation of these basement rocks and lithostructural understanding of these mineralised faults/ fractures is necessary for further detailed exploration.

Uranium mineralization at Juba- Banjhapali area is hosted by pyritiferous feldspathic arenite (PFA) of the basal Rehatikhol formation in Singhora Protobasin which occurs as isolated patches aligned in NNW- SSE and NNE- SSW direction assaying 0.01% – 0.079% U_3O_8 (beta/gamma) (free of thorium). Polymetallic sulphide mineralisation of Fe- Pb- Cu- As- Ag also associated with uranium in Pyritiferous Feldspathic Arenite (PFA). This significant mineralisation in sediments, proximal to unconformity makes pyritiferous feldspathic arenite a very important horizon for mineralisation. Similar set of conditions are investigated by detailed Petromineralogical and geochemical characterisation of this unit in the adjacent areas of Juba- Banjhapali domain. Study area (Chiwarakuta- Malaikhaman sector) of this project lies just south of Juba- Banjhapali domain and expected to bear similar potential in terms of mineralisation. Hence this project is formulated to characterise this PFA unit along with other units of Rehatikhol Formation for better understanding of U mineralisation potential in adjacent area.

The unconformity type deposits are generally found to occur under thick pile of sediments and therefore, poses severe constraints for its exploration. Most of the unconformity deposits are known to occur below 400-500m depth near the unconformity plane intersected by major faults/shear zones showing broad alteration envelope around concealed deposits which generally shows its signature up to the surface. In the proposed area, a number of post Singhora fault/shear zones trending N-S to NNE-SSW, NW-SE and ENE-WSW intersect the cover sediments which could be favourable locales for uranium migration and enrichment. Thorough understanding of these faults/ shear by detailed lithostructural mapping integrated with available previous data can enable to identify possible locals and controls of uranium mineralisation. This project is aimed to cover these aspects of investigation also to look for role of these structures (if any) in mineralisation.

Presence of fluorite mineralisation in the environs of Singhora Protobasin also reported along faults/ fractures. It is found to be associated with polymetallic sulphides, oxides and Uranium mineralisation in Kodopali and Burhadongar area in basement rocks (Yadava et. al, 2007). Fluorite forms in the late stages of crystallisation of hydrothermal fluids and hence its REE geochemistry is characteristics of hydrothermal fluid chemistry from it derived therefore it is considered as indicator mineral in IOCG system (Tobias U. Schlegel et. al, 2020). Presence of fluorite in Proterozoic Rehatikhol sediments near Chiwarakuta is really conspicuous and inspire to look for other characteristics of IOCG system. Uranium, polymetallic sulphide and fluorite mineralisation in the rocks of Sambalpur Granitoids and sediments of Rehatikhol Formation emphasise on more detailed petro- geochemical studies of these rocks in

Chiwarakuta- Malaikhaman sector. Hence, this project is designed to achieve following objectives-

- Detailed litho-structural mapping and radiometric survey to understand the litho-structural setup and mineralisation in the area.
- Petromineralogical and geochemical characterisation of Rehatikhol Formation (mainly sandstone) and basement granite to decipher provenance, tectonic setting, paleoweathering and paleoclimatic conditions.
- Study of uranium and fluorite mineralisation in Chiwarakuta- Malaikhaman area to deduce possible controls and association of mineralisation.
- To integrate the geological and geochemical characters for understanding the mineralisation characteristics.

1.2 RESEARCH PLAN/ METHODOLOGY

a) Field work: Field investigations using GPS, Brunton Compass, toposheets, hand lens with UV light, radiation detectors.

- Detailed litho- structural mapping and radiometric survey of 55 sq. km area on 1: 10000 scale.
- Systematic sampling for lab studies, field data collection, and field based sedimentological studies.
- Identification of radioactive, sulphide and fluorite mineralisation and its field based mutual relation and controls.
- Ground checking of heliborne survey inferred signatures and lineaments.

(b) Petrography: Using Leica petrological microscope with image analyser.

- Thin-Section study: To study mineralogy, texture and associated ore minerals of sandstones and granite.

- Study of radioactive minerals: To locate/identify radioactive mineral, its mode of occurrence and association with other oxide and sulphide minerals (by CN film autoradiography), identification of mineral phases in radioactive sample by XRD technique.
- Modal analysis of Rehatikhol sandstones using James Swift- automatic point counting system.

(c) Geochemistry:

- Radiometric analysis of basement rocks and overlying lithounits for their U, Th and K content (by gamma ray spectrometry).
- Geochemical analysis for major, minor, trace elements (by WD-XRF and ICP- AES).
- REE analysis of basement rocks and other lithounits (by ICP- AES).
- Fluoride analysis by ion selective electrode method.
- Plotting of various geochemical diagrams including Chondrite Normalised REE plot.

(d) Data processing for interpretation and integration of data.

1.3 DELIVERABLES

This project resulted in following deliverables-

- Geological map of 55 sq. km area on 1: 10000 scale.
- Various cross sections depicting lithostructural setup and mineralisation in area.
- Discovery of uraniferous anomalies at Kermeli, Kurapali and many thoriferous anomalies.
- Determination and interpretation of radio elemental distribution in various lithounits of basement rocks and Rehatikhol Formation.
- Hydro uranium anomaly (54 ppb) in Rehatikhol sediments in Chiwarakuta village just near to fluorite occurrences.

- Petromineralogical and geochemical characterisation of Sambalpur Granitoids.
- Classification of Rehatikhol Formation into 5 lithounits and their petromineralogical and geochemical characterisation.
- Comparative geochemical studies of mineralised PFA of Juba, Chhibarra and unmineralised PFA of various localities in study area.
- Paleocurrent analysis of Rehatikhol Formation.
- Fracture and joint trend analysis of different sectors.
- Deduction of provenance, tectonic setting, paleo weathering conditions and paleoclimate of Rehatikhol Formation.
- Possible controls of uranium and fluorite mineralisation in study area.

More emphasis has been given on the Rehatikhol Formation of Singhora Group in this project. Petromineralogical studies along with geochemical analysis were carried out to generate data in order to classify sandstones and draw interpretations on the provenance, paleoweathering and tectonic setting of the Rehatikhol Formation. Various geochemical indices and plots were generated to depict the above mentioned interpretations.

1.4 RELEVANCE TO AMD PROGRAMME

The principle mandate of AMD is to establish indigenous uranium resources. The deliverable of this project has successfully led to new understanding and potentiality of the area. The identification of radioactive mineralisation, rocks of economic and petrological interest in various localities has opened new avenues of research and exploration through the entire basin.

1.5 LOCATION AND ACCESSIBILITY

The study area falls in the different quadrants of Survey of India toposheet numbers 64 O/3 and 64 O/7 (Figure 1.1). The study area comprises Chiwarakuta- Rehatikhol-

Malaikhaman- Dongar Raksha sector and lies in the geographic coordinates between the latitude N 21˚15’00’’ to N 21˚18’50’’ and longitude E 83˚12’30’’ and E 83˚17’30’’. It has an average elevation of 248 metres (813 feet).

It is located at Chhattisgarh and Odisha border on NH-6 and connected with Nagpur (475 km) and Raipur (178 km) (Figure1.2). Nearest town is Saraipali, located about 156 km far from Raipur and 120 km from Bilaspur.

Air: The nearest airport is Raipur airport, located about 182km from Chiwarakuta.

Railways: Raigarh (88 km), Mahasamund (145 km) and Raipur (190 km) are the major railway station by which study area can be approached.

1.6 GEOMORPHOLOGY

Geomorphologically, the area is represented by a low lying plain, plateau with some undulating hills. Southern and Eastern part study area occupied by rugged hilly terrain ranging from 300 to 400 m above MSL. The elevation of the area varies from 238 to 424 m above MSL. In the eastern part the area is hilly and covered by forest. The maximum basin elevation is 685 m above MSL in the southern part.

The Physiography of the basin is controlled by geological formations namely, sandstone, siltstone, shale and Limestone. Seasonal rivers and nalas of the study area are tributaries to Mahanadi River in north and Ong River in south constitute the main channel system in the area. Drainage of the area is mostly dendritic with some structurally controlled rectangular and trellis pattern. Parallel drainage has been developed on cuesta and steep linear ridges. Various tributaries and distributaries of Mahanadi River and Ong River form the drainage network. In sandstone terrain, the drainage pattern is dendritic.

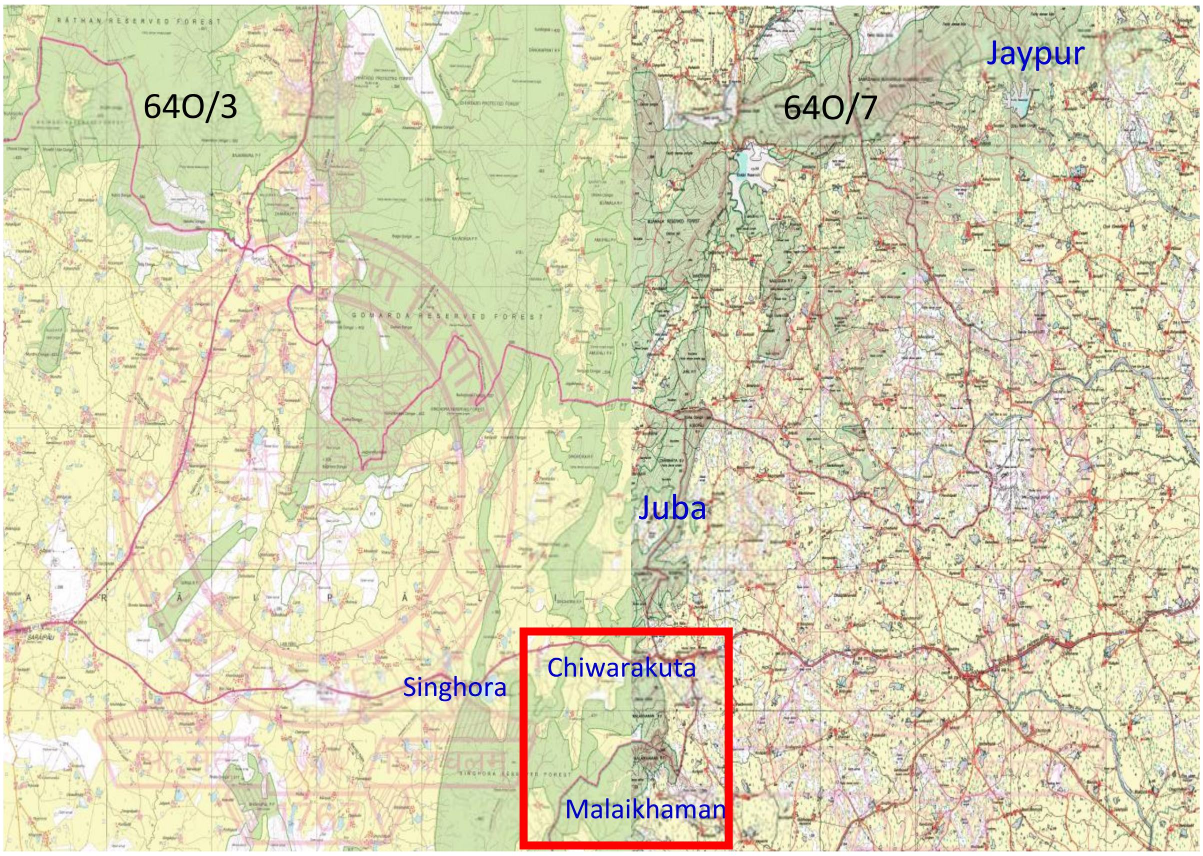

Figure 1.1 Mosaic of toposheet 64 O/3 & O/7 showing the study area block and topography.

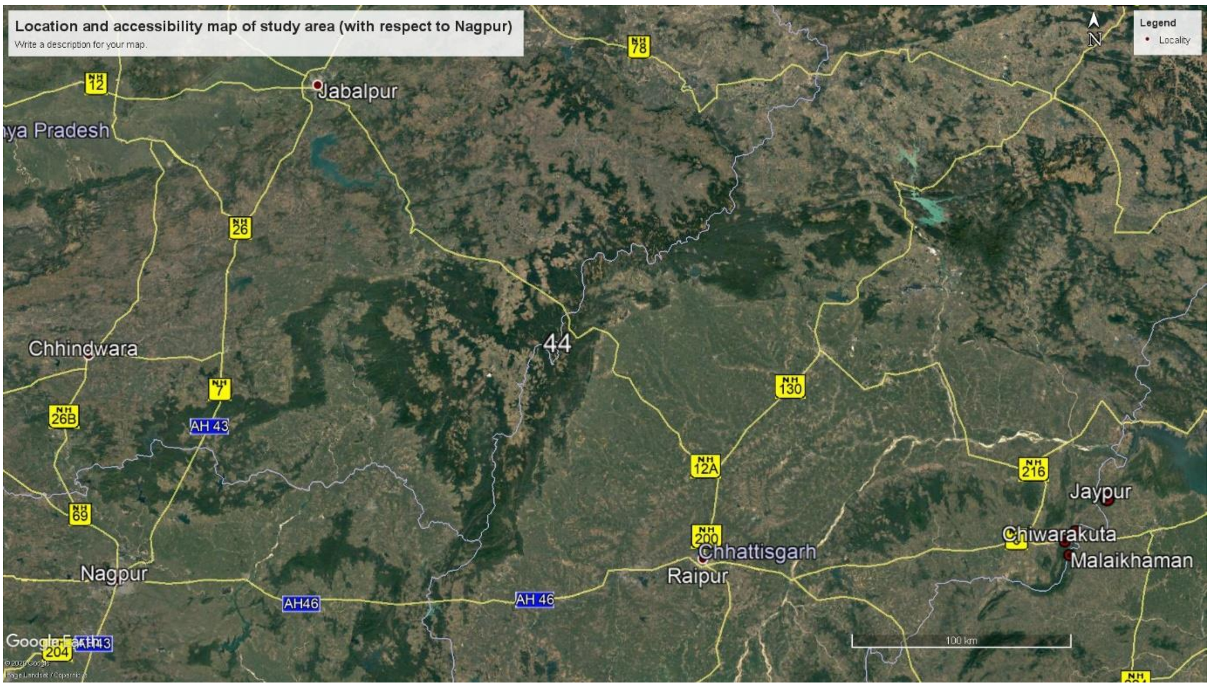

Figure 1.2 Google earth image showing accessibility of Chiwarakuta with respect to Nagpur.

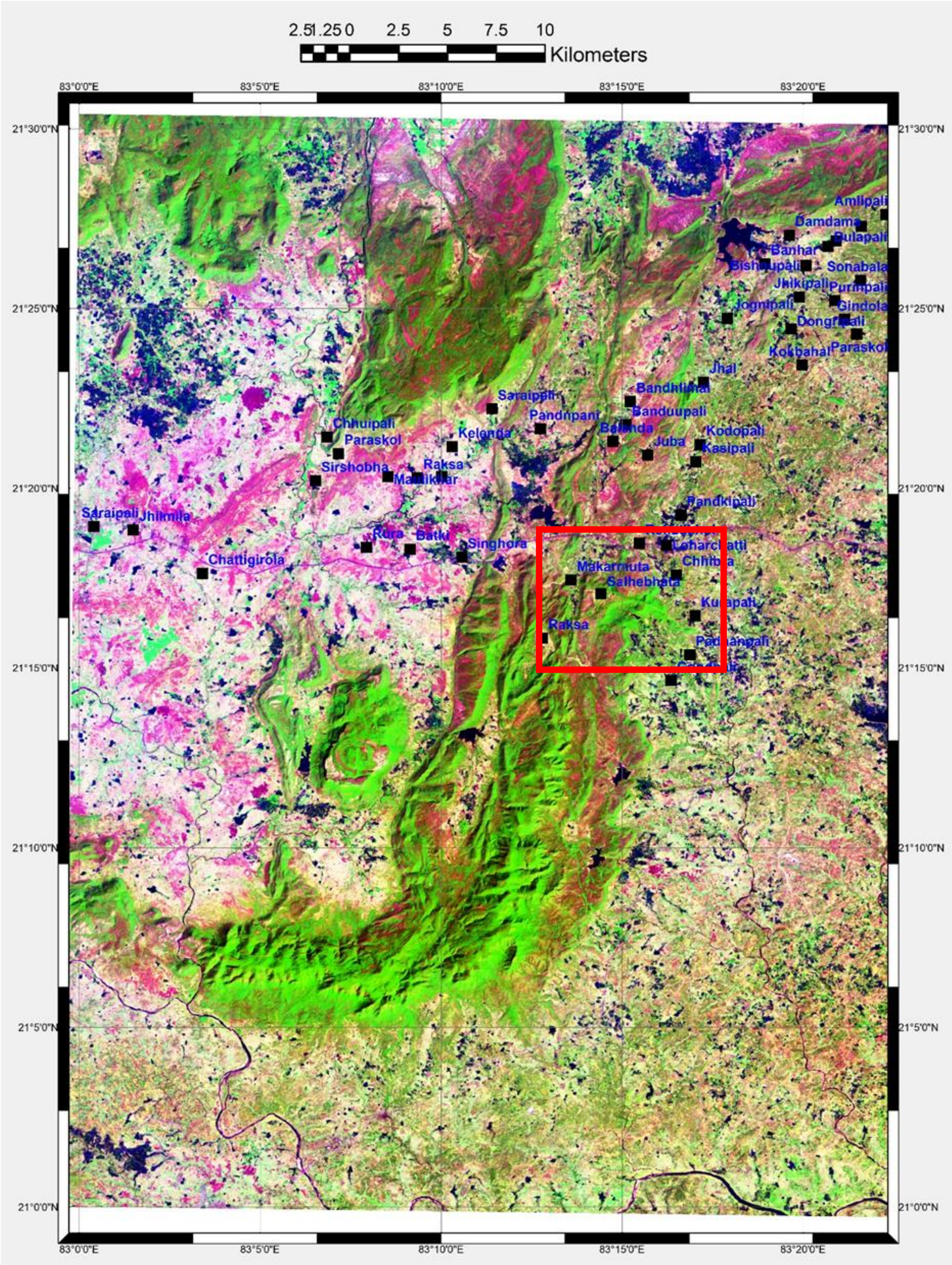

Figure 1.3 FCC satellite imagery (Bands 7, 5, 1) of Saraipali- Sohela area. (Source: USGS, Landsat 8).

Drainage texture is coarse in sandstone while it is fine in shale. In limestone countries the drainage is internal due to solution activity. In granitic terrain, the drainage is usually joint/fracture controlled forming a coarse dentritic pattern. Prominent landforms are plateau, cuesta, mesa, linear ridges and escarpment. The major lineaments are NNE, NE, NW and N-S extracted and inferred from satellite imagery of Sohela- Saraipali area (Figure 1.3).

1.7 CLIMATE

The area is characterized by tropical climate. The climate is hot and humid due to its proximity to tropic of cancer and dependence on monsoon for rains. During the months of summer, the temperatures rises to ~ 45ºC. Winter is pleasant with the temperature dropping up to ~10ºC. The rainfall of the area is dominated by the South West Monsoon, which starts in the middle of June and ceases by the end of September or beginning of October. The area receives about 1300 mm (51 in) of rainfall, mostly in the monsoon season ranging from late June to early October.

1.8 FLORA AND FAUNA

The study area is cladded with sub-tropical, thick, dry deciduous mixed forest and categorised under Reserved Forest. The main species of flora in this area are Teak (Tectona grandis), sal (Shorea robusta), Palas (Butea monosperma), Haldu (Adina dardifolia, salai (Boswellia serrata), Mahua (Madhuca latifolia), Kalam (Mitragyne parvifolia) and Neem (Azadiracta indica), Biza (Phylan this), Bel (Aegla mamelos), Mango and Char.

The fauna is represented by Panther (Panthera pardus), Slot Bear (Melursus ursinus), common Jangle Cat (Felis chaus), Wild Boar (Sus scrofa), Common Langur (Prebsytis entellus), Black Buck (Antilope ceryicapra), Blue Bull (Boselaphus tragocamelus), Sambher (Ceryus unicolor), Squirrel (Funambullus pennanti), Porcupine (Hystrix indica) and field rats (Bandicotabengalensis).

1.9 PREVIOUS WORK

Majority of earlier studies on the Chhattisgarh basin were concentrated in the western and south – central part of the basin where the succession is characterized by development of algal stromatolites and mature sandstone, characteristic stable platformal association (Dutt, 1964,; Murti, 1987). Many workers had carried out their important scientific works on Singhora sub basin of Chhattisgarh basin. The pioneering work in the area on 2”=4 miles scale was carried out by Smith (1898). Later Narayana Murthy (1956), Banerjee (1964), Gupta (1969), Mohanty (1970) mapped parts of the basin and the adjacent areas. They classified the lithopackage of Chandarpur sandstone of Chhattisgarh Supergroup. The age of the succession is not very preciously constrained, Kruezer et al (1977) suggested K-Ar date of 700-750 Ma for the basal part of the succession. Whereas Schnitzer (1977) proposed that the succession may range between 800 to 1100 Ma in age. Sinha and Hansoti (1994), later modified the stratigraphy of Singhora Group by their work on pyritiferous feldspathic arenite (Juba Member), presence of doleritic sill in Rehatikhol Formation, identification of porcellanites in Rehatikhol and other Formations.

Dutt (1964) studied in the south western part of the Chhattisgarh Basin and classified the succession into five series, the Chandarpur Sandstone, Charmuria Limestone, Gunderdehi Shale, Khairagarh Sandstone and Raipur Shale-Limestone. Schnitzer (1969; 1971) established five cycles of sedimentation, separated by unconformities in the east central part of the basin. Murti (1987) worked in the south central part of the basin, assigned a “Supergroup” status to the Chhattisgarh succession and classified the rocks into two groups separated by an unconformity, the lower, Chandarpur Group, and the upper, Raipur Group. Each group comprises several formations. The basal conglomerate, arkose and subarkose were classified as the Lohardih Formation. The Chaporadih Formation comprises of medium to very fine grained sandstone which grades up into to medium grained quartz arenites of Kansapathar

Formation. Datta (1998) worked in the central part of the basin and retained the classification of Murti (1987). Das et al. (1992) divided the Chhattisgarh Basin into Hirri and Baradwar sub-basins, with Singhora and Barapahar as protobasins. They classified the Chhattisgarh Supergroup into three unconformity-bound groups, the Singhora Group, the Chandarpur Group and the Raipur Group in an ascending order. Das et al. (1992) considered that the Singhora Group is the lowermost unit of the Chhattisgarh Supergroup and occurs between the granite gneissic complex of the basement and the Chandarpur Group. The Singhora Group was further classified into four formations, Rehatikhol, Saraipali, Bhalukona and Chuipali (Das et al. 1992; 2003). Patranabis-Deb (2004) and Patranabis-Deb and Chaudhuri (2008) made three fold classification of the succession around the eastern part of the basin. They classified the succession into the Chandarpur, Raipur and Kharsiya Groups, but in contrast to Das et al. (1992), they suggested that the Chandarpur Group represents the basal stratigraphic unit in the eastern part of the basin. Recently, four-tier lithostratigraphy for the Chhattisgarh Supergroup is also referred classifying it into four groups namely, Singhora, Chandarpur, Raipur and Kharsiya as Group (Chakraborty et al., 2015).

Exploration activity in Singhora basin has commenced long back in late 80's. Uranium mineralisation along southeastern margin of Chhattisgarh basin has been located in the conglomerate, arkose and arenite of Singhora Group at Kalangpali (0.017% U_3O_8 β/γ), Juba (0.010-0.079% U_3O_8 β/γ), Goverdhangiri (0.026-0.13% U_3O_8 β/γ), Bagianala (up to 0.80% U_3O_8 β/γ) and Borehole No. KJB/6 (0.017% x1.5m and 0.019x0.40m), KJB/10 (0.011% x0.20m), KJB/18 (0.041% x0.55m & 0.018x 0.80m) and KJB/38 (0.014% x0.30m). However, uranium mineralisation in the sheared basic rock and granite gneiss are located all along the basin margin. (Sinha and Hansoti 1995, Mishra & Rao 1995, Kamlesh Kumar 1998, Yadava and Agarwal 1999, Pant and Chaturvedi 1999, Yadava and Rajeeva Ranjan 2000 and Yadava et al 2007).

Uranium mineralisation with polymetallic (U, Pb, Cu, As) association hosted in Juba Member (pyritiferous feldspathic arenite-PFA) of Rehatikhol Formation of Singhora Group was first discovered by Dr D K Sinha during FS 1994-95, at Juba-Banjhapali area, Singhora Protobasin, Mahasamund District, Chhattisgarh. Further detailed field and laboratory studies by him during FS 1995-96 established uranium mineralisation as epigenetic, hydrothermal in nature, apparently controlled by prevalent N-S & NNW-SSW faults/shears. Various aspects of geological studies, nature of uranium mineralisation, polymetallic association, structural studies, petromineralogical, geochemical and sulphur isotope study results are lucidly elaborated and explained in Annual reports (FS 1994-95 & 1995-96). Detailed work on ore minerography has been carried out on uraniferous polymetallic sulphide bearing arenite of Juba by Jain et al, 1998 that imparted hydrothermal polymetallic sulphides association of Fe- Pb- Cu- Zn-Ag- As with U mineralisation. Prominent illite/ sericite as well as kaolinite alteration haloes trending along NW-SE, NE-SW and ENE-WSW fracture trends are also identified in Salhebhata- Malaikhaman sector as a result of lithogeochemical survey (n=472) (Sharma and Jana, 2013) that led to uranium haloes (above threshold of 15.26 ppm). Reconnaissance radiometric survey and mapping on 1:50000 scale has been carried out by A.R. Mukundhan in F.S. 1996- 1997 that resulted identification of uraniferous radioactive anomaly in quartz reef near Malaikhaman (T.S. 64 O/8).

Integration, processing of radiometric, magnetic and EM data of high resolution heliborne geophysical survey that was carried out over Singhora Protobasin (FS 2011-12, Singhora Block-I, 5828 Lkm) has delineated a target block of 1500 m x 400 m near Bandupali, NE of Juba area, where the NE-SW trending EM conducting body is interpreted to continue in basement rocks starting from unconformity surface that coincides with inferred magnetic fracture/anomaly trend (Maurya and Sridhar, 2018).

CHAPTER 2
REGIONAL GEOLOGY

2.1 INTRODUCTION

A crustal-scale shear zone, referred to as the Central Indian Shear Zone (Ramakrishnan & Vaidhyanadhan, 2010) divides the Precambrian terrain of central India into two crustal provinces, northern and southern. The Bastar Craton, belonging to the southern crustal province, hosts gneisses, migmatites, supracrustals and cover sediments spanning in age from late Archaean to Mesoproterozoic. Proterozoic platformal sediments of Chhattisgarh, Abujhmar, Indravati, and Kharihar basins unconformably overlie these gneissic complex - supracrustal rocks of Bastar craton. Phanerozoic Gondwana sediments are deposited along Mahanadi and Pranhita - Godavari grabens, which are in turn covered by Deccan traps and recent alluvium.

The Chhattisgarh basin, located at the margin of the Bastar craton (East Indian craton), is the third largest Proterozoic basin of Peninsular India. The Chhattisgarh basin (33,000 km2 in area) documents ~2.3-km thick succession of mixed siliciclastic-carbonate–phosphorite/ evaporite lithology and lies unconformably over the granitic/gneissic basement of the Archaean/ Palaeoproterozoic Bastar Craton (Chakraborty et al., 2015, Murti, 1987). Regionally and tectonically, the Chhattisgarh Basin is bounded by Godavari and Mahanadi Rifts to the southwest and north east and by Central Indian Suture Zone (CITZ) and Eastern Ghat Mobile Belt (EGMB) to the northwest and southeast respectively (Figure 2.1). In detail, the Chhattisgarh Basin lies on the central Indian craton (Bastar craton) and surrounded by Sambalpur Granitoids in the east (2,380 ± 44 Ma; Choudhary et al., 1996), Bilaspur-Raigarh-Surguja Belt of Sausar Group in the north (1,541 ± 26 to 1,100 ±20 Ma; Pandey et al., 1995), Nandgaon volcano-plutonics in the southwest (2,462± 25 to 2,039 ± 79 Ma; Pandey et al.,

1995) and Khairagarh volcano-sedimentary rocks in the west (2,120 ± 35 Ma; Sinha, 1996). Metasediments and granitoids of Baster craton (3,610 ± 336 to 2,110 ± 41 Ma; Pandey et al., 1995) lie to the south of the basin (Figure 2.2).

Based on sedimentation pattern, contact relationship (unconformable/ gradational), succession lithologs and relative dominance of lithology, the Chhattisgarh basin has been divided into three sub-basins: (i) the Singhora Protobasin, (ii) the Baradwar Sub-basin, and (iii) the Hirri Sub-basin and the sedimentary succession is classified under three constituent groups viz. Singhora, Chandarpur and Raipur (Das et al., 1992, 2003). Recently, four-tier lithostratigraphy for the Chhattisgarh Supergroup is also referred classifying it into four Groups namely, Singhora Group, Chandarpur Group, Raipur Group and Kharsiya Group (Chakraborty et al., 2015).

Based on sedimentary assemblages, facies and stratigraphic architecture, it has also been inferred that the basin evolved as an intracratonic rift (Chaudhuri et al. 2002; Patranabis-Deb and Chaudhuri, 2008). It shows structural disturbances along the western, northern and eastern margins. The western and northern margins of the basin are delimited by NNE-SSW and E-W to ENE-WSW faults respectively. Broad open warps and large scale faults trending NNW-SSE, NNE-SSW, E-W and NE-SW within the strata express the deformation in the eastern part of the basin. These large-scale faults are believed to be the rejuvenated basin opening faults (Chaudhuri et al. 2002). Younger cross faults trend NE-SW and N600- 700 W to S600-700 E which are occupied by quartz veins. Younger doleritic sills and dykes trending NNE-SSW and NW-SE traverses Singhora Group of rocks.

Study of aeromagnetic data by M. Sridhar et al (2017) over Singhora protobasin and adjoining area revealed NW-SE trending aeromagnetic signatures related to Sonakhan Greenstone Belt extends below the Singhora sedimentary rocks and forms the basement in the west. The analysis suggests that TCAL (Trans-Chhattisgarh Aeromagnetic Lineament) is a block fault with northern block down-thrown and affected the basement rocks comprising the Sonakhan Greenstone Belt and Sambalapur Granitoids. The episode of faulting represented by the TCAL is pre-Singhora sedimentation and played a vital role in basin evolution (M. Sridhar et al., 2017). Stratigraphy proposed by various authors in different parts of Chhattisgarh basin is given in Table 2.1.

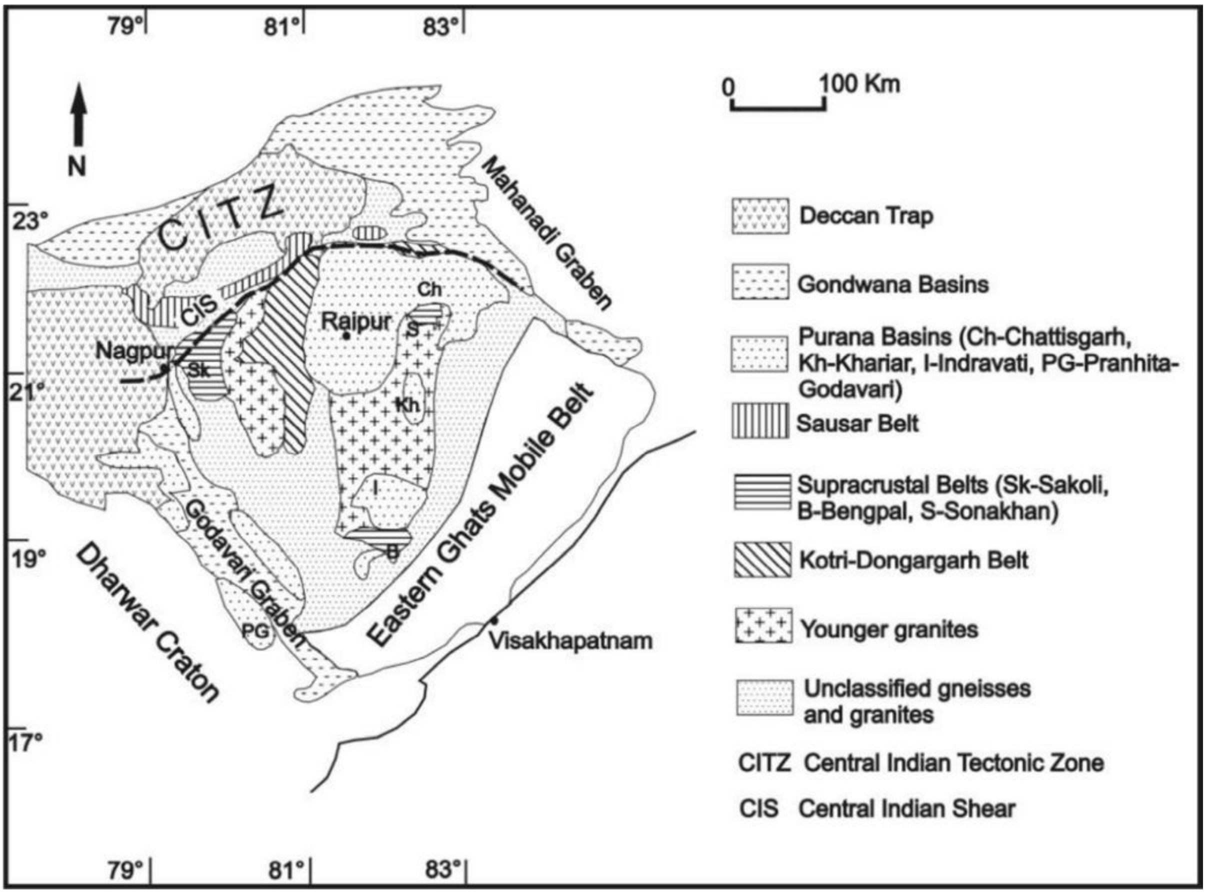

Figure 2.1 Bastar Craton surrounded by other cratons, mobile belts and grabens (modified after Ramakrishnan and Vaidhyanadhan, 2010, Dhang & Patranabis, 2012).

2.2 GEOCHRONOLOGY OF CHHATTISGARH BASIN

The Chhattisgarh Basin is geochronologically one of the best constrained Proterozoic basins in India. Unlike other Indian basins, such as Vindhyan and Cuddapah, reports of geochronological data are restricted within lower, middle or upper parts of their respective successions, the availability of concordant tuffaceous strata at different stratigraphic levels

Table 2.1 Stratigraphic classification of different parts of the Chhattisgarh Basin by different workers (modified after Dhang & Patranabis 2012).

Dutt (1964)- Southwestern part	**Schnitzer (1969)- East central part**	**Murti (1987)- South central part**		**Das, et.al. (1992; 2003)**		**Patranabis Deb and Chaudhuri (2008)**		**Chakraborty et al., 2015**	
Raipur Shale-	Maniari Shale (100m)		Tarenga Shale (180m)		Maniari Formation (70m)	Kharsiya	Nandeli Shale (300m)	Kharsiya	Nandeli Shale
Limestone	Hirri Kharkhena Dolomite					Group	Sarnadih Sandstone (250m)	Group	Sarnadih Sandstone
(450m)	(50-100m)						~~~*Unconformity*~~~		~~~*Unconformity*~~~
	Belha Limestone (80m)								
	Patharia-Umaria Shale		Chandi Limestone		Tarenga Formation		Sukhda Tuff (70m)		Maniari Formation)
	(50m)		(670m)		(180m?)				
	~~*Unconformity*~~~						Churtela Shale (150m)		Tarenga Formation
Khairagarh	Nandini Lst. (80-100m)	Raipur		Raipur				Raipur	
Sandstone	Bhatapara Lst./Dolo (50m)	Group		Group	Chandi Formation (670m)		Saradih Lst. (100m)	Group	Chandi Formation
(variable thickness)	Lilagarh Shale (50m)								
	Akaltara Dolo./Arenite		Gunderdehi Shale						
	(40m)		(430m)						Gunderdehi
	~~*Unconformity*~~~~					Raipur	Gunderdehi Shale (450m)		Formation
					Gunderdehi Formation	Group			
Gunderdehi Shale	Karuid Shale (100-150m)		Charmuria Limestone						Charmuria Limestone
(180m)	Karuid Limestone (50m)		(490m)				Sarangarh Limestone		
	Seorinarayan Shale (100m)		~~~*Unconformity*~				(150m)		
Charmuria	Sarangarh Lst.(30-50m)				Charmuria Limestone				
Limestone			Kansapathar/Kond. Fm.		(490m)		Bijepur Shale (100m)		
(300m)	~~~*Unconformity*~~~~		(+125m)						
					Kansapathar Fm.(20-200m)		Kansapathar Fm. (60m)		Kansapathar Fm.
	Chandarpur Quartzite		Chaporadih Fm. (15m)					Chandarpur	
Chandarpur	(200m)	Chandarp			Chaporadih Fm. (20-200m)		Gomarda Fm. (650m)	Group	Chaporadih Fm.
Sandstone		ur Group		Chandarpur		Chandarpur			
(300m)	Conglomerate (300m)		Lohardih Fm.(240m)	Group	Lohardih Fm. (20m)	Group	Lohardih Formation (150m)		Lohardih Fm.)
~~*Unconformity*~~	~~~~*Unconformity*~~~		~~~*Unconformity*~~		~~~~*Unconformity*~~~		~~~*Unconformity*~~~~		~~*Unconformity*~~
Archaean granite,	Crystalline Complex		Archaean Basement		Chhuipali Fm. (300m?)		Basement complex		Chuipali Fm.
dolerite, etc.				Singhora	Bhalukona Fm.(~20m)			Singhora	Bhalukona Fm
				Group	Saraipali Fm. (60m)			Group	Saraipali Fm.
					Rehatikhol Fm.(20m+)				Rehatikhol Fm.
					~~*Unconformity*~~~				~~*Unconformity*~~
					Archean and Lower				Archean and Lower
					Proterozoic Basement				Proterozoic Basement

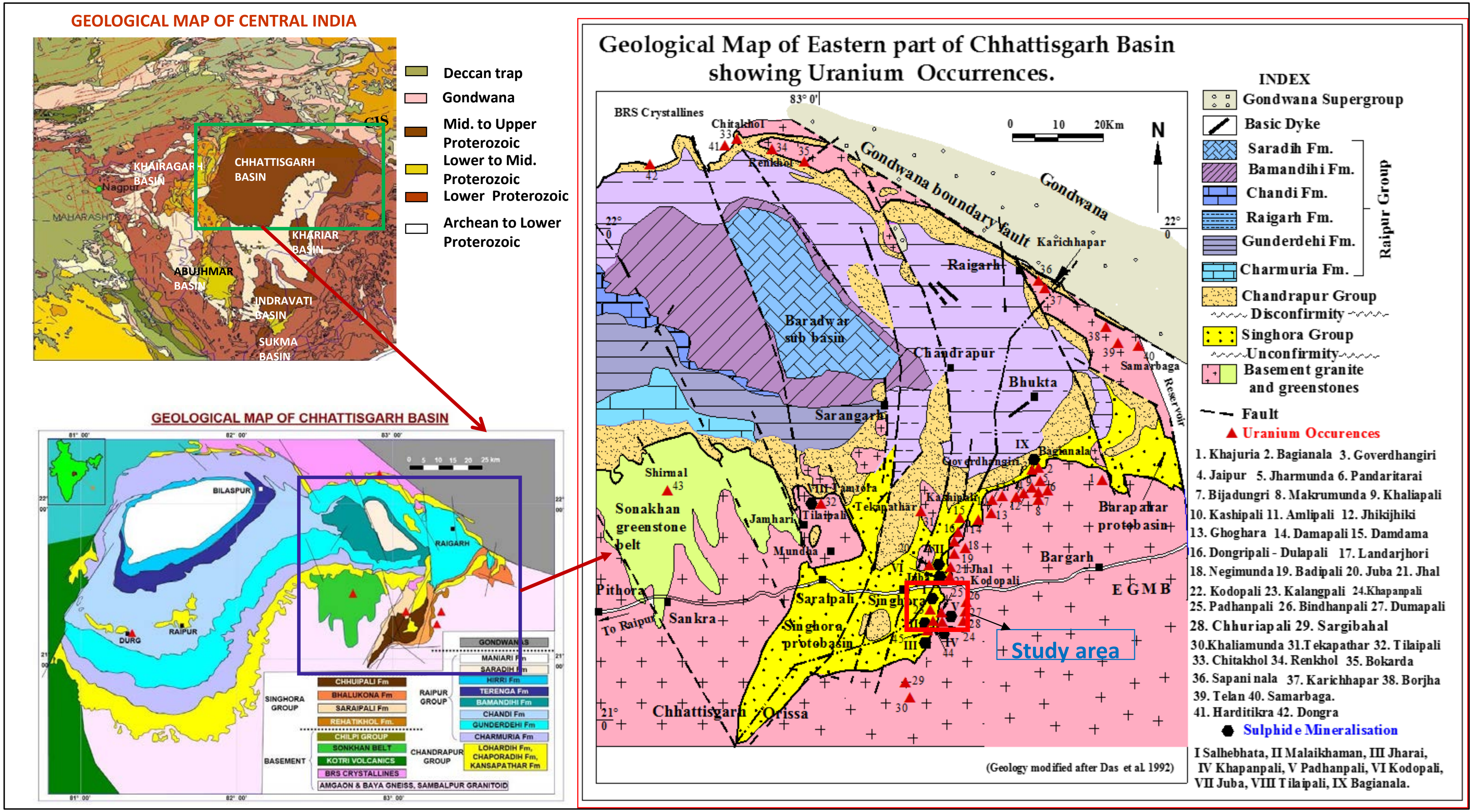

Figure 2.2 Regional geological map of Chhattisgarh basin and location of study area in it.

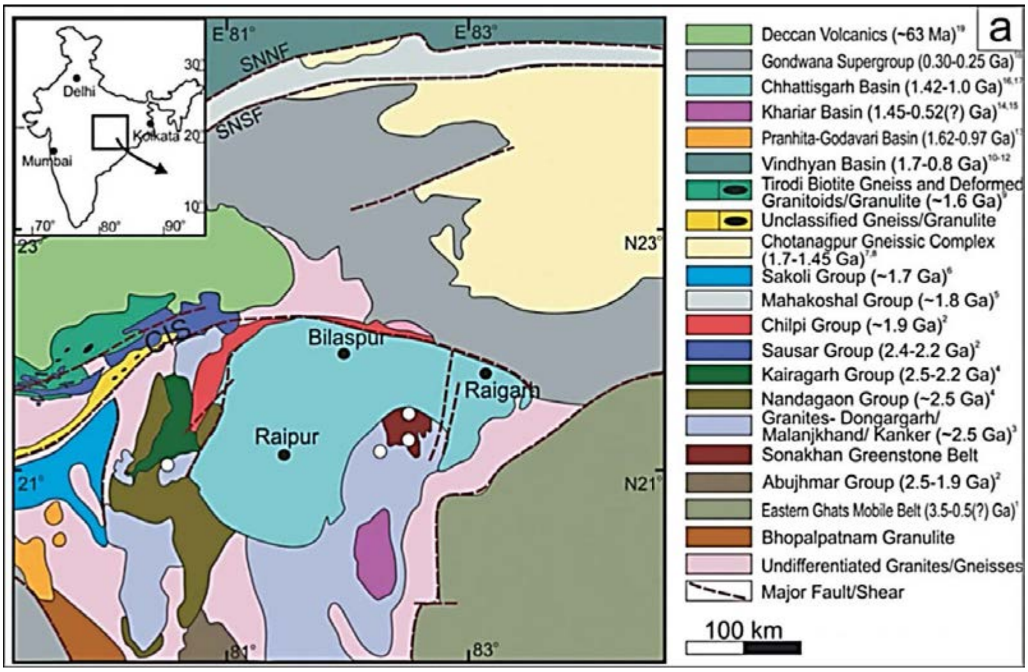

Figure 2.3 Geological map of central India showing the location of Chhattisgarh Basin, basement granitoids, and adjacent litho-units in Bastar craton (modified after Saha and Patranabis-Deb 2014). Sources of age data: 1: Dasgupta et al. (2013); 2: Mohanty (2015); 3: Manikyamba et al. (2016); 4: Khanna et al. (2019); 5: Bora et al. (2013); 6: Ahmad et al. (2009); 7: Dey et al. (2017); 8: Mukherjee et al. (2017); 9: Bhowmik et al. (2011); 10: Sarangi et al. (2004); 11: Gopalan et al. (2013); 12: George et al. (2018); 13: Amarasinghe et al. (2015); 14: Das et al. (2009); 15: Ratre et al. (2010); 16: Das et al. (2011); 17: Patranabis-Deb et al. (2007); 18: Mukhopadhyay et al. (2010); 19: Renne et al. (2015). (Source: B. G. George and J. S. Ray, 2020).

within the Chhattisgarh lithopackage allowed workers to apply a well-constrained age bracket with robust/near-robust geochronological systematics (U–Pb zircon SHRIMP, Sm–Nd monazite) in terms of both initiation and closing age for the basin.

These studies have indeed driven the Neoproterozoic time frame for the basin into the background (Patranabis-Deb et al.2007; Das et al. 2009; Bickford et al. 2011a, b) and established its 'Mesoproterozoic' time frame on a strong basis. The Patranabis-Deb et al. (2007) reported 990–1020 Ma age zircon grains from a tuffaceous layer present in the upper part of the Chhattisgarh succession, exposed near the Sukhda area. Subsequently, studies involving zircon and monazite grains retrieved from tuff/volcanoclastic layers spanning its basal part, that is, the Singhora tuff (c. 1500 Ma Sm–Nd monazite electron probe microanalysis (EPMA), Das et al. 2009;1405+9 Ma, Bickford et al. 2011a) present at the contact between the Rehatikhol and Saraipali Formation of the Singhora Group and the uppermost part, that is, the Dhamda tuff (correlatable with the Sukhda tuff; 993+8 Ma U–Pb SHRIMP zircon, Bickford et al. 2011a–b) sandwiched within the Tarenga Formation, have put the Chhattisgarh lithopackage in a well-constrained time domain, between c. 1500 and 1000 Ma. Recently, Das et al. (2017) studied zircon dating of lithounits of Singhora Group that yield youngest zircon population between 1643 Ma to 1619 Ma implying the age of sedimentation is <1600 Ma. Based on geochronological study of Bandhalimal sill intruded in Rehatikhol Formation, it is proposed that the rocks of Rehatikhol Formation are older than 1,100 Ma (Sinha et al, 2011). This study suggest time of initiation of Chhattisgarh Basin (>1,100 Ma) with the help of petrography, geochemistry and radiometric age of doleritic sill. This age estimation corroborates to the age deduced from the Conophyton species reported from Rehatikhol Formation (Sinha et al., 2002). Therefore, on the basis of above evidences it is concluded that rocks of Singhora Group are older than 1,100 Ma. Geochronological ages are shown in Figure 2.3 belonging to environs of Chhattisgarh basin. Summarizing the recently reported geochronological dates, it is concluded that the Chhattisgarh Basin belongs to 'Mesoproterozoic' time with its sedimentation history spanning around 400 Ma, that is, between 1400 Ma (1405±9 Ma, Bickford et al. 2011a, b) and 1000 Ma (Patranabis-Deb et al. 2007).

Another geochronogical data of dolerite dyke, from Damdama area, which is intrusive into the basement and overlying sediments of Chandarpur Group in the central Indian craton, yielded Rb-Sr internal isochron age of 1641 ± 120 Ma (Pandey et al., 2012). This study is the first reliable age report on the onset of sedimentation in the Chandarpur Group. The total minimum time span of Chandarpur and Raipur Group may be 1.6 Ga to 1.0 Ga

(Mesoproterozoic). The rocks of unconformably underlying Singhora Group of Chhattisgarh Supergroup thus indicates Paleoproterozoic age (older than 1.6 Ga).

2.3 SINGHORA GROUP

The Late Archean to Early Proterozoic Sonakhan Greenstone Belt that is represented by bimodal volcano-sedimentary assemblage (Sonakhan Group) intruded by younger granites, gabbros, ultramafics and dolerites (Das et al., 1992) forms basement of Singhora Group in the west while Sambalpur granitoids forms basement in eastern part. The lowermost Singhora Group developed in an embryonic basin to the east, consists of four formations of arenite (Rehatikhol), argillite± carbonate (Saraipali), arenite (Bhalukona) and argillite± carbonate sequence (Chuipali Formation). Singhora Group covers an area of over 1,000 km^2 with about 400 m thickness of sedimentary column. The Chandarpur Group, unconformably overlie the Singhora Group. The basal Singhora basin is inferred as a 'protobasin' underlying the aerially extensive main Chhattisgarh basin (Das et al., 1992; Chakraborty et al., 2009). Sinha and Hansoti (1995) have proposed modifications to the stratigraphy of Singhora Group in which they have mentioned presence of porcellanites in the Rehatikhol, Saraipali and Chuipali Formations and sill and dyke of basic compositions (Table 2.2). Rehatikhol Formation has been accepted as the oldest Formation of Chhattisgarh Supergroup (Das et al., 1992; Mukherjee and Ray, 2010).

Restricted within the southeastern part of the basin, the lithopackage belonging to this group records early sedimentation history in the basin. A wide variety of depositional environment ranging from alluvial fan/ braid plane system to distal marine shelf beyond storm wave base with a transition delta in between has been inferred based on process based sedimentological studies involving different lithostratigraphic intervals of Singhora Group (Chakraborty et al. 2009, 2011). Detailed description of rocks of Singhora Group of rocks is mentioned under local geology chapter.

Table 2.2 Stratigraphic succession of Chhattisgarh Super group in Study Area.
(after Das et al., 1992 and Sinha & Hansoti, 1995)

Raipur Group	Shale, Limestone and Dolerite Dykes	
---------- Unconformity ----------		
Chandarpur Group	Sandstone, shale	
---------- Unconformity ----------		
Chuipali Fm.	Shale, limestone, porcellanite	Singhora Group (Study Area)
Bhalukona Fm.	Glauconitic sandstone	
Saraipali Fm.	Shale, limestone, porcellanite	
Rehatikhol Fm.	Conglomerate, sandstone, shale, porcellanite and doleritic sill.	
---------- Unconformity ----------		
Sambalpur Granitoid/ Sonakhan Group - Archean to Lower Proterozoic Age		

2.4 CHANDARPUR GROUP

Rocks of the Chandarpur Group are widely exposed all along the southern margin of the Chhattisgarh basin lying unconformably over the crystalline basement. This group has been divided into three Formations, namely, the arenaceous Lohardih, the fine grained glauconitic arenaceous to argillaceous Chaporadih and the arenaceous Kansapathar Formations in ascending order (Murti 1987; Das et al. 1992). The topmost Kansapathar Formation (also known as Kondkeraat places) is persistent. Patranabis-Deb and Chaudhuri (2002, 2007) identified the Gomarda Formation below the Kansapathar Formation in the Raigarh area as roughly equivalent to the Chaporadih Formation of Das et al. (1992). The Chaporadih Formation is also widespread. Such distribution is consistent to their fan-delta depositional setting (Patranabis-Deb and Chaudhuri 2002).

The Chandarpur Group (Figure 2.2) consist of siliciclastics deposited in an array of alluvial, coastal and shallow marine environments within multiple cycles of transgression and progradation. The succession is marked by rapid lateral facies changes indicating rapidly shifting depositional systems, variable rates of sediment influx, and uneven rates of subsidence and creation of accommodation in different parts of the basin.

The Lohardih Formation, unconformably overlies granites and gneisses of the basement, has a maximum preserved thickness of 150 m, and is characterized by a heterogenous assemblage of conglomerate, feldspathic sandstone with wide range of textural and mineralogical variations, locally developed minor matured quartzose sandstone, and shale. The Lohardih Formation grades upward into the c. 650 m thick Gomarda Formation characterized by extreme lithologic variation between shale and sandstone, with a dominant component of sandstone - mudstone heterolithics (Patranabis-Deb, 2004).

The upper heterolithic unit of the Gomarda Formation grades upwards into the Kansapathar Sandstone. The latter sandstones are well sorted, medium-grained, subarkosic to quartzose, and occur as small lenticular shoaling-up bars.

2.5 RAIPUR GROUP

The Raipur Group is well developed in the Hirri sub-basin and is divided into six formations (Das et al. 1992). The contact between the Chandarpur Group and the Raipur Group is sharp in both the Hirri and Baradwar sub-basins except at places south of Durg where it is gradational. Murti (1987) described the erosional contact between Chandarpur Group and Raipur Group at Birkoni and Tumgaon (north of Mahasamund) but Patranabis-Deb and Chaudhuri (2008) do not report any unconformable contact between these two groups in the Baradwar sub-basin. The Formations of Raipur Group are described below-

The Charmuria Formation, the oldest formation of the Raipur Group, is characterized by typical black flaggy limestone that grades to purple shale. The Gunderdehi Formation consisting mostly of calcareous purple to grey shale includes sandstone and siltstone lenses. The Saradih Limestone, overlies the Gunderdehi Shale with a gradational contact, comprises a thick unit of interbedded dolomite and red shale at its basal part, whereas its upper part is dominated by a grey limestone facies of very well bedded rythmite of micrite and marl. The Chandi Formation dominated by purple to grey stromatolitic limestone is the largest Formation (by thickness and area) in the Hirri sub-basin; but, it is very poorly developed in the Baradwar sub-basin. The Tarenga Formation consists dominantly of silty to very fine mudstone with minor calcareous, cherty and dolomitic beds. The Formation is divisible into three members, i.e., the Kusmi, Dagauri and Belha, from bottom upward in the Hirri sub-basin. The Hirri Formation consists dominantly of grey black dolomite and black shale. It is stromatolitic and gypsiferous at places. Maniari Formation is the youngest formation of the Chhattisgarh Supergroup and consists of gypsiferous purple to pink shale and argillaceous dolomite.

2.6 BASIC INTRUSIVES

The Chhattisgarh basin records intrusions of basic dykes spanning over 1000 Ma; the oldest is in the Calymmian (1.64 Ma, Rb-Sr internal isochron age) and the youngest corresponds to Danian (Deccan volcanism~65 Ma). The younger intrusives penetrated the Chandarpur or the Raipur Group of rocks in various parts of the basin. The dolerite dyke at Mahrum, in the southern margin of the Hirri sub-basin (Mukherjee and Ray 2010) intrudes the Chandarpur sandstone and is associated with faults and quartz vein. Dhanagarh and Karrakot dykes intrude the Chandarpur Group and the Maniari Formation, whereas the dyke at Raipur and Janjgir cuts the Chandi Formation. A 100 m wide N–S running intrusive dolerite has also been found along Nala section of village Bhalmar (Dungri, Orissa) within the siltstone /sandstone of Chandarpur Group. A diabasic intrusive in Bandhalimal near the south western margin of the Singhora basin has been dated at 1421 ± 23 Ma (Das et al. 2011). Dolerite dyke is also reported from Damdama area, which is intrusive into the basement and overlying sediments of Chandarpur Group, yielded Rb-Sr internal isochron age of 1641 ± 120 Ma (Pandey et al., 2012). It is oldest age of basic intrusive rock in Chhattisgarh basin.

CHAPTER 3

LOCAL GEOLOGY

The study area is part of Singhora Protobasin that lies SE of main Chhattisgarh Basin and comprises mainly rocks of Singhora Group. The rocks of Singhora Group covers an area of 1000 sq km with about 400 m thickness of sediments and developed in embryonic proto basin (Das et al. 1992). The rocks of Singhora Group in the study area overlie the Sambalpur granite of Lower Proterozoic age (~2380± 44 Ma, Chaudhary et al. 1996) having nonconformable contact and divided into four Formations, viz. Rehatikhol Formation (Conglomerate, arenite, shale, porcellanite/chert), Saraipali Formation. (Shale, limestone, porcellanite), Bhalukona Formation (quartz arenite, glauconitic sandstone) and Chuipali Formation. (Shale, limestone, porcellanite). Faulted contact between basal Rehatikhol Formation and underlying basement rock was also noted at some places (near Rehatikhol). Rocks of Chandarpur Group and Chuipali Formation of Singhora group are not present in the detail map area of project but these has been covered under reconnaissance survey (Figure 3.1).

Basement granite mostly forms low lying land and mostly soil covered while rocks of Singhora Group forms escarpment, cuesta, plateau and hogback topography following high RL contours. Detailed radiometric survey, geological mapping (1:10,000), geochemical sampling and ground checking of heliborne survey data has been carried out over 55 sq km for this project along with reconnaissance survey and geological mapping (1:25000) over 385 sq km in adjacent area. The rocks of Singhora group are affected by number of reactivated basement faults and fractures resulting repetitive sequence of Formations. Polymetallic sulphides, uranium and fluorite mineralisation are observed in Singhora group of rocks as well basement rocks. Detailed description about these is mentioned in further chapters. Apart from these, rocks of economic and petrological importance are mapped and investigated.

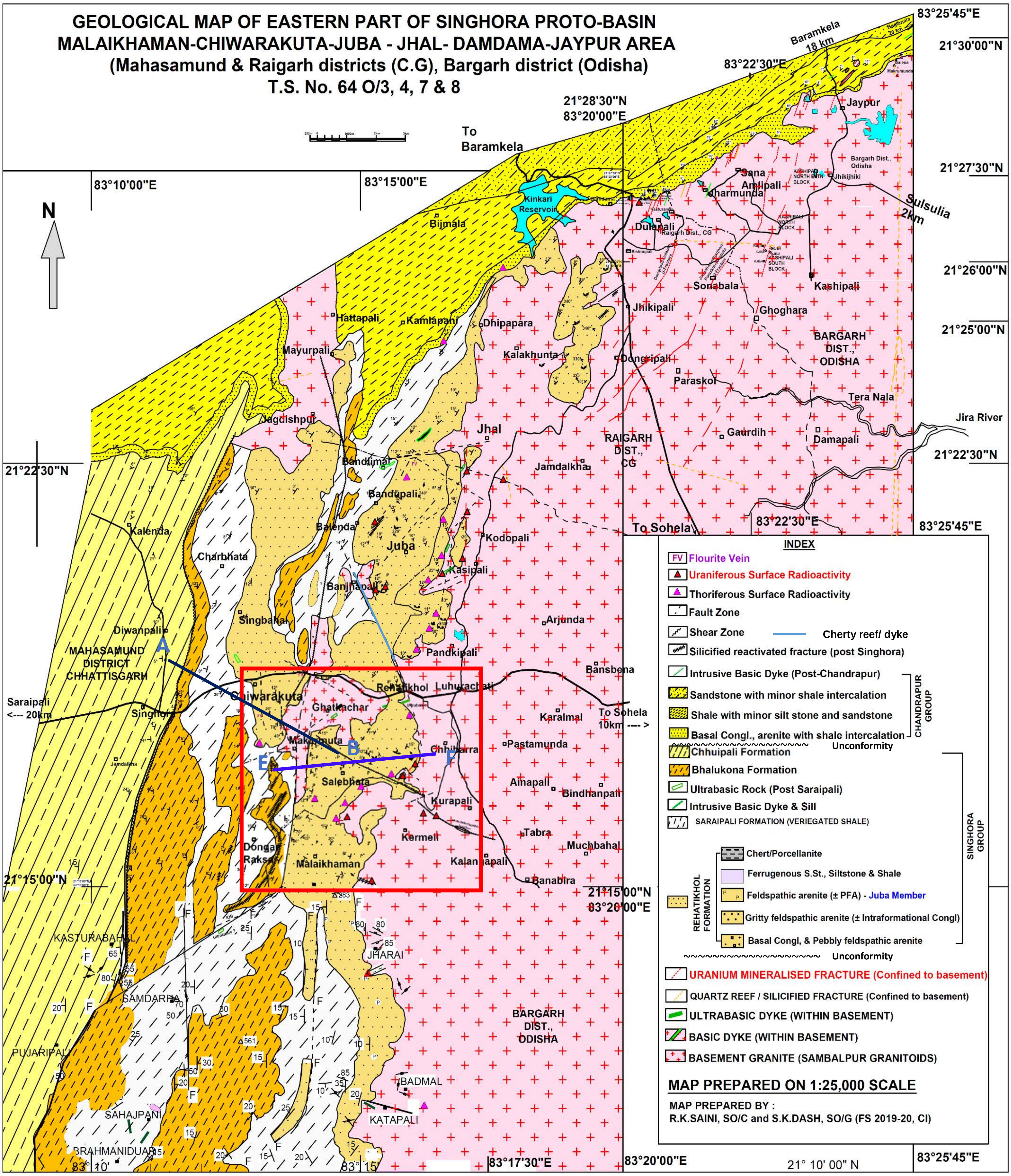

Figure 3.1 Geological map of eastern part of Singhora basin showing study area of project (mapped on 1:25000 scale FS 2019-20).

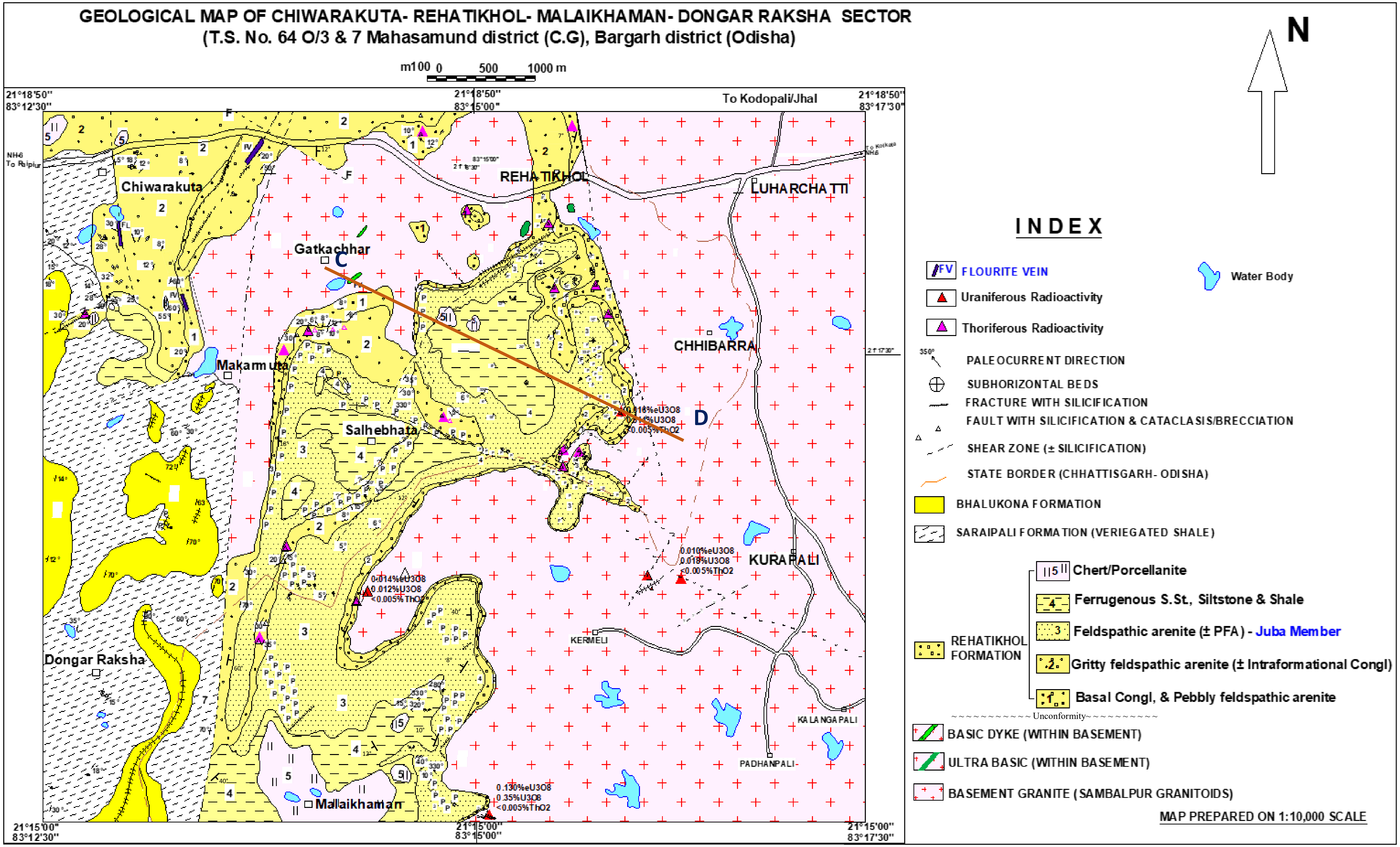

Figure 3.2 Detailed geological map of study area covering Chiwarakuta- Rehatikhol- Malaikhaman- Rehatikhol sector (mapped on 1:10000 scale).

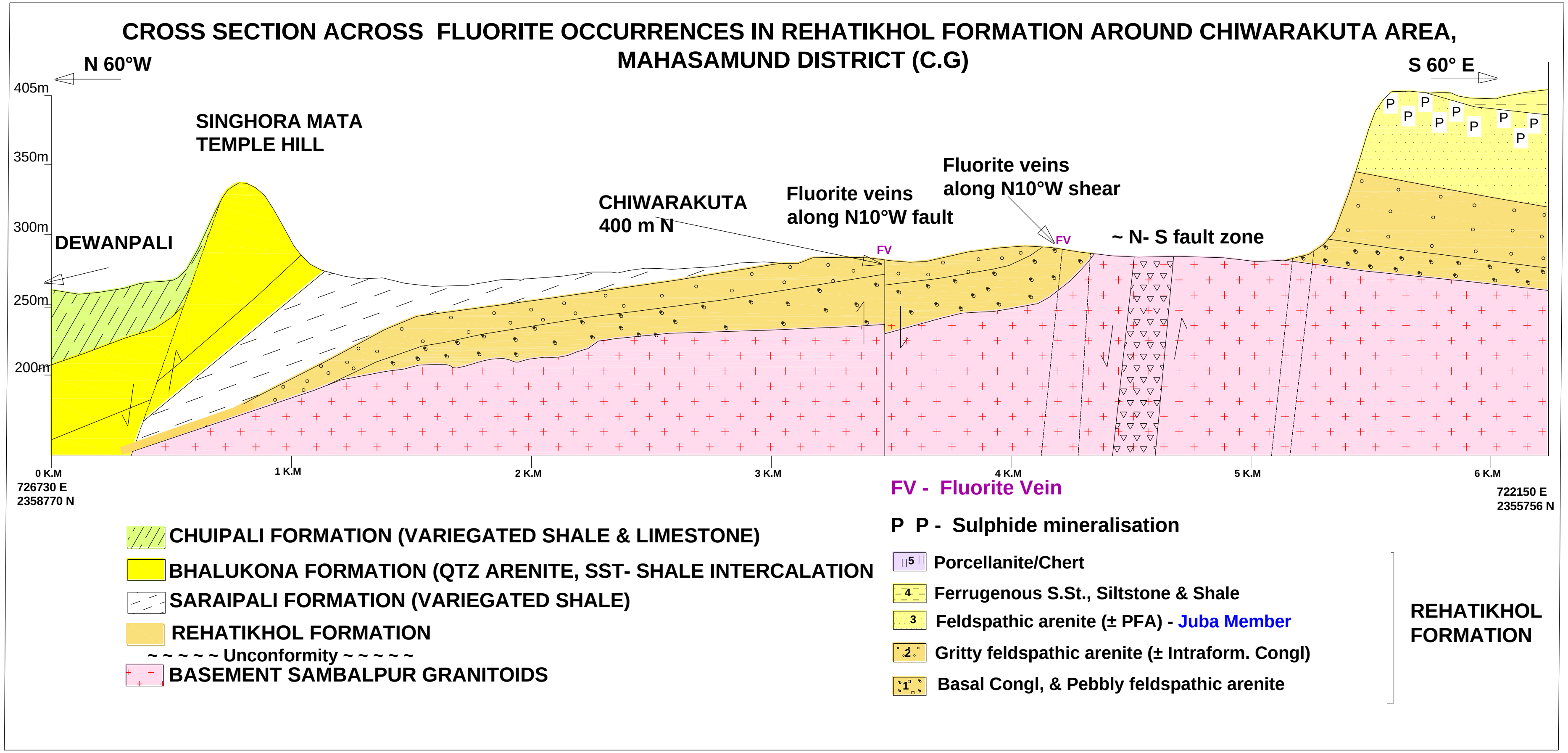

Figure 3.3 Cross section depicting lithostructural setup across fluorite occurrences in Chiwarakuta area. (Section line A-B in Figure 3.1)

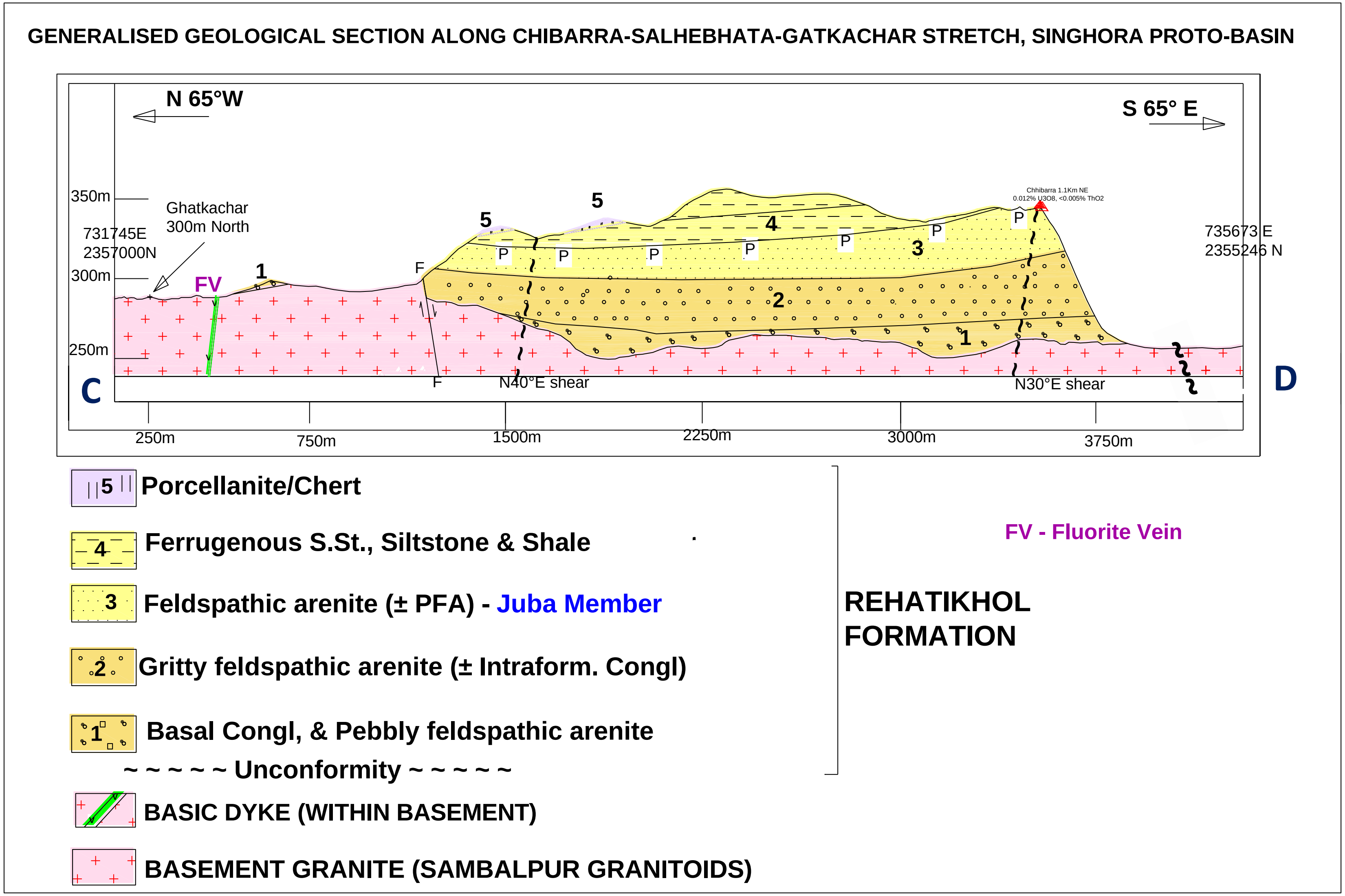

Figure 3.4 Cross section across Chhibarra anomaly and Gatkachhar fluorite mineralisation. (Refer section line C- D from Figure 3.2)

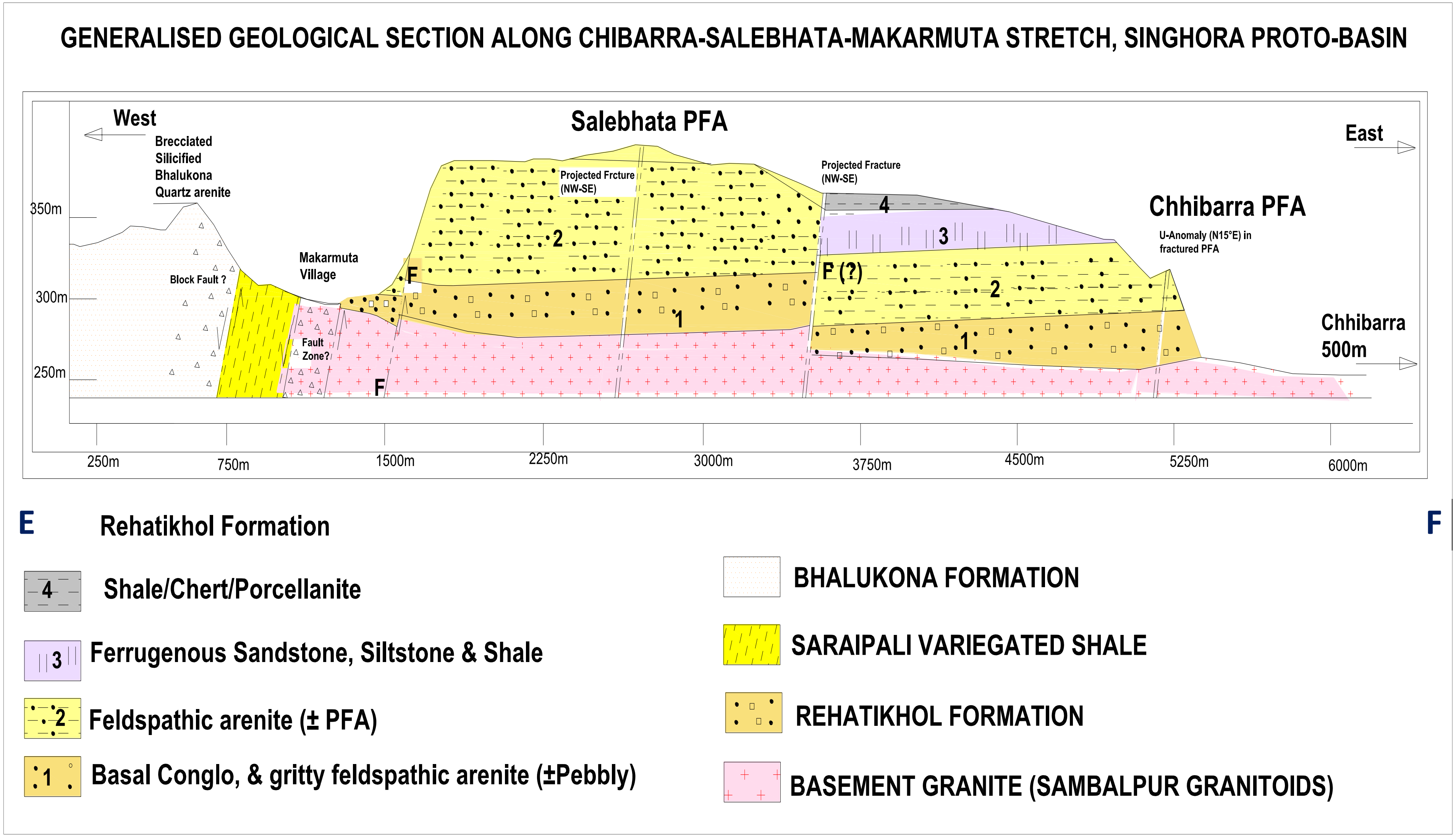

Figure 3.5 Generalised geological cross section along Makarmuta- Salhebhata- Chhibarra tract (along E- F section line in Figure 3.1).

Figure 3.6 Pink porphyritic granite having K- feldspar as phenocryst, SE of Murmuri chowk.

Figure 3.7 Leucocratic bt granitoid in NW of Chhibarra. (Plg >K- feldspar).

Figure 3.8 Medium grained leucocratic granite of Banabira (less biotite).

Figure 3.9 Thick granitic regolith (below yellow line) at nonconformity below thin polymictic cobbly conglomerate, Kermeli.

Figure 3.10 Feldspathic veins in basement granitoid at SE of Gatkachhar.

Figure 3.11 Epidote veins cutting gneissosity of granite gneiss, Kermeli

Cross sections of Chiwarakuta-Chhibarra-Salhebhata- Malaikhaman sector

Geological cross sections are prepared along the section lines marked on the regional as well detailed geological map (Figure 3.1 and Fig 3.2). From east to west in section line (A-B), cross section (Figure 3.3) depicts sequence of Rehatikhol Formation affected by ~N- S faults resulting local dip reversal, further west a major N- S fault zone in basement followed by sheared contact (N350°) of Rehatikhol formation and basement granitoids is present. Further west, fluorite mineralisation encountered in a shear zone parallel to it. Further west, a parallel fault with minor throw having fluorite mineralisation in gritty feldspathic arenite observed followed by Saraipali Shale- Bhalukona quartz arenite and Chuipali shale towards west.

Cross section (Figure 3.4) depicts from east to west (along C-D section line)- basement Sambalapur granitoid having unconformable contact with Rehatikhol Formation affected by basin marginal fault- further west again basement exposed as inlier around Gatkachhar having fluorite mineralisation at the contact of basic intrusive. Uraniferous Chhibarra anomaly is present along NNE trending fracture zone in the section line.

A generalised geological cross section has been prepared along E-F section line (along Chhibarra- Salhebhata- Makarmuta stretch) (Figure 3.5). Cross section demonstrates sediments of Rehatikhol Formation overlying basement granitoids, presence of post-depositional faults/fractures, PFA with sulphide bleeding at Chhibarra and Salebhata along faults/fractures, granite inlier near Makarmuta (interpreted as a tectonic inlier than a basement high), block faulting west of Makarmuta, wherein Saraipali shale with Bhalukona Formation is juxtaposed against granites with complete absence of Rehatikhol Formation. A down-thrown western block with more than 100m is expected/inferred west of Makarmuta/east of Dongar Raksha villages, as upper part of Saraipali/Lower Bhalukona Formation is juxtaposed with granites.

The local geological set-up is summarized below.

3.1 BASEMENT ROCKS

3.1.1 Sambalpur Granitoid

Sambalpur Granitoids form the basement for the sediments of Singhora Group with varying mineralogical composition as observed megascopically, which includes pink porphyritic granites (Figure 3.6), grey biotite granite (Figure 3.7) and medium grained leucocratic granitoid (Figure 3.8). The basement granitoid is coarse grained pink feldspar dominated porphyritic granite at the periphery of Murmuri outlier and Pandkipali.

The basement granites of Jhal- Kasipali- Chhibarra-Kurapali area (dominantly pink porphyritic granite/ grey granite and medium grained leucogranites) are distinctly different from those of Dulapali- Amlipali- Jaypur area (two mica granite and leucogranites). These granites are reported to contain high intrinsic uranium values and is also noted at some places with high background radioactivity, especially in the SE part. Mostly, basement granitoid is soil covered and forms peneplain land with low RL contours. Presence of thick regolith has been observed at west of Kermeli indicating prolonged weathering and basement low during the deposition (Figure 3.9). Mafic xenoliths are also observed in porphyritic granite near Rehatikhol village. Basement is traversed by quartz reef, feldspathic veins (Figure 3.10), quartzo feldspathic injections, mafic dykes and pegmatites with large crystal of K feldspar. Pervasive epidotitisation with thin epidote veins are observed at many places. Patches of older granite gneiss belonging to EGMB (?) are located at west of Kermeli. Epidote veins cutting across gneissosity are noted in these gneisses (Figure 3.11).

Inliers of basement granite are observed at Makarmuta- Gatkachhar- Murmuri, Juba-Banjhapali and Jagdishpur- Mayurpali areas occurring as faulted/tectonic inliers. Capping of Rehatikhol sediments are also seen over the inliers at Gatkachhar and Murmuri as outliers. The granites in Juba – Banjhapali inliers are mostly pink granite / pink porphyritic granite showing chloritisation, indicating hydrothermal activity. These granitoids are intruded by basic rocks near Gatkachhar and by garnet bearing ultrabasic rocks near Rehatikhol.

3.2 SINGHORA GROUP

There are four Formation in Singhora Group but three Formation are only exposed in study area (Figure 3.12). Field observation of these Formations are as follow-

3.2.1 Rehatikhol Formation

Rehatikhol Formation of Singhora Group is having a nonconformity contact with basement granites with a basal polymictic conglomerate horizon along unconformity. At some places, faulted contact is also seen at Gatkachhar, west of Kasipali, Kodopali & Burha Dongar, resulting in presence of tectonic outliers at these places.

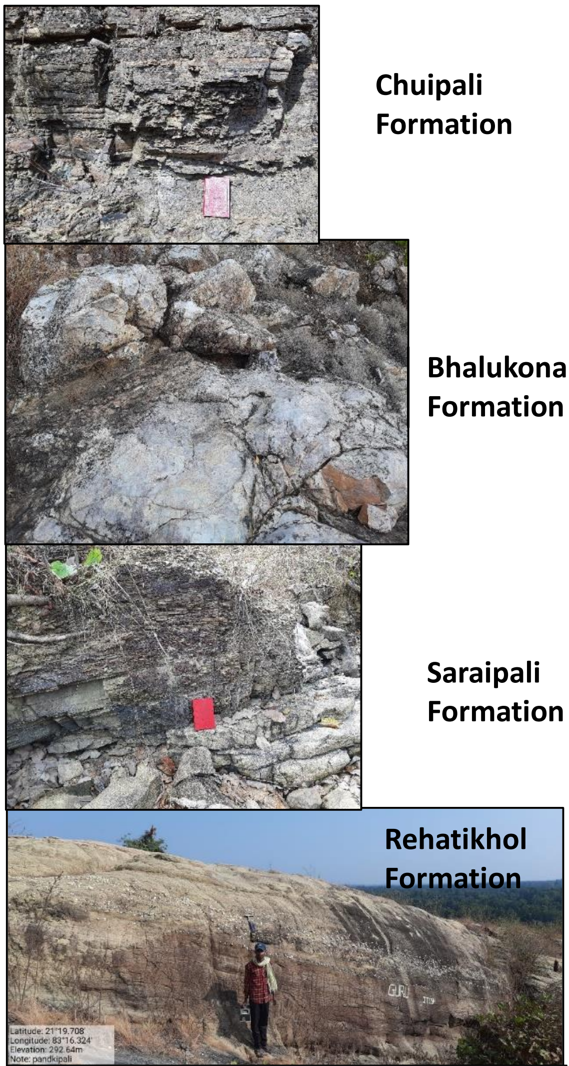

Figure 3.12 Generalised photo litholog of Singhora Group’s Formations.

Rehatikhol Formation is classified into 5 lithounits based on grain size variation, mineralogical composition and sedimentological aspects, and are briefly described below.

(a) Basal Polymictic Conglomerate : Polymictic basal conglomerate of Rehatikhol Formation lies just above the nonconformity plane and comprises granule to pebble size sub-rounded clasts and at some places cobble size set in arkosic (coarse grained even granule sized)

Figure 3.13 Basal polymictic conglomerate at Rehatikhol.

Figure 3.14 Clast of granite, chert and quartz in basal polymictic conglomerate at Rehatikhol.

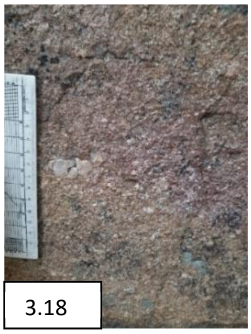

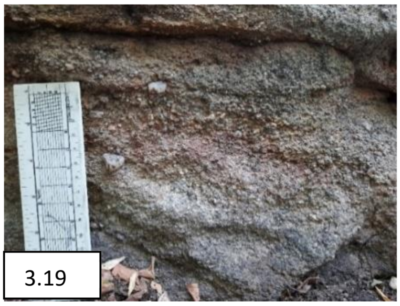

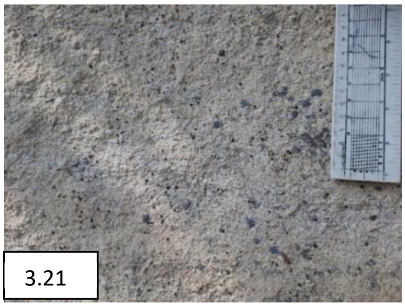

Figure 3.15 Clast supported diamictic conglomerate at Murmuri outlier.

Figure 3.16 Oligomictic conglomerate having feldspathic arenitic matrix in upper sequence of Rehatikhol Formation, SW of Chhibarra.

Figure 3.17 Fining upward sequence from conglomerate to pebbly arenite, SW of Chhibarra.

Figure 3.18 Pebbly feldspathic arenite/ sandstone near NW of Chhibarra.

Figure 3.19 Grain size variation in pebbly/ gritty feldspathic arenite, SE of Murmuri.

Figure 3.20 Pebbly arenite intercalation in feldspathic arenite, SW of Chhibarra.

Figure 3.21 Feldspathic arenite, SW of Chhibarra.

Figure 3.22 Liesegang ring structure in feldspathic arenite/ sandstone, SE of Murmuri chowk.

Figure 3.23 Sulphide bleeding along minor fractures in PFA near Malaikhaman.

Figure 3.24 General texture of PFA and pyrite wrapped around the rounded grains of PFA (NE of Salhebhata).

Figure 3.25 Ferruginous glassy vein intruded in fractured PFA (500 m NW of Salhebhata)

Figure 3.26 Ferrugenious medium grained sandstone, SW of Salhebhata.

Figure 3.27 Banded porcellanite of Rehatikhol Formation near Chiwarakuta.

Figure 3.28 Megaripples showing paleocurrent direction towards NW in feldspathic arenite (south of Rehatikhol)

Figure 3.29 Asymmetric megaripples in feldspathic sandstone showing N350º paleocurrent direction, N of Salhebhata

Figure 3.30 Reverse graded bedding in pebbly sandstone (south of Gatkachhar) matrix (Figure 3.13). The clasts are mainly composed of quartz, lith-fragments of quartzite/ quartz arenite, granite, minor chert set in gritty matrix of quartz, altered and non-altered feldspar (Figure 3.14). These beds are mostly matrix supported conglomerate except few beds of clast supported in upper portion. The basal conglomerate is not exposed all along and at many places upper sequence directly lies in contact with basement. The thickness of this lithounit varies along the basin margin (few meters to more than 10 m).The conglomerate of Rehatikhol Formation occurs as a repetitive sequence along with pebbly to gritty sandstone/ arenite in the NW part of Chhibarra and Pandkipali, Kasipali- Kodopali area. This lithounit is affected by joint and fractures, due to basin margin fractures/ faults, hence occur mostly as rolled boulders and fractured outcrops. Many diamictic to oligomictic conglomerate horizon also present at different levels in basal part of Rehatikhol formation (Figure 3.15 & 3.16). These beds show fining upward sequence (Figure 3.17) dominantly having fluviatile origin and deposited in alluvial fan environment as debris flows. This unit is not exposed throughout the contact and is best seen at west of Chhibarra, near Malaikhaman, Ghatkachar and Rehatikhol.

(b) Gritty/ pebbly feldspathic arenite: This lithounit occurs as intercalation within conglomerate in the basal part but in upper sequence it has a significant thickness of 5 – 20 m thickness. It consists mainly coarse to granule sized subangular quartz, feldspar (pebbly at places) as observed megascopically (Figure 3.18). Many feldspar grains are epidotised and also show kaolinisation (?). Repetitive fining upward sequence has been observed in the above lithology.

There is gradational contact with lower member and upper member. This unit shows significant grain size variation with graded bedding (Figure 3.19). This lithounit occurs as low dipping cover rock having escarpment faces, highly jointed and fractured near basin margin and along other major fractures. Oligo/diamictic conglomerate horizon is present at different levels having well rounded recycled vein quartz in arenitic matrix (Figure 3.20). At some places asymmetric megaripples were observed showing NNW paleocurrent direction. Lenticular bedding with lenses of shale was seen at Singhbhal area. These beds also appear to be of fluviatile origin. Thickness varies from few meters to more than 20 meters. This unit is well exposed and attains maximum thickness at Makarmuta while minimum thickness at Kermeli-Malaikhaman.

(c) Feldspathic arenite ±Pyritiferous feldspathic arenite (FA±PFA): The pebbly feldspathic arenite sequence is overlain by this lithounit and consists of medium grained sub-rounded quartz, altered and non-altered feldspar (Figure 3.21). It is very hard, compact and occurs as very low dipping (nearly horizontal) containing some occasional intercalation of oligomictic conglomerate layers. At some places liesegang ring structure also observed indicating authigenic precipitation during diagenesis (Figure 3.22). This is the thickest unit of Rehatikhol Formation and designated as Juba Member by Sinha et al, 1995 with the presence of pyritiferous feldspathic arenite as bed. Due to presence of diagenetic pyrite, which is between 2-5%, often reaching 10% at places, this pyrite bearing layer of feldspathic arenite is known/designated as PFA layer by Sinha et al, 1995. Significant sulphide mineralisation along with moderate to high radioactivity observed at Juba, Banjhapali and Chhibarra, where this lithounit is intensively fractured and having diffused quartz grains (smoky quartz also) along with both altered and non-altered feldspar. Megascopically, sulphides can be identified as disseminated pyrite dominantly along with galena and chalcopyrite (?). Sulphides are mostly diagenetic in PFA but epigenetic addition also seen in the vicinity of fractures/faults/shears.

In PFA, sulphides occur as disseminations, along veins and as sulphide bleeding on bleached outcrops (Figure 3.23). Sulphides can be identified as disseminated pyrite dominantly along with minor galena, bornite and chalcopyrite (Juba and Chhibarra). Sulphides also have been seen wrapped around the rounded quartz–feldspar grain and in intergranular spaces (Figure 3.24). The sulphide content in PFA increase significantly as lithounit seems to be more jointed and fractured along with silica veins. Feldspar gives reddish tinge on oxidation and adsorption of Fe when PFA oxidise. Some ferruginous glassy veins also observed to be intruded in feldspathic arenite near Salhebhata (Figure 3.25). These veins possibly contributed Fe in PFA for epigenetic pyrite and silica overgrowth causing diffused quartz grains. Minor/thin micaceous siltstone bands are present within this lithounit.

At upper levels, it grades into medium grained ferruginous sandstone with subrounded quartz grain and with thin shale intercalation in between (Figure 3.26) at N of Salhebhata and East of Makarmuta. Superimposed ripples and planer cross bedding have been observed near N of Salhebhata. Asymmetrical mega ripples/ anti dunes also observed in feldspathic arenite. These beds also have been deposited in fluvial system.

(d) Shale – siltstone - ferrugenious sandstone: Light green colored shale and deep red colored siltstone sequence occurs above the feldspathic arenite of Rehatikhol Formation. These also forms very low dipping thin sequence and intercalated by thin layers of porcellanite/ chert. Iron oxide coating is observed along and across the fissility plane in shale. Fine to medium grained, deep red colored ferruginous sandstone lies above the shale-siltstone (Figure 3.26). Pebbly horizon marks initiation of this sequence. It consists of well-rounded to rounded medium grained quartz, altered feldspar grain set in ferruginous matrix. Superimposed ripple marks was observed in ferruginous siltstone in rolled boulders near Salhebhata. Fine grained, deep red colored ferruginous sandstone lies above the shale –siltstone. It is best exposed around Salhebhata- Malaikhaman tract.

(e) Porcellanite: Dark grey coloured glassy band of porcellanite occurs at top of Rehatikhol Formation having minor intercalation of clayey tuffaceous matter and shale (Figure 3.27). These are indication of acidic volcanic activity in Singhora basin and very important in the view of U mineralisation. Thickness of these beds varies from few meters to 10 meters. Pyrite is associated with porcellanite in Chiwarakuta area.

The total thickness of Rehatikhol sediments vary between 60-120m in southern and central part, whereas it becomes progressively less in northern part. All lithounits are not developed/exposed throughout eastern margin, but best developed in Chhibarra-Salebhata-Makarmuta stretch and Jhal- Balenda stretch. Thickness of basal units of Rehatikhol formation (polymictic conglomerate and gritty feldspathic arenite) is less (15- 20m) around Kermeli-Malaikhaman tract. Juba member (PFA) directly overlies the basement rock at some places (Malaikhaman to Kermeli foot track).

Sedimentary Structures in Rehatikhol Formation

Major sedimentary structures are mainly megaripples (Figure 3.28 & 3.29), graded bedding and cross beds. Paleocurrent data also has been taken from these structures. Reverse graded bedding in pebbly intercalation in Gritty feldspathic arenite also observed at many places (Figure 3.30). Although lithounits are highly affected by 3 – 4 major fractures trends, hence proper outcrop for sedimentological studies are not available and whatever outcrop present that have altered data due to deformation. Therefore data has been taken on the less disturbed outcrops. Most of the paleocurrent data lies towards NNW or NW direction with an average NW paleocurrent direction. The general trends of beds in the study area towards NNE (avg N15^0 E) diping towards NW direction with 8^0 to 15^0 dip amount. Sedimentary log of the Rehatikhol Formation incorporating all 5 lithounits has been prepared based on the detailed mapping in the Rehatikhol- Chhibarra area (Figure 3.31). Overall sequence shows fining upward in addition to localized coarsening sequence as a result of reverse graded bedding in the basal portion. Based on the characteristics of lithounits and sedimentary log, fluviatile depositional environment for the basal portion and marginal marine depositional environment (near shore beach to deltaic) for the upper portion can be inferred.

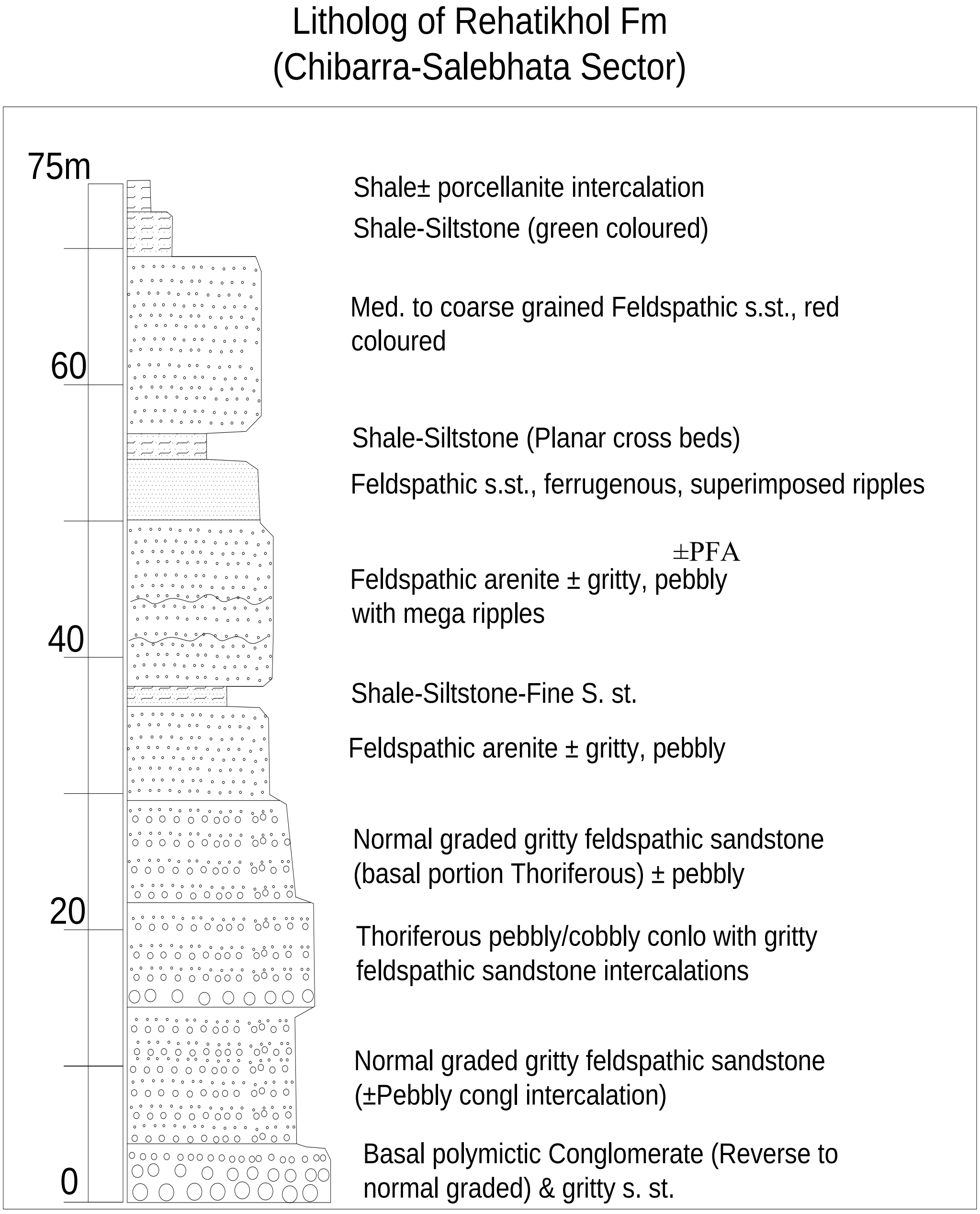

Figure 3.31 Generalised sedimentary litholog of Chhibarra- Salhebhata sector.

Paleocurrent analysis

Paleocurrent analysis in the Juba N sector: Major sedimentary structures in above sector are mainly megaripples, graded bedding and cross beds. Paleocurrent data has been taken mostly on the asymmetric megaripples (90%) coupled with few data from cross beds. Although lithounits are highly affected by 3 – 4 major fractures trends, hence proper outcrop for sedimentological studies are not available and whatever outcrop present that have altered data due to deformation. So data has been taken on the less disturbed few outcrops. Further data has been plotted on Rose diagram (Figure 3.32) with significant population of data. Most of the paleocurrent data lies towards NNW or NW direction with an average NNW paleocurrent direction (N328^{o}). It indicates that sediments have been transported from bevelled basement highland situated in SSE direction of sector. Dispersion in data is in the range of ~50^{o} angle that is less and indicate accuracy of data and consistency of paleocurrent direction.

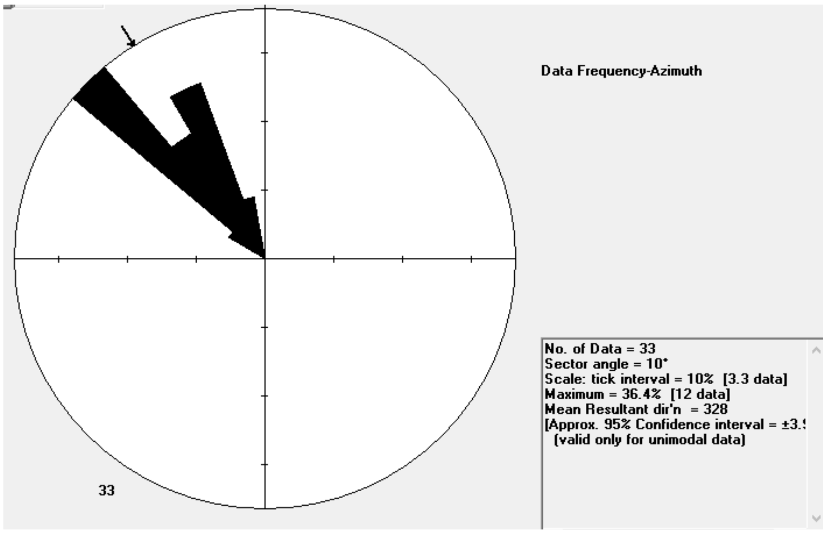

Figure 3.32 Rose diagram of paleocurrent data from N of Juba

Paleocurrent analysis in the Malaikhaman- Salhebhata sector

Paleocurrent data also taken from the megaripples present in the upper portion of feldspathic arenite (± PFA) member in the southern part of study area i.e. Malaikhaman- Salhebhata sector. Rose diagram of these data shows unimodal unidirectional paleocurrent direction towards NW (avg direction N 314^{o}). Dispersion in the data is slightly more than Juba N sector indicating more fluctuation in paleocurrent direction/ shift in the channels (Figure3.33).

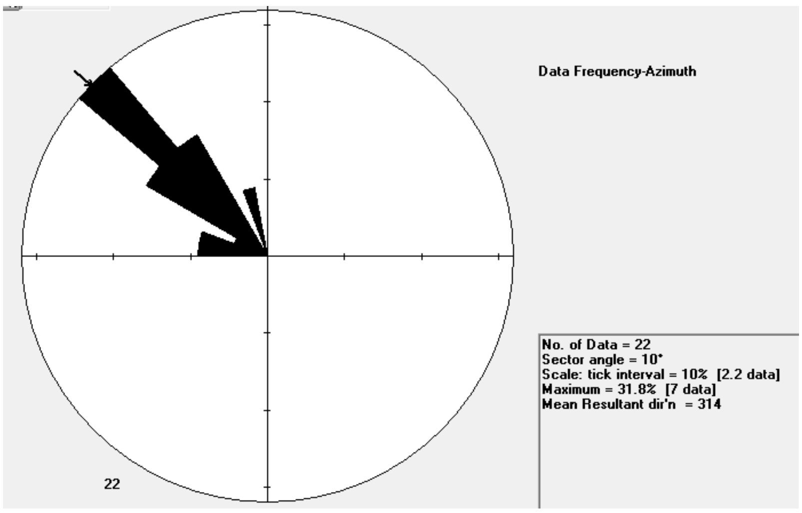

Figure 3.33 Rose diagram of paleocurrent data in Malaikhaman- Salhebhata sector.

Integrated rose diagram for both sector

Rose diagram prepared (Figure 3.34) for all the paleocurrent data in assigned area infers unimodal NW paleocurrent direction (avg N 323°). Data is taken mostly from feldspathic arenite member from asymmetric megaripples/ dunes. Paleocurrent analysis infers alluvial depositional environment for the basal portion of Rehatikhol Formation. Most of the data are taken from feldspathic arenite member of Rehatikhol Formation.

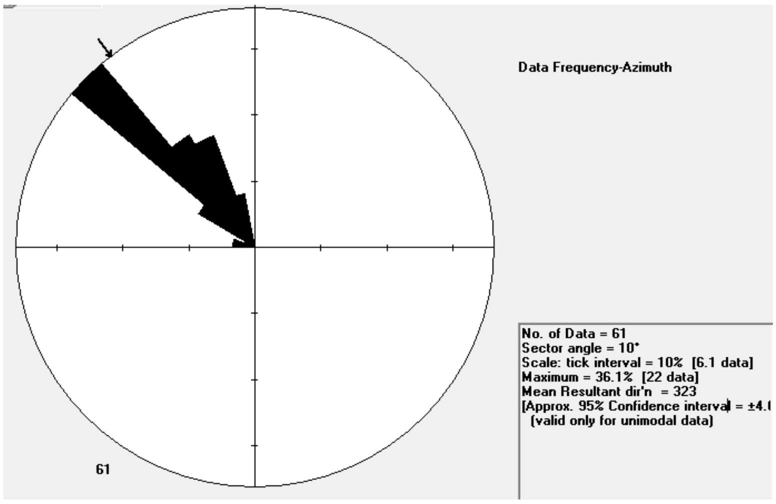

Figure 3.34 Rose diagram of paleocurrent data of Rehatikhol Formation, Malaikhaman- Salhebhata- Juba N sector.

3.2.2 Saraipali Formation

It comprises argillaceous rocks (shale) with porcellanite and minor limestone. Saraipali shale is found to be gradational with Rehatikhol Formation at most of the places. The shale-porcellanite horizon and/or shale-siltstone-fine sandstone horizon which marks the upper part of Rehatikhol Formation grades to dominant variegated gentle dipping purple shale of Saraipali Formation at all places. In fact it is difficult to exactly demarcate the boundary between upper Rehatikhol shale and Saraipali shale and the contacts are marked and plotted based on dominance of shale and appearance of purple shale as that of Saraipali Formation.

Because of block faulting (?), Saraipali shales are juxtaposed with basement granite at west of Makarmuta area, where the former is deformed, highly crumbled and crenulated along the fault zone and show ferrugenisation and silicification. It has intercalation of ferruginous sandstone/ siltstones as seen at Chiwarkuta road cutting, where it shows steep dip & drag folds due to faulting. Shale-siltstone of Saraipali Formation is calcareous in nature as seen SE of Dongar Raksha. Carbonate rock has been observed just adjacent to brecciated silicified zone at ~1 km SE of Dongar Raksha village near waterfall on Dongar Raksha-Malaikhaman forest foot path. Perforated surface with many cavities has been developed on the whole outcrop and it comprises coarse grained calcite grains. It could be limestone of Saraipali formation, juxtaposed with Bhalukona Formation with faulted contact. The Saraipali shale which are otherwise a gentle westward dipping horizon, is often seen to possess steep dip due to post-sedimentation faults, observed at many places, best exemplified along Raksha- Malaikhaman tract. The upper part of Saraipali Formation possibly contains shale-arenite intercalation which progressively/gradationally becomes dominantly arenite of Bhalukona Formation.

3.2.3 Bhalukona Formation

This Formation comprises mainly quartz arenite, siltstone with minor shale intercalation. Bhalukona arenites are occupying the top contours of south of Malaikhaman, east of Sargunabhata- Brahmanidwar stretch and are gradational with Saraipali shale. Occasional sulphide mineralisation and ferrugenisation was seen where this lithounit is jointed and fractured. Makarmuta-Raksha ridge with Bhalukona Formation (?) is truncated in the south by a NE-SW trending ferruginous breccia zone, near Sargunabhata village. This zone is with high iron content with brecciated fragments of chert, arenite. Yellow ochre has developed on weathered surface at places. Bhalukona rocks are also exposed along shear zone at ridge on which Singhora Mata Temple is located. Bhalukona sediments represent deposition under beach/ upper shore face environment condition.

3.2.4 Chuipali Formation: Chuipali Formation consists mainly of shale and stromatolitic limestone that are exposed west of Singhora Temple hill. During traverse from Dewanpali-Dongripali to Singhbhal dam, the Chuipali shale found to trending nearly E- W and dipping towards south. It is light green coloured shale having structural contact with rocks of Bhalukona quartz arenite at Singhora Temple hill. Chuipali sediments represent deposition under marine shelf condition. Rehatikhol sediments are studied in detailed compare to Bhalukona and Chuipali Formations.

3.3 CHANDARPUR GROUP

In the northern part of study area, Chandarpur Group of rocks are exposed from Kinkari reservoir-Damdama-Jaypur stretch and further east and north of it. In Damdama-Jaypur stretch, Chandarpur Group sediments directly overlie basement Sambalpur granitoids with a nonconformity contact, marked by a polymictic thoriferous conglomerate layer. It is followed upward by arenites, arenite-shale, shale, shale-siltstone-sandstone, sandstone units together constituting the Chandarpur Group of Chhattisgarh Supergroup. The lithounits show NE-SW to ENE-WSW strike with gentle (5-8°) dips towards NW in general.

3.4 STRUCTURE

Systematic collection of structural data, which includes attitude of primary sedimentary structures, secondary structures viz. joints, fracture/fault trends were collected and the data interpreted. The litho- contacts and structural data are plotted on 1:10000 scale (Figure 3.2). Major structural grain in the area is NNE-SSW, mostly present in basement rocks as fracture zones. The basin has also this trend, so also the strike of lithounits at most places follow this trend. Reactivation of these basement fractures are evident in Singhora sediments, as prominent fractures, joints and shear zones. Apart from this dominant structural grain, NW-SE, NE-SW and E-W fractures/ joints are also recorded. It is commonly observed that mostly NNE-SSW trend structures are mineralized (U with sulphides), although association of U mineralisation cannot be ruled out for NW-SE and NE-SW fractures that are mostly associated with silicification.

Major structural grain in Salhebhata- Makarmuta- Chhibarra- Rehatikhol area is ~N-S trending dominant fractures along with NW-SE, NE-SW joints/silicified fractures also. Several faults/fractures were identified in southern part of study area i.e. Makarmuta- Raksha- Chhibarra- Chiwarakuta area. N035º trending intermittently uranium mineralised shear zone identified at 1.5 km SW of Chhibarra village where elongated grain and development of foliation having silicification has been observed. Another major shear zone identified at south of Kurapali Village in basement granitoid trending N320º where S-C fabric in granite mylonites have been developed due to sinistral shearing (Figure 3.35). This shear zone extending into basement below the sediments of Rehatikhol Formation and also reactivated that is evident by the intense silica veining and faulting/ fracturing in same trend at N of Salhebhata. Sulphide mineralisation is also present along this fault/ fracture in feldspathic arenite/ sandstone.

Stretched pebbles also noted in pebbly layers in PFA in the continuity of this shear zone at NW of Salhebhata (Figure 3.36). NE trending fractures are very prominent in Rehatikhol sediments around Salhebhata- Chhibarra sector. Presence of slickensides alone NNE trending fault in PFA also noted at west of Chhibarra. NE trending silicified fracture with comb structure observed at N of Malaikhaman (Figure 3.37). In addition, it was observed that rocks of Rehatikhol Formation are traversed by ~N- S silica veins, having escarpment face between Makarmuta and Salhebhata gives an indication of presence of fault. Further study in that area clear about presence of N-S trending fault along which rocks of Saraipali formation (shale) are juxtaposed with basement granite which in turn is juxtaposed with Bhalukona Formation with intense deformation near Makarmuta village. Various clear cut evidences of this major fault zone are noted in the field that are summarised in Figure 3.38- 3.42. Further SW, ferrugenised breccia zone of significant dimension located having trend towards NE direction (Figure 3.43).

Inter- relationship of fractures in Salhebhata- Makarmuta- Chhibarra sector:

Based on detailed studies, the inter-relationship of N-S, NE-SW and NW-SE fractures have been deduced in the sector. Some of the field photographs depicting the relationship is shown in Figure 3.44- 3.46. Based on field evidences/observation, mutual relation

	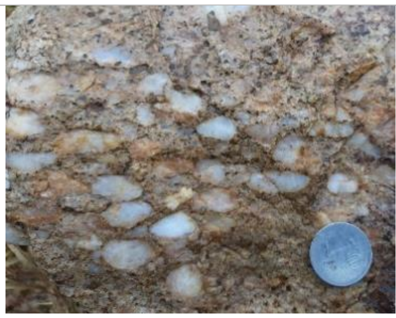	
Figure 3.35 S-C fabric in granite mylonites showing sinistral shear in NW trending shear zone (W of Kermeli).	Figure 3.36 Stretched pebbles in oligomictic conglomeratic intercalation in PFA, NW of Salhebhata.	Figure 3.37 Comb structure in quartz vein trending N030º N of Malaikhaman.

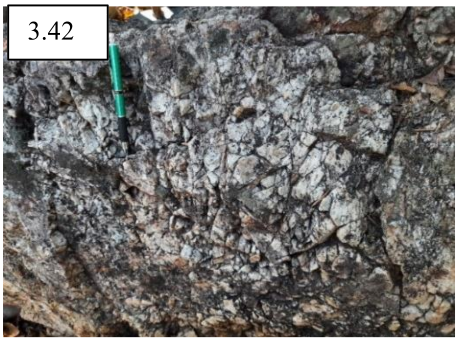

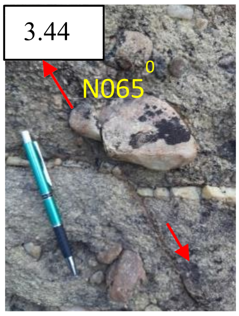

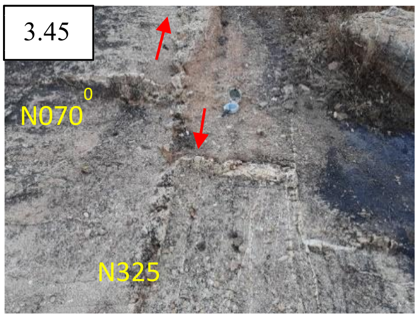

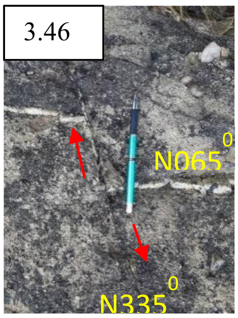

Figure 3.38 N- S trending silicification in gritty feldspathic sandstone adjacent to major N- S trending normal fault (S of Makarmuta).

Figure 3.39 Steeply dipping gritty feldspathic arenite towards E near N- S trending fault.

Figure 3.40 Nearly sub vertical gritty feldspathic arenite in the fault zone.

Figure 3.41 Drag folds and kink bend developed in shale of Saraipali formation near fault.

Figure 3.42 Breciation in quartz arenite in the fault zone.
Figure 3.43 Ferrugenised breccia from NE of Sargunabhata.
Figure 3.44 Displacement in N- S trending quartz vein and clast along N65º fault/ joint.
Figure 3.45 Displacement in N070º trending quartz vein along N325º fault plane traversed by quartz vein.
Figure 3.46 Displacement in N065º trending quartz vein along N335º fault/ joint plane. (Figure 3.54 to 3.56 are from 1.5 km NE of Makarmuta).
Figure 3.47 Sheared feldspathic sandstone having preferred orientated and elongated quartz grain. Trending N035º (~1.5 km NW of Chhibarra).

of dominant 3 sets of fractures (NW-SE, N-S and NE-SW) established in the Salhebhata-Makarmuta- Gatkachhar- Chhibarra sector. Field evidences show N-S is oldest, affected by NE-SW (younger) and NW-SE, often silicified (youngest). These evidences could be related to chronology of reactivation of theses fractures. Intensity of NE shearing can be seen as development of schistose rock from feldspathic arenite along it near Chhibarra (Figure 3.47).

3.4.1 Fracture Analysis: In the entire area covering basement rocks, Singhora sediments and overlying Chandarpur sediments, the fracture data is studied and summarized in Rose Diagram (Figure 3.48) below. Data has been collected mostly from sediments (>80%). It reveals that NNE-SSW (N20E-S20W) fractures are the dominant set in the area, followed by NE-SW (N40E-S40W). These two fracture sets are associated with intense ferrugenisation, chloritisation, silicification with evidences of shearing/ cataclasis and most importantly associated with uranium mineralisation, especially as observed in basement rocks and Chhibarra area.

NW-SE or NNW-SSE trending fractures are mostly occupied by quartz reef or are intensely silicified. Surface uranium mineralisation along this fracture is seen as spots/patches/zones east of Malaikhaman, near Banjhapali (?) barring which no significant uranium mineralisation could be observed associated with NNW-SSE fractures.

3.4.2 Joint Analysis: Rose diagram for more than 200 joints set data has been prepared as shown in Figure 3.49 which reflects presence of different sets, with dominance of NNE-SSW, N-S, NW-SE and E-W sets. Data has been collected mostly from sediments (>80%).

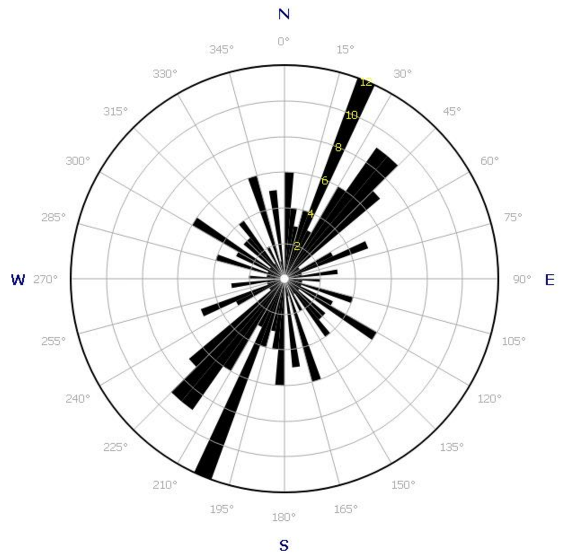

Figure 3.48 Rose diagram for fracture trends.

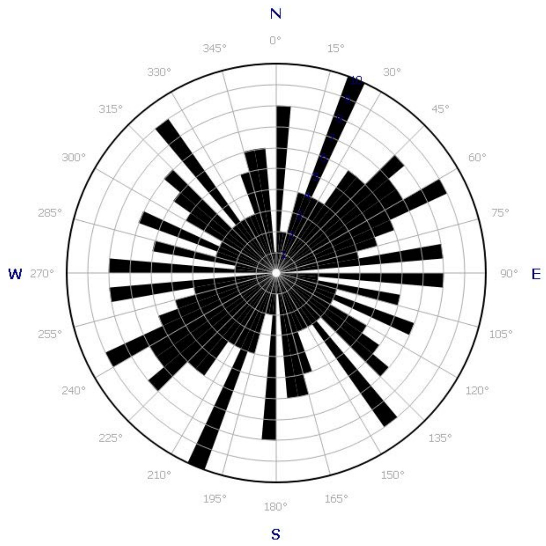

Figure 3.49 Rose diagram for joint

Rose diagrams for Chiwarakuta- Chhibarra- Malaikhaman sector

Rose diagram of fractures (Figure 3.50) shows predominance of NNE-SSW fracture trend along with WNW- ESE, NNW- SSE and NE-SW trends while rose diagram for joints (Figure 3.51) shows dispersed trends mainly in NNE- SSE, N- S, E- W, NE-SW and WNW-ESE trends.

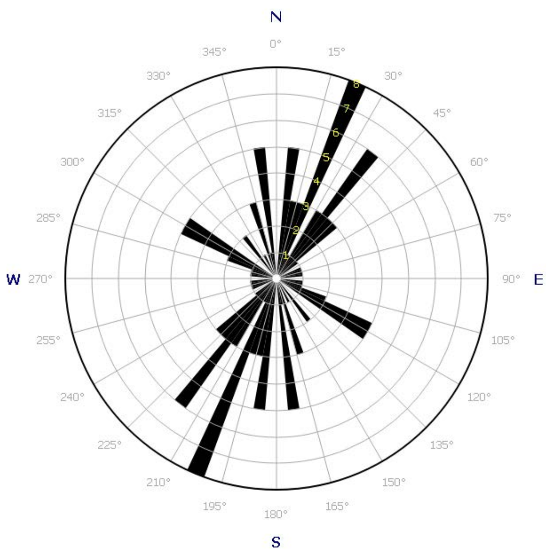

Figure 3.50 Rose diagram for fractures.

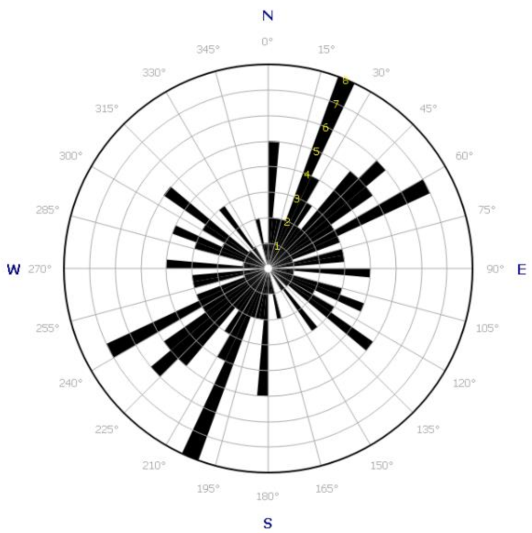

Figure 3.51 Rose diagram for joints.

CHAPTER 4
PETROMINERALOGICAL STUDIES

Petromineralogical studies of sedimentary rocks enables to ascertain mineralogical composition, grain size and textural characteristics, diagenetic aspects, classification and nomenclature. Composition of sediment has been used to determine relationships between tectonic setting and provenance (Dickinson and Suczek, 1979; Johnsson, 1993). Petromineralogical characteristics of basement igneous rocks gives information about petrogenesis, temperature, pressure and emplacement conditions of these rocks apart from compositional and classification aspects. Mineralogical composition of clastic sedimentary rocks are manifestations of provenance rocks. Sedimentary rocks encompasses the information about history of physical and chemical conditions prevailing at the time of their deposition.

Petromineralogical characteristics of sediments are reflection of provenance characteristics, weathering and climatic conditions, transportation processes, depositional environment, tectonic setting and diagenetic changes. Sedimentary rocks are an important source of information about previous orogenic conditions and may contain detritus that describes the evolution of orogenic settings (Johnsson, 1993). The most important factors noted by Johnsson (1993) are source rock composition, chemical weathering, abrasion, sorting during transportation and diagenesis. These factors are affected by three main interrelated components, namely tectonic setting, climate and the nature of the depositional system. Each of these factors affects the characteristics of the others, producing different clastic compositions. Petromineralogical study of any rock is a tool to characterize and classify the rock type and its tectonic provenance. As sediments are transported long distances from the source area, lithics become separated from relict quartz and are chemically broken down according to Goldich stability series. This results in quartz-rich sandstones that are characteristic of continental interiors and passive margin platform settings, and massive, mud-rich deltas characteristic of passive continental margin slope settings.

Petromineralogical study imparts details of rock forming as well as ore minerals and their association that helps to identify nature of mineralization. Petromineralogical studies of basement rock and other sedimentary rocks overlying basement have been carried out with the help of Leica Make Petrological Microscopes, Modal P-2700 attached with Image analyser for photomicrography at Petrology Lab of AMD, Nagpur. The results of the study are summarised below:

4.1 BASEMENT ROCKS

Study area mostly comprises granitoids as basement rocks with few basic and ultrabasic rocks intruded in it. Megascopically, 4 variant in Sambalpur granites has been identified viz. pink porphyritic granite, grey biotite granite and medium grained leucogranites. Apart from these, muscovite- biotite granite also present in Damdama- Jaypur area that excluded from project area but also similarly important as source of Singhora sediments.

4.1.1 Grey biotite granite of Chhibarra

Megascopically, rock is medium to coarse grained, hard, compact and massive in nature. The rock is medium to coarse grained and shows brecciated texture under microscope (Figure 4.1). This rock essentially consist of quartz, plagioclase and K-feldspar with biotite and zircon as accessory minerals. The deformation coupled with mineral alteration changed the original attributes of the rock. Deformation imprints may be due to fracturing in rock by nearby faults otherwise rock may be unreformed. Quartz is anhedral, interstitial (Figure 4.1 & 4.2) and myrmekitic at places. Plagioclase is of albite- oligoclase in composition and often shows sericitisation (Figure 4.3). Microcline is predominant K-feldspar with minor orthoclase.

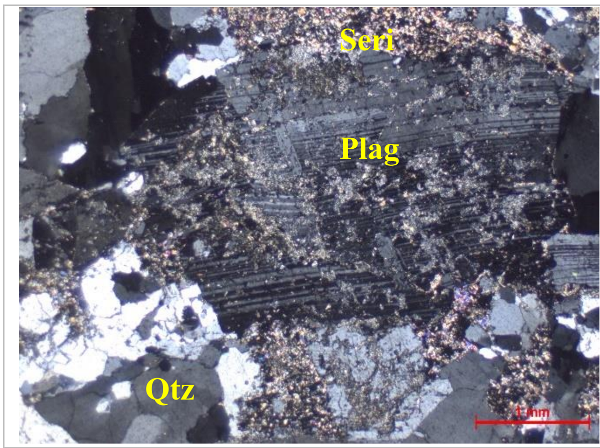

Figure 4.1 Coarse grained deformed and altered granite, TL, air, 2N.

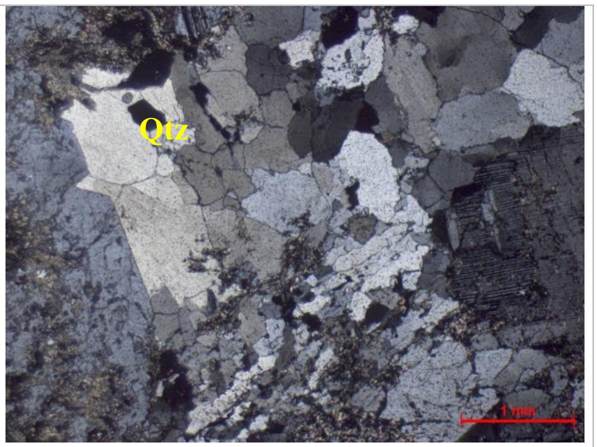

Figure 4.2 Medium to coarse grained subhedral to anhedral quartz grains, TL, air, 2N.

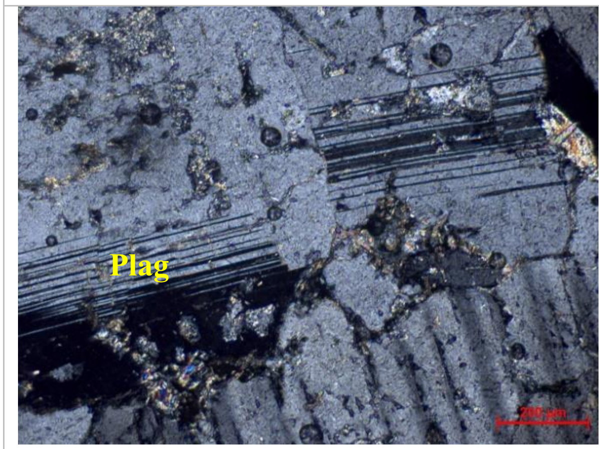

Figure 4.3 Deformation in albitic plagioclase lamellae TL, air, 2N.

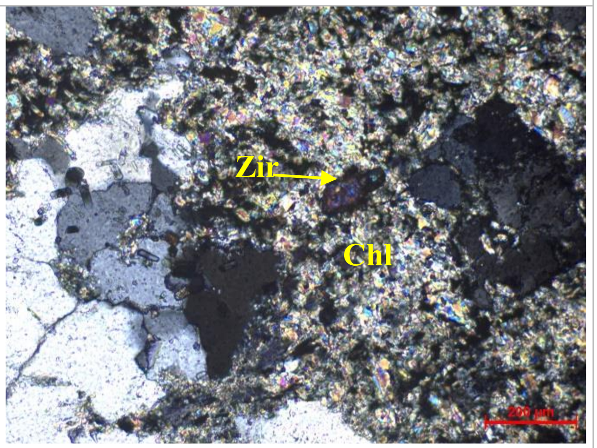

Figure 4.4 Zoned zircon and chlorite flakes in altered granite, TL, air, 2N.

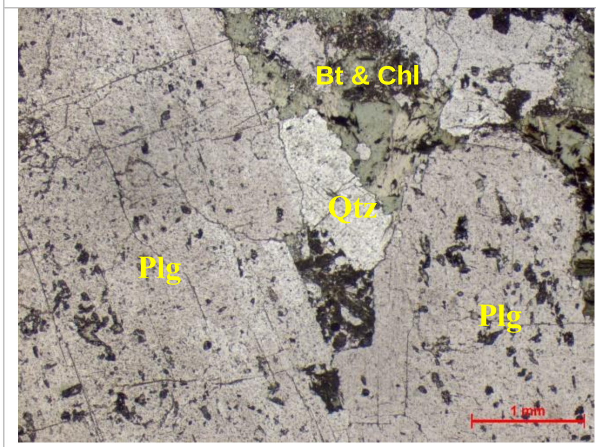

Figure 4.5 General texture of course grained biotite granodiorite of Murmuri, TL, air, 1N.

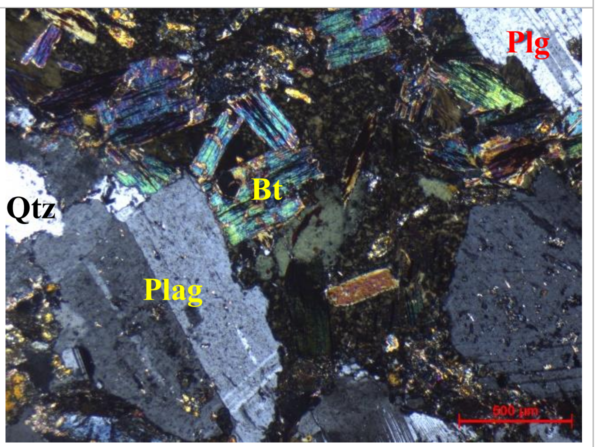

Figure 4.6 Green biotite and plagioclase in biotite granodiorite of Murmuri, TL, air, 2N.

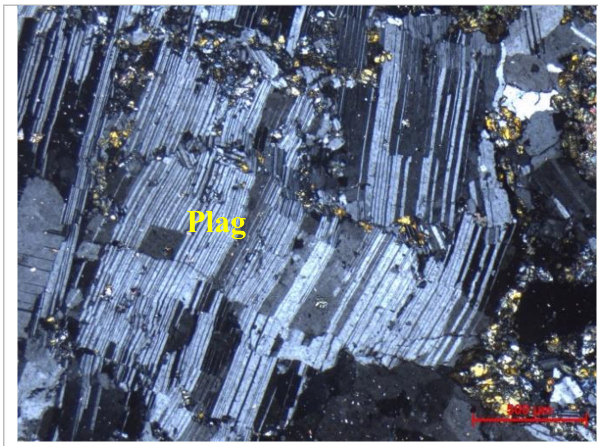

Figure 4.7 Deformed/ banded lamellae of plagioclase and micro shear zones in biotite granodiorite of Murmuri, TL, 2N.

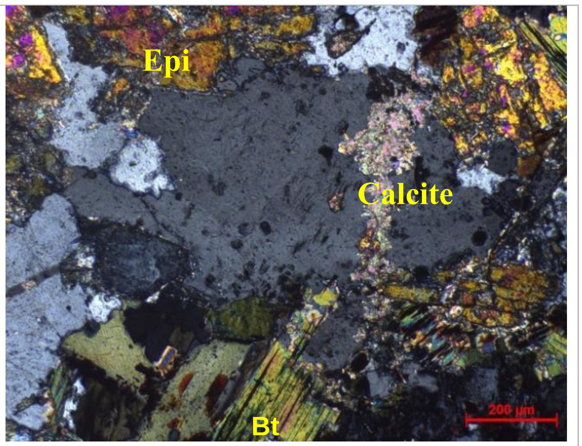

Figure 4.8 Formation of calcite (intruding into quartz) and epidote from plagioclase as a result of saussuritisation, TL, 2N.

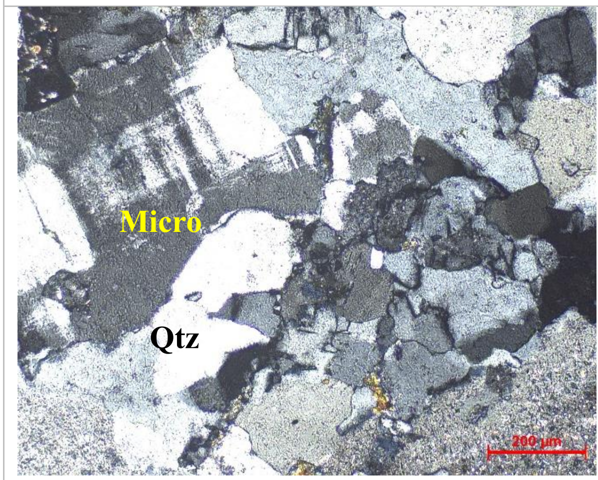

Figure 4.9 Quartz and microcline with general texture of granodiorite, TL, air, 2N.

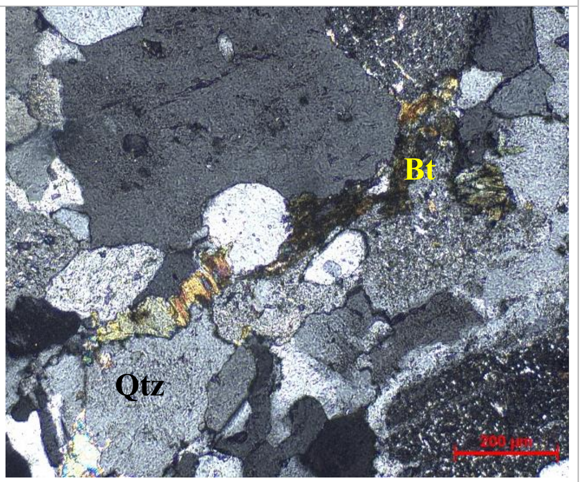

Figure 4.10 Biotite as interstitial segregation in granodiorite, TL, air, 2N.

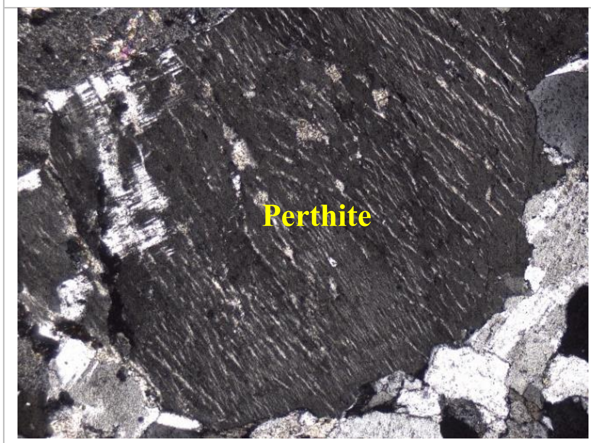

Figure 4.11 Microclinisation of flame perthite in less altered Granite, 10x, TL, air, 2N.

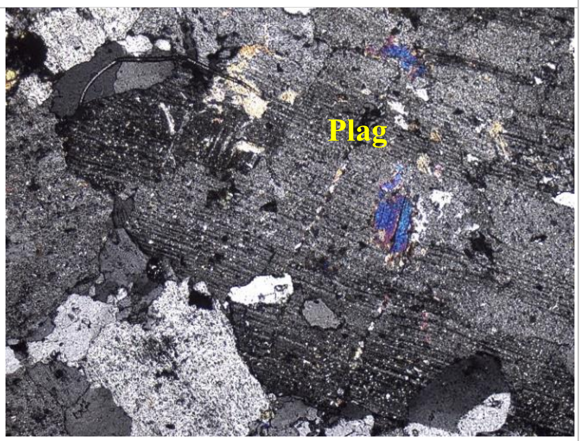

Figure 4.12 Sericitisation of deformed plagioclase and muscovite flakes in altered Granite, 5x, TL, air, 2N.

Biotite occurs as interstitial segregations of the major minerals, whereas zircon occur as disseminated grains (Figure 4.4). The rocks original hypidiomorphic texture is mostly obliterated due to variable degree deformation in the form of fracturing, crushing and granulation. The fractures are of more than one generation, as displayed by the textural attributes. Sericitisation and chloritisation (Figure 4.4, 4.5) are the mineral alterations observed. Besides, intense infiltration of calcite is prominent feature observed. Some anhedral opaque minerals also observed in chloritic matter. The mode of occurrence of secondary minerals along the fractures and weak planes, imply post-deformational hydrothermal nature. The rock is identified as biotite tonalite.

4.1.2 Pink porphyritic biotite granite of Rehatikhol- Murmuri

Rock sample is medium grained, greyish to pinkish in colour, hard, compact and massive in nature. It contains occasional phenocryst of K- feldspar giving porphyritic texture to the rock. Quartz, K- feldspar, plagioclase and biotite can be identified megascopically.

The rock essentially contains quartz and plagioclase (Figure 4.5), K- feldspar with biotite as prime accessory mineral, constituting more than 5% of the rock by volume (visual estimation), hence, named as biotite granodiorite. Apatite, sphene, anatase and goethite constitute other accessory/ minor minerals. Quartz is anhedral and interstitial. Plagioclase is of albite- oligoclase in composition and often shows low degree sericitisation. Biotite is mainly light green coloured and occurs as interstitial segregations of the major minerals (Figure 4.6). Stubby prismatic apatite occur as disseminated grains. Granular sphene and anatase are often found occurring in association with biotite. Goethite occurs as irregular segregations. Deformation imprints as granulation, brecciation and bending/ dislocation of twin lamellae in plagioclase are noted along with presence of micro shear zones (Figure 4.7). Sericitisation and sassuritisation of plagioclase by formation of epidote (zoisite) and calcite (Figure 4.8), chloritisation (Figure 4.5), epidotisation and formation of secondary muscovite from biotite are observed as alterations. Based on mineralogical composition, rock is named as biotite granodiorite.

4.1.3 Medium grained biotite granite of Kurapali- Muchbhal

Rock sample is medium grained, light grey in colour, hard, compact and massive in nature as observed megascopically. Under microscope, rock is medium to coarse grained consisting essentially quartz, plagioclase and K-feldspar (Figure 4.9) with biotite as prime accessory mineral, constituting more than 5% of the rock by volume (visual estimation), hence, named as biotite granodiorite. Allanite and zircon constitute other accessory minerals.

Quartz is anhedral and interstitial (Figure 4.9 & 4.10). Plagioclase is of albite - oligoclase in composition. K-feldspar is subordinate to plagioclase. Biotite occurs as interstitial segregations of the major minerals (Figure 4.10). Allanite and zircon occur as disseminated grains. Microclinisation of flame perthite is also noted (Figure 4.11). Major sericitisation (Figure 4.12) and minor sassuritisation of plagioclase; chloritisation and epidotisation of biotite are the mineral alterations observed. Rock is identified as biotite granodiorite.

4.1.4 Basic rock in Gatkachhar

Megascopically, rock sample is fine to medium grained, dark grey in colour, hard, compact and massive in nature. The rock essentially composed of calcic plagioclase of labrodorite composition and calcic clino-pyroxene with intergranular and glameroporphyritic (Figure 4.13) textures. Skeletal titano-magnetite (Figure 4.14), anatase, pyrite constitute minor minerals. The original mineralogy of the rock is variably altered. Chlorite, sericite and calcite are the secondary minerals formed due to moderate degree alteration of the major minerals. Rock can be named as altered dolerite.

4.2 REHATIKHOL FORMATION

Based on megascopic mineralogical composition, textural aspect, grain size and sedimentological studies in field, Rehatikhol Formation is classified into 5 lithounits viz. basal polymictic conglomerate ± pebbly feldspathic arenite, gritty/ gravelly feldspathic arenite ± conglomerate, feldspathic arenite ± PFA, ferruginous sandstone- siltstone- shale and porcellanite. Petrographic characteristics of these lithounits are following-

4.2.1 Basal polymictic conglomerate ± pebbly feldspathic arenite

The basal conglomeratic horizon is matrix supported, very poorly sorted conglomerate containing pebble to cobble size clast (sometime boulder size) of quartz (upto 90%), feldspar, rock fragments of granite/ chert / occasional altered basic rock, silicified rocks in very coarse to granule size feldspathic arenite matrix. Quartz occurs as arenaceous matrix as well as subrounded pebbles and cobbles. Feldspar is mostly altered (sericitised and saussuritised) and occurs as matrix as well as clast upto pebble size. Composition of clast and matrix indicates granitic source for these beds. Unsorted, subangular to subrounded immature clast set in arkosic matrix indicate sediments have been supplied from nearby provenance by rapid sedimentation as debries flow with high viscosity under higher gradient conditions of channel. Thin section study has been only carried out for pebbly feldspathic arenite horizon.

Pebbly arenite/ conglomerate is constituted by clast supported framework (Figure 4.13). It is poorly sorted, composed of sub rounded to rounded pebbles/ granules, medium to coarse sand sized clasts (Figure 4.13). It is bound by fine to very fine sand sized detritus and sericite matrix. The sand sized clasts are mainly composed of quartz with subordinate feldspar. Quartz is of both monocrystalline and poly crystalline nature with overgrowth at places and K-feldspar is represented by perthite and microcline (Figure 4.14). The pebbles are constituted by silicified rocks, vein quartz, quartz and feldspar. Occasional mica flakes also observed in matrix. Zircon, monazite and xenotime are the heavy minerals observed. The clast composition indicates mainly a granitic/ gneissic source rock, the sorting and roundness indicates the provenance source is not too far from the depositional basin and gradient of sediment supply channel is very high.

4.2.2 Gritty/ gravelly feldspathic arenite

It is light greenish to cream coloured, sub compact and moderately hard, very coarse to granule sized feldspathic arenite as observed megascopically. Rock is consist of granule to pebble sized quartz (>60%), K-feldspar (upto 20 %) with minor lithic fragments of graphic granite and chert set in siliceous and sericitic matrix (<15%) in clast supported framework. Clasts are poorly sorted to moderate sorted and subangular to subrounded in nature (Figure 4.15). Plane contact as well as sutured contact has been observed between the clast indicating high degree of compaction (Figure 4.16). Feldspar is subrounded and mainly microcline (Figure 4.17) and perthitic composition. Quartz shows polycrystalline and monocrystalline both nature indication igneous or metamorphic origin (Figure 4.17). Muscovite flakes also observed in sericitic matrix (Figure 4.18). Sorting and roundness of grains improve in this horizon and grain size of clast decrease compare to underlying basal polymictic conglomerate and pebbly feldspathic arenite.

4.2.3 Feldspathic arenite

Megascopically, rock sample is medium to coarse grained, whitish cream coloured, hard, compact and massive in nature. Feldspar and occasional micaceous mineral can be identified in hand specimen. Grain size variation is prominent and some pebbly layers also present at some levels in this Member.

Rock is consist of medium to very coarse sand size grains with some granule size sediments under microscope and contains mostly clast supported framework (Figure 4.19).

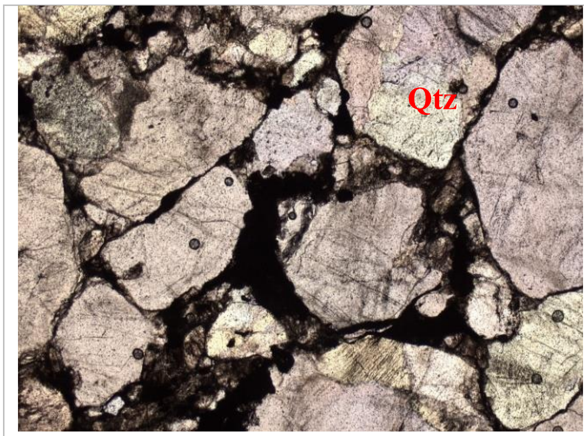

Figure 4.13 Poorly sorted pebbly feldspathic arenite with subangular to subrounded clast, 2.5x, 1N, TL, air.

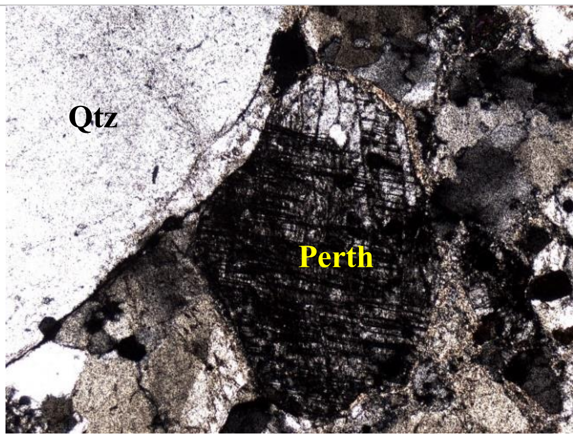

Figure 4.14 Subrounded feldspar and overgrowth in quartz in pebbly feldspathic arenite, 2.5x, 2N, TL, air.

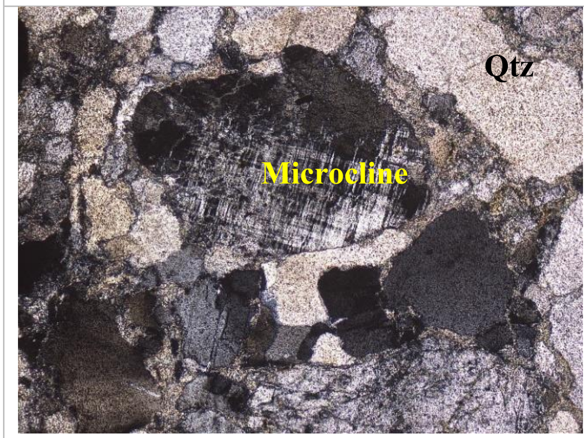

Figure 4.15 Poorly sorted, gritty feldspathic arenite, subangular to subrounded microcline and quartz, 5x, TL, air, 2N.

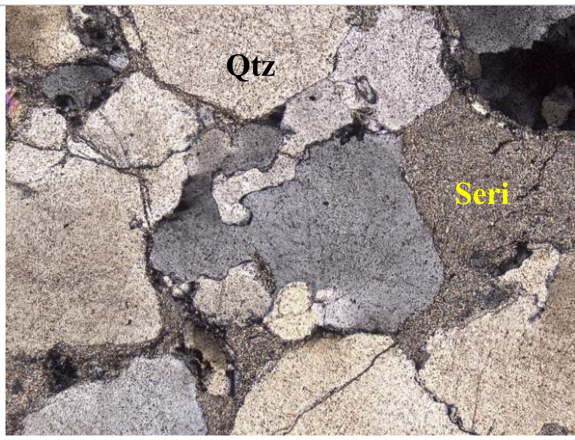

Figure 4.16 Plane and sutured contact between clast and sericitc matrix (< 15 %) in gritty feldspathic arenite, 5X TL, air, 2N.

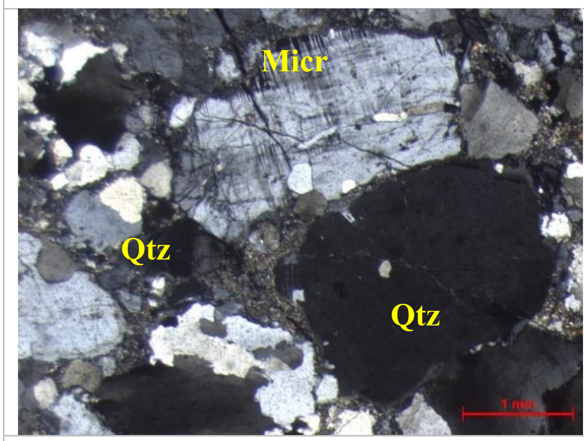

Figure 4.17 Mono and poly crystalline quartz, microcline and sericitic matrix in gritty feldspathic arenite, TL, 2N, air, Chiwarakuta.

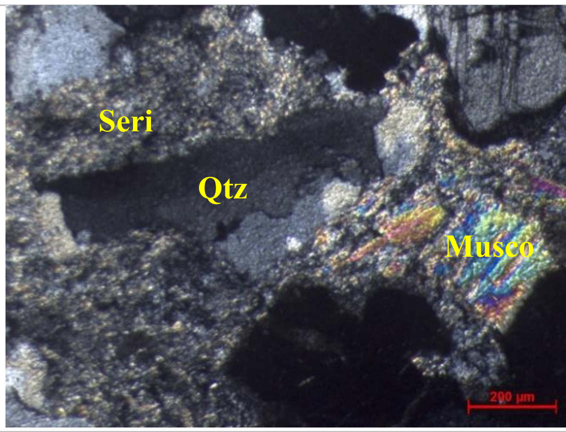

Figure 4.18 Muscovite flake in sericitic and siliceous matrix in gritty feldspathic arenite, TL, 2N, air, Chiwarakuta.

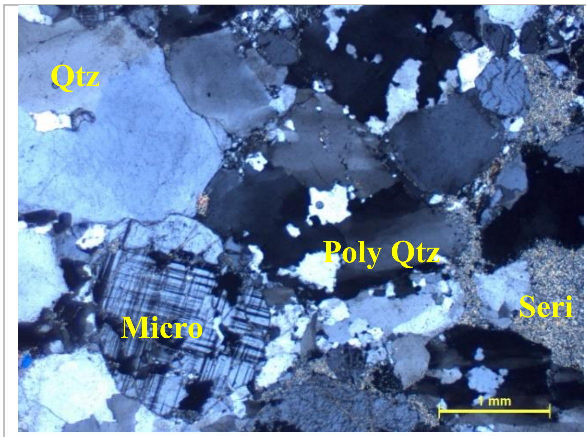

Figure 4.19 Feldspathic arenite of Malaikhaman, Tl, 2N, air.

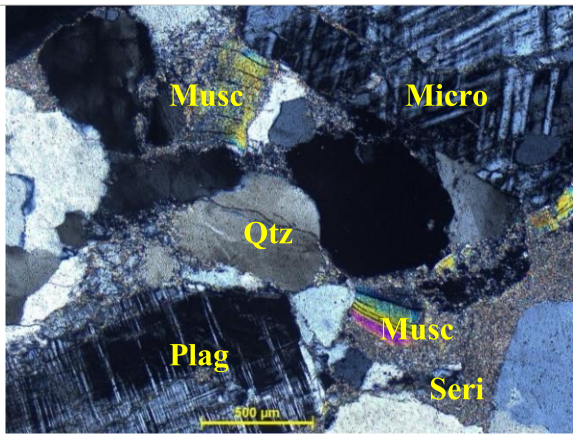

Figure 4.20 Plagioclase, muscovite, microcline and quartz with sericitic matrix in Feldspathic arenite, TL, 2N, air.

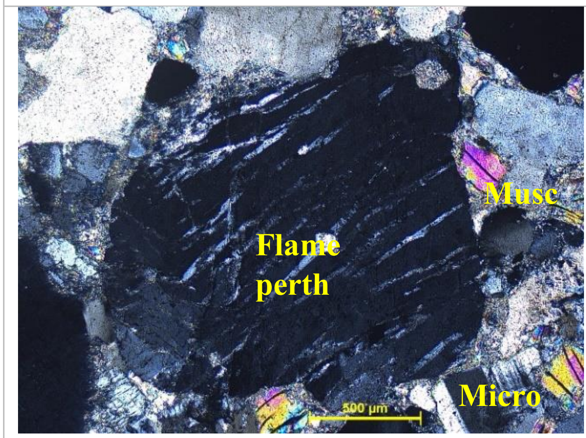

Figure 4.21 Flame perthite, muscovite, microcline in feldspathic arenite, TL, 2N, air.

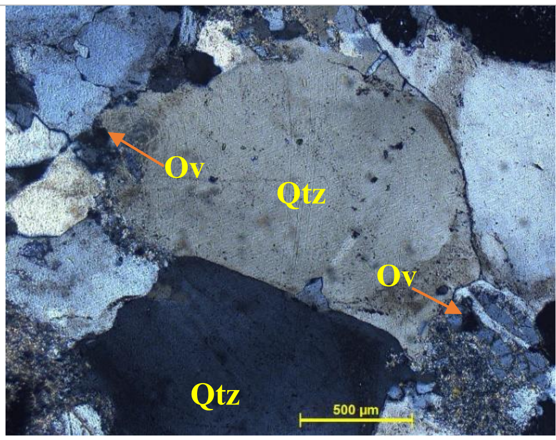

Figure 4.22 Silica overgrowth due to pressure solution and plane contact between quartz grains of felds. arenite, TL, 2N, air.

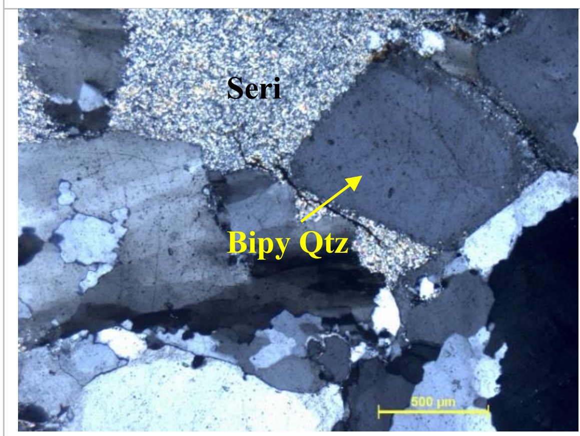

Figure 4.23 Euhedral bipyramydal quartz grain with corroded grain boundary in sericitic and siliceous matrix of feldspathic arenite, TL, 2N, Air.

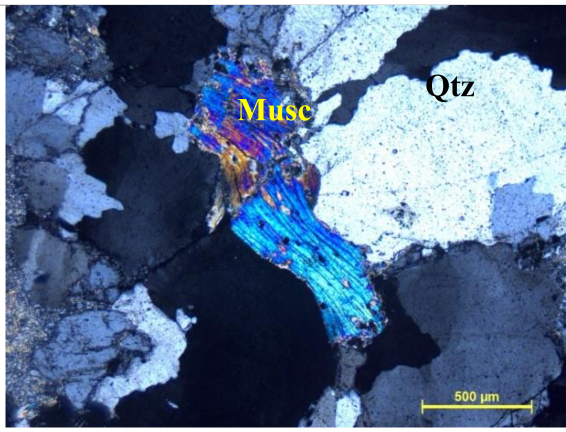

Figure 4.24 Bending in muscovite feldspathic arenite without pyrite of Malaikhaman, Tl, 2N, air.

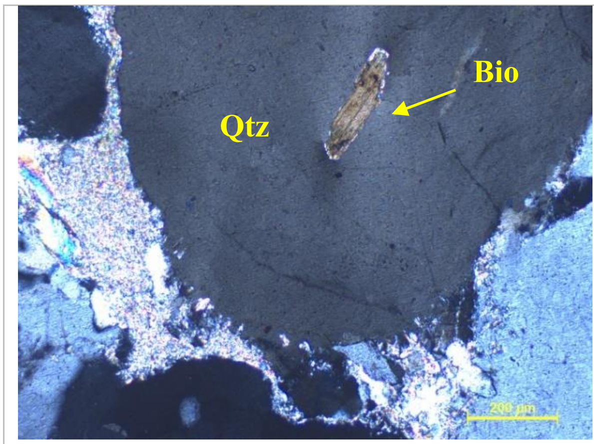

Figure 4.25 Biotite inclusion within quartz clast in feldspathic arenite of Rehatikhol, TL, 2N, air.

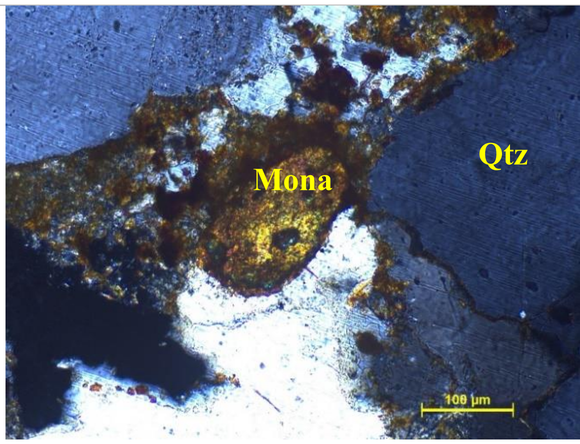

Figure 4.26 Detrital monazite in feldspathic arenite, TL, 2N, air.

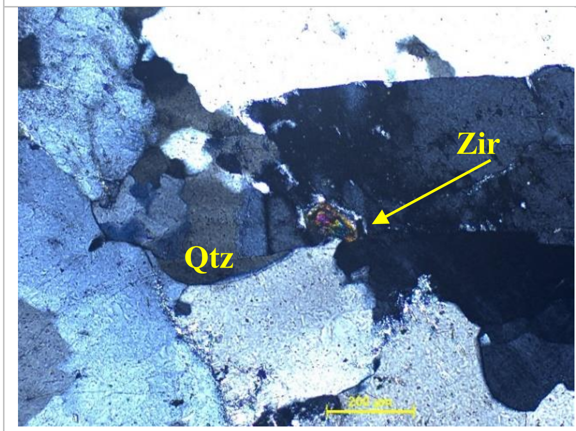

Figure 4.27 Zoned zircon grain and plane contact between quartz grains in feldspathic arenite, TL, 2N, air.

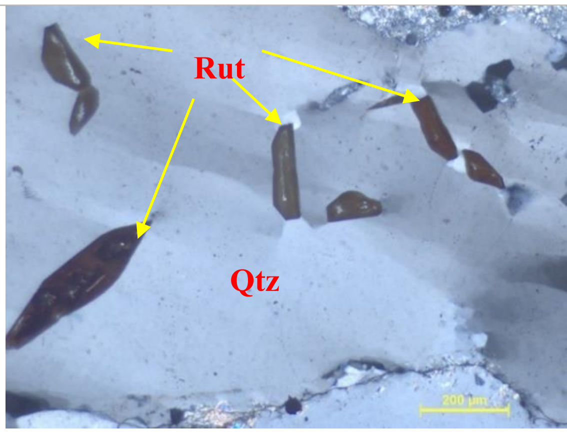

Figure 4.28 Rutile inclusion in quartz clast of feldspathic arenite, TL, 2N, air.

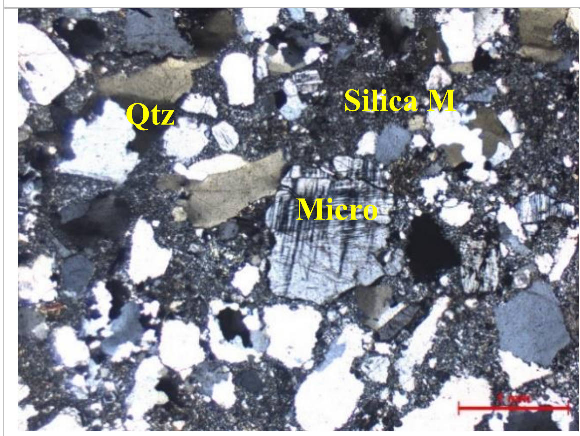

Figure 4.29 Quartz, microcline, perthite feldspar clast in siliceous matrix in PFA, Tl, air, 2N.

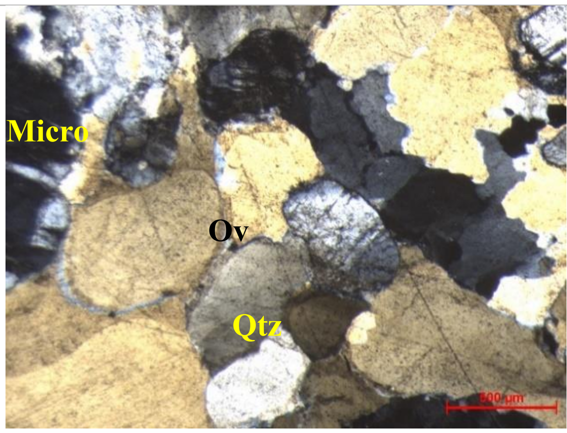

Figure 4.30 Subrounded quartz and microcline with plane and sutured contact, TL, 2N, air.

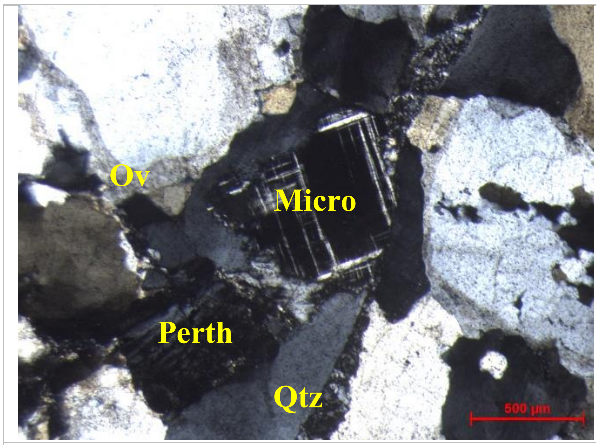

Figure 4.31 Microcline and perthite with quartz as clasts in minor sericitic, arenaceous and pyritic matrix, TL, air, 2N.

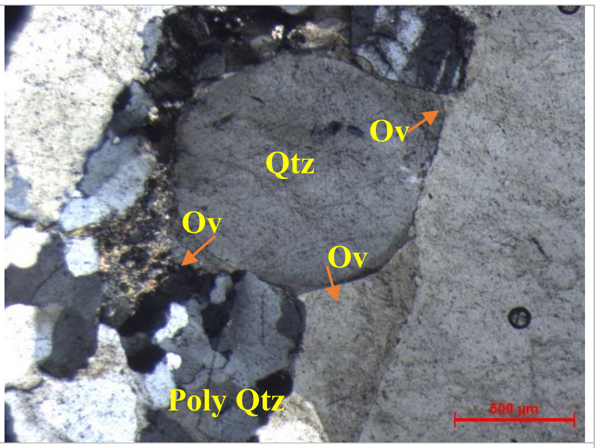

Figure 4.32 Well rounded quartz grain (most possiblly recycled) and silica overgrowth in PFA, TL, 2N, air.

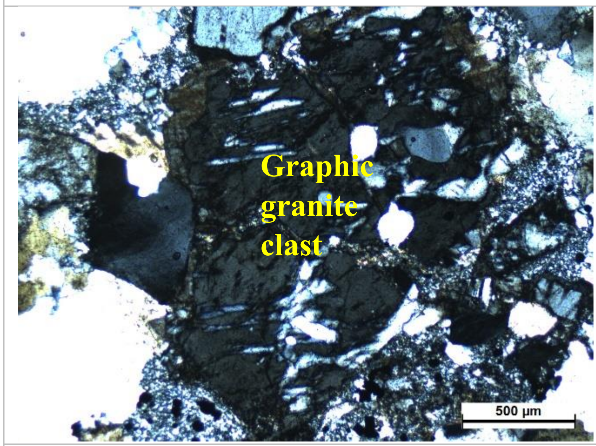

Figure 4.33 Graphic granite clast (intergrowth of quartz in feldspar) in pebbly PFA 2.5x, Tl, ,2N, air.

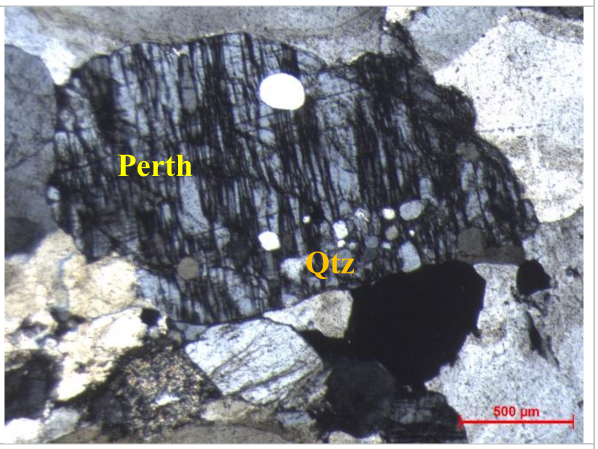

Figure 4.34 Rounded quartz inclusion in subrounded grain of flame perthite, Tl, 2N, air.

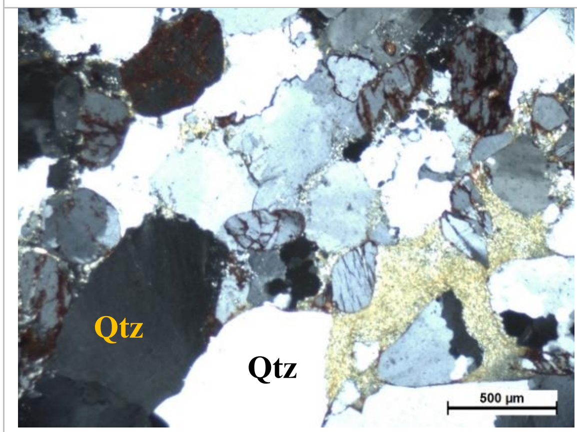

Figure 4.35 Iron inside quartz and feldspar fractures give red stains on the surface. No opaques, Tl, 2N, air.

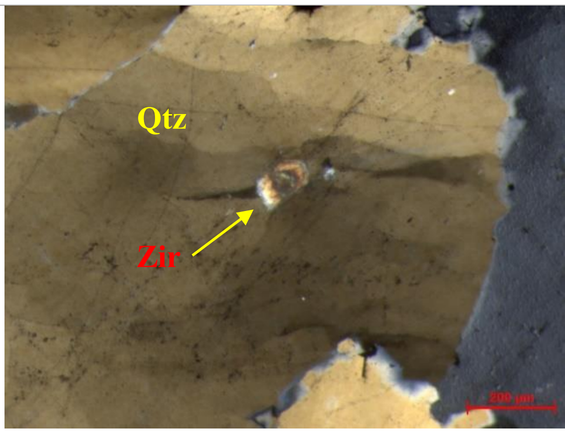

Figure 4.36 Wavy extinction in quartz (strained), zoned zircon as inclusion, Tl, 2N, air.

It is poorly sorted consisting of fine to coarse sand, granules and pebbles size subangular to subrounded clasts bound by matrix and cement (Figure 4.19). Quartz is dominant clast with subordinate feldspar. Quartz is represented by both mono-crystalline and poly-crystalline grains (Figure 4.19), whereas feldspar is represented by clasts of flame perthites, microcline and occasional plagioclase (Figure 4.19- 4.21). The grains and pebbles are constituted by polycrystalline quartz of igneous and metamorphic source rock, vein quartz and feldspar of granitic origin. Fine quartz, feldspar, clay, muscovite and sericite constitute matrix (Figure 4.21) whereas secondary overgrown silica in optical continuity with detrital quartz constitute the binding cement (Figure 4.19 & 4.22). Mostly plane contact between clast are present indicating high degree of compaction and silica overgrowth due to pressure solution (Figure 4.22).

Some suspected bipyramydal and euhedral quartz grains has also been observed in feldspathic arenite indicating their acidic volcanic origin (Figure 4.23). It is inferred that localised acidic volcanic activity has been started in provenance during the sedimentation of Rehatikhol Formation with the introduction of feldspathic arenite member. Bended muscovite flakes and inclusion of biotite in quartz are the micaceous minerals that noted in this unit (Figure 4.24 & 4.25), showing their origin from two mica granite (a younger phase of Sambalpur Granite). Detrital monazite (Figure4.26) and zoned zircon (Figure 4.27) constitute heavy mineral assemblage.

Rutile inclusion in quartz with undulose extinction (Figure 4.28) shows acidic rock as provenance of these sediments. Poor sorting indicates nearby provenance with less transportation whereas predominant quartzo-feldspathic clast composition indicates mainly a granite source rock.

4.2.3.1 Pyritiferous feldspathic arenite

Megascopically, rock sample is medium grained, grey in colour, hard, compact and massive in nature. Pyrite and feldspar can be identified in hand specimen. Grain boundaries of quartz grains are diffused (due to overgrowth).

Rock is medium to very coarse grained with occasional granule size grained under microscope and contains mostly clast supported framework (Figure 4.29, 4.30 & 4.31). It is poorly to moderately sorted consisting of fine to coarse sand, granules and pebbles size subangular to subrounded clasts bound by matrix and cement (Figure 4.29 & 4.31). The clasts are mainly composed of quartz with subordinate feldspar, mainly microcline and perthites (Figure 4.31). Quartz is represented by both mono-crystalline and poly-crystalline grains, whereas feldspar is represented by clasts of perthite and microcline (Figure 4.31). The pebbles are constituted by vein quartz, metamorphic quartz, plutonic quartz and feldspar of granitic origin. Fine quartz, feldspar, clay, pyrite and sericite constitute matrix whereas secondary overgrown silica in optical continuity with detrital quartz constitute the binding cement (Figure4.30- 4.32).

Silica overgrowth is very prominent in this unit compare to other units. Silica overgrowth is main causative factor of diffused grain boundaries as seen megascopically. Plane and sutured contact between clast are present mostly indicating high degree of compaction and compressive deformation (Figure 4.30 & 4.31). Larger grains of quartz and feldspar show more roundness comparatively that indicate their long transportation with provenance. Occasional well rounded grains of quartz with silica overgrowth also observed that possibly infer recycled sediment input (Figure 4.32). Presence of polycrystalline subrounded quartz infers their metamorphic provenance and could be older metamorphic enclaves in Sambalpur Granitoids. Apart from these, graphic granite clast (intergrowth of quartz and feldspar, Figure 4.33), quartz with biotite inclusion, subrounded perthites and quartz inclusion in subrounded perthites

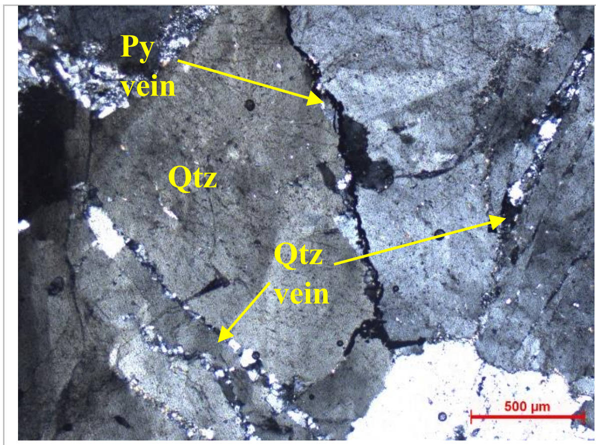

Figure 4.37 Deformed quartz clast with quartz and pyrite vein in PFA, Tl, 2N, air.

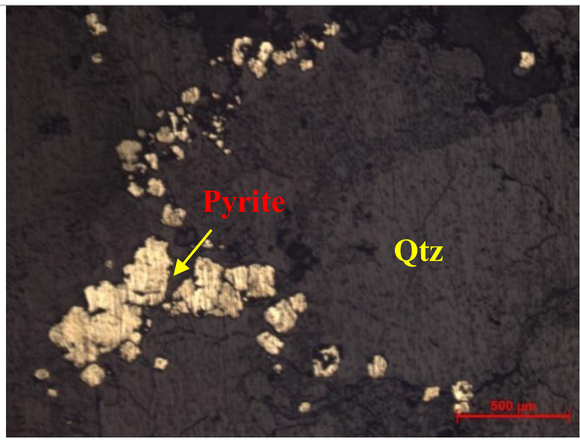

Figure 4.38 Disseminated pyrite in matrix of PFA, Rl, 1N, air.

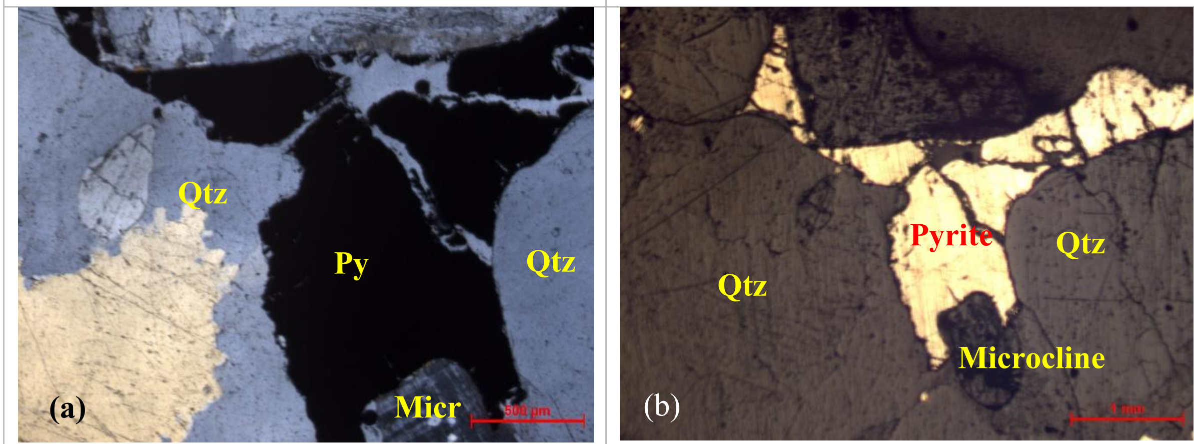

Figure 4.39 Pyrite as intergranular matrix in PFA (a) Tl, 1N, air. (b) RL, 1N, air.

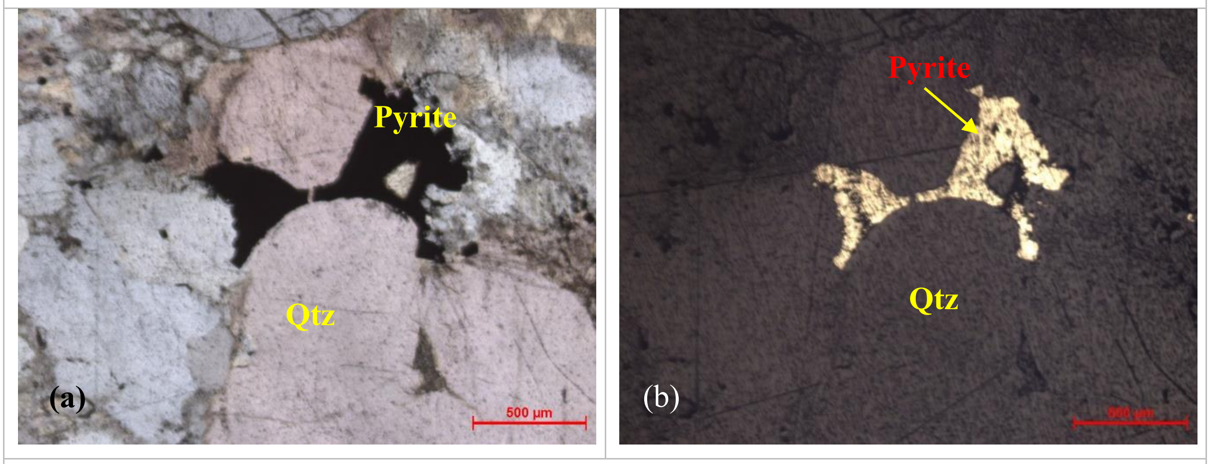

Figure 4.40 Cluster of pyrite wrapped around the quartz grains in intergranular space.
(a)Tl, 1N, air. (b) Rl, 1N, air.

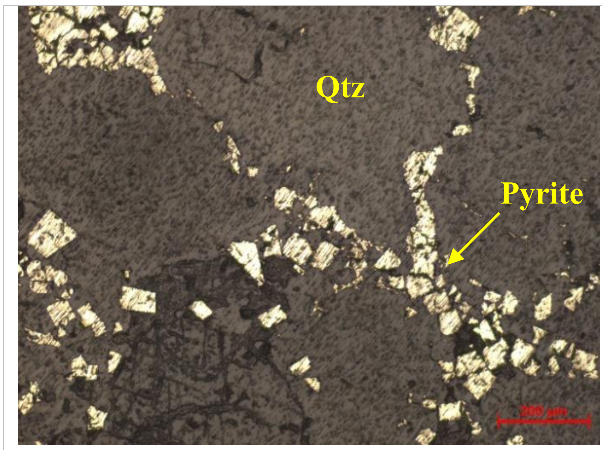

Figure 4.41 Pyrite around grain boundary of quartz within matrix of PFA, Rl, 1N, air.

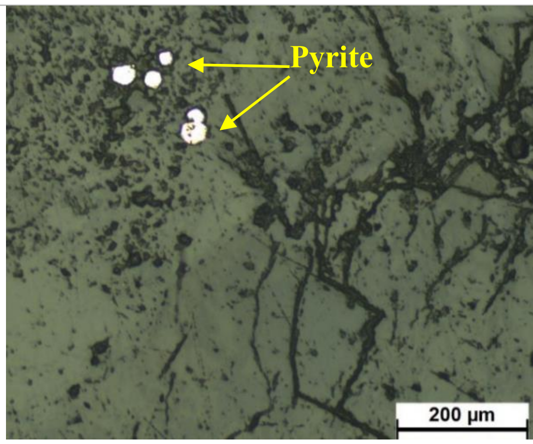

Figure 4.42 Subrounded pyrite grains inferring detrital pyrite, Rl, 1N, air.

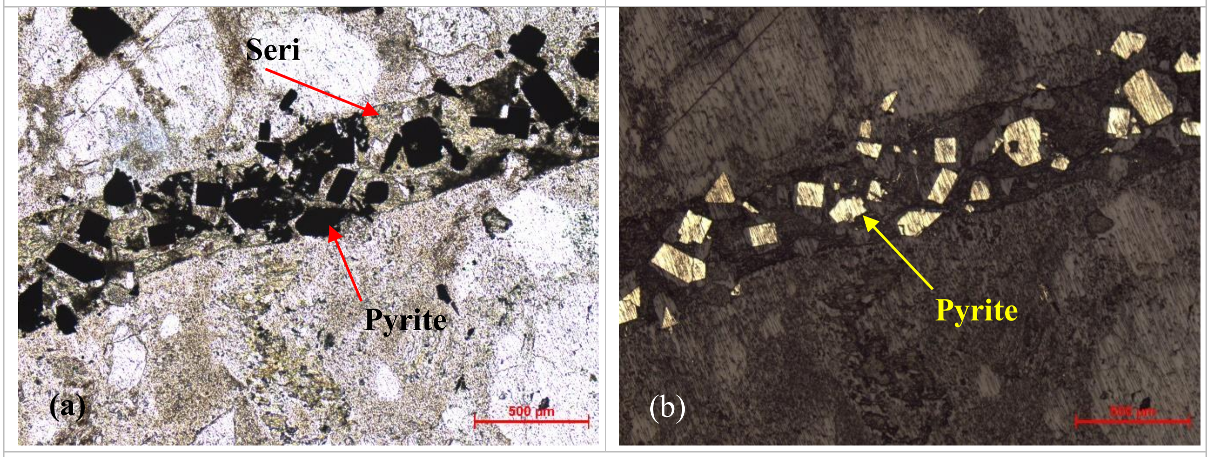

Figure 4.43 Euhedral cubic pyrite in sericitic vein within siliceous matrix in PFA.
(a) TL, 1N, air. (b)RL, 1N, air.

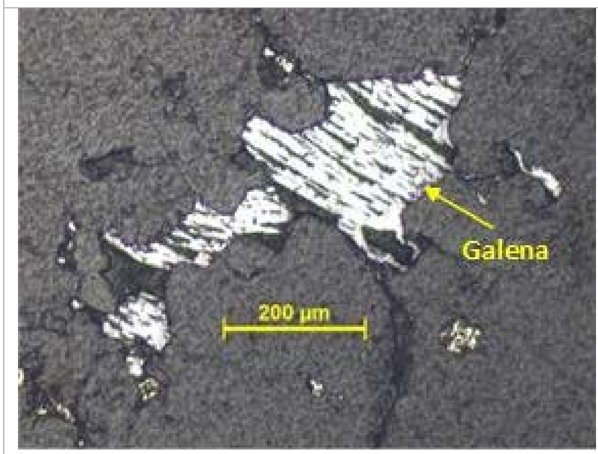

Figure 4.44 Epigenetic galena as fracture filling in PFA, Chhibarra, RL, 1N, air.

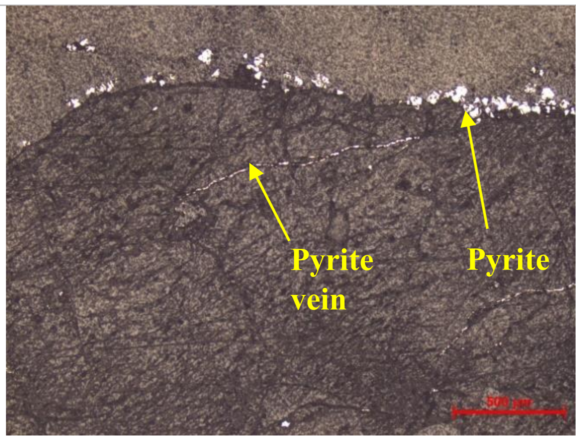

Figure 4.45 Pyrite dissemination in matrix around quartz grain boundary and thin pyrite vein, Rl, 1N, air.

(Figure 4.34) also encountered that indicate sediment input of PFA is mainly from granitic provenance (Sambalpur granitoids). Presence of iron oxide stains in fractures of quartz and feldspar also noted in oxidised surface of sample due to oxidation of pyrite and subsequent mobilisation into fractures (Figure 4.35). Zoned zircon as inclusions in quartz grain are noted indicating granitic source of these grains (Figure 4.36). Some quartz grain shows wavy extinction inferring deformation in it (Figure 4.36). Zircon (Figure 4.36) and monazite constitute heavy minerals. Poor sorting indicates nearby provenance with less transportation whereas predominant quartzo-feldspathic clast composition indicates mainly a granite source rock with minor contribution from sedimentary litho-units, as reflected by pebble nature. The high incidence of potash feldspar and granite fragments suggests that the detritus were derived from a granitic source (Blatt 1967; Basu 1976). Deformation imprints in some PFA are represented by strained quartz grains with wavy extinction, injection of silica and pyrite vein along micro fracture plane (Figure 4.37).

Euhedral to subhedral pyrite is observed occurring in association with matrix and cement as disseminations (Figure 4.38, 4.39 a & b). Anhedral clusters of pyrite also found to be wrapped around quartz grain in intergranular spaces (Figure 4.40 a & b) that could be possibly diagenetic origin. Disseminated euhedral pyrites are also noted in pyritiferous matrix of PFA (Figure 4.41) that could be of both diagenetic and epigenetic origin for that further study is required to ascertain precisely. A nearly subrounded grains of pyrite (Figure 4.42) are also noted that infers presence of detrital pyrite (?) could be attributed as transportation in anoxic conditions. Epigenetic hydrothermal pyrite is also present in PFA unit and it is represented by euhedral cubic pyrite along the sericitic and siliceous (cherty?) vein (Figure 4.43 a & b) that typically indicate hydrothermal activity and alteration. Presence of epigenetic galena also noted in Chhibarra PFA that was also identified megascopically (Figure 4.44). Remobilised pyrite can be identified as small stringes and thin veins in grains of quartz and feldspar (Figure 4.45). It is originated from mobilisation of existing diagenetic and epigenetic pyrite and precipitation in weak plane and spaces. So, PFA unit comprises diagenetic, epigenetic and remobilised pyrite and represent strong reduced facies in Rehatikhol Formation. Sulphur isotope study of these pyrites also confirmed their diagenetic, epigenetic and remobilised origin (Sinha et al. 2001).

4.2.4 Ferruginous sandstone

It is medium grained and cherry reddish to pinkish coloured sandstone consisting subrounded to rounded grain of quartz and feldspar set in ferruginous matrix as observed megascopically. Matrix content seems to be higher than other sandstones of Rehatikhol Formation. Some smoky quartz grains and altered feldspar with goethitic matter observed in this unit.

It is characterised by subrounded to rounded, medium to coarse sand sized grain set in matrix supported framework (Figure 4.46). This sandstone is poorly to moderately sorted and consisting of mainly quartz grains of polycrystalline to monocrystalline nature with minor feldspar and muscovite. Intergranular spaces are filled with sericitic (mostly) and siliceous matrix that is later ferrugenised (Figure 4.47 & 4.48). Matrix supported framework is prominent in this sandstone. Grain contacts are manifested in the form of point and plane contact indicating comparatively less compaction and deformation than other sandstone of Rehatikhol Formation (Figure 4.46). Feldspar is represented by perthites and microcline with minor alteration in some grains. Quartz grains with wavy extinction and elongated quartz grains are also noted (Figure 4.49). Varying degree of roundness has been observed in this sandstone from subrounded to subangular. Well-rounded grains of quartz also present in sandstone inferring their recycled origin (Figure 4.50). Apart from these, some suspected bipyramydal quartz grains that could be derived from acidic volcanic source also noted (Figure 4.51). Detrital zircon (Figure 4.52) and monazite (Figure 4.53) constitute heavy mineral assemblage indicating acidic igneous provenance. This sandstone of Rehatikhol Formation characterised relatively higher matrix content and some ferruginous input either from oxidation of overlying pyrite bearing porcellanite or volcanic activity in near provenance area. Sericitic matrix of this sandstone is found to have iron oxide staining thus indicating later solution activity.

4.2.5 Porcellanite

Evidences of volcanoclastic sedimentation in Singhora basin are manifested by presence of porcellanite layers intercalated with shale in upper Rehatikhol Formation and as massive porcellanite in Saraipali and Chuipali Formation. Megascopically, porcellanite are characterised by dark greyish cryptocrystalline layers with goethitic or limonitic oxidised surface. Thin laminated bands of tuffaceous matter also associated along with occasional fine pyrite cubes and disseminations.

Rock is very fine grained and cryptocrystalline in nature under microscope. Devitrified wavy glassy bands are pervasive in the rock giving it laminated appearance (Figure 4.54). High magnification microscopy indicates these bands are composed of thin lensoidal cherty shards that evolved from devitrification of glassy matter. It mainly consist of devitrified cherty shards, euhedral to subhedral quartz (Figure 4.55) and occasional plagioclase laths. Globular shaped fine calcite as dissemination also noted in cryptocrystalline and sericitic matrix (Figure 4.56). Sericite flakes and lenses of chert are set in matrix with goethitic stains along some laminations (Figure 4.57). Magnetite and pyrite constitute opaque mineral assemblage. Magnetite occurs as occasional anhedral altered grain (Figure 4.58 a & b) while pyrite occurs as fine disseminations (Figure 4.59). Pyrite is anhedral and have desiccated grain boundary (Figure 4.60). Presence of pyrite indicate reducing condition prevailing at the time of porcellanite formation and it also noted in Juba porcellanite (Figure 4.61). Limonitic stains are pervasively noted on the oxidised surface of porcellanite that derived from the oxidation of pyrite porcellanite (Figure 4.62).

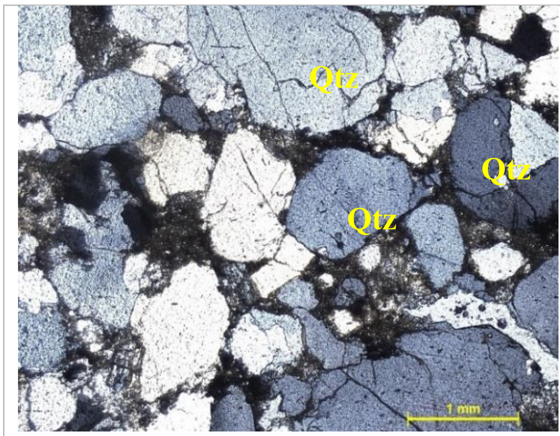

Figure 4.46 General texture of ferrugenised sandstone, Tl, 1N, air.

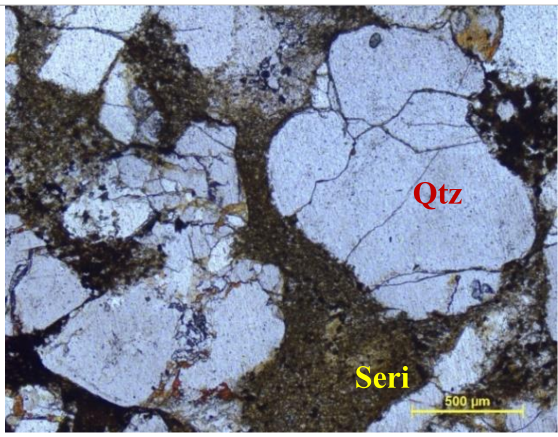

Figure 4.47 Quartz clast in ferruginous and sericitic matrix of ferrugenous sandstone, TL, air, 2N.

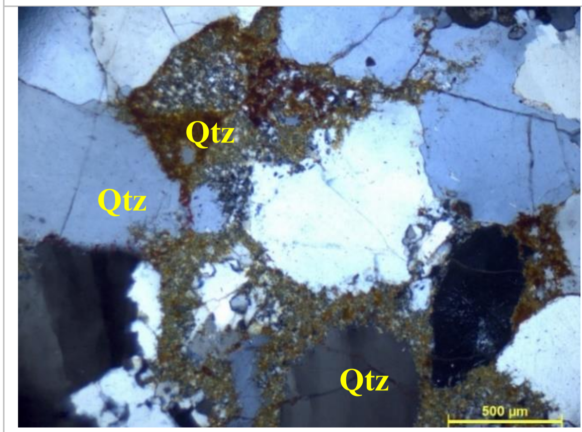

Figure 4.48 Quartz showing wavy extinction in ferruginous sandstone with sericitic matrix and iron stains, TL, air, 2N.

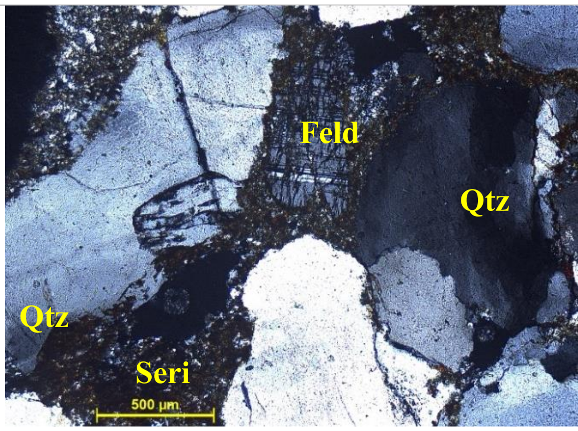

Figure 4.49 Perthite and elongated quartz grains with wavy extinction (strained) in ferruginous sandstone, TL, air, 2N.

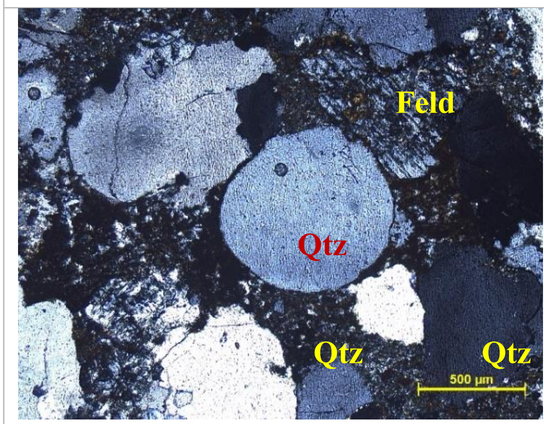

Figure 4.50 Rounded recycled quartz clast in ferrugenious sandstone Tl, 2N, air.

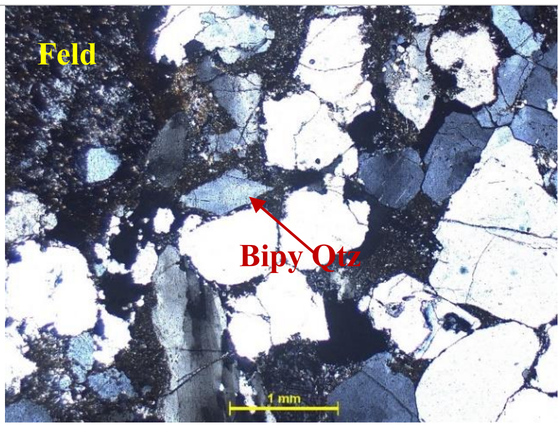

Figure 4.51 Euhedral bipyramydal (?) quartz grain, sericitic and siliceous matrix in ferruginous sandstone, TL, 2N, Air.

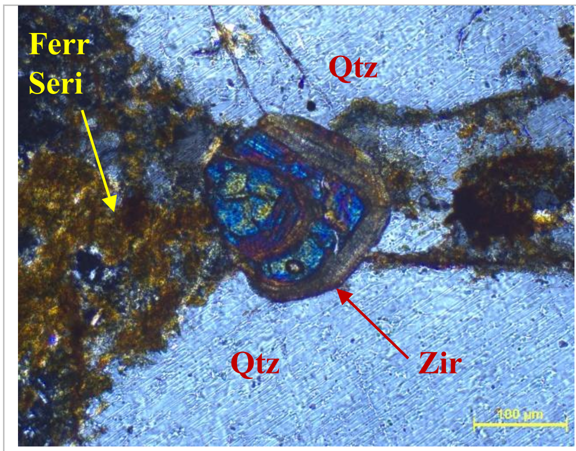

Figure 4.52 Zoned zircon grain in ferruginous sandstone with sericitic matrix, TL, air, 2N.

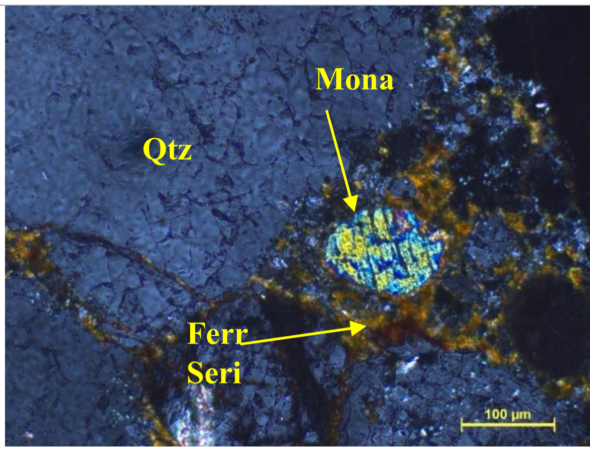

Figure 4.53 Monazite grain in ferruginous sandstone with in sericitic matrix, TL, air, 2N.

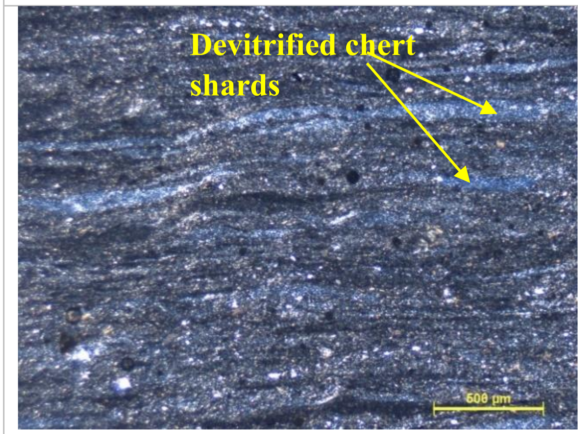

Figure 4.54 Devitrified chert and banding of cherty and quartz with few opaques in porcellanite, Chiwarakuta, TL, air, 2N.

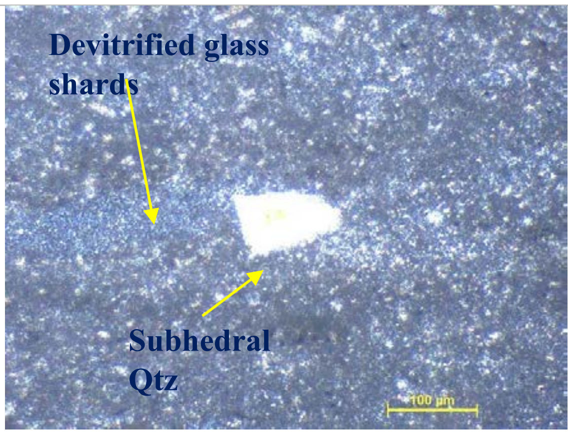

Figure 4.55 Euhedral to subhedral quartz with corroded boundary in porcellanite, TL, 2N, Air.

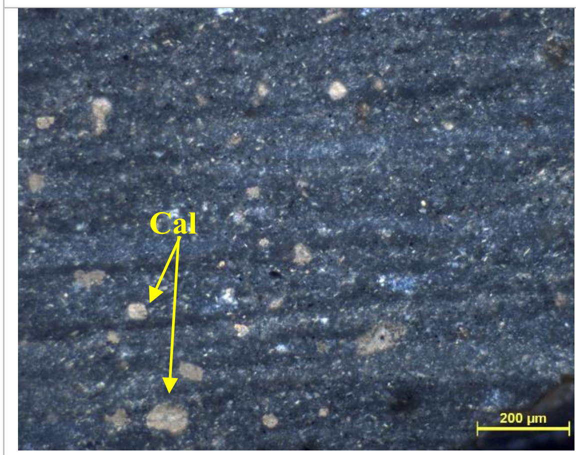

Figure 4.56 Globular shaped calcite as disseminations in porcellanite, Chiwarakuta, TL, air, 2N.

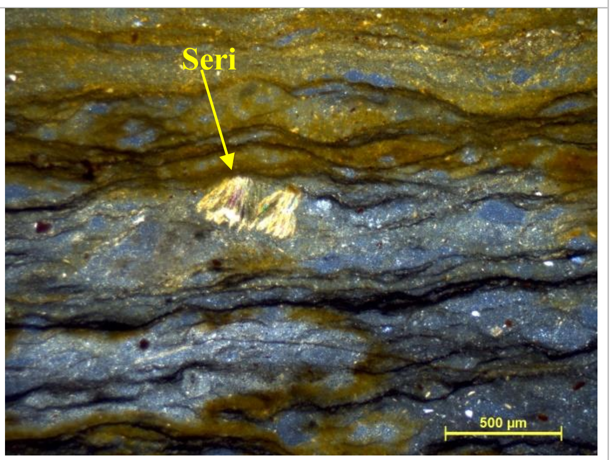

Figure 4.57 Sericite and lenses of chert within limonitic and goethitic layers porcellanite, Chiwarakuta, TL, air, 2N.

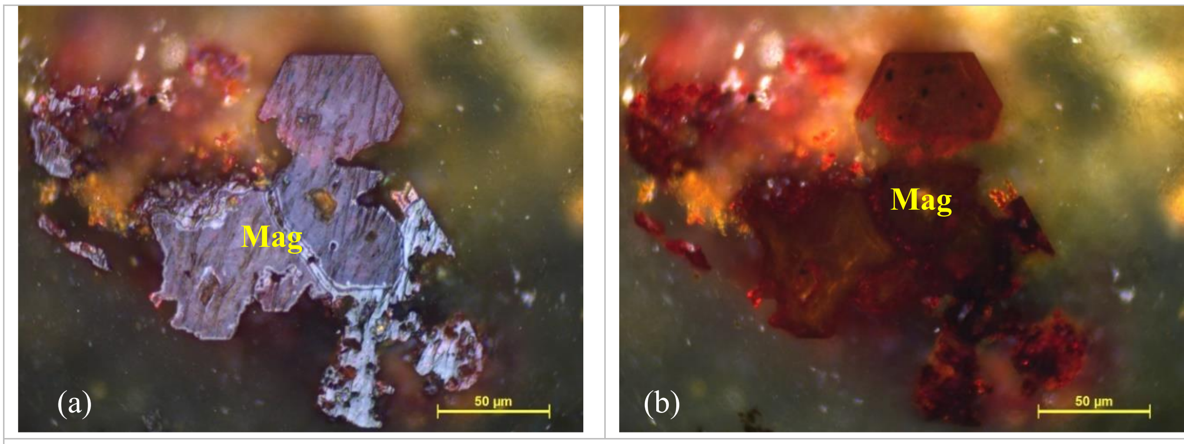

Figure 4.58 Anhedral altered magnetite in porcellanite, Chiwarakuta.

(a) RL, oil, 1N. (b) RL, oil, 2N.

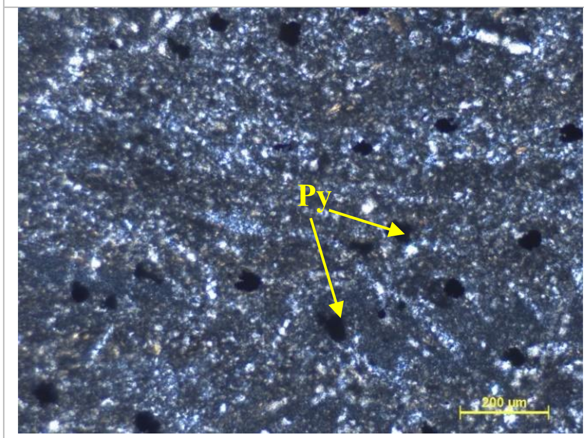

Figure 4.59 Devitrified chert with few disseminated pyrite in porcellanite, Chiwarakuta, TL, air, 2N.

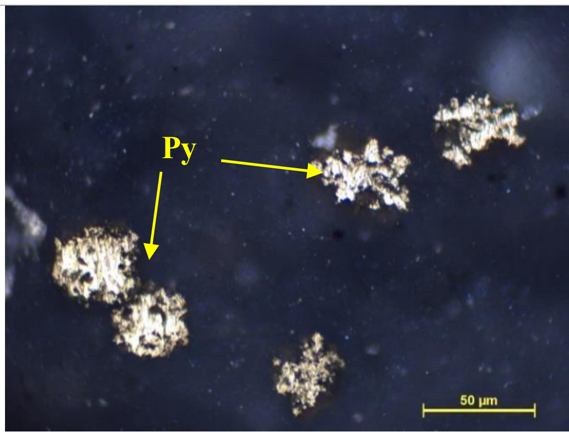

Figure 4.60 Group of anhedral pyrite with desiccated grain boundary in porcellanite, Chiwarakuta, RL, oil, 1N.

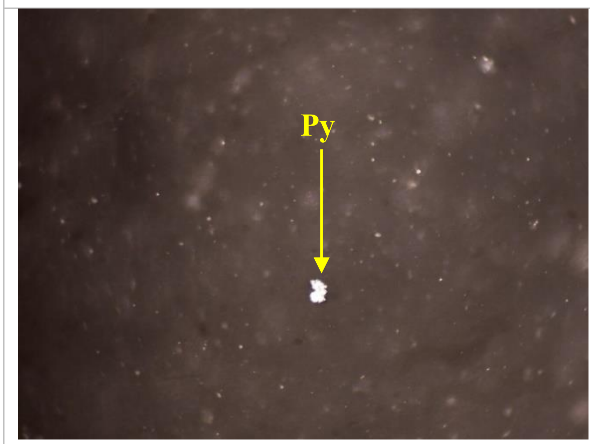

Figure 4.61 Rare specks of pyrite noted in Juba porcellanite, RL, oil, 1N.

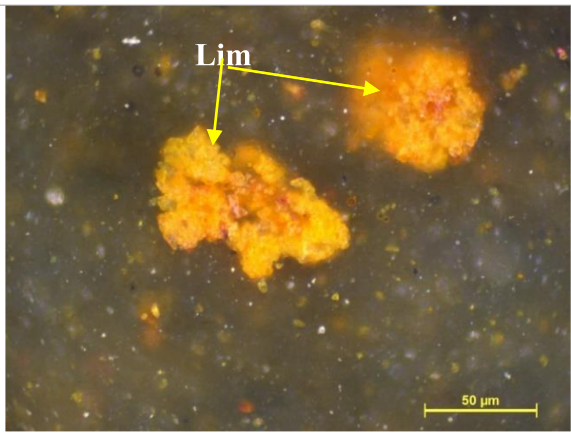

Figure 4.62 Limonitic stains in porcellanite, Chiwarakuta, RL, oil, 1N.

Devitrified shards structure, presence of euhedral to subhedral quartz, presence of feldspar laths, sericite and field evidences indicates their volcanic origin.

4.2.3.1 Modal Analysis of PFA for classification and tectonic setting inferences

The classifications of sandstones are mainly based on the petrographic characteristics of rocks derived from particular provenances. Dickinson and Suczek (1979) and Dickinson et al. (1983) divided clastic sedimentary rocks into three broad provenance classifications, namely, continental block, recycled orogen and magmatic arc. The petrographic characteristics for this study were determined using the Gazzi- Dickinson (Ingersoll et al., 1984) point counting method. James swift- automatic point counter is used for point counting purpose.

4.3.2.2 Gazzi- Dickinson point counting method

This technique is used to statistically measure the volumetric components of a sedimentary rock for classification, chiefly sandstone. A randomly oriented thin section of sedimentary rock is selected to perform point counting using this method. A minimum of 300 representative points should be used to perform the count. These counts are then converted to percentages and used for compositional comparisons in provenance studies. The QFL diagram plots all quartz (Q, including mono- and poly-crystalline varieties) grains together with Feldspar (F) and all unstable Lithics/ Rock fragments (L/R), thus emphasizing grain stability. The emphasis on grain stability shows the influence of weathering, provenance relief and transport mechanism on source rock composition (Dickinson and Suczek, 1979). Petrographic analyses were performed on 8 thin sections prepared from the rock samples collected from PFA (5), feldspathic arenite (2) and ferruginous sandstone (1) of Rehatikhol, Malaikhaman-Chhibarra area. Each thin section was analyzed using the Gazzi-Dickinson point counting method and a total of 500 counts per slide were obtained (Ingersoll et al., 1984). The composition of sandstones of Rehatikhol Formation determined by this method is given in Table 4.1.

Table 4.1 Mineralogical (modal) composition of feldspathic arenite, pyritiferous feldspathic arenite and ferruginous sandstone based on modal analysis by point counting method.

Sample No.	Field nomenclature	Quartz (Q)	Feldspar (F)	Rock Fragment(R)	Matrix	Muscovite	Zircon	Monazite	pyrite	Other opaques	others	Total
MKN/PFA/19	PFA	426	109	0	16	0	2	0	30	0	0	583
CHB/PFA/04	PFA	409	114	0	18	2	1	0	43	0	0	587
CHB/PFA/02	PFA	412	64	4	15	5	3	0	12	1	0	516
JB/PFA/20	PFA	338	75	3	20	5	5	1	30	0	0	477
CHB/PPFA/3	PFA	442	68	0	26	2	2	0	32	0	0	572
MKN/SST/30	Feldspathic arenite	345	127	2	22	7	1	1	0	0	2	507
RTKL/FA/02	Feldspathic arenite	339	84	12	41	20	2	0	0	1	0	499
RTKL/FSST/09	Ferruginous sandstone	364	44	1	72	17	3	1	0	0	1	503
		%										
MKN/PFA/19	PFA	73.07	18.70	0.00	2.74	0.00	0.00	0.00	5.15	0.00	0.00	
CHB/PFA/04	PFA	69.68	19.42	0.00	3.07	0.34	0.34	0.00	7.33	0.00	0.00	
CHB/PFA/02	PFA	79.84	12.40	0.78	2.91	0.97	0.97	0.00	2.33	0.19	0.00	
JB/PFA/20	PFA	70.86	15.72	0.63	4.19	1.05	1.05	0.21	6.29	0.00	0.00	
CHB/PPFA/3	PFA	77.27	11.89	0.00	4.55	0.35	0.35	0.00	5.59	0.00	0.00	
MKN/SST/30	Feldspathic arenite	68.05	25.05	0.39	4.34	1.38	1.38	0.20	0.00	0.00	0.39	
RTKL/FA/02	Feldspathic arenite	67.94	16.83	2.40	8.22	4.01	4.01	0.00	0.00	0.20	0.00	
RTKL/FSST/09	Ferruginous sandstone	72.37	8.75	0.20	14.31	3.38	3.38	0.20	0.00	0.00	0.20	

Table 4.2 QFR composition of sandstones of Rehatikhol Formation for their classification.

Sample No.	Field nomenclature	Quartz (Q)	Feldspar (F)	Rock Fragment(R)	Total	Quartz (Q) %	Feldspar (F)%	Rock Fragment(R) %
MKN/PFA/19	PFA	426	109	0	535	79.63	20.37	0.00
CHB/PFA/04	PFA	409	114	0	523	78.20	21.80	0.00
CHB/PFA/02	PFA	412	64	4	480	85.83	13.33	0.83
JB/PFA/20	PFA	338	75	3	416	81.25	18.03	0.72
CHB/PPFA/3	PFA	442	68	0	510	86.67	13.33	0.00
MKN/SST/30	Feldspathic arenite	345	127	2	474	72.78	26.79	0.42
RTKL/FA/02	Feldspathic arenite	339	84	12	435	77.93	19.31	2.76
RTKL/FSST/09	Ferruginous sandstone	364	44	1	409	89.00	10.76	0.24

Feldspathic arenite consist of 67.94- 68.04 % quartz, 16.0- 25.05 feldspar, 0.39- 2.40 rock fragments, 4.34- 8.22% matrix and minor others. Pyritiferous feldspathic arenite is constituted by 69.68- 77.27 % quartz, 11.89- 18.70 feldspar, 2.33- 7.33% pyrite, upto 0.78% rock fragment, 2.74- 4.55% matrix and minor others. Similarly, ferruginous sandstone consist of 72.37 quartz, 8.75% feldspar, 0.20% rock fragments 14.31% matrix and others. Muscovite and sericite also contribute upto 4.01% component in modal population of feldspathic arenite. Matrix content is progressively increase from pyritiferous feldspathic arenite to feldspathic arenite followed by ferruginous sandstone. Counted point were collected to plot QFR diagram so calculated for % QFR for classification and to deduce provenance of sediments. With the help of point counts following triangular diagrams are prepared to classify the sandstone type and its provenance.

Pettijohn classification diagram (1987): A widely used classification of sandstone types which divides sandstones into arenites (less than 15% of rock is mud matrix) and wackes (more than 15% but less than 75% of the rock is mud matrix). The arenites are subdivided into quartz arenite (more than 95% quartz grains), feldspathic arenite (more than 25% feldspar and more feldspar than rock fragments), subfeldspathic arenite (5–25% feldspar grains and more feldspar than rock fragments), lithic arenite (more than 25% rock fragments and more rock fragments than feldspar), and sublitharenite (5–25% rock fragments and more rock fragments than feldspar). All samples of Pyritiferous feldspathic arenite of Rehatikhol Formation falls in subfeldspathic arenite clan in QFR diagram of Pettijohn classification (Figure 4.63). Samples of feldspathic arenite falls in feldspathic arenite to subfeldspathic arenite clan and ferruginous sandstone is found to be sub feldspathic arenite in QFR diagram (Figure 4.64).

Folk Classification Diagram: Folk proposed a classification for sandstones based on the relative abundances of quartz (Q), feldspars (F), and rock fragments (R). These are the main poles of the classification diagram. All 5 samples of PFA fall in subarkosic field of Folk triangular diagram (Figure 4.65) while samples of feldspathic arenite falls in arkose to subarkose field (Figure 4.66). Ferruginous sandstone is also found to be subarkosic composition according to Fold classification (Figure 4.66).

4.2.3.3 Provenance classification of sandstones

Dickinson ternary plot for Provenance: The composition of source rocks has a great influence on the ultimate composition of sandstone. So, provenance studies are mainly based on modal analysis of detrital framework grains (Dickinson and Suczek, 1979; Dickinson et al., 1983). Dickinson (1985) classified sandstone on the basis of their characteristic petrofacies, which is primarily controlled by the tectonic setting of their provenance. He used detrital modes of 88 sand suites, which reflect different tectonic settings of provenance terrains, and grouped the provenance related to continental sources, into three major types viz-

1). Continental Block: Craton interior, Transitional Continental

2). Basement Uplift.

3). Magmatic Arc: Dissected arc, Transitional arc and undissected arc.

4). Recycled Orogenic

The Q-F-R diagram emphasizing factors controlled by provenance, relief, weathering and transport mechanism as well as source rock based on total quartzose (Q), feldspathic (F) and lithic (R) modes. In this diagram, the studied sample data mainly fall in the Continental Block (Figure4.67 & 4.68), more specifically in the regime of craton interior and transitional continental provenance which suggest that sediments are derived within craton. All samples of pyritiferous feldspathic arenite, feldspathic arenite and ferruginous sandstone indicate similar inferences in QFR ternary diagram (Figure 4.67 & 4.68). Singhora proto basin is part of Bastar Craton so source of sediments must be interior part of part of craton. In general, sediments derived from continental interiors and deposited within intracratonic basins or along passive margins are rich in detrital quartz and poor in lithic fragments, especially volcanic lithics Dickinson and Suczek (1979).

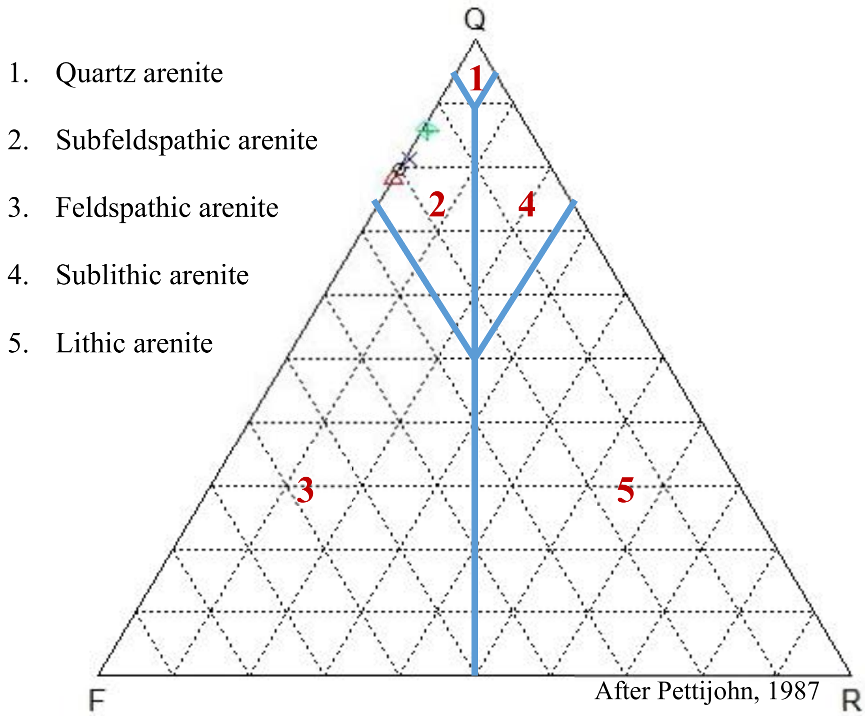

Figure 4.63 Ternary QFR diagram of sandstone classification for pyritiferous feldspathic arenite of Rehatikhol Formation. (After Pettijohn et al,. 1987).

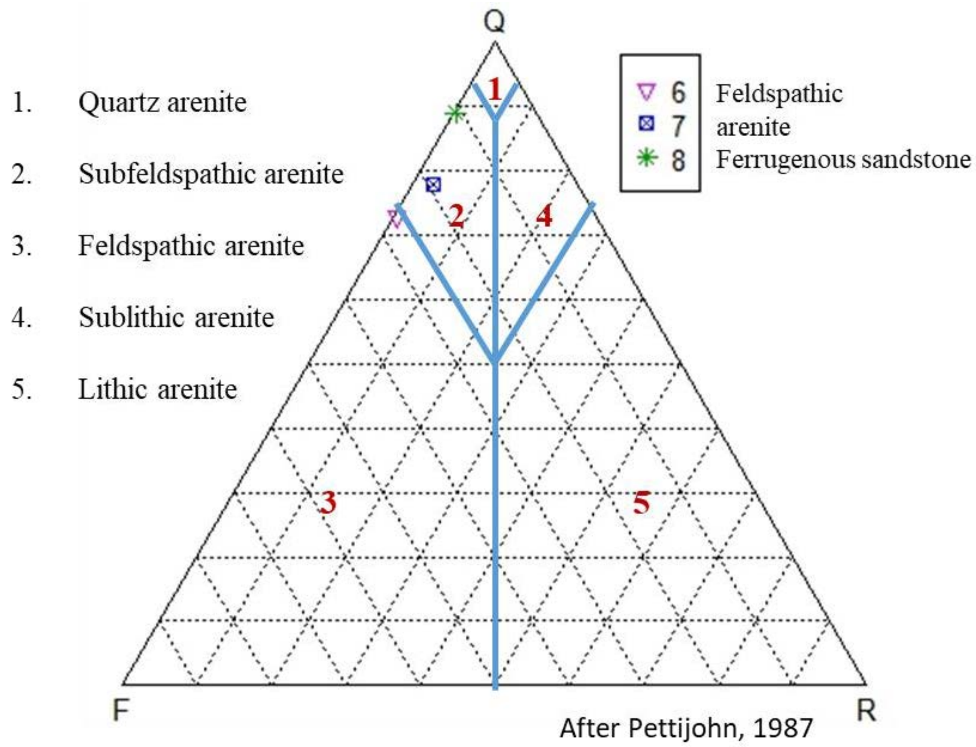

Figure 4.64 Ternary QFR diagram of sandstone classification for feldspathic arenite and ferruginous sandstone of Rehatikhol Formation. (After Pettijohn et al,. 1987).

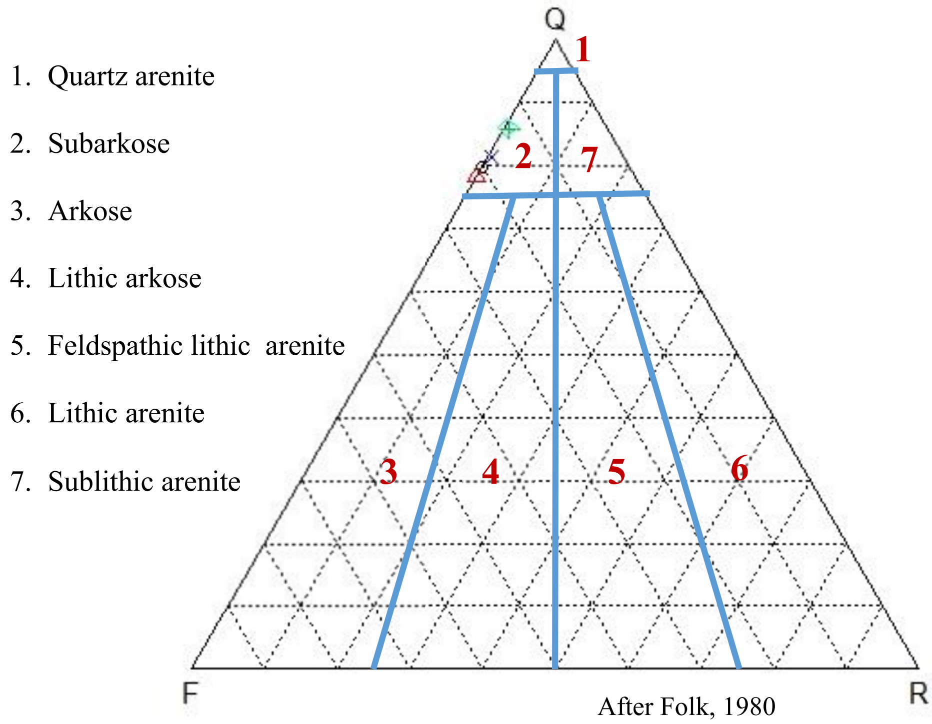

Figure 4.65 Ternary QFR diagram of sandstone classification for pyritiferous feldspathic arenite of Rehatikhol Formation. (After Folk, 1980).

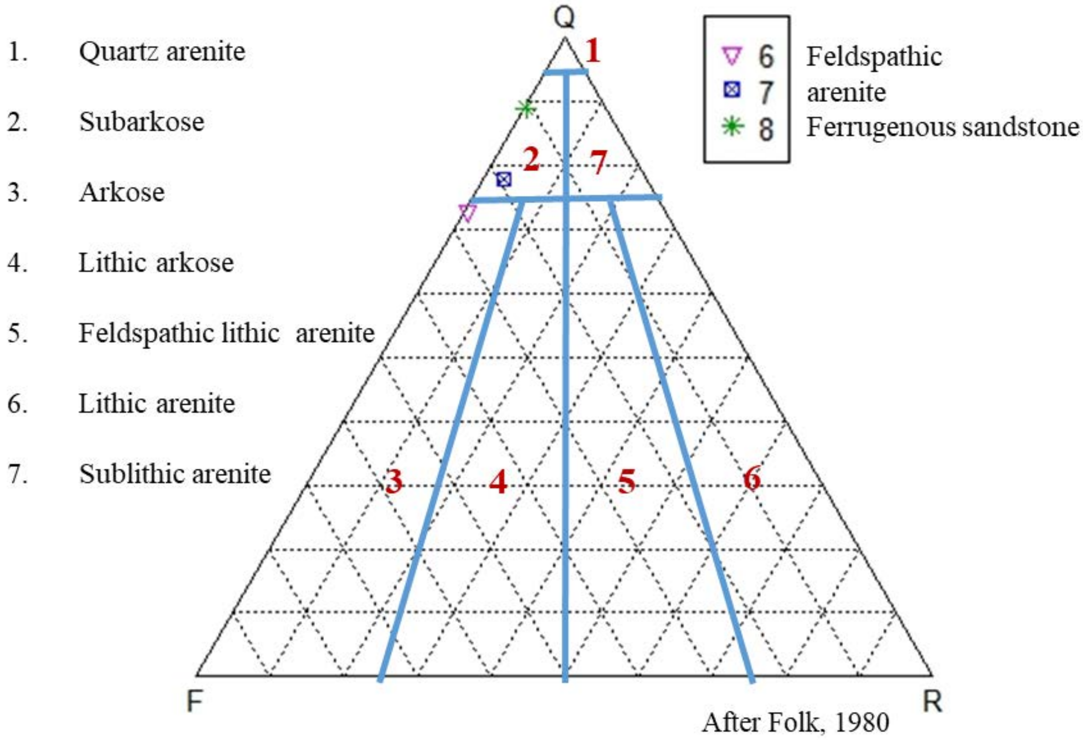

Figure 4.66 Ternary QFR diagram of sandstone classification for feldspathic arenite and ferruginous sandstone of Rehatikhol Formation. (After Folk, 1980).

Feldspathic arenite and sub feldspathic arenite are primarily derived from feldspar rich rocks like granite but apart from appropriate provenance geology, climate and source area relief are also important factors. Under humid conditions feldspars weather to clay minerals so semi-arid and cold climate favour feldspathic arenite formation. It is known that the feldspar may escape destruction and thus be transported and deposited with quartz sands if rates of uplift, erosion, and deposition are great enough. Under such conditions, irrespective of the climate, weathering processes are incomplete and the sands derived from such terrain are high in feldspar content. Arkoses, therefore, may be said to indicate either a climatic extreme or high relief. Hence, feldspathic (microcline and perthites) nature of Rehatikhol sandstone suggest semi-arid and cold climatic condition prevailing in source area.

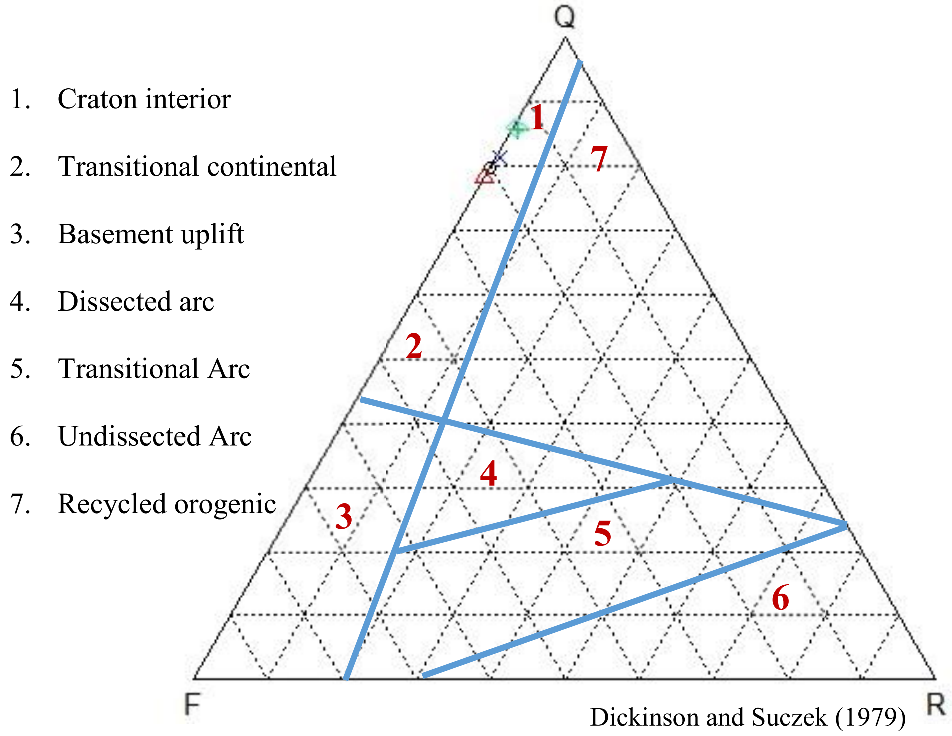

Figure 4.67 Provenance discriminant diagram of PFA of Rehatikhol Formation after Dickinson and Suczek (1979).

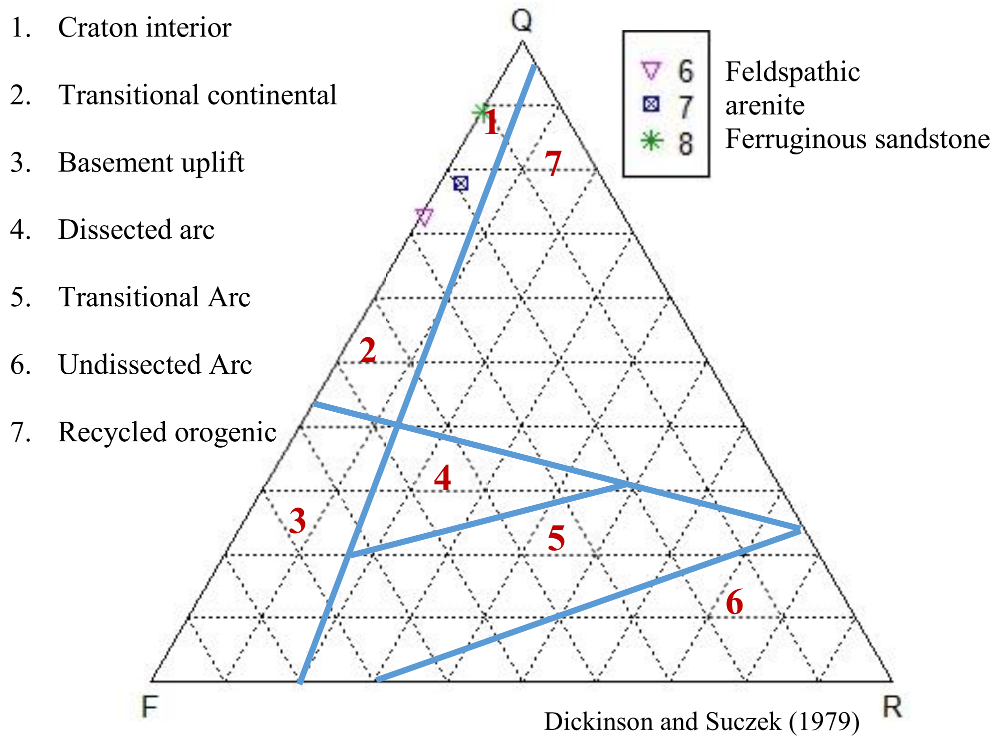

Figure 4.68 Provenance discriminant diagram of feldspathic arenite and ferruginous sandstone of Rehatikhol Formation after Dickinson and Suczek (1979).

CHAPTER 5
GEOCHEMISTRY

5.1 INTRODUCTION

Geochemistry is qualitative and quantitative approach to determine the distribution and migration of chemical elements in earth materials enabling us to understand various earth processes. Geochemical characterisation of igneous and sedimentary rocks is greatly used for classification, tectonic setting, source rock studies, crystallisation, chemical precipitation, paleoweathering and paleoclimatic studies. The composition of source rocks has a great influence on the ultimate composition of sandstone. So, provenance studies are mainly based on modal analysis of detrital framework grains (Dickinson and Suczek, 1979) and bulk rock geochemistry (Bhatia; 1983, 1985; Bhatia and Crook, 1986).

The chemical and mineralogical compositions of clastic sedimentary rocks are influenced by source rock characteristics, weathering, sorting processes during transportation, sedimentation and diagenetic processes. Hence, the composition (both mineralogical & chemical) of sedimentary rocks is generally used for identification of provenance, weathering conditions and tectonic settings (Taylor and McLennan, 1985). Geochemistry of sandstone is useful to understand provenance characterization, paleoclimatic conditions and intensity of chemical weathering. Major elements of sediments are helpful for determination of their original detrital mineralogy. The K_2O/Al_2O_3 ratio, Index of Compositional Variability (ICV), Chemical Index of Alteration (CIA), SiO_2-Al_2O_3+K_2O+Na_2O diagram and Al_2O_3-CaO+Na_2O-K_2O (A-CN-K) plot are useful geochemical parameters for the study of provenance, paleoclimate conditions, maturity and intensity of weathering (Nesbitt and Young, 1984).

Trace elements such as La, Y, Sc, Hf, REEs etc. are used as indicators of provenance, geological processes and tectonic setting due to their relatively low mobility and insolubility during sedimentary processes. In geochemical provenance studies geochemical analysis of shales is used because of their homogeneity before deposition, post deposition impermeability and higher abundance of trace elements. The relatively immobile elements such as Sc, Zr, REEs show very low concentrations in natural waters and are thus transported from the source rock to the clastic rocks almost quantitatively. Various weathering indices such as CIA, CIW and PIA are calculated to estimate the weathering at source and post deposition alteration of sandstones. Geochemical interpretation are being corroborated with petrographic characteristics and outcome is deduced to give overall inferences.

Geochemistry of basement rocks i.e. Sambalpur granitoids and intrusives into it, has been studied in detail to determine their geochemical characteristics. Geochemical characterisation of Rehatikhol sediments also carried out to deduct provenance, tectonic setting, paleoweathering and paleoclimatic conditions. Furthermore, relationship of paleoclimate conditions with intensity of chemical weathering in source area also has been interpreted using geochemical diagrams. A total 82 samples of Granitoid, pyritiferous feldspathic arenite, pebbly PFA, mafic, ultramafic and shale samples from study and surrounding area have been analysed for major oxides and selected trace elements using WD-XRF technique.

5.2 METHODOLOGY

5.2.1 WD-XRF

In XRF, X-ray are produced by a source irradiate sample. In most cases the source is an X-ray tube. The element present in the sample will emit fluorescent X-ray radiation with discrete energies (equivalent to colour for optical light) that are characteristic for these elements. A different energy is equivalent to different colour. By measuring the energies (determining the colours) of the radiation emitted by the sample it is possible to determine which elements are present. This step is called qualitative Analysis. By measuring these intensities of the emitted energies (colours) it is possible to determine how much of each element is present in the sample. This step is called quantitative analysis. Wavelength dispersive XRF uses a crystal to separate the various wavelengths: for every angle of incident radiation, the only wavelength reflected to the detector is the one that conforms to Bragg"s formula: $n\lambda = 2d \sin\theta$

Where n is a whole number, λ is the wavelength of the x-ray radiation used; d is a constant characteristic of every crystalline substance (i.e. the x-ray crystal); and θ is the angle on incidence of the x-radiation on the sample. So, by changing the angle of the crystal, you can select for specific elements of interest. In the ARL PERFOM'X -269 at AMD/CR Nagpur, this is all done automatically and any combination of elements can be analyzed. The system changes crystals for the various elements, calculates the overlap of elements within the spectrum and yields results in any form desired: qualitative, ratio, quantitative, graphic. The ARL PERFORM'X -269, WDXRF(MAGIX PRO) is capable of measuring all elements from beryllium (atomic number 4) to uranium (atomic number 92) and beyond (at trace levels, often below one part per million, and up to 100%).

Major, trace elements of representative samples from study area have been analyzed using Wavelength Dispersive X-Ray Fluorescence Spectroscopy (WD-XRFS). The analytical technique used is governed by both, element–technique amenability and concentration of the element of interest. For these analysis, samples are first cleaned using ultrasonic cleaner and then dried and powdered with the help of crushers, ball mill and pulveriser to –100 mesh. Finally, the powdered samples are grounded to –250 to – 300 mesh in agate mortar and then samples are prepared as compressed powder pellets or fused glass discs and excited with x-ray radiation, normally generated by an x-ray tube operated at a potential of between 10 and 100 kV.

Table 5.1 Precisions, accuracy and detection limit of WD-XRF.

Element/Oxide	**Precission**	**Accuracy (%error)**	**Detection Limit**
Si, Al, Ti, Fe, Ca, K	<1%	<5%	0.01%
Na_2O and MgO		4-5%	
Mn and P		5-10 % (if conc is <0.1%)	
Trace Elements		<5% (if conc>100 ppm) ± 5% (if conc is >30 ppm but <100 ppm) ± 10 %(if conc is <30ppm).	10 ppm

Na, Mg, Al, Si, P, K, Ca, Ti, Mn, Fe and selected trace elements, including Rb, Sr, Y, Nb, Zr, Cr, Ni, Cu, Zn, Ga, Ba, Pb, Th and U. Detection limits for many of these trace elements lie in the range 5 to 10 ppm rock under routine operating conditions. Quantitative analyses of major and trace elements were made on Fully Automated Sequential ARL Performa's 269 WD-XRFS. The spectrometer is a sophisticated platform to enable accurate and rapid analysis of up to 90 elements in nearly any solid or liquid sample.

The ARL PERFORM'X spectrometer has a novel compact design and offers the superior benefits of XRF analysis including repeatability, sensitivity and ease of use while establishing new standards of speed, consistency and flexibility on a broad range of samples. Precision, accuracy (% error) and detection limit of WD-XRF instrument at AMD/CR Nagpur has been given in table 5.1

5.2.2 Inductively coupled plasma- atomic/optical emission spectroscopy (ICP- AES/OES)

The ICP was developed for optical emission spectrometry (OES) by Fassel et al. at Iowa State University in the US and by Greenfield et al. at Albright & Wilson, Ltd. in the UK in the mid-1960s. In ICP-OES, the sample is subjected to plasma where the component elements are excited to a higher energy state. These excited atoms return to their ground state by releasing emission rays. The wavelength of the emission ray is characteristic of the element and the intensity of the emission ray gives the concentration of the element. The first step for analysis of a sample by ICP-OES is preparing the sample solution and the corresponding standards for introduction to the instrument. This depends on the physical and chemical properties of the analyte of interest and the sample matrix. Then a suitable ICP methodology is to be programmed using the software provided with the instrument. First a calibration curve is prepared with the prepared standards and then the sample concentrations are measured relative to the standards. Finally the results are tabulated and reported as required. In principle all the elements of periodic table except for Argon can be analysed by ICP-OES. But practically all the elements except inert gases, oxygen, nitrogen, halogens (except iodine) and some radioactive elements are estimated routinely by ICP-OES. Particularly the REEs, refractory elements and light elements such as Li, Be and B show excellent sensitivity in ICP-OES.

Geological Scope of ICP-OES- Major, minor and trace elements from different Geological samples such as rock, minerals, hydro-geochemical, core rock can be analyzed by ICP-OES.

- ✓ 10 major oxides (i.e. SiO_2, Al_2O_3, Fe_2O_3, MgO, CaO, Na_2O, K_2O, TiO_2, MnO and P_2O_5) in normal silicate rock samples can be determined with detection limit as low as % (except for K_2O and P_2O_5).
- ✓ Li, ba, Sr, Sc, Y, La, Zr, V, Nb, Cr, Co, Ni, Cu, Zn are conveniently estimated by ICP-OES.
- ✓ Mo, Ag, Cd, Hg, Pb can be measured in mineralized samples.
- ✓ Sn, W, U and Th can be measured above 50µgg-1.
- ✓ Some rare earth elements can be measured at sub ppm levels for while others are estimated at ppm levels except for Pm.

Detection limit of ICP-AES for different elements is tabulated in Table 5.2. Rare Earth Elements (REE) and few trace elements of representative samples from study area have been analyzed using Inductively Coupled Plasma- Atomic/Optical Emission Spectroscopy (ICP-AES/OES) model Horiba Jovin Vyon-Ultima-2 (France make) at AMD/CR Nagpur. The analytical technique used is governed by both, element–technique amenability and concentration of the element of interest. Analysis of fluoride has been carried by Ion Selective Electrode method at chemistry lab, CR, Nagpur.

5.3 GEOCHEMISTRY OF BASEMENT ROCKS

The data obtained from WD-XRF and Chemistry laboratories, Nagpur are processed for different ratios and indices. The analytical data hence obtained is used to plot various binary, ternary and discrimination diagrams. Interpretations thus made on the basis of the variation diagrams will help in substantiating the observations made in the field and the result obtained from petrographic studies. Further corroboration of the data will help in the characterization of the rocks and their geochemical behaviour.

5.3.1 Major oxide and trace element Geochemistry of Granitoids

Geochemical characterisation of Sambalpur granitoids has been attempted in the present work for nomenclature of various litho-units, to assess source magma composition, identifying chemical variations, intra-elemental abundance and inter-elemental relationship etc. Besides, major and trace element data are also useful in understanding the nature of possible source and the tectonic environment of emplacement of granites and their distinct characteristics.

The samples (n= 6) of pink porphyritic biotite granite from Gatkachhar- Rehatikhol area have characterized by variable SiO_2 (64.63-72.67%), Al_2O_3 (14.68-16.23%), highly variable FeO (T) (1.48-5.82%), CaO (0.12-3.96 %), Na_2O (1.35-4.22%) and K_2O (1.67-5.25%) (Table 5.3). The samples also characterized variable P_2O_5 (0.06- 0.20%) Rb (48-189 ppm), Sr (73- 759 ppm), Zr (118-189ppm) and Ba (986-2423 ppm) and <10- 80 ppm Pb (Table 5.3). These samples are collected just near to basin margin and from Gatkachhar inlier.

Table 5.2 Detection limit (in ug/L) of ICP-OES for different elements at chemistry lab, CR, Nagpur (for pure solutions).

Element	**Ag**	**Al**	**As**	**Au**	**B**	**Ba**	**Be**	**Bi**	**Ca**	**Cd**	**Ce**	**Co**	**Cr**	**Cu**
Det. limit	0.6	1	1	1	1	0.03	0.09	1	0.05	0.1	1.5	0.2	0.2	0.4
Element	**Cu**	**Dy**	**Er**	**Eu**	**Fe**	**Ga**	**Gd**	**Ge**	**He**	**Hg**	**Ho**	**In**	**Ir**	**K**
Det. limit	0.4	0.5	0.5	0.2	0.1	1.5	0.9	1	0.5	1	0.4	1	1	1
Element	**Mo**	**Na**	**Nb**	**Nd**	**Ni**	**Os**	**P**	**Pb**	**Pd**	**Pr**	**Pt**	**Rb**	**Re**	**Rh**
Det. limit	0.5	0.5	1	2	0.5	6	4	1	2	2	1	5	0.5	5
Element	**Ru**	**S**	**Sb**	**Sc**	**Se**	**Si**	**Sm**	**Sn**	**Sr**	**Ta**	**Tb**	**Te**	**Th**	**Ti**
Det. limit	1	10	2	0.1	2	10	2	2	0.05	1	2	2	2	0.4
Element	**TI**	**Tm**	**U**	**V**	**W**	**Y**	**Yb**	**Zn**	**Zr**					
Det. limit	2	0.6	10	0.5	1	0.2	0.1	0.2	0.5					

Table 5.3 Summary of major oxide and trace elements data of pink porphyritic biotite granite (n=6) of Rehatikhol- Gatkachhar.

Major oxide in %	**SiO_2**	**TiO_2**	**Al_2O_3**	**FeO**	**MgO**	**MnO**	**CaO**	**Na_2O**	**K_2O**	**P_2O_5**
Average	68.28	0.34	15.18	4.02	2.28	0.06	2.36	3.59	3.30	0.14
Maximum	72.67	0.47	16.23	5.82	3.29	0.10	3.96	4.22	5.25	0.20
Minimum	64.63	0.15	14.68	1.45	0.67	0.02	0.12	1.35	1.67	0.06

Trace elements in ppm	**Cr**	**Ni**	**Cu**	**Zn**	**Ga**	**Rb**	**Sr**	**Y**	**Zr**	**Nb**	**Ba**	**Ce**	**Pb**	**Th**	**U**
Average	61.5	61.8	17.7	77.3	27.0	105.2	502.0	-	162.0	-	1496.3	129.5	-	34.2	-
Maximum	84	78	23	102	31	189	759	58	189	229	1966	167	80	49	55
Minimum	34	53	15	35	25	48	73	<10	118	<10	986	89	<10	24	<10

Table 5.4 Summary of major oxide data of biotite granite of Kashipali- Chhibarra- Bindhanpali area.

Major oxide in %	**SiO_2**	**TiO_2**	**Al_2O_3**	**FeO**	**MgO**	**MnO**	**CaO**	**Na_2O**	**K_2O**	**P_2O_5**
Average	70.78	0.23	15.10	1.05	1.11	0.05	1.77	4.12	3.65	0.42
Maximum	75.40	0.46	17.10	3.55	2.21	0.08	4.30	4.44	5.09	0.72
Minimum	67.20	0.05	13.56	0.04	0.13	0.02	0.47	3.67	1.76	0.02

Trace elements in ppm	**Cr**	**Ni**	**Cu**	**Zn**	**Ga**	**Rb**	**Sr**	**Y**	**Zr**	**Nb**	**Ba**	**Ce**	**Pb**	**Th**	**U**
CHB/GR/7	29	90	17	25	28	200	55	47	71	33	357	15	116	45	35
BPL/GR/8	22	55	18	32	28	155	252	5	99	15	633	60	85	45	24
PKL/GR/9	55	84	12	44	24	149	544	5	134	5	1803	166	33	22	5

The samples (n= 8) of biotite granite from Kashipali- Chhibarra- Bindhanpali area (slightly away from basin margin) have characterized variable SiO_2 (67.63-75.40%), Al_2O_3 (13.56-17.10%), highly variable FeO (T) (0.04-3.55%), CaO (0.47-4.30 %), Na_2O (3.67-4.44%) and K_2O (1.67-5.09%) (Table 5.4). Three samples out of these analysed for trace elements that shows variable Rb (149-200 ppm), Sr (55- 544 ppm), Zr (71-134 ppm) and Ba (357-1803 ppm) and 33-116 ppm Pb (Table 5.4). These samples are collected just near to basin margin and from Gatkachhar inlier. One sample of granitoid (pink porphyritic granite rich in alkali feldspar phenocryst near Murmuri outlier) characterised 59.2% SiO_2, high Al_2O_3 (20%), moderate FeO (T) (0.85%), CaO (2.57 %), Na_2O (3.67-5.62 %) and K_2O (5.1 %). Sample of feldspathic injection in WNW shear zone near Kurapali characterised 62.45% SiO_2, 1.60% TiO_2, 17.15% Al_2O_3, 0.43% Fe_2O_3 (T), 1.23% CaO, 2.05% N_2O and high K_2O (14.39%) with 394ppm Rb, 15ppm Sr, 61ppm Zr and 2032ppm Ba. The pink biotite granites of Juba (n=2) area characterised SiO_2 (72-74.50 %), Al_2O_3 rages 14.47-15.05%, FeO (T) varies 0.25-0.45 %, CaO less and ranges 0.20- 40 %, Na_2O ranges 3.67-4.44% and K_2O ranges 1.67-5.09%.

5.3.1.1 Implication on classification, tectonic setting and magmatic activity

Various binary and ternary diagram has been plotted from the major and trace element of data of Sambalpur Granitoids to draw inferences about their classification, tectonic setting and magmatic activity. In the classical AFM diagram after Irvine and Baragar, 1971 (Figure 5.1), all the studied samples fall in a typical calc alkaline Al enrichment field. In the Ab-Or-An triangular plot of O`connor (1965) for feldspar, it is observed that all variant of basement granite samples are rich in albite and orthoclase and fall in granite to granodiorite, except of three sample which fall in tonalite and trondhjemite field of plot (Figure 5.2). In SiO_2 vs Na_2O+K_2O plot for plutonites (Middlemost 1994) all samples fall in granite to granodiorite field (Figure 5.3). Majority of the granite samples plot in peraluminous to meta-aluminous field except one sample of quartzo feldspathic injections in granitoid plot in peralkaline field

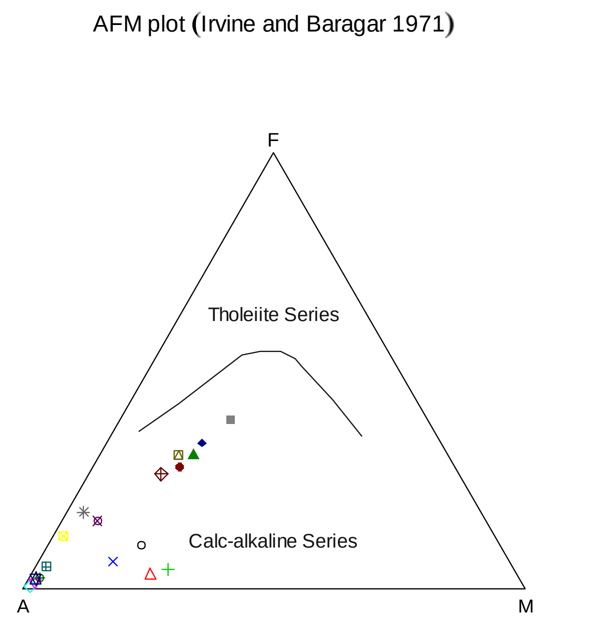

Figure 5.1 AFM ternary plot for granitoid of the study area (after Irvine and Barager, 1971).

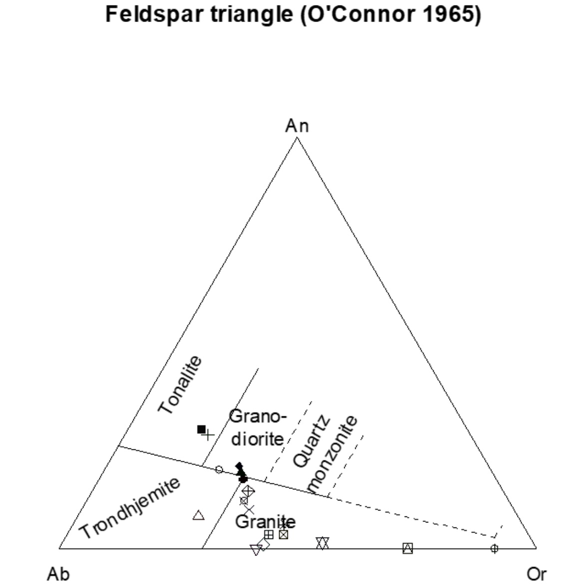

Figure 5.2 Ab-Or-An triangular plot of O`connor (1965) for feldspar of granitoids.

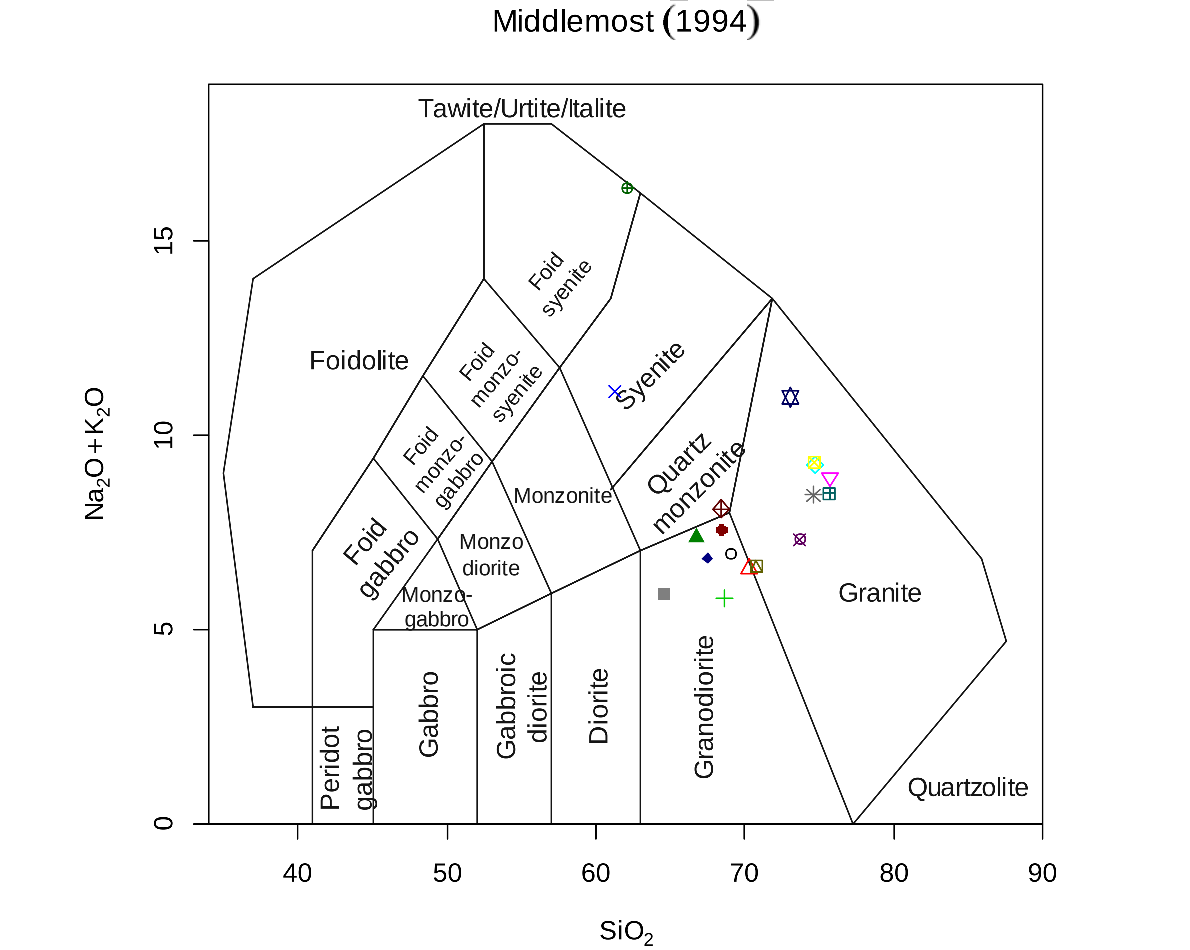

Figure 5.3 TAS classification plots of granitoid of study area (after Middlemost, 1994).

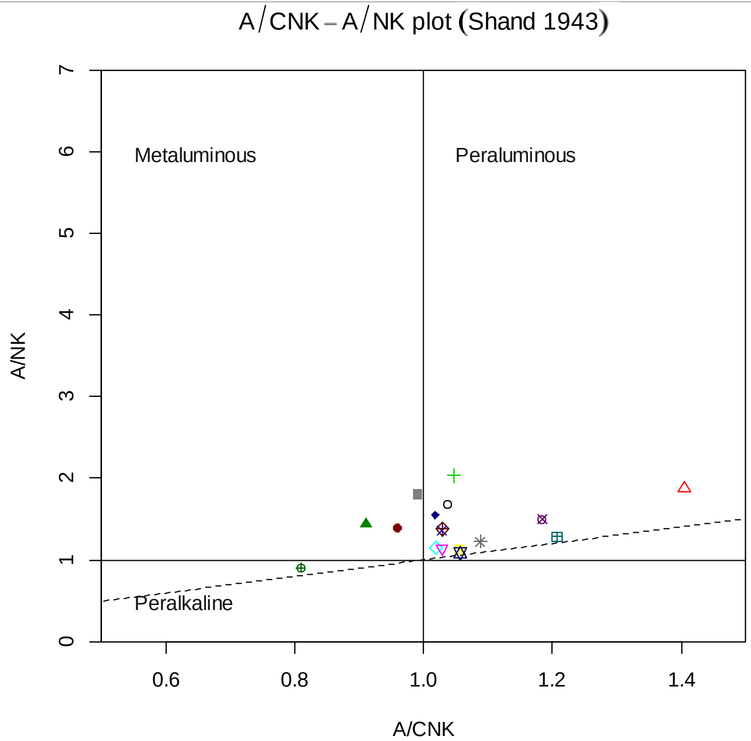

Figure 5.4 A/NK vs. A/CNK plot for Sambalpur Granitoids (after Shand, 1943).

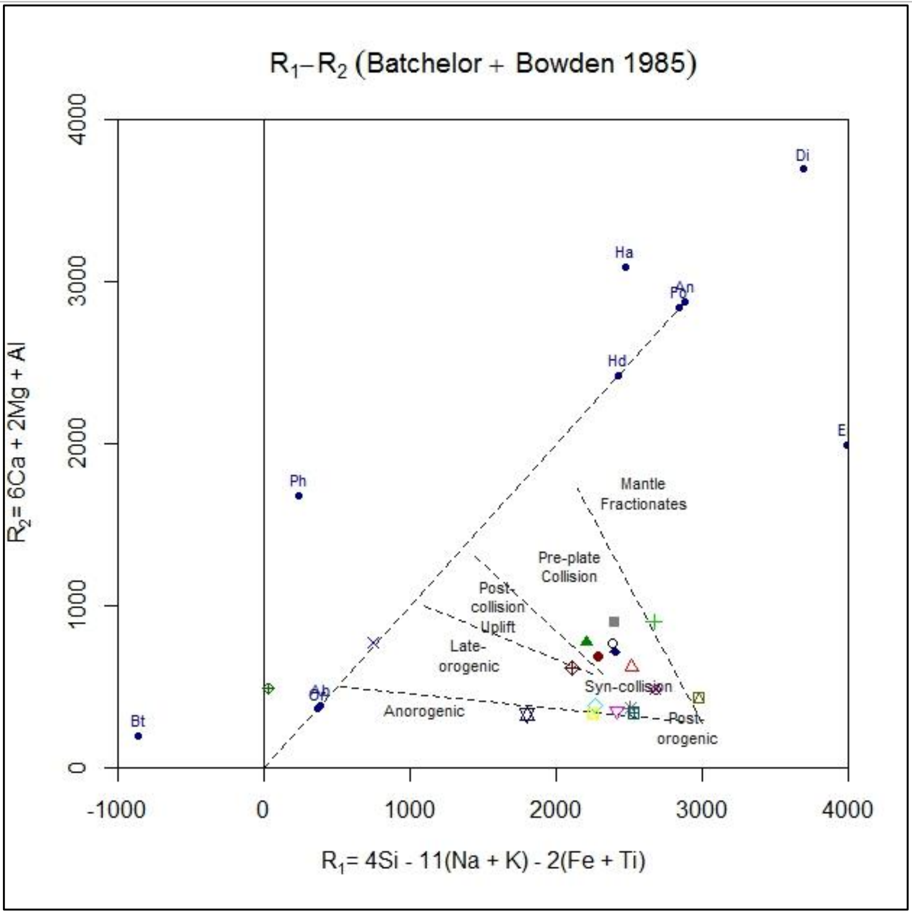

Figure 5.5 R1 vs R2 plot of Batcher and Bowden 1985 for tectonic setting of granitiods of study area.

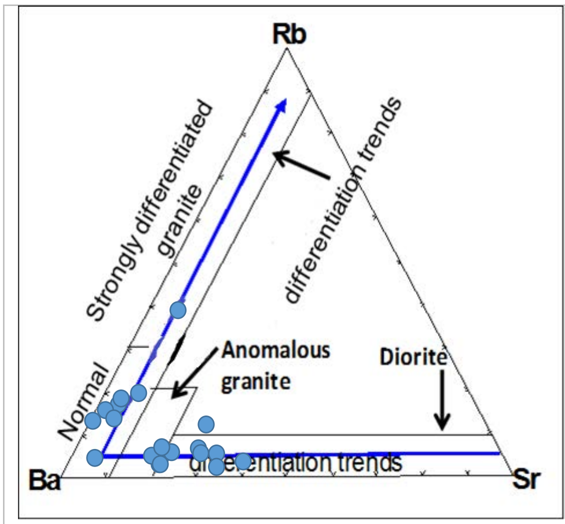

Figure 5.6 Rb- Sr- Ba ternary diagram of EI Bouseily (1975) for granitoids.

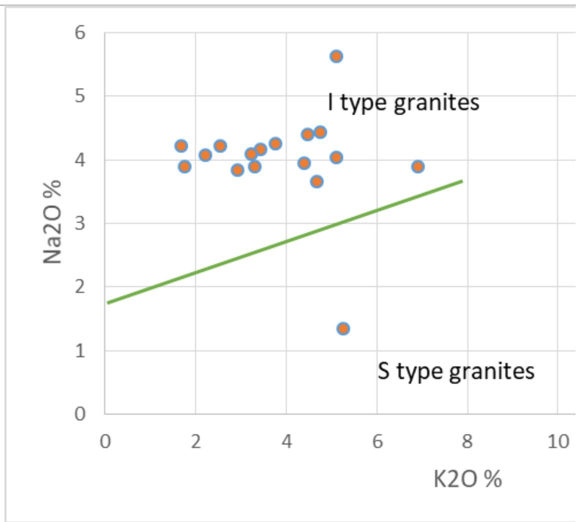

Figure 5.7 Na_2O-K_2O binary plot for granitoids (after Chappell and White, 2001)

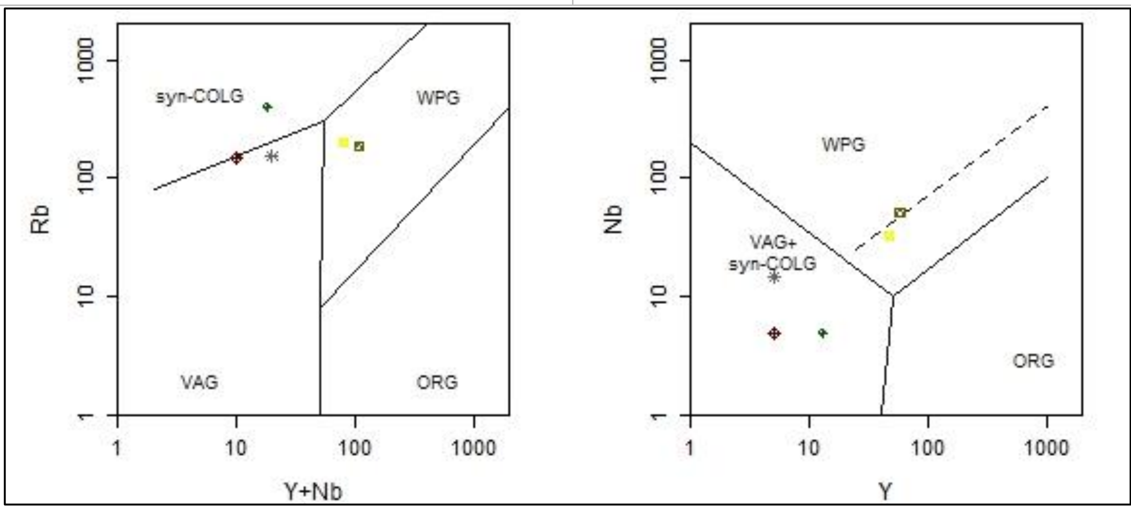

Figure 5.8 Nb vs Y and Rb vs (Y+Nb) tectonic discrimination plots of granitoids (after Pearce et al.1984).

in A/CNK vs A/NK plot (Shand, 1943) (Figure 5.4). Batcher et al.(1985) used combination of element as R1 vs R2 plot was R1=4Si-11(Na+K)-2(Fe+Ti) and R2= 6Ca+2Mg+Al (Figure 5.5) to see tectonic setting of the rocks. Majorities of the samples of granite plot in syn collision to pre plate collision field, i. e. granite rock is basement type not an intrusive phase. Rb-Ba-Sr ternary diagram of EI Bouseily, 1975 (Figure 5.6) for granite are plotted. It has observed that all the granite samples followed the trend of differentiation. Granite is normal to anomalous granite type.

Granites in study area have less Rb/ Sr ratio (1.03), less differentiation index (82.80), major oxide data and K_2O vs Na_2O diagram of Chapell and white, 2001 (Figure 5.7) indicates their I type granite nature. One sample of feldspathic injection corresponds to S type granite field. Pearce et al.(1984) used combination of trace element such as Nb vs Y and Rb vs (Y+Nb) to distinguish between granitoids, the samples of basement granite of the area plot (Figure 5.8) in syn- collision granite and WPG (within plate granitoid).The Pearson correlation matrix (Table 5.5) of major element compositions show very good correlation of SiO_2 with MgO, Al2O3, CaO, TiO_2 and MnO (>0.5) whereas good correlation with FeO(t), Na_2O and P_2O_5 and least correlation with K_2O and Na_2O. Among K_2O and Na_2O, correlation with K_2O is higher than Na_2O and between CaO and FeOt, CaO is higher. All these observations suggest moderate differentiation within the magma which gave rise to the granites. SiO_2 shows negative correlation with Al_2O_3 and K_2O, CaO. FeO follows TiO_2 as ilmenite is among an important accessory mineral in the granites. CaO shows positive correlation with P_2O_5 which indicate possibility of apatite mineral in granite.

Table 5.5 Pearson correlation coefficients of major elements in Granitoids.

	SiO_2	**TiO_2**	**Al_2O_3**	**FeO**	**MgO**	**MnO**	**CaO**	**Na_2O**	**K_2O**	**P_2O_5**
SiO_2	**1.00**									
TiO_2	-0.69	1.00								
Al_2O_3	-0.82	0.50	1.00							
FeO	-0.29	0.05	-0.14	1.00						
MgO	-0.66	0.20	0.39	0.73	1.00					
MnO	-0.57	0.06	0.35	0.54	0.88	1.00				
CaO	-0.64	0.27	0.37	0.42	0.80	0.87	1.00			
Na_2O	-0.08	-0.45	0.07	-0.13	0.11	0.39	0.36	1.00		
K_2O	-0.14	0.63	0.14	-0.33	-0.52	-0.63	-0.48	-0.50	1.00	
P_2O_5	-0.49	0.54	0.63	-0.48	0.06	0.24	0.33	0.11	0.23	1.00

Table 5.6 Summary of CIPW Norms of the Sambalpur Granitiod of the study area.

	Q	C	Or	Ab	Or+Ab	An	Ns	Di	Hy	Il	Tn	Ru	Ap	Sum	Diff Index
KSP/GR/1	25.28	2.18	15.01	35.71	50.72	12.09	0.00	0.00	4.41	0.15	0.00	0.30	1.59	96.71	88.09
CHB/GR/2	30.48	6.54	13.12	34.52	47.64	3.96	0.00	0.00	5.16	0.13	0.00	0.33	1.59	95.82	82.09
CHB/GR/3	27.31	2.49	10.40	33.00	43.40	16.63	0.00	0.00	5.51	0.17	0.00	0.37	1.71	97.58	87.34
GPL/GR/5	29.87	1.63	28.01	37.57	65.58	0.64	0.00	0.00	0.32	0.09	0.00	0.02	1.35	99.50	96.09
KPL/GR/6	32.51	1.63	26.36	37.23	63.59	0.00	0.00	0.00	0.40	0.06	0.00	0.02	1.24	99.45	96.10
CHB/GR/7	29.02	0.78	30.09	34.09	64.18	2.16	0.00	0.00	0.59	0.03	0.00	0.05	0.06	96.85	95.35
BPL/GR/8	32.31	1.15	27.55	31.03	58.58	3.66	0.00	0.00	0.90	0.07	0.00	0.11	0.04	96.81	94.54
PKL/GR/9	21.54	0.70	22.14	36.04	58.18	9.45	0.00	0.00	4.89	0.09	0.00	0.23	0.27	95.36	89.17
KPL/GR/10	0.07	0.00	85.04	8.09	93.14	0.00	2.16	0.00	0.95	0.01	0.38	1.44	2.02	100.16	95.36
JB/GR/14	22.24	0.80	40.78	33.00	73.78	0.99	0.00	0.00	0.42	0.01	0.00	0.04	0.00	98.28	97.00
JB/GR/15	33.54	2.48	26.00	33.42	59.43	1.98	0.00	0.00	0.50	0.02	0.00	0.04	0.00	97.99	94.95
GTK/GR/15	33.40	2.47	19.57	32.93	52.50	6.87	0.00	0.00	1.68	0.05	0.00	0.12	0.14	97.22	92.76
GTK/GR/16	39.59	8.33	31.01	11.39	42.40	0.00	0.00	0.00	4.82	0.07	0.00	0.29	0.21	95.72	81.99
GTK/GR/18	20.73	0.21	9.88	35.72	45.61	18.64	0.00	0.00	8.20	0.22	0.00	0.36	0.36	94.31	84.97
RTKL/GR/19	22.69	0.00	20.23	35.31	55.54	11.32	0.00	0.00	5.92	0.13	0.52	0.07	0.37	96.56	89.55
RTKL/GR/20	20.41	0.00	19.06	34.59	53.65	12.19	0.00	1.18	6.19	0.16	0.81	0.00	0.46	95.05	86.25
RTKL/GR/21	24.05	0.67	17.28	32.44	49.72	12.46	0.00	0.00	6.73	0.20	0.00	0.25	0.40	94.48	86.22

CIPW norm of these granites are calculated that reveal that rock is Alkali rich granite with higher albite and orthoclase content along with quartz and plagioclase. The basement granitoids show normative albite, quartz, k-feldspar and anorthite with have an average content of 32.42, 24.75, 26.20 and 6.72% respectively (Table 5.6).

Table 5.7 Summary of REE analysis of Sambalpur Granitoids in and around study area.

Sample No	La	Ce	Pr	Nd	Sm	Eu	Gd	Tb	Dy	Ho	Er	Tm	Yb	Lu	Y	∑REE	∑LREE	∑HREE	LREE/HREE
Max	62	104	30	34	7	1	9	1	3	1	2	1	2	1	16.6	258	238	20	11.9
Min	16	23	5	14	2.5	0.5	4	1	2	1	1	1	1	1	8.3	73	61	12	5.083
Avg	48	75.8	16	27.4	5.7	0.9	6.4	1	2.2	1	1.4	1	1.2	1	11	189	173.8	15.2	11.43

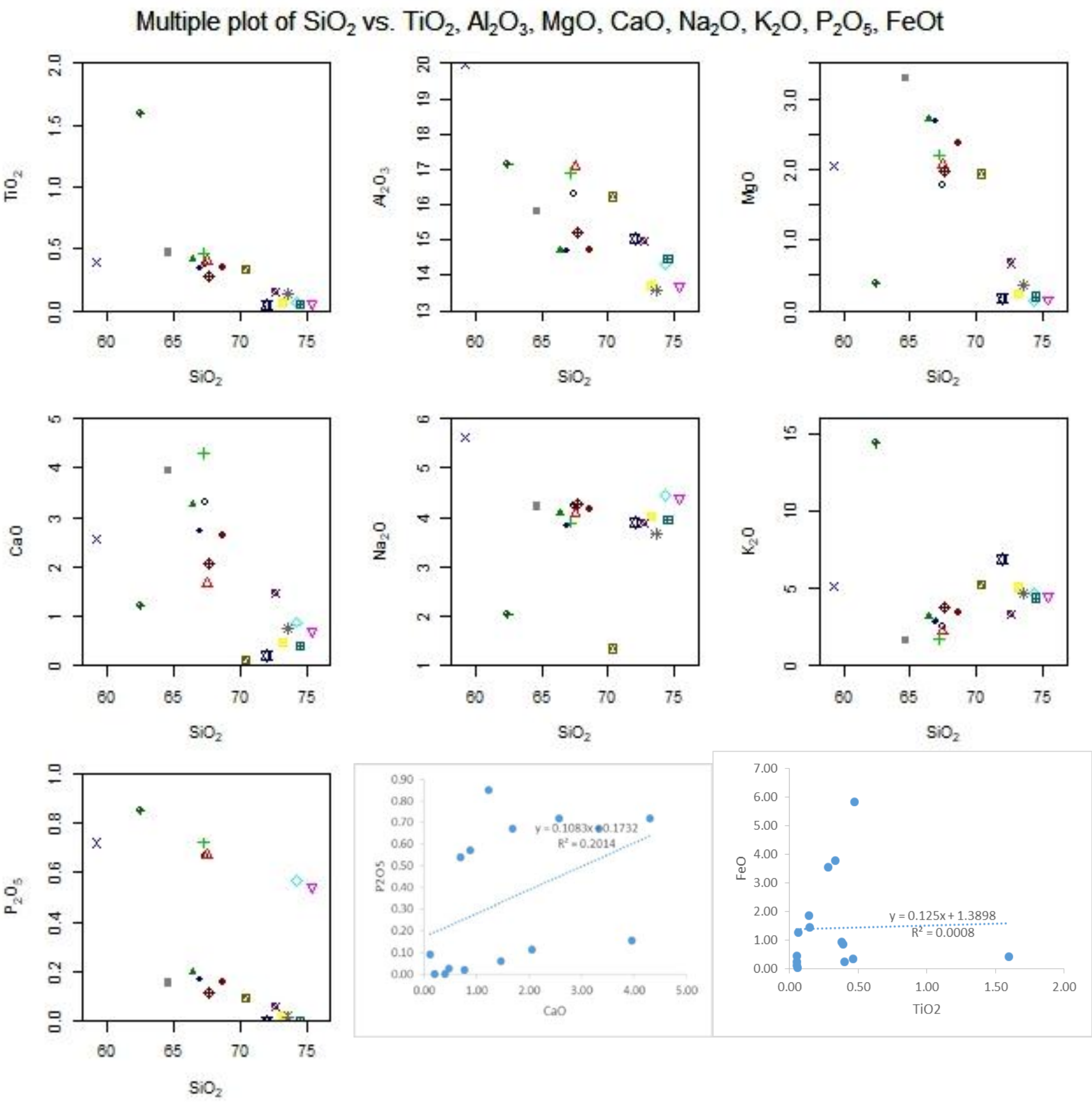

Figure 5.9 Hawkers variation diagram for SiO_2 vs other major oxide of granitoids.

In Harker variation diagrams (Figure5.9) the overall decreasing trends of MgO, FeOt, CaO, TiO_2 and P_2O_5 with progressive increase of SiO_2 have been observed which probably indicates the early fractionation of plagioclase (due to decrease of CaO), amphiboles (due to decrease of CaO, FeOt, MgO, TiO_2) and resistants such as apatite, zircon, rutile, ilmenite etc (Haruna et al., 2013).

5.3.2 REE geochemistry of Sambalpur Granitoids

Samples (n=8) of basement granitoids are analysed for their REE content at Chemistry Lab , CR. Rare Earth Elements geochemistry is important tool to characterize igneous rock to understand various aspects of their petrogenesis. Yttrium is also included with the REE group, because they share chemical and physical similarities with the lanthanides. The REE data of selected samples (n= 8) have been studied to understand the distribution and pattern of REE abundance and their petrogenetic significance. Overall, these granites show moderate abundance and distribution pattern of REE (ΣREE 65-251 ppm) where the total abundance of REE is less than Clarke's value (145.81 ppm) (Clark, 1924) for average abundance in granite. The granites of Murmuri, Chhibarra and Kashipali (Pink porphyritic biotite granite) are more differentiated as these possess more total REE (average 217 ppm) than the clark values of granites.

The representative REEs (n=8) (Table 5.7) shows that the granites are more enriched in LREEs than HREEs. The average concentration of REEs show that, in LREEs, Ce is dominant with 75.8 ppm followed by La (48 ppm), Nd (27.4 ppm), Pr (16 ppm), Sm (5.7 ppm) and Eu (0.83 ppm). In HREEs, Y is dominant with 11 ppm followed by Gd (6.5 ppm), Dy (2.1 ppm), Er (1.3ppm), Yb (1.16 ppm), Ho (1 ppm), Tb (1 ppm), Tm (1 ppm) and Lu (1ppm).

The higher concentration of LREE relative to HREE suggests high order of fractionation. Such enrichment is commonly recorded in Precambrian Basement Complexes. REE data of Juba granites samples has been excluded in chondrite normalised plot due to majority of data are below detection limit. Large negative Eu anomalies (Eu/Eu*) are recorded in the granites of the study area. Besides, feebly negative to positive Ce anomalies (Ce/Ce*) indicate enrichment of LREE

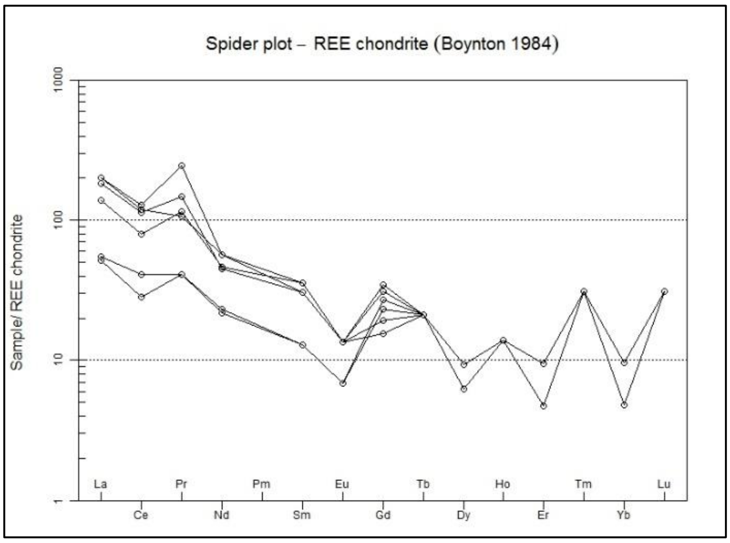

Figure 5.10 Chondrite normalised REE plot of Granitoids of study area.

and points toward the presence of Ce-rich monazite in the residual phase. The depletion or enrichment of Ce and Eu usually occurs in the natural environment, which may be linked to their oxidation state and mobility under different oxidation-reduction conditions. Ce^{3+} is more easily oxidized to Ce^{4+} with higher oxygen fugacity and is much less mobile resulting in positive Ce anomaly ($\delta Ce > 1$). Eu is an incompatible element in the trivalent form (Eu^{3+}) in an oxidizing magma, but is preferentially incorporated into plagioclase in its divalent form (Eu^{2+}) in a reducing magma.

This ion-exchange process is the basis of the negative Eu anomaly ($\delta Eu < 1$). The Eu anomalies are chiefly controlled by plagioclase. Thus, removal of plagioclase from a felsic melt by crystal fractionation or partial melting of a rock in which plagioclase is retained in the source will give way to negative Eu anomaly. The depletion of REEs has been attributed to various processes including magmatic differentiation, hydrothermal leaching or a combination of both.

5.4 GEOCHEMISTRY OF REHATIKHOL FORMATION

5.4.1 Major Oxide and trace element geochemistry

The major and trace elemental distribution of the Rehatikhol Formation (n=61) comprising seven major lithofacies i.e. polymictic conglomerate (n=4), gritty feldspathic arenite (n=6), pyritiferous feldspathic arenite (n=25), feldspathic arenite (n=9), ferruginous sandstone (n=5), shale (n=8) and Porcellanite (n=4) is described and tabulated below (Table 5.8 & 5.9).

Major oxides distribution in various lithofacies

Polymictic conglomerate: The conglomerates of Rehatikhol Formation (n=4) are characterized by high SiO_2 (77.45–87.23 wt%), moderate Al_2O_3 (6.83 – 13.60 wt%), K_2O (2.17 –5.84 wt%), Na_2O(0.79-1.30 wt%), CaO (0.08-0.42 wt%), low $Fe_2O_3(t)$ (0.66 –1.16 wt%). MgO content is generally low (<0.01-0.53 wt %), TiO_2 content is (0.21 – 0.37 wt%) and P_2O_5 content is (0.06 – 0.32 wt%).

Gritty feldspathic arenite: The sandstones of this lithounit (n=6) are characterized by high SiO_2 (73.17-85.99 wt%), moderate Al_2O_3 (7.39-15.97wt%), K_2O (2.26 –6.90 wt%), Na_2O (0.94-1.10 wt%), low CaO (0.02-0.05 wt%), low Fe_2O_3(t) (0.29 –1.17 wt%). MgO content is generally low (<0.01-0.74 wt%), TiO_2 content is (0.04 – 0.22 wt%) and P_2O_5 content is (0.01 – 0.04 wt%).

Pyritiferous feldspathic arenite (PFA): The sandstones of this lithounit (n=25) are characterized by high SiO_2 (80.40-89.78 wt %), low Al_2O_3 (4.93-9.29 wt %), K_2O (1.21 –4.80 wt %), Na_2O (0.74-1.08 wt%), low to moderate CaO (0.02-0.25 wt%), moderate Fe_2O_3(t) (0.65 –6.95 wt%). MgO content is generally low (<0.01-0.15 wt %), TiO_2 content is (0.02 – 0.18 wt %) and P_2O_5 content is (0.01 – 0.19 wt %).

Feldspathic arenite: The sandstones of this lithounit (n=9) are characterized by moderate SiO_2 (72.18-87.13 wt%), high Al_2O_3 (7.30-13.88 wt%), K_2O (2.83-7.11wt%), Na_2O (0.82-1.84 wt%), moderate to high CaO (0.03-4.25 wt%), low Fe_2O_3(t) (0.03 –0.62 wt%). MgO content is moderate (0.01-0.79 wt%), TiO_2 is (0.04 – 0.14 wt%) and P_2O_5 is (0.01 – 0.26 wt%).

Ferruginous sandstone: The sandstones of this lithounit (n=5) are characterized by moderate SiO_2 (67.59-80.51 wt %), high Al_2O_3 (9.70-22.40 wt %), K_2O (1.51- 7.07 wt%), Na_2O (0.97-2.75 wt%), low CaO (0.03-0.09 wt%), high Fe_2O_3(t) (0.78 –5.69 wt %). MgO content is moderate to high (0.66-1.58wt %), TiO_2 content ranges 0.04 – 0.23 wt% and P_2O_5 content is 0.02 – 0.07 wt%. The samples also characterized variable Cr (132-239ppm), Ni (11-43ppm), Cu (18-43ppm), Rb (48-276ppm), Sr (up to 91ppm), Y (up to 107ppm), Zr (up to 146ppm), Nb (up to 76ppm) and Ba (277-1006ppm.

Shale: The shales of this lithounit (n=8) are characterized by low to moderate SiO_2 (56.36-63.45 wt%), very high Al_2O_3 (21.23-23.41wt%), K_2O (5.53-6.86 wt%), Na_2O (0.10-0.55 wt%), moderate CaO (0.64-0.79 wt%), moderate Fe_2O_3(t) (1.61-8.55 wt%). MgO content is moderate to high (0.81-1.06 wt%), TiO_2 is (0.61-0.78 wt%) and P_2O_5 is (0.06 – 0.10 wt%).

Porcellanite (n=04): The samples have characterized variable to high SiO_2 (76.59-86.36%), low to moderate Al_2O_3 (6.65-10.06%), variable Fe_2O_3 (T) (2.39-8.82%), MgO (0.61-1.52%), CaO (0.34-0.40%), Na_2O (1.30-1.49%) and K_2O (0.35-1.66%) with 81-356ppm Cr, 33-103ppm Rb, 45-135ppm Sr and 292-451ppm Ba.

Table 5.8 Summary of major oxides data of Rehatikhol Formation in study area.

	Rock type	**SiO_2**	**TiO_2**	**Al_2O_3**	**Fe_2O_3(t)**	**MgO**	**MnO**	**CaO**	**Na_2O**	**K_2O**	**P_2O_5**
Min	Porcellanite (n=4)	76.59	0.12	6.65	2.39	0.61	0.01	0.34	1.30	0.35	0.14
Max		86.36	0.25	10.06	8.82	1.52	0.04	0.40	1.49	1.66	0.31
Avg		80.95	0.22	8.98	4.92	0.93	0.03	0.37	1.40	1.12	0.25
Min	Shale (n=8)	56.36	0.61	21.23	1.61	0.81	0.01	0.64	0.10	5.53	0.06
Max		63.45	0.78	23.41	8.55	1.06	0.03	0.79	0.55	6.86	0.10
Avg		59.33	0.71	22.55	5.47	0.94	0.02	0.69	0.24	6.32	0.07
Min	Ferrugnous sandstone (n=5)	67.59	0.04	9.70	0.78	0.66	< .01	0.03	0.97	1.51	0.02
Max		80.51	0.23	22.40	5.69	1.58	0.50	0.09	2.75	7.07	0.07
Avg		74.89	0.09	14.45	3.24	0.98	--	0.05	1.50	4.07	0.04
Min	Feldspathic arenite (n=9)	72.18	0.04	7.30	0.03	0.01	<0.11	0.03	0.82	2.83	0.01
Max		87.13	0.14	13.88	0.62	0.79	0.24	4.25	1.84	7.11	0.26
Avg		80.35	0.10	10.41	0.41	0.23	--	1.10	1.21	5.10	0.07
Min	PFA (n=25)	80.40	0.02	4.93	0.65	<0.01	<0.01	0.02	0.74	1.21	0.01
Max		89.78	0.18	9.29	6.95	0.15	0.04	0.25	1.08	4.80	0.19
Avg		85.59	0.05	7.16	2.59	0.06	--	0.07	0.94	2.49	0.05
Min	Gritty feldspathic arenite (n=6)	73.17	0.04	7.39	0.29	<0.01	<0.01	0.02	0.94	2.26	0.01
Max		85.99	0.22	15.97	1.17	0.74		0.05	1.10	6.90	0.04
Avg		79.75	0.11	11.90	0.68	0.39		0.04	1.02	5.00	0.02
Min	Polymictic conglomerate (n=4)	77.45	0.21	6.83	0.66	<0.01	<0.01	0.08	0.79	2.17	0.06
Max		87.23	0.37	13.60	1.16	0.53	-	0.42	1.30	5.84	0.32
Avg		83.07	0.28	9.75	0.95	0.17	-	0.19	0.98	4.01	0.15

Average Upper Continental Crust (UCC) and post Archean Australian Average Shale (PAAS) spider plots (values after Taylor and McLennan, 1985) for major oxide of Rehatikhol sediments are plotted to draw inference about enrichment and depletion of major oxides (Figure 5.11 & Figure 5.12). Comparative study revealed that all lithounits show SiO_2 enrichment except in shale that show depletion due to Al_2O_3 and K_2O dilution. Quartz in Rehatikhol sandstones is main causative factor of silica enrichment along with feldspar. All lithounits are characterised by depletion of TiO_2 and $Fe_2O_3$with respect to PAAS (Shale is less depleted). It shows absence of Fe- Ti oxide mineral like ilmenite, rutile, biotite and sphene that indicate all sandstone of Rehatikhol Formation do not have influx of basic composition sediments.

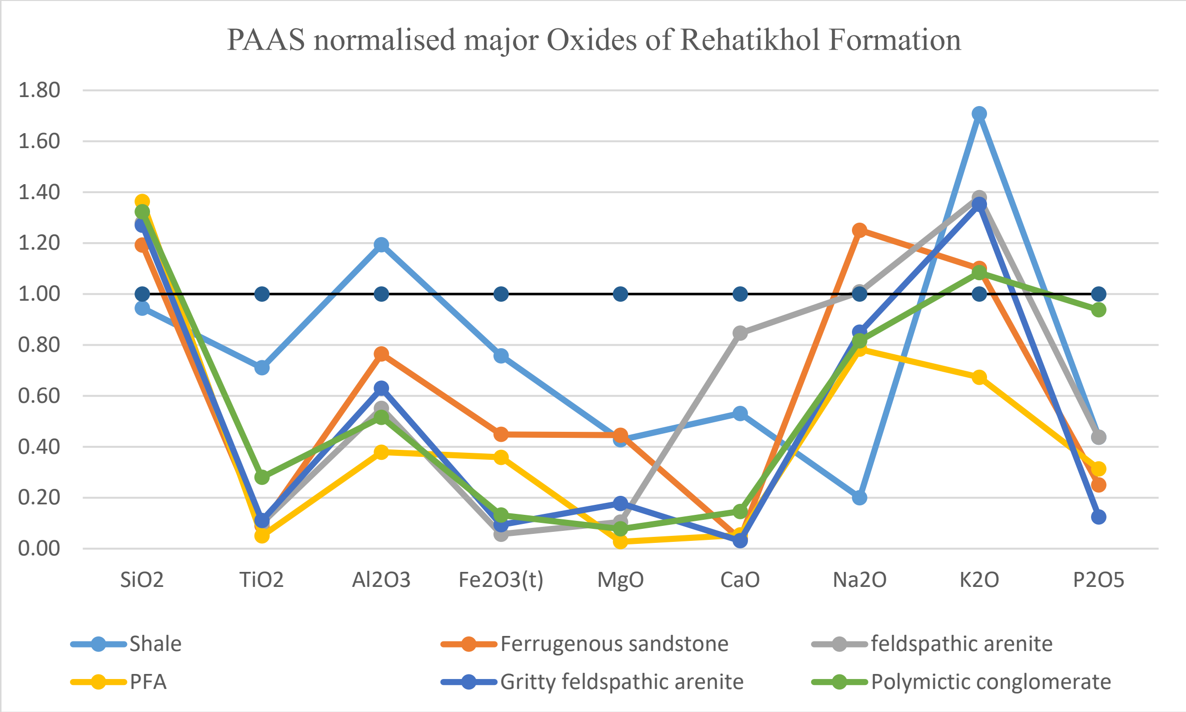

Figure 5. 11 Post Archean Australian Average Shale (PAAS) normalised spider plot of major oxide of Rehatikhol sediments (values of PAAS after Taylor and McLennan, 1985).

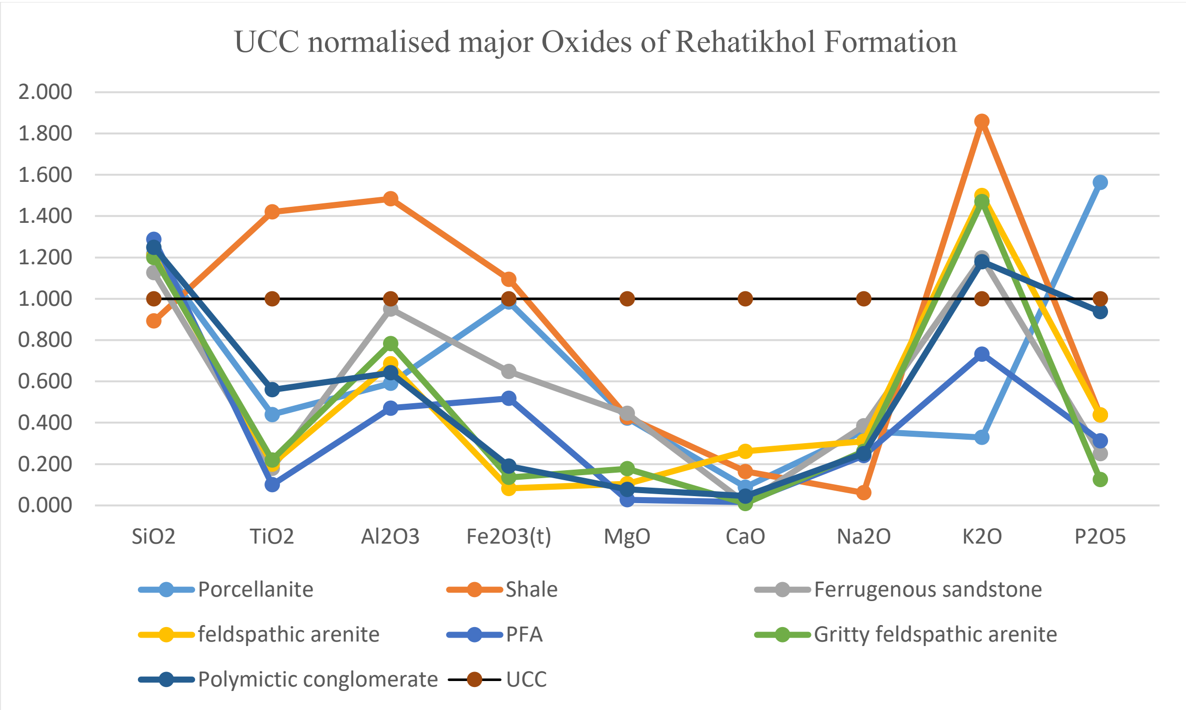

Figure 5.12 Upper Continental Crust (UCC) normalised spider plot of major oxide of Rehatikhol sediments (values of UCC after Taylor and McLennan, 1985).

Shale shows significant enrichment of TiO_2 and slight enrichment of Fe_2O_3 with respect to UCC that infers minor presence of fine Fe- Ti oxide bearing heavies derived from basic igneous source. It indicate supply of sediments also have basic influx during the deposition of shale. XRD study of shale is required to confirm it further. Depletion of CaO, Na_2O and Al_2O_3 in sandstones are mainly due to removal of plagioclase during transportation by chemical weathering. K_2O is enriched due to microcline and perthites in all sandstones of Rehatikhol Formation except PFA that indicate relatively more maturity of this unit or dilution due to high silica overgrowth as observed in petrography. Although K feldspar is also less in this unit and samples of this unit fall in subfeldspathic arenite in QFL ternary diagrams. K_2O enrichment due to presence of K feldspar indicate moderate weathering in source area. Porcellanites are found to be enriched P_2O_5 content that is conspicuous. Porcellanite and ferruginous sandstone are less depleted in Fe_2O_3 content in UCC normalised plot due to presence of pyrite in porcellanite and iron oxide staining in sericitic matrix in ferruginous sandstone. All the geochemical characteristics are corroborated by petromineralogical studies.

UCC normalised spider plot has been prepared for trace element data of Rehatikhol Formation (Figure 5.13). Overall, Th and Ce are enriched in sediments indicating presence of monazite. Basal polymictic conglomerate is highly enriched in Th content indicating their thoriferous nature. Sandstones are depleted in Zr, Ti, Nb, Y and P while enriched in U and Ba.

5.4.1.1 Classification of sandstones based on major oxides geochemistry

The sandstones of the Rehatikhol formation (n=45) comprising four lithofacies have been classified using K_2O vs Na_2O bivariate plot (after Pettijohn (1963) in which all the samples falls in arkosic field (Figure 5.14). Also in the Log (SiO_2/Al_2O_3) vs Log (Fe_2O_3/K_2O) (Figure 5.15) classification Diagram (After Herron, 1988), majority of the samples from gritty-pebbly feldspathic arenites and feldspathic arenites falls in arkosic and sub-arkosic field while some samples got clustered along lithicarenite- sublithic arenite boundary.

Table 5.9 Summary of Trace element data of Rehatikhol Formation in study area.

Sample No.	Rock type	Cr	Ni	Cu	Zn	Ga	Rb	Sr	Y	Zr	Nb	Ba	Ce	Pb
Average	Porcellanite (n=4)	162.75	22.00	25.00	74.25	24.75	59.75	81.50	24.50	60.75	28.75	374.75	118.25	58.50
Max		356	25	27	121	27	103	135	35	86	36	451	160	80
Min		81	19	20	38	22	33	45	14	45	17	292	66	29
Average	Shale (n=8)	58.25	20.25	15.38	39.88	26.38	316.88	26.00	59.67	129.50	13.00	821.00	81.63	48.60
Max		70	30	18	59	32	414	32	76	184	14	946	90	140
Min		45	13	12	29	24	231	20	34	105	12	637	66	13
Average	Ferruginous sandstone (n=5)	191.60	23.20	26.40	28.40	27.00	172.20	65.50	82.33	86.60	41.75	670.80	73.80	200.00
Max		239	43	43	38	34	276	91	107	146	76	1006	115	425
Min		236	30	43	32	23	48	16	0	85	10	277	115	96
Average	feldspathic arenite (n=9)	67.71	50.00	19.78	28.67	25.14	202.00	63.71	45.33	93.33	29.29	1120.57	76.83	77.86
Max		165	105	40	61	28	289	91	57	146	60	1573	132	181
Min		24	5	5	18	22	93	32	31	60	5	482	18	19
Average	PFA (n=25)	102.56	70.26	47.36	33.00	26.88	84.08	45.78	108.80	111.48	34.93	644.48	60.72	295.06
Max		215	127	214	150	48	164	110	248	309	97	1650	162	721
Min		24	11	11	10	16	39	11	25	10	11	251	26	67
Average	Gritty feldspathic arenite (n=6)	133.17	38.50	21.83	24.00	27.50	182.67	79.00	35.33	96.67	35.00	1119.50	64.50	100.00
Max		224	100	30	29	28	241	109	61	135	60	1352	101	198
Min		26	17	16	21	27	106	68	12	54	15	734	20	60
Average	Polymictic conglomerate (n=4)	172.50	19.00	26.00	24.25	26.25	139.75	84.00	133.75	512.50	50.25	1815.25	248.75	205.50
Max		260	28	27	28	28	232	102	293	761	67	2853	407	265
Min		107	12	24	21	25	67	54	57	374	33	1104	163	169

Note: Some of the REE data are analysed below the detection limit of ICP- AES, hence taken as half of detection limit or removed from the data sheet. Pb data is reported as semi quantitative data hence can be used only for qualitative analysis. U mineralised PFA comprises galena also that's why Pb values are higher in some samples.

5.4.1.2 Provenance, tectonic setting and paleoclimatic conditions

Chemical composition of sandstones of Rehatikhol Formation is mostly controlled by the source rock from which the erosion, deposition and diagenetic processes lead to development of this sedimentary rocks. Provenance erosion is controlled by tectonics and finally deposited and preserved portions of the detritus can give insight into the provenance setting. Apart from the major elements it is often observed that trace element content increases in clayey portions compared to the silica rich arenite portions. Therefore, trace elements concentration can give ideas on paleo weathering and erosion time span, topography and distance between the source and deposition area, styles and agents of transportation etc.

Since different tectonic condition have their own characteristic provenance set up with typical sedimentation processes, geochemical signatures of sedimentary rocks will be different from back arc, fore arc, inter arc basins, active and passive margins collisional or rift settings. After plotting the data in the Al_2O_3 versus TiO_2 (Figure 5.16) bivariate discrimination diagram (Hayashi et al. 1997) the samples plot in the felsic source rock field. TiO_2 and Zr concentrations in siliciclastic rocks are good indicators of source rock. Hayashi et al. (1997) have devised a scheme for discriminating the source of sedimentary rocks on the basis of TiO_2 /Zr weight ratios. As per that scheme of discrimination, the TiO_2 /Zr weight ratios in the studied samples indicate their derivation dominantly from felsic to intermediate igneous rocks (Figure 5.17). Provenance plot of Rosers and Korsch, 1988 based on discriminant function F1 and F2 also indicate felsic igneous to intermediate igneous source (Figure 5.18). The bivariate plot of K_2O/Na_2O vs SiO_2 (Figure 5.19) represents passive margin setting. The bivariate plot of Al_2O_3/SiO_3 vs. Fe_2O_3 (t) + MgO (after Bhatia, 1983) for Rehatikhol sediments shows passive margin tectonic setting too (Figure 5.20). The bivariate plot (after Roser and Korsch 1986) is also used to make out about the influence of climatic conditions on the chemical maturity of sandstone can be studied, and thereby the prevalent palaeoclimatic conditions

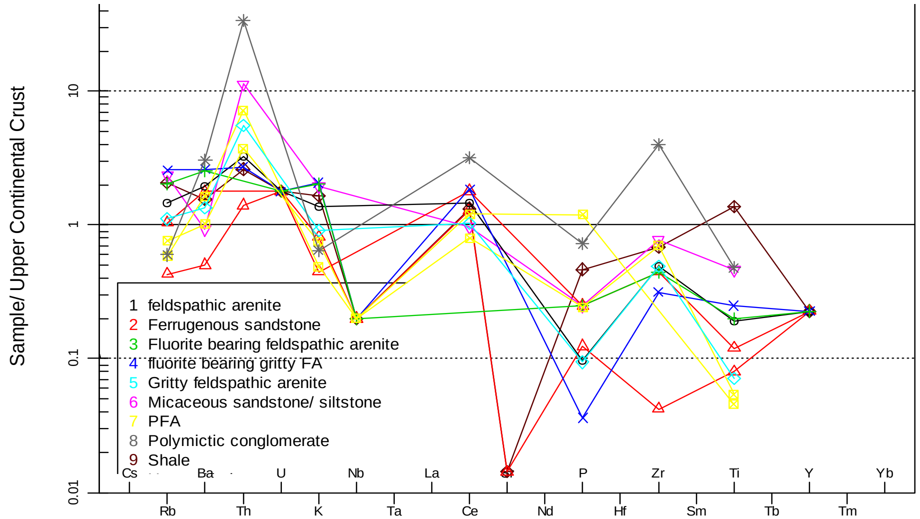

Figure 5. 13 UCC normalised spider plot of trace elements of Rehatikhol sediments (Taylor and McLennan, 1995).

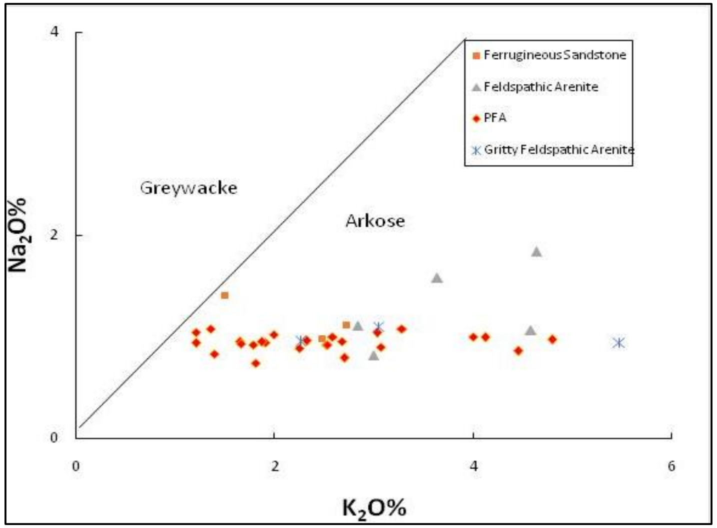

Figure 5.14 Na_2O vs. K_2O plots for discriminating greywacke and arkose after Pettijohn ,1963).

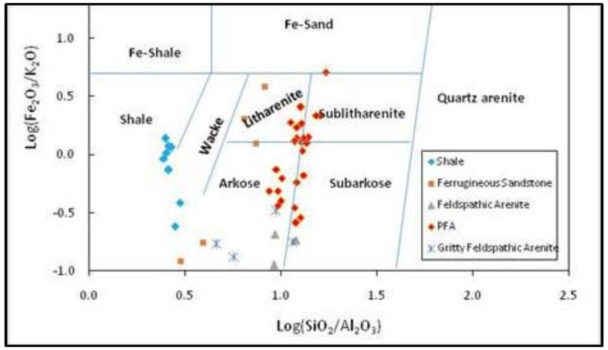

Figure 5.15 Log (SiO2/Al2O3) vs Log (Fe2O3/K2O) plot of sandstone classification Diagram (After Herron, 1988).

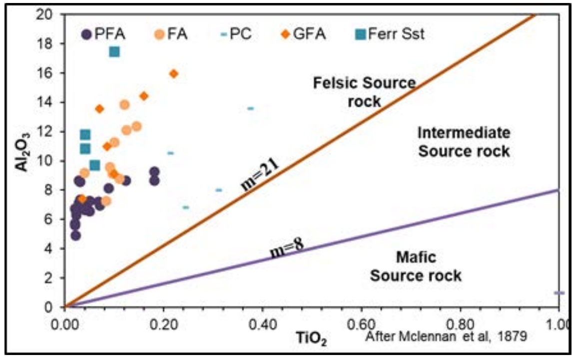

Figure 5.16 Al_2O_3 versus TiO_2 bivariate discrimination diagram for provenance of Rehatikhol sediments (Hayashi et al. 1997).

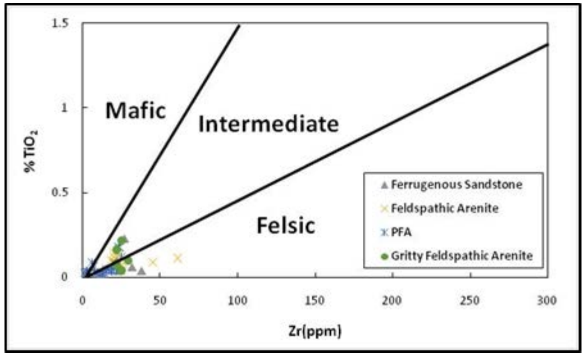

Figure 5.17 Provenance diagram of TiO_2 vs. Zr for the sandstones of Rehatikol Formation (after Hayashi et al., 1997).

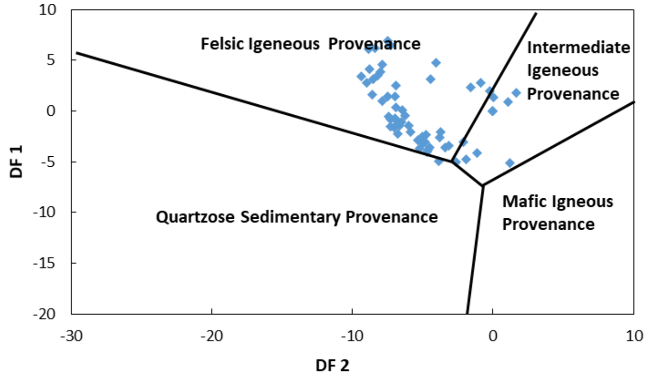

Figure 5.18 Provenance plot after Rosers and Korsch, 1988.

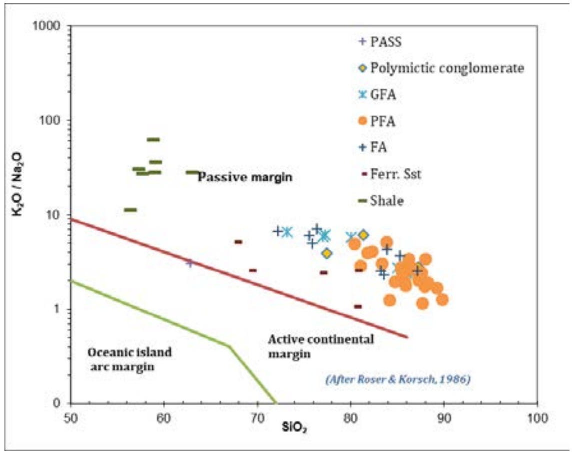

Figure 5.19 Plots of log K_2O/Na_2O vs. SiO_2 relations for Rehatikol sediments on the tectonic setting discrimination diagrams.

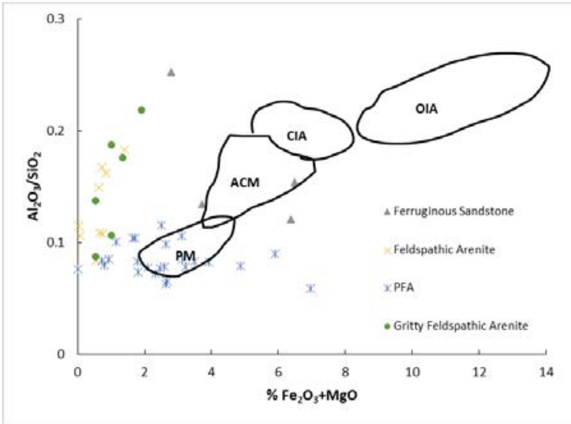

Figure 5. 20 Al_2O_3/SiO_3 vs. Fe_2O_3(t)+MgO plots of Rehatikhol sediments. Fields after Bhatia (1983).

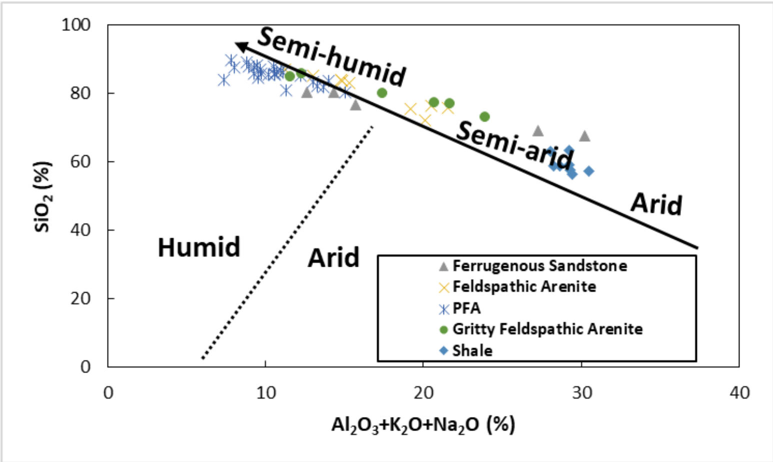

Figure 5.21 Chemical maturity of Rehatikhol sediments and their palaeoenvironment of deposition (after Suttner and Dutta, 1986).

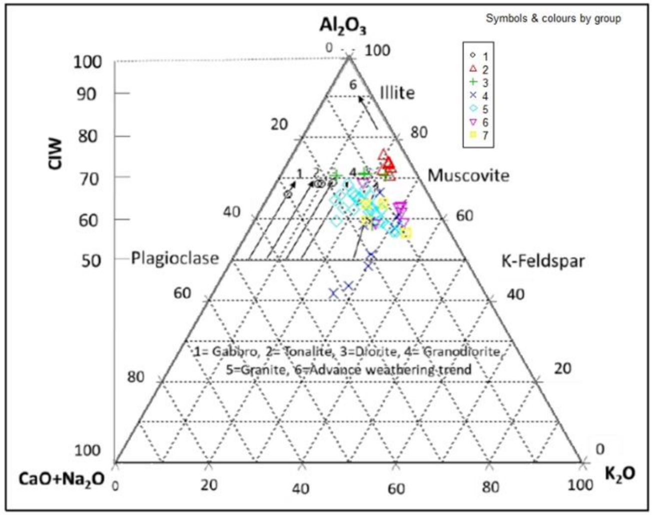

Figure 5.22 A-CN-K ternary diagram of Al_2O_3–(CaO+Na_2O)–K_2O for Rehatikhol sediments (after Nesbitt and Young 1984).

during provenance weathering can be deciphered, using SiO_2 vs. (Al_2O_3 +K_2O+Na_2O) bivariate plot (Suttner and Dutta, 1986). The plots of sandstones in SiO_2 vs. (Al_2O_3 +K_2O+Na_2O) (Figure 5.21) binary space apparently (ignoring the effect of reworking/recycling) indicate derivation of the precursor sediments dominantly under a semi-humid palaeoclimatic condition.

5.4.1.3 Paleoweathering

Intensity of chemical weathering of source rocks is controlled mainly by source rock composition, duration of weathering, climatic conditions and rates of tectonic uplift of source region. During chemical weathering Ca, Na and K are largely removed from source rocks. The amount of these elements surviving in soil profiles and in sediments derived from them is a sensitive index of the intensity of chemical weathering (Nesbitt et al., 1997).

If the siliciclastic sedimentary rocks are free from alkali related post-depositional modifications, then their alkali contents (K_2O + Na_2O) and K_2O / Na_2O ratios are considered as reliable indicators of intensity of weathering of source material. The degree of source rock weathering is quantified variously. A few indices of weathering have been proposed based on molecular proportions of mobile and immobile element oxides (Na_2O, CaO, K_2O and Al_2O_3).

- Chemical Index of Alteration (CIA; Nesbitt and Young, 1982) is well established as a method of quantifying the degree of source weathering.
- Weathering of the deposited sediments and elemental redistribution during diagenesis can be assessed using Plagioclase Index of Alteration (PIA; Fedo et al., 1995) and Chemical Index of Weathering (CIW).
- Index Compositional Variation ICV (Cox, R et al , 1995) is calculated for the maturity of the sediments as well as prevailed climatic conditions and source weathering. The ICV tends to be highest in minerals that are high in weathering intensity and decreases in more stable minerals (less weathered minerals). As per (Cox, R et.al, 1995), sandstones or shales with

ICV > 1 are compositionally immature with the first cycle of sediments deposited in tectonically active settings. The equations of the above indices are:

$$CIA = \{Al_2O_3 / (Al_2O_3 + CaO + Na_2O + K_2O)\} \times 100$$

$$PIA = \{(Al_2O_3 - K_2O) / ((Al_2O_3 - K_2O) + CaO + Na_2O)\} \times 100$$

$$CIW = \{Al_2O_3 / (Al_2O_3 + CaO + Na_2O)\} \times 100$$

$$ICV = (Fe_2O_3 + K_2O + Na_2O + CaO + MgO + MnO) / Al_2O_3$$

Following the procedure provided by McLennan (1993) CIA, PIA and CIW values have been determined for Rehatikhol sediments and summary is tabulated in table 5.10.

Table 5. 10 Summary of various alteration indexes of Rehatikhol Formation.

		CIA	CIW	PIA	ICV
Shale	Average	73.23	93.24	90.58	0.69
	Maximum	75.87	94.19	91.95	0.78
	Minimum	71.66	86.54	82.84	0.79
Ferruginous sandstone	Average	68.77	84.60	79.54	0.86
	Maximum	71.66	91.13	87.53	0.99
	Minimum	58.94	78.84	67.68	0.56
Feldspathic arenite	Average	59.68	80.77	69.04	0.80
	Maximum	66.65	86.77	80.95	1.00
	Minimum	53.02	72.30	52.84	0.59
PFA	Average	63.14	80.84	72.63	0.89
	Maximum	68.75	85.10	78.78	1.59
	Minimum	57.09	72.20	64.61	0.64
Gritty felds. arenite	Average	62.73	86.56	78.08	0.73
	Maximum	69.39	89.78	82.38	0.77
	Minimum	59.04	79.82	68.67	0.60

The studied samples of sediments of Rehatikhol formation are plotted in the A–CN–K ternary diagram in which majority of the samples are plotted above the feldspar tie line (Figure 5.22) define an intermediate trend, which indicates moderately weathered Al_2O_3 rich source.

Average CIA values (62.73 %), CIW (average = 86.56%), PIA values (average =78.08%) and ICV (0.73) of gritty feldspathic arenite correspond to the moderate source weathering similarly PFA also characterised by CIA (63.14% average), average CIW (80.84 %), PIA (72.63 %) and ICV (0.89) representing moderate (slightly higher than earlier) source weathering. Low average CIA value (59.68 %) in feldspathic arenite of Rehatikhol Formation indicate incipient source weathering under cold, semi-arid climatic conditions although average CIW, PIA and ICV values are slightly higher due to presence of K_2O and N_2O in the form of perthites and microcline or may be due to post depositional feldspar alteration due to diagenesis and lithification. The intensity of weathering in source rock area increased with the time from deposition of basal Members to upper Member shale (Figure 5.23). Similar inferences are drawn from the average value of alteration index in ferruginous sandstone. Higher PIA values from PFA and pyritiferous feldspathic arenite are due to their higher total Fe_2O_3 content.

Shale of Rehatikhol Formation characterised by higher average CIA (73.23%), CIW (93.24%), PIA (90.58 %) and lower ICV (0.69) values indicating moderate weathering in source area and with higher maturity of shale. Petromineralogical studies also supports these inferences as significant K feldspar is observed in all sandstone of Rehatikhol Formation indicating their immaturity and moderate source weathering under cold climatic conditions.

5.4.2 REE geochemistry of Rehatikhol Formation

REE are relatively immobile in hydrothermal and sedimentary processes hence no or very less fractionation taken over while mineralisation of U from fluids by these processes. Therefore, REE characteristics of U phases and whole rock can be a better tracer to understand the source of mineralising fluids from these have derived. Uraniferous PFA samples of Chhibarra anomaly, uraniferous PFA samples of Juba anomaly, unmineralised PFA and feldspathic arenite has been analysed for REE, U, Th, F content for comparative study. Comprehensive summary of analysis is tabulated below in Table 5.11. Highly radioactive PFA sample of Juba with high U content characterised relatively very high total REE (average 134.54 ppm) followed by high total REE content in Chhibarra PFA with U (avg 31.56 ppm).

Table 5. 11 Summary of REE and U, Th and F data (in ppm) of PFA of Juba- Chhibarra and Feldspathic arenite of Malaikhaman.

Sample No.	**MKN/SST/30**	**CHB/PFA/5**	**SBT/PFA/6**	**CHB/PFA/8**	**MKN/PFA/19**	**JB/PFA/9**	**JB/PFA/10**	**JB/PFA/13**	**JB/PFA/15**	**CHB/PFA/2**	**CHB/PFA/3**	**CHB/PFA/4**	**CHB/PFA/7**
La	2.5	2.5	2.5	2.5	2.5	2.5	2.5	2.5	2.5	2.5	2.5	2.5	2.5
Ce	2.5	2.5	2.5	13	9	7	4	22	4.5	4	3	3	2.9
Pr	2.5	2.5	2.5	5	2.5	6	8	4	4.5	3.9	3.2	3.8	3.8
Nd	5	6	6	2.5	2.5	5	3	5	3	2.9	3	5	6
Sm	2.5	2.5	2.5	2.5	2.5	9	14	4	3.9	3.6	2.4	1.9	2.3
Eu	0.25	0.25	0.25	0.25	0.25	5	9	0.4	1	0.4	0.35	0.3	0.1
Gd	1	1	1	1	1	30	57	3	4	4	1.5	1.5	4
Tb	1	1	1	1	1	5	12	1.5	3	1.45	1.35	1.4	1.4
Dy	1	1	1	1	1	38	81	3	8	6	3	4	7
Ho						8	16	1.25	1.5				
Er	1	1	1	1	2	22	43	3	6	3	1	1	4
Tm						2	4	1.6	1.5				
Yb	<0.5	1	1	<0.5	1	13	24	2	4	3.8	1.9	2.9	4.8
Lu	<0.5	<0.5	<0.5	<0.5	<0.5	2.1	3.2	1.1	1.1	0.4	0.35	0.3	0.35
Y	2	3	4	2	1	217	487	18	50	39	21	24	6
∑REE	19.25	21.25	21.25	29.75	25.25	154.60	280.70	54.35	48.50	35.95	23.55	27.60	39.15
∑LREE	15.25	16.25	16.25	25.75	19.25	34.50	40.50	37.90	19.40	17.30	14.45	16.50	17.60
∑HREE	4	5	5	4	6	120.1	240.2	16.45	29.1	18.65	9.1	11.1	21.55
LREE/HREE	3.81	3.25	3.25	6.44	3.21	0.29	0.17	2.30	0.67	0.93	1.59	1.49	0.82
Th	<10	<10	<10	40	30	18	19	20	24	5	5	5	5
U	<10	<10	<10	<10	<10	140	270	120	290	100	50	80	80
Zr	16	10	16	22	11	12	12	12	12	30	34	51	30
F	1300	<50	<50	<50	<50	<50	<50	<50	<50	600	<50	<50	<50

Note: Some of the REE data are analysed below the detection limit of ICP- AES, hence taken as half of detection limit or in proportion to other similar samples. Unmineralised PFA and feldspathic arenite characterised very less total REE content (average 23.55). Positive correlation of U content with total REE indicates REE might be associated U bearing phases. Chondrite normalised spider plot shows nearly similar pattern between mineralised PFA of Chhibarra and Juba (Figure5.24) indicating similar mineralising processes and potential of the area.

Mineralised samples characterised by high Pr, Gd, Tb, Ho and Tm. LREE/ HREE ratio indicate that uraniferous PFA of Juba are relatively highly enriched in HREE. Similar inferences also noted in uraniferous PFA of Chhibarra that could be due to presence of HREE rich coffinite/ xenotime. Unmineralised PFA and feldspathic arenite characterised depleted HREE in comparison to LREE. HREE enrichment is characteristic of mineralisation in both Juba and Chhibarra PFA. All HREE are found to have positive correlation with U in PFA as seen in Pearson correlation matrix (Table 5.12). HREE enrichment indicates that U mineralisation is caused by hydrothermal fluids that could be derived from a less fractionated magmatic source (may be aroused through deep fractures). Y also shows very strong positive correlation with HREE indicating contribution from suspected xenotime (may be of hydrothermal origin?) though only mineralised PFA have high Y. U also shows good positive correlation with Y that support these inferences.

5.4.3 Major oxide and trace elements geochemistry: Comparative study with PFA of Juba

Comparative study of U mineralised PFA of Juba, Chhibarra (study area) and unmineralised PFA of study area has been carried out for major and trace elements distribution. Summary of comparison of major oxide and trace elements is tabulated in Table 5.13. Uraniferous Juba PFA is found to be slightly more siliceous, depleted in K_2O and Al_2O_3 in comparison to other PFA, possibly because of introduction of U bearing siliceous hydrothermal fluid infiltration that caused rise in silica at the expense of K_2O and Al_2O_3 by alteration of K feldspar to clay. Average Cu, Zn, Rb, Cr and Pb contents are higher in mineralised PFA that is due to epigenetic polymetallic sulphide mineralisation associated with U mineralisation. PAAS and UCC normalised major oxides and trace elements plots are prepared for comparative depletion and enrichment of chemical species. All studied PFA shows nearly similar pattern in PAAS normalised major oxide plots (Figure 5. 25). This similarity indicates that major oxides didn't altered much while U mineralising processes and other PFA also have similar major

Table 5.12 Pearson correlation matrix between U and REE of U mineralised PFA.

	Ce	Pr	Nd	Sm	Eu	Gd	Tb	Dy	Ho	Er	Tm	Yb	Lu	Y	Th	U
Ce	1															
Pr	-0.06	1.00														
Nd	0.28	-0.20	1.00													
Sm	0.00	0.98	-0.25	1.00												
Eu	-0.11	0.98	-0.24	0.99	1.00											
Gd	-0.11	0.98	-0.20	0.99	1.00	1.00										
Tb	-0.14	0.97	-0.31	0.97	0.98	0.98	1.00									
Dy	-0.15	0.98	-0.23	0.98	0.99	1.00	0.99	1.00								
Ho	-0.54	0.99	-0.34	1.00	1.00	1.00	0.98	1.00	1.00							
Er	-0.11	0.99	-0.22	0.99	1.00	1.00	0.99	1.00	1.00	1.00						
Tm	-0.45	0.95	-0.47	0.94	0.93	0.95	0.98	0.96	0.96	0.95	1.00					
Yb	-0.18	0.98	-0.19	0.97	0.99	1.00	0.98	1.00	1.00	1.00	0.95	1.00				
Lu	0.11	0.97	-0.20	0.98	0.96	0.95	0.94	0.94	1.00	0.96	0.95	0.93	1.00			
Y	-0.14	0.98	-0.29	0.98	0.99	0.99	0.99	1.00	1.00	0.99	0.97	0.99	0.95	1.00		
Th	0.47	0.56	-0.16	0.54	0.48	0.43	0.49	0.42	-0.60	0.48	-0.46	0.40	0.68	0.44	1.00	
U	-0.02	0.69	-0.44	0.63	0.60	0.57	0.68	0.59	0.30	0.62	0.40	0.58	0.70	0.61	0.82	1

Table 5.13 Summary of major oxide and trace elements of PFA of Rehatikhol Formation.

	U mineralised PFA of Juba			U mineralised PFA of Chhibarra (study area)			Unmineralised PFA of Study area		
	Max	**Min**	**Avg**	**Max**	**Min**	**Avg**	**Max**	**Min**	**Avg**
SiO_2	89.78	84.14	87.24	86.63	83.35	85.26	89.22	80.40	85.02
TiO_2	0.02	0.02	0.02	0.03	0.03	0.03	0.18	0.03	0.07
Al_2O_3	6.78	4.93	6.02	8.66	7.13	7.93	9.29	6.57	7.41
Fe_2O_3(t)	6.95	2.32	3.26	3.47	0.90	1.76	5.77	0.65	2.55
MgO	0.04	0.01	0.02	0.12	0.02	0.06	0.15	0.01	0.08
CaO	0.25	0.06	0.11	0.08	0.04	0.06	0.14	0.02	0.05
Na_2O	1.08	0.92	0.99	1.08	0.92	0.99	1.04	0.74	0.91
K_2O	1.99	1.21	1.53	3.28	2.52	2.77	4.80	1.39	2.79
P_2O_5	0.19	0.04	0.08	0.06	0.03	0.04	0.11	0.01	0.03
Cr	187	165	176.33	215	44	155	170	24	59.07
Ni	77	17	36.20	127	30	70.00	118	11	82.50
Cu	214	27	63.17	90	33	54.00	133	11	39.27
Zn	30	17	20.60	150	20	55.25	116	10	31.07
Ga	48	17	30.83	43	28	32.50	28	16	23.80
Rb	121	42	67.17	132	68	89.75	164	39	89.33
Sr	57	12	32.80	84	29	59.50	110	11	46.50
Y	130	44	81.67	248	95	174	69	25	49.00
Zr	129	46	101.60	155	55	120.00	309	10	112.75
Nb	58	15	36.50	29	11	18.00	97	17	40.22
Ba	903	251	400.33	786	549	622.25	1650	303	748.07
Ce	77	26	38.33	68	50	56.75	162	31	70.73
Pb	2540	122	924.50	1682	478	910.75	721	67	301.77

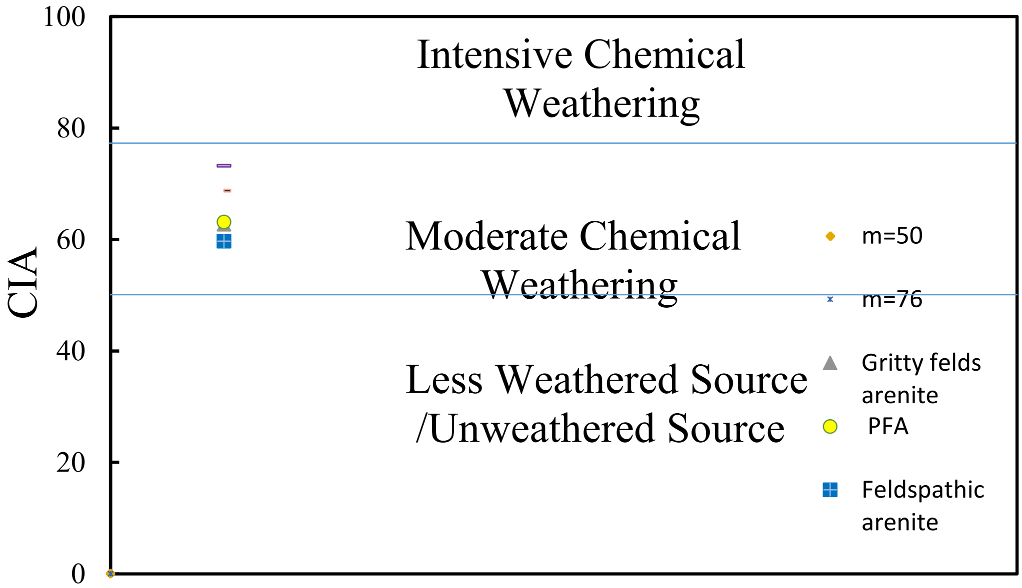

Figure 5. 23 Plot of CIA values of Rehatikhol Formation and corresponding weathering conditions.

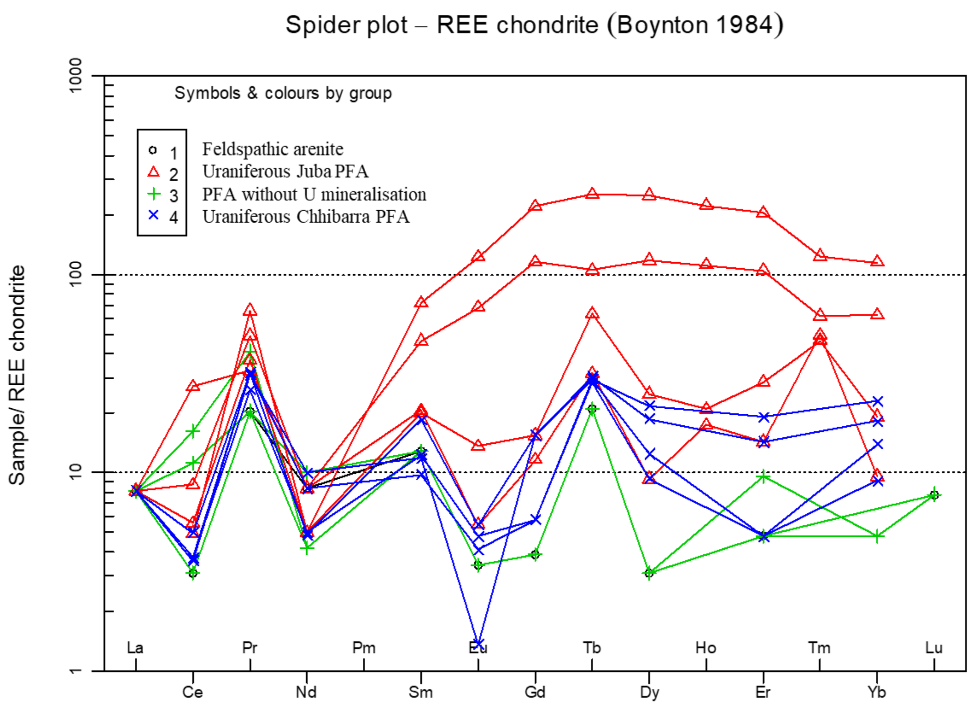

Figure 5. 24 Chondrite normalised REE plot of U mineralised and non-mineralised PFA.

oxide composition and have similar potential for further exploration. It indicates role of secondary phenomenon in U mineralisation that is hydrothermal fluids. UCC normalised trace elements plots show that K, Rb, Ba and Ti are more depleted in U mineralised PFA than unmineralised PFA (Figure 5.26). Mineralised PFA shows enrichment of Y and Yb.

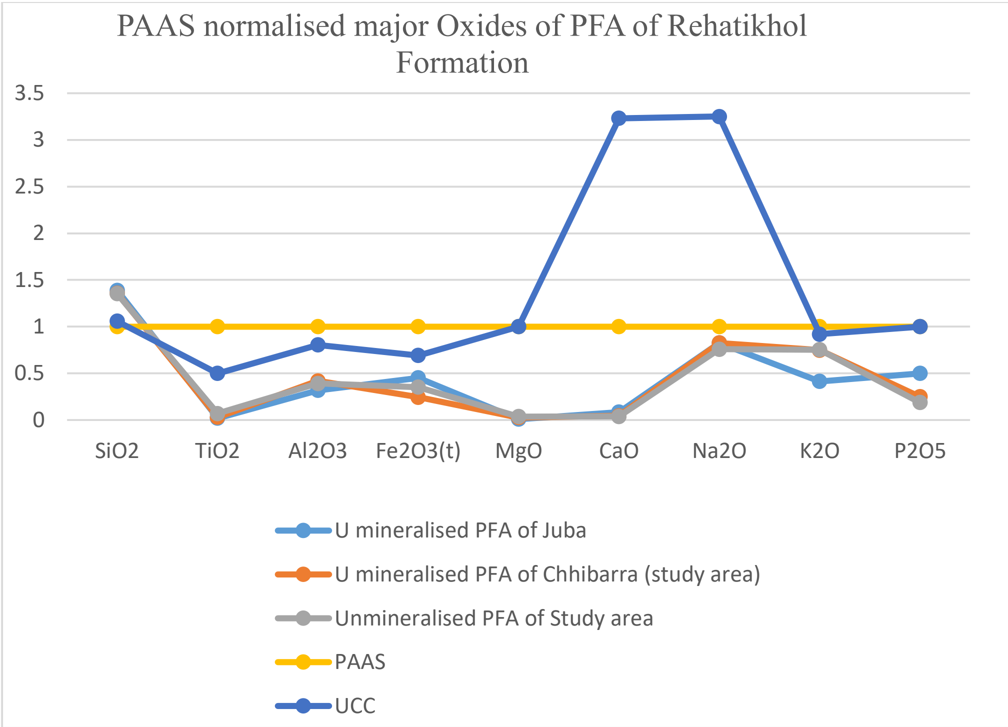

Figure 5. 25 PAAS normalised major oxide plots of PFA of Rehatikhol Formation (values of major oxides after Taylor and McLennan, 1985)

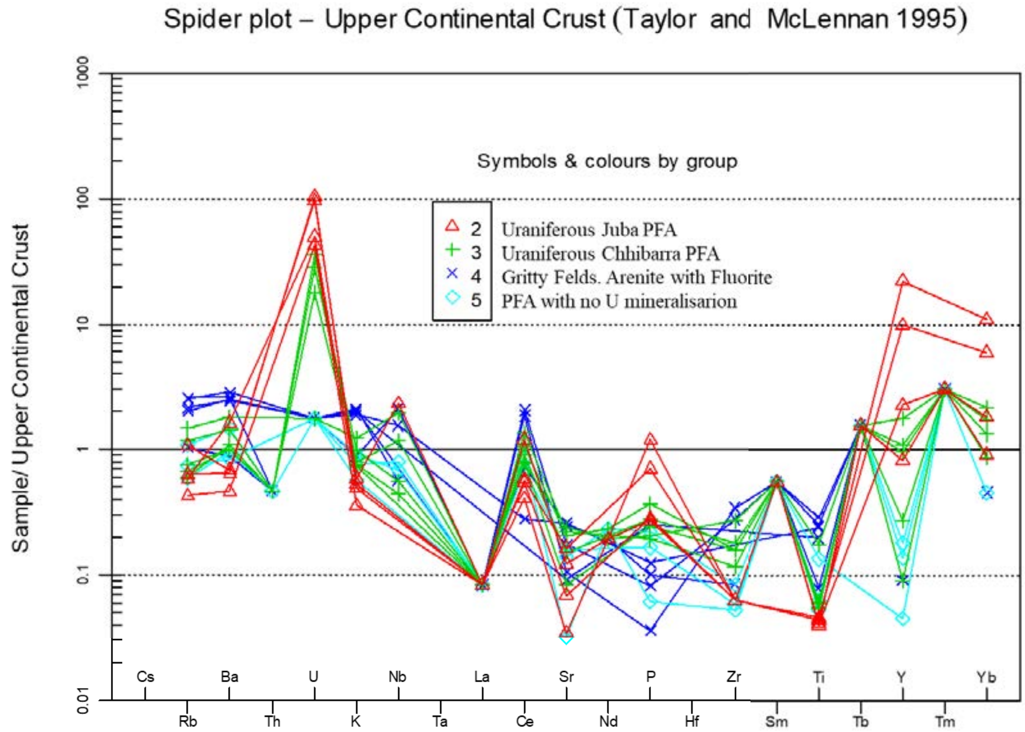

Figure 5.26 UCC normalised trace elements spider plot of PFA of Rehatikhol Formation (values of major oxides after Taylor and McLennan, 1995).

CHAPTER 6
RADIOACTIVE MINERALISATION

6.1 INTRODUCTION

Detailed radiometric survey has been carried out to identify and study radioactive mineralisation of U and Th in the project area. Radiation Survey Meter (RSM), Scintillometer and Portable Gamma Ray Spectrometer are used to measure radiation in the survey area. Systematic field traverses have been planned to carry out radiometric survey using these radiation detector over rocks of Singhora Group as well as basement rocks. More emphasis of radiometric survey has been kept on major reactivated faults/ fractures and their intersections, PFA unit of Rehatikhol Formation and projected basement fractures near to the unconformity plane that are mineralised in basement. Background radioactivity in basement Sambalpur Granites has been measured with an average of 8- 10 uR/ hr while in sediments of Rehatikhol Formation, it is 10- 12 uR/ hr. leucocratic biotite granites of Banabira- Bansbena area show slightly higher average radioactivity (12-15 uR/ hr) due to enriched intrinsic radio elemental concentration. Elevated ppm of U concentration is resulted from PPM analysis of some of these granite sample. Highest average radio elemental concentration in basement is observed in biotite- muscovite granite of Jaypur- Damdama area. These granite could be younger and more evolved phase of Sambalpur Granitoids.

Slightly higher average radioactivity has been observed in some lithounits of Rehatikhol Formation due to heavy minerals concentration that are radioactive (like zircon and monazite) or due to epigenetic introduction of U in sediments through faults and fractures. Basal conglomerate, intraformational conglomerate and some gritty layers show anomalous radioactivity but all are thoriferous in nature. Only elevated radioactivity in PFA unit of Rehatikhol Formation is corresponding to elevated U concentration. Significant amount of sulphides in this unit indicate strong reducing condition that are favourable for U fixation and concentration. A total 94 samples has been analysed for radiometric PPM analysis to understand radio elemental distribution and migration in different lithounits (basement rock as well as sediments).

6.2 RADIOELEMENTAL DISTRIBUTION

The radiometric data of different lithounits is interpreted to find out average U, Th, K, U/ Th and their range. A comprehensive summary table of radiometric U and Th of various lithounit is given below (Table 6.1). Physical assay results of samples has been interpreted for U/ Th ratio depicting mobilization and concentration of U relatively to Th.

Table 6.1: Summary of radio-elemental distribution in various litho-units in study area.

Rock Type	RaeU_3O_8	ThO_2	U/Th	Th/U	Avg U	Avg Th	avg K (in %)	avg U/Th	avg Th/U
Ferrugenised breccia					3	3		1	1
Porcellanite (n=6)	<1-4	3-9.0	0.16-0.5	02-6.0	2.25	6.5	0.97	0.32	3.43
Shale (n=9)	04-06.0	20-28	0.17-0.25	4-5.62	5.11	24.67	4.83	0.21	4.92
Siltstone					3	17	1.70	0.18	5.56
Ferruginous sandstone (n=5)	0.5-3	2-21.0	0.12-0.50	02-8.0	1.5	9	1.98	0.28	5.4
PFA (n=20)	1-19.0	2-19.0	0.40-9.5	0.06-3.85	4.50	4.10	1.49	1.48	1.74
Feldspathic arenite (n=9)	1-7.0	1-18.0	0.11-0.77	1.30-9.09	3.22	8.22	2.07	0.33	4.06
Feldspathic arenite with fluorite (n=5)	01-2.0	4-14.0	0.14-0.5	2.0-7.14	1.8	8.40	4.66	0.25	4.74
Gritty feldspathic arenite (n=8)	1-5.0	4-64.0	0.08-0.75	1.33-12.50	2.62	14.88	3.04	0.30	5.84
Basal polymictic conglomerate (n=1)					8	80	3.1	0.1	10
Granitoids with Fluorite (n=2)					2	<2	5.1	2	0.5
Quartzo feldspathic injection (n=1)					5	<1	12.3	5	0.2
Migmatites/gneiss (n=2)	13-14.0	77-78	0.17-0.18	5.56-5.86	13.5	77.50	4.55	0.18	5.72
Quartzo feldspathic rock (n=3)	3-18.0	3-17.0	0.18-6.0	0.17-5.56	14.0	7.33	6.13	5.56	1.94
Sambalpur granitoids (n=21)	01-12.0	01-36.00	0.06-1.33	0.50-16.67	3.64	14.48	3.19	0.37	5.24

Average of U/ Th and Th/ U for different lithounits has been calculated only for below threshold values (U/ Th< 0.35 for basement rocks and U/ Th< 2 for sediments). U/ Th values above threshold value are categorised as anomalous values. Basement granitoids shows approximate standard ratio of average U/ Th ratio (0.25- 0.35). High anomalous value (U/Th>0.35) observed in some granitoid samples (U/Th= 0.32- 10.5, n = 4) of Kermeli-Kurapali area along shear zone showing remobilisation of U and structural controls along WNW shear zone.

The Sambalpur granites are reported to be fertile in nature containing average 8-10ppm U. But granitoids that are exposed very near to the basin margins (mostly pink porphyritic granite), are depleted in intrinsic U content (1- 3 ppm RaeU_3O_8) and shows very less average U/Th ratio (<0.25) while granites away from basin margin (medium grained leucogranites ?) are enriched in U content (6-12 ppm) and shows slightly higher U/Th ratio (>0.30). Samples of granite near to the basin margin that are depleted in its uranium content indicate possibly uranium might have leached out of the system and gone into the sediments of Singhora basin (?). Muscovite- biotite granites that are exposed in northern part of study area around Damdama- Jaypur sector also shows higher intrinsic U content (6- 8 ppm) and shows slightly higher U/Th ratio. Quartzo- feldspathic injections in basement rocks around Kermeli- Kurapali also have high intrinsic U content (3-18 ppm) and higher average U/Th ratio (5.56) showing enrichment of U.

Sediments of Singhora group show either approximate standards U/ Th ratio as of granite/ sediments or Th is enriched except Pyritiferous feldspathic arenite horizon of Rehatikhol formation. This horizon shows enrichment of U and elevated average U/Th ratio (1.48) indicating enrichment of U due to sulphides fixation/ reduction. High anomalous value (U/Th>2) observed in some PFA samples (U/Th= 2- 17, n = 5) of Chhibarra, Salhebhata and Gatkachhar area. Radiometric ppm values show that U/ Th value of shale of Rehatikhol Formation ranges between 0.18 -0.25 (approx. to standard ratio) that shows no enrichment of Th and U by sedimentary processes in these lithounits. The basement granitoid (pink porphyritic granite) around Rehatikhol- Gatkachhar area supports this also showing approximate range (U/ Th 0.06- 0.21). Granitoids of similar composition situated far away from study area towards eastward could have supplied the sediments for the shale. Low value of U/ Th in sandstones and conglomerate is due to detrital monazite/ zircon concentrated by mechanical processes. Two samples of two mica granite from Jaypur area shows relatively high U values (8 ppm).

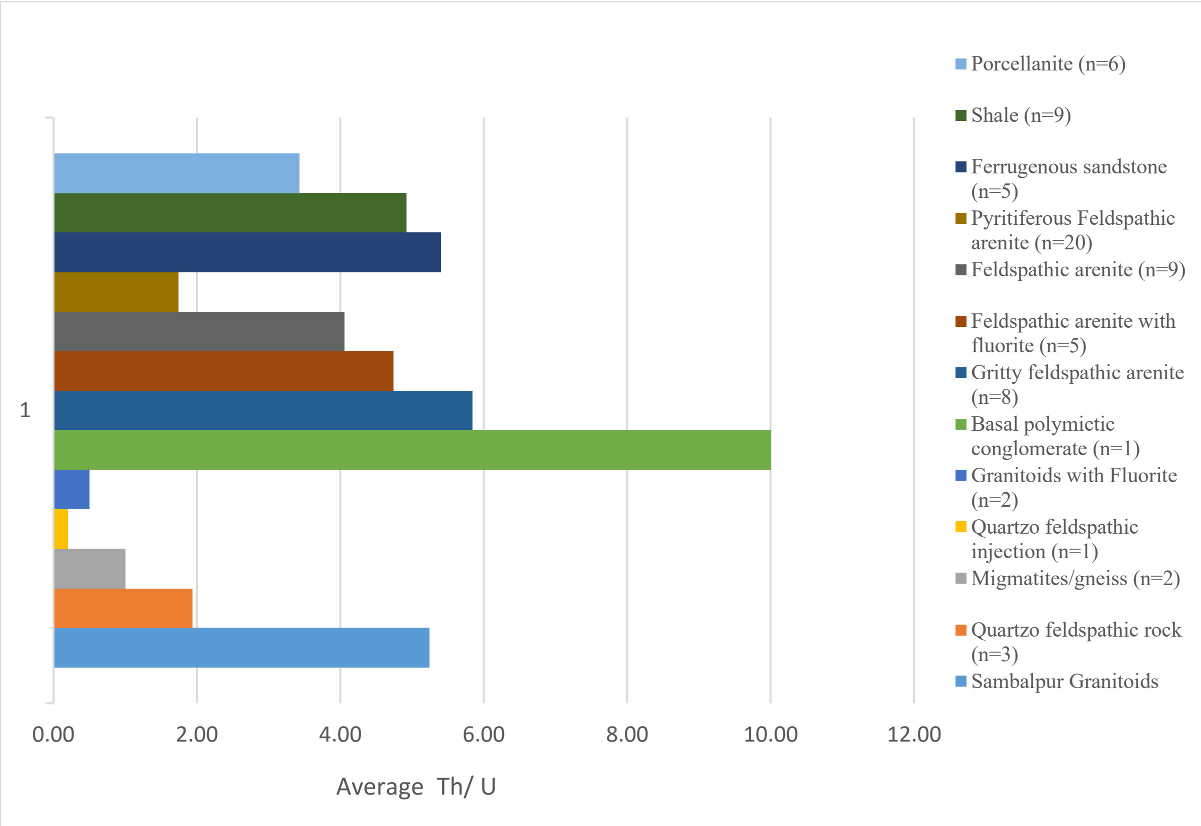

Figure 6.1 Bar chart showing comparison of Th/ U ratio of various lithounits.

Radiometric data has been also interpreted for average Th/ U ratio and bar chart has been prepared for comparison (Figure 6.1). Uranium enrichment is obvious in quartzo feldspathic injections and feldspathic injections in basement rocks. Fluorite bearing granitoids also show enrichment of U comparative to Th. Pyritiferous feldspathic arenite around Rehatikhol, Salhebhata and Gatkachhar area shows U/ Th mostly less than 1 but it is relatively higher than other lithounits. Elevated average U/ Th ratio in PFA indicate concentration of U in lithounit. High anomalous value (U/Th>2) observed in some PFA samples (U/Th= 2- 17, n = 5) of Chhibarra, Salhebhata and Gatkachhar area. Most of the sediments of Rehatikhol Formations are enriched in Th indicating migration of U to other lithounits while PFA horizon shows anomalous Th/ U ratio in samples collected near faults and fractures indicating lithostructural controls of mineralisation (due to presence of sulphides).

6.3 RADIOACTIVE ANOMALIES

Several radioactive fractures/zones/patches/spots were recorded during geological mapping and radiometric survey, including in basement granitoid, in Rehatikhol Formation of Singhora Group. All the earlier reported anomalies of CR & ER in the surveyed area and newly located anomalies during ongoing project (uraniferous and thoriferous) were studied and plotted. An attempt has been made here to study, compile, plot, interpret and re-evaluate the uranium mineralisation with the broader objective of reassessment and reappraisal of the area.

6.3.1 Thoriferous mineralisation

Thoriferous mineralisation is very conspicuous along the eastern part of Singhora proto-basin and is a result of mechanical transport as placers. In contrast, uranium mineralisation is structure controlled and epigenetic in nature.

- Thoriferous radioactivity recorded at many places around W of Kodopali & Pandkipali, Chhibarra- Salhebhata - Gatkachhar areas in basal polymictic conglomerate at Singhora unconformity contact.
- Upper conglomerate /Pebbly Feldspathic Arenite horizon: West of Pandkipali, Kodopali, near Makarmuta-Ghatkachar, overlying PFA at Juba, Bandhalimal, Salhebhata-Malaikhaman areas (Figure 6.2).
- Low order radioactivity reported in pebbly PFA at SW of Chhibarra.

- High order thoriferous radioactivity is reported in ferruginous feldspathic sandstone at 1.5 km NW of Pandkipali (0735081, 2360549), 100mx5-10m.
- Low order thoriferous radioactivity recorded in granite gneiss near Kermeli.

Figure 6.2 High order thoriferous radioactivity at N of Malaikhaman.

Figure 6.3 Uraniferous high RA in PFA at Chhibarra anomaly.

Petrological studies of few thoriferous samples revealed that high radioactivity is mainly due to significant concentration of zircon and monazite as heavy minerals. All the samples of suspected thoriferous anomalies are not analysed by gamma ray spectrometry hence the data is tabulated below in Table 6.2 is based on PGRS. Radiometric assay result of the reported thoriferous anomalies is tabulated in Table 6.3.

Table 6.2 Summary of thoriferous anomalies (based on PGRS data) in the study area.

Sl. No.	location	UTM coordinates	Radioactivity xbg (µR/hr.)	Brief Description
7	SW of Chhibarra	0734318 2355055	3- 20xbg (20-100µR/ hr)	High order RA in polymictic conglomerate over a dimension of 400x 100 m.
8	SE of Murmuri Chowk	0733372 2357556	2- 3x bg (up to 24µR/ hr)	Low order RA in pebbly to gritty feldspathic arenite over 10 m length.
9	NW of Chhibarra	0734422 2357145	4-5xbg(27-32µR/ hr)	Low order RA observed in gritty feldspathic arenite of Rehatikhol formation having epidotised feldspar.
10	NW of Chhibarra	0734693 2357135	5-7xbg(26-38µR/ hr	Low order RA observed in pebbly feldspathic arenite of Rehatikhol formation having feldspar epidotised, and almost 50m extent

Table 6.3: Radiometric assay result of thoriferous anomalies in Rehatikhol Formation and basement rock in and around study area.

Sample No.	% eU_3O_8	% U_3O_8	% ThO_2	Location	Co-ordinate UTM / Lat-Long		Rock Type
CHB/PPFA/01	0.011	<0.010	0.018	Chhibarra	734573	2355098	Pebbly PFA
CHB/PPFA/02	0.011	<0.010	0.017		734571	2355105	Pebbly PFA
SBT/CG/11	0.020	<0.010	0.038	S of Salebhata	21^{0}16’ 25.89”	83^{0}13’53.68“	Conglomerate
PKL/SST/21	0.013	<0.010	0.024	Pandkipali	735040	2360595	Ferruginous sandstone
PKL/SST/27	0.054	<0.010	0.110		735080	2360545	
PKL/SST/28	0.069	<0.010	0.130		735083	2360547	
PKL/SST/29	0.140	<0.010	0.260		735082	2360548	
CHB/PC/02	0.023	<0.010	0.044	Chhibarra	734353	2355074	Polymictic conglomerate
CHB/PC/03	0.046	<0.010	0.088		734348	2355071	
CHB/PC/04	0.013	<0.010	0.024		734348	2355071	
PKL/CG/05	0.017	<0.010	0.032	Pandkipali	735413	2359958	Diamictic conglomerate
PKL/CG/06	0.039	<0.010	0.079		735565	2360432	
KML/GR/24	61ppm	13ppm	77ppm	SW of Kermeli	21^{0}16’ 18.68”	83^{0}14’35.76 “	Granite Gneiss
KML/GR/25	62ppm	14ppm	78ppm		21^{0}16’ 18.68”	83^{0}14’35.76 “	

6.3.2 Uranium Mineralisation

Hosted by Rehatikhol sediments

Besides Juba-Banjhapali, uranium mineralisation has been located west of Chhibarra, associated with NNE-SSW to NE-SW fractures hosted on surface by fractured PFA and epigenetic sulphides (Figure6.5). Pyrite and galena are associated in RA samples as observed megascopically. Samples of PFA from Chhibarra anomaly, assayed 0.011- 0.020 % U_3O_8 (β/γ) with ThO_2 < 0.005%.

Hosted by basement rocks

Uranium mineralisation in basement rocks is summarised below-

a. Spotty anomaly reported in Granite mylonites along WNW shear zone at SW of Kurapali analysed 0.010% eU_3O_8, 0.018% U_3O_8 with <0.005%ThO_2. There is intense zone of shear that passes between the Kurapali and Kermeli village of Bargarh district and extend through the sediments of Rehatikhol formation north of Salhebhata. Multiepisodic silicification, breciation and quartzo feldspathic injection are observed in this shear zone. Some spotty low order RA also observed in this shear zone near Kurapali in the sheared granite. It is affected by NNE fractures/ faults and spotty low order RA zone also observed along N035^0 trending fracture. It is affected by NNE fractures/ faults. It extends below Rehatikhol sediments with strong reactivation imprints at north of Salhebhata.

b. NE- SW fracture with silicification, breciation and quartzo feldspathic injection at W of Kermeli village, Bargarh district analysed upto 0.014% eU_3O_8, 0.012% U_3O_8 with <0.005%ThO_2 (n=2).

6.3.2.1 Detailed study of Malaikhaman anomaly

Nearly WNW (N290- N310^0) trending shear zone passes between Padhanpali-Malaikhaman tract that intruded by an uraniferous quartz reef with very high order RA and secondary U mineralisation. Radiometric assay result (Table 6.4) of this Malaikhaman anomaly (in brecciated quartz reef) reveals upto 0.130 % eU_3O_8, 0.035 % U_3O_8 with <0.005%ThO_2 (n=6). Most of the samples show disequilibrium towards daughter product due to high concentration of secondary U minerals. Basement granite is intensively mylonitised along this sinistral shear zone with the development of S-C fabric (Figure 6.4) and minor phyllonite (Figure 6.5) at some places. This zone is later intruded by the parallel uraniferous quartz reef and veins that have lensoidal and curvilinear form (Figure 6.6) at places possibly indicating later activation of shearing affecting it. The marginal portion shows intense breciation and recrystallisation (resilicification?) with very high order radioactivity (Figure 6.7) along with secondary U mineralisation and minor sulphide mineralisation.

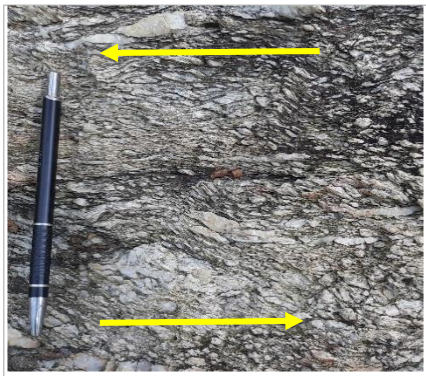

Figure 6.4 S-C fabric in granite mylonite showing sinistral shear, E of Malaikhaman.

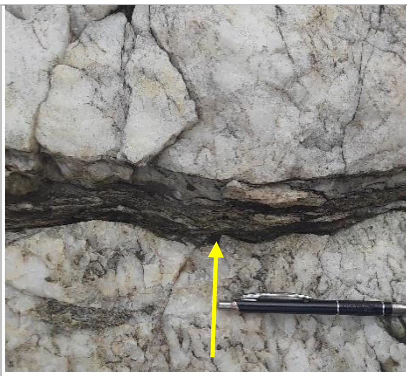

Figure 6.5 Phyllonite relict in the quartz reef, E of Malaikhaman.

Figure 6.6 Lensoidal quartz reef intruded into granite mylonites.

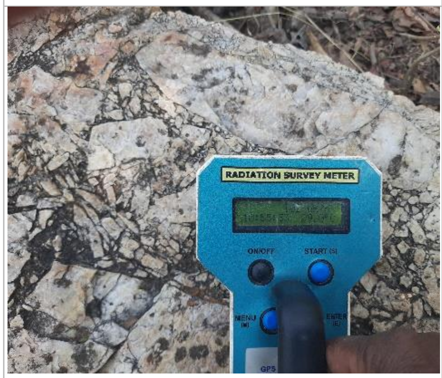

Figure 6.7 High radioactivity in brecciated quartz reef, E of Malaikhaman.

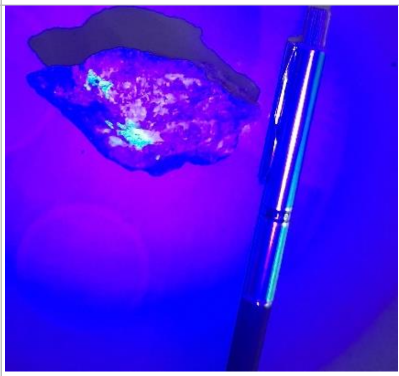

Figure 6.8 Secondary U mineral showing fluorescence under UV light.

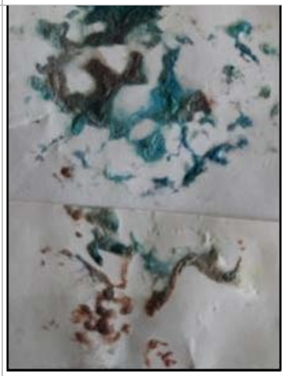

Figure 6.9 Positive chromogram test (Brown colour).

Table 6.4: Radiometric assay result of Malaikhaman anomaly samples.

Sample No.	**%eU_3O_8**	**% U_3O_8**	**% ThO_2**	**Latitude**	**longitude**	**Rock Type**
MKN/QRF/1	0.015	<0.010	<0.005	21^{0}15’ 00.76”	83^{0}15’07.85 “	Brecciated quartz reef
MKN/QRF/3	0.100	0.041	<0.005	21^{0}15’ 00.77”	83^{0}15’07.84 “	
MKN/QRF/4	0.082	0.032	<0.005	21^{0}15’ 00.76”	83^{0}15’07.84 “	
MKN/QRF/5	0.042	0.047	<0.005	21^{0}15’ 00.77”	83^{0}15’07.85 “	
MKN/QRF/6	0.110	0.029	<0.005	21^{0}15’ 00.77”	83^{0}15’07.84 “	
MKN/QRF/7	0.130	0.035	<0.005	21^{0}15’ 00.77”	83^{0}15’07.84 “	

This breciation episode could be associated with the mineralisation since the high radioactivity only limited to the brecciated marginal portion and traceable upto 10- 20 m on the both margins. Lemon yellow colour secondary U mineral (autonite?) observed as fracture coating on RA samples giving flouroscence under UV light (Figure 6.8). Shearing is so intense that quartz grains are almost become linear due to stretching in the central part and it dilute away from the zone suddenly. Mylonite is also silicified due to infiltration of silica from the quartz reef/vein. This shear zone is affected by a NNE trending ferrugenised fracture/ fault sinistrally and further extend beneath the sediment of Rehatikhol formation without affecting these. Epidotitisation is major alteration in the basement rock in the adjacent area. No evidences of reactivation of this shear zone observed in sediments in same continuity but joints sets of same trend are noted.

Petrological studies on Malaikhaman anomalies samples

Petrological studies has been carried on the samples of Malaikhaman anomaly for better understanding of U and associated mineralisation and their controls. Attempt has been made to locate/identify radioactive mineral, its mode of occurrence and association with other oxide and sulphide minerals (by CN film autoradiography).

Megascopic Characters: The studied samples are part of fractured/brecciated quartz reef showing high order mineralisation with secondary minerals and sulphide. The host rock is appears to be highly brecciated/fractured quartz reef emplaced within sheared granite. Sulphide minerals can be seen megascopically. Chromogram test on highly active samples gives positive result (brown spots) and indicate presence of leachable U (Figure 6.9). Blue spots are due to Fe associated with pyrite and other minerals.

Microscopic Characters: Under microscope, the rock shows high deformation manifested as fractured quartz rich rock with angular strained fragments, dusty inclusions in quartz with strain orientation, presence of fracture filling veins with secondary uranyl minerals, apatite, fluorite chalcopyrite and pyrite. Sassuritisation of feldspars are also noticed along vein margins. It consists predominantly of quartz (~ 90-95% by volume), with vein containing brecciated quartz fragments with secondary uranyl minerals, saussurite, apatite, fluorite, pyrite and chalcopyrite.

High radioactive sample was presently studied to decipher causative factors of high radioactivity, radioactive phases and associated minerals, including sulphides. The mosaic view of the mineralized vein is shown in Figure 6.10. Brecciation signatures of quartz reef showing angular fragments of quartz and plastic flow behaviour is reflected in Figure 6.11 a & b. Secondary silicification is also noted along the fractures. Presence of saussurite and secondary uranyl minerals is shown in Figure 6.12 and secondary uranyl minerals aligned along the vein with presence of apatite and fluorite is shown in Figure 6.13. The rock has shown high density alpha tracks on CN film (72 hours exposure) corresponding to secondary uranyl minerals along the fracture filling vein (Figure 6.14 a & b).

Presence of apatite (Figure 6.15 & 6.13) and fluorite (Figure 6.13 & 6.16) with secondary uranyl minerals along the vein is characteristic of the rock. Strain orientation of dusty inclusions (Figure 6.17), strained quartz with alignment along the vein (Figure 6.18), shearing effect and polymetallic association in vein are reflected below. Sphalerite with sulphide disease (exsolution texture) (Figure 6.19) and brecciated pyrite also observed. Chalcopyrite disease is exsolution texture and results from simultaneous crystallisation of sphalerite and chalcopyrite. Saussuritisation of sheared fragments of feldspars is common in and around the mineralized vein. Host rock is named as fractured quartz reef.

Ore Minerals / Opaques: Besides secondary uranyl minerals pyrite and chalcopyrite (Figure 6.19 & 6.20) are the common association along the mineralized vein.

XRD analysis

One high radioactive sample of brecciated quartz reef from Malaikhaman anomaly has been analysed using X ray diffraction (XRD) technique to identify radioactive mineral, opaque minerals and silicate mineral phases. Uraninite and kasolite (in traces) are identified atomic minerals along with Goethite, Hematite, magnetite, pyrite and galena (traces) as ore minerals.

Biotite, chlorite, fluorapatite, strengite, jarosite and quartz are other rock forming minerals identified.

XRF analysis

Three samples from the anomaly (MKN/QRF/4, 5 & 7) analysed high SiO_2 (82.94-86.56%), CaO (2.00-3.40%), P_2O_5 (1.85-2.66%), Na_2O (1.16-1.45%) with Al_2O_3 (5.15-5.75%), Fe_2O_3 (T) (2.22-3.66%), K_2O (0.04-0.16%) and low MgO (0.03-0.11%), MnO (<0.01-0.01%) (Table 6.5), which is also reflected in its mineralogy as dominant quartz, saussurite, apatite and fluorite with secondary uranyl mineral (autonite is inferred due to high Ca & P_2O_5) with total iron attributing to Fe-sulphides (Pyrite & Chalcopyrite).

Figure 6.10 Mosaic view of apatite-fluorite-sulphide-uranium bearing vein within sheared quartz reef, 1N, 2.5x, TL.

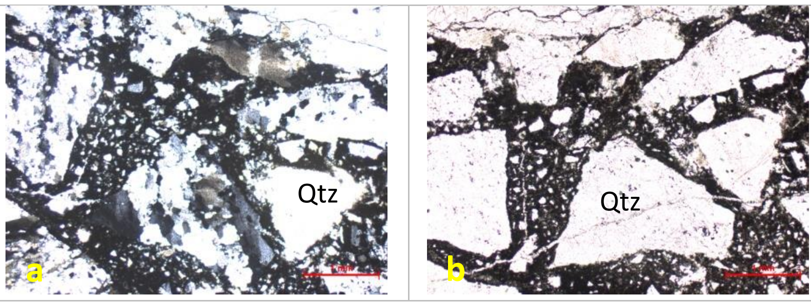

Figure 6.11a & b Brecciation of quartz reef and plastic flow within mineralized vein, 2N, 2.5x, TL.

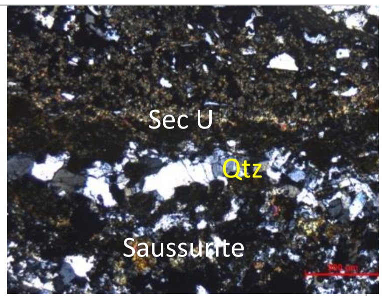

Figure 6.12 Saussurite and secondary uranyl mineral along vein in sheared quartz reef, 2N, 5x, TL.

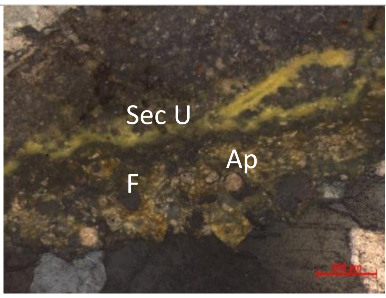

Figure 6.13 Secondary uranyl mineral with apatite, fluorite and sulphide minerals along vein, 1N, 10x, TL.

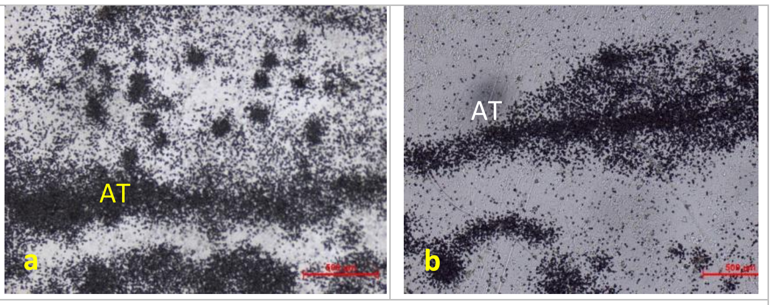

Figure 6.14a & b Alpha tracks (AT) corresponding to secondary U-minerals along vein, 1N, 5x, TL.

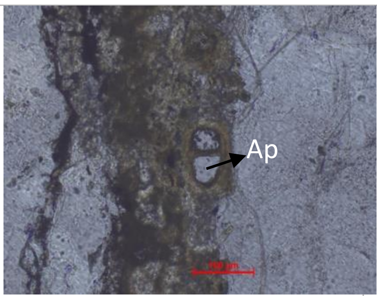

Figure 6.15 Apatite along the vein in sheared quartz reef, 1N, 20x, TL.

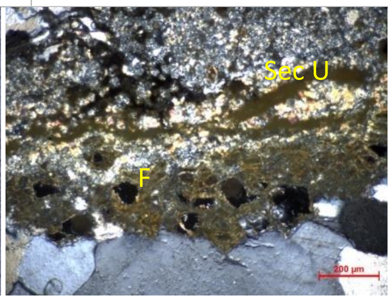

Figure 6.16 Secondary uranium minerals with fluorite along the vein in sheared quartz reef, 2N, TL.

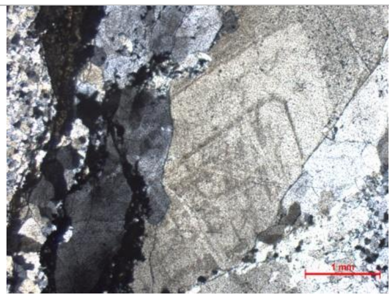

Figure 6.17 Strain orientation of dusty inclusion in sheared quartz reef, 2N, 2.5x, TL.

Figure 6.18 Strained quartz in and around the mineralized vein, 2N, 2.5x, TL.

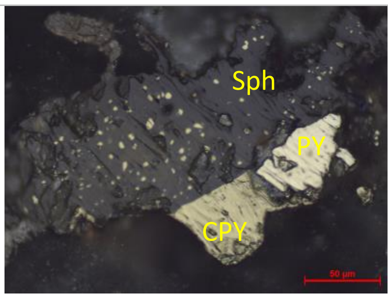

Figure 6.19 Chalcopyrite disease (chalcopyrite inclusion within sphalerite) in brecciated quartz reef, RL, oil, 1N.

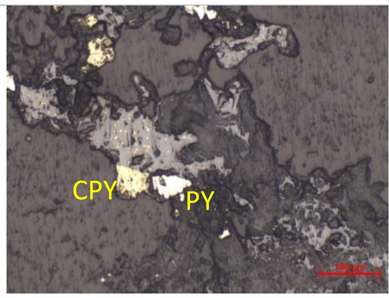

Figure 6.20 Pyrite and chalcopyrite along the vein, 1N, 20x, TL.

Besides, high Cr (159-240ppm), Zn (128-197ppm), Y (59-97ppm), Pb (371-640ppm) and uranium (613-851ppm) also analysed in the rock. Cu (30-32ppm) and Ni (17-19ppm) is analysed. Based on XRF analysis, physical assay and petrological studies, U-Cu-Pb-Zn association with apatite and fluorite in vein is evident. Affinity of U with fluorite is clear with this study in the environs of Singhora basin.

REE & Fluorine analysis result of Malaikhaman anomaly samples

REE analysis result of 5 radioactive samples of Malaikhaman anomaly (brecciated quartz reef with secondary U minerals, polymetallic sulphide, fluorite and apatite vein) received from chemistry lab CR (ICP- AES) is tabulated in Table 6.6. Chondrite normalised plot (Nakamura 1974) of these samples shows nearly flat pattern of HREE with minor depletion of LREE. All radioactive samples analysed high F content (Table 6.7) indicating presence of fluorite associated with U. The total REE content of quartz reef is low and varies from 39.6 -71.3 ppm (Table 6.7). The quartz reef is characterised by minor depletion of LREE ($(La/Yb)_N$ = 0.53-1.56). All samples shows minor positive Eu anomaly and nearly flat pattern of HREE (Figure 6.21). The positive Eu anomaly coupled with LREE depletion in these productive quartz veins suggests a source which is enriched in Eu and depleted in LREE due to crystal fractionation. Chondrite normalised REE pattern of mineralised quartz reef is nearly similar with positive Eu anomaly to gold bearing quartz veins of Hutti gold field, Karnataka (Rao et al, 2015) and Archean Basement-Hosted Gold Deposit in Pinglidian, Jiaodong Peninsula, Eastern China (Ruihong Li et al, 2019). It indicate possibility of Au association also with Malaikhaman quartz reef. Presence of polymetallic sulphides, ferrugenised breccia (in near vicinity), hydrothermal fluorite and apatite mineralisation coupled with U mineralisation also indicate a possibility of IOCG system in study area.

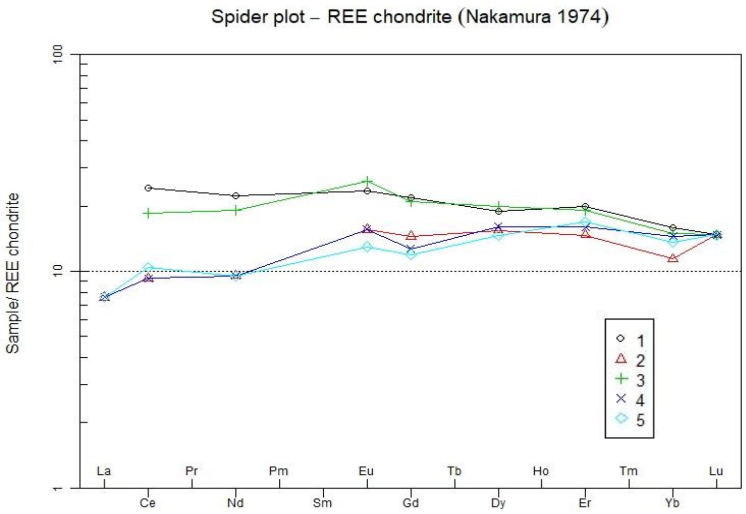

Figure 6.21 Chondrite normalised REE spider diagram of Malaikhaman anomaly samples.

Table 6.5 XRF analysis result of Malaikhaman anomaly samples.

	MKN/QRF/4	MKN/QRF/5	MKN/QRF/6
Concentration in Wt %			
SiO_2	86.56	82.94	84.22
TiO_2	0.04	0.06	0.09
Al_2O_3	5.15	5.75	5.29
Fe_2O_3(T)	2.22	3.04	3.66
MgO	0.08	0.11	0.03
MnO	<0.01	0.01	<0.01
CaO	**2.00**	**3.40**	**2.40**
Na_2O	1.16	1.45	1.41
K_2O	0.04	0.14	0.16
P_2O_5	**1.85**	**2.66**	**1.91**
Concentration in ppm			
Cr	40	194	159
Ni	19	18	17
Cu	30	32	30
Zn	**168**	**128**	**197**
Ga	27	26	30
Rb	17	24	28
Sr	47	213	80
Y	68	59	97
Zr	55	47	110
Nb	51	47	63
Ba	39	248	155
Ce	10	27	20
Pb	**416**	**371**	**640**
Th	46	41	53
U	**613**	**851**	**663**

Table 6.6 REE data of Malaikhaman anomaly samples (in ppm).

Sample No.	MKN/QRF/03	MKN/QRF/04	MKN/QRF/05	MKN/QRF/06	MKN/QRF/07
La	8	<5	6	<5	<5
Ce	21	8	16	8	9
Pr	<5	<5	<5	<5	<5
Nd	14	6	12	6	6
Sm	<5	<5	<5	<5	<5
Eu	1.8	1.2	2	1.2	1
Gd	6	4	5.8	3.5	3.3
Tb	<2	<0.2	<2.0	<2.0	<2.0
Dy	6.5	5.3	6.8	5.5	5
Ho	<2	<2.0	<2.0	<2.0	<2.0
Er	4.5	3.3	4.3	3.6	3.8
Tm	<2	<2.0	<2.0	<2.0	<2.0
Yb	3.5	2.5	3.3	3.2	3
Lu	0.5	0.5	0.5	0.5	0.5
Y	33	28	35	27	27

Table 6.7 Summary of REE data of Malaikhaman anomaly (concentration in ppm).

Sample No.	**∑REE**	**∑LREE**	**∑HREE**	**LREE/ HREE**	**(La/Yb) N**	**(La/Sm) N**	**(Sm/Yb)N**	**%F**
MKN/QRF/3	71.3	47.3	24	1.971	1.54	2.01	0.77	0.05
MKN/QRF/4	38.8	20.2	18.6	1.086	0.68	0.63	1.08	0.13
MKN/QRF/5	62.2	38.5	23.7	1.624	1.23	1.51	0.81	0.15
MKN/QRF/6	39.5	20.2	19.3	1.047	0.53	0.63	0.84	0.03
MKN/QRF/7	39.6	21	18.6	1.129	0.56	0.63	0.90	0.10

CHAPTER 7
FLUORITE AND SULPHIDE MINERALISATION

7.1 FLUORITE MINERALISATION

Fluorite mineralisation has been observed in study area at different locations in basement rocks as well as Singhora sediments (Figure 7.1). Fluorite mineralisation is found-

(a) in Gritty feldspathic arenite and pebbly layers of Rehatikhol Formation at

(i) ~1km N of Makarmuta, (Figure 7.2) (ii) 400 m S of Chiwarakuta

(iii) 1.5 km NE of Chiwarakuta

(b) in Feldspathic Arenite at the intersection of ENE- WSW, NE-SW and NW- SE fractures near 0.8 km NE of Bandhalimal

(c) in basement rock at contact of mafic rock

(i) 200 m SE of Ghatkachar. (ii) in basement fracture north of Kodopali outlier, near Jhal.

Fluorite vein bearing feldspathic arenite samples of different trends have been studied in petrology lab for petromineralogical studies. Fluorite of different veins/directions has been separated using bromoform in MPU lab and some samples sent to chemical lab for major, trace elements including U, REE and bromoheavies and fluorite vein samples have been sent to stable isotope studies. The fluorites mainly occur as purple, deep/navy blue, violet color and whitish translucent variety.

Fluorite is hosted by deformed conglomerate in Makarmuta area. Rock consisting fractured/ strained clasts of quartz and chert have contact with sheared and brecciated basement granite at N of Makarmuta (Figure 7.2, 7.3 & 7.4). The clasts are stretched/elongated in the direction of shearing (Figure 7.3). The clasts got brecciated due to progressive deformation and fractures and interclast spaces are later filled with silica and fluorite by apparent late stage hydrothermal fluids. Shear cleavage also developed as result of shearing (Figure 7.4). Fluorite of 3 different colors (colorless to whitish translucent, purple/ violet and deep navy blue) are present as veins (Figure 7.5 -7.10) and coating along with silicification in the gritty feldspathic arenite and conglomerate layers. There is possibility that different colors of fluorite are due to varying trace elements and REE composition in its lattice might have arisen due to its crystallization from multiple generation hydrothermal activity. Three different shear zones are identified in Chiwarakuta- Makarmuta tract that are parallel to the major structural fabrics (mostly faults) passing through Makarmuta and west of Gatkachhar (Figure 2.2). It has been observed that navy blue color fluorite is youngest since its veins cut across other existing colored fluorite (Figure 7.7). Silicification is also closely associated with fluorite mineralisation. Multiple generations of fluorite mineralisation and silicification is present in Rehatikhol Formation around Chiwarakuta area. Different generations of fluorites are shown with respect silica vein in Figure 7.9- 7.11. At least 3 generations of fluorite mineralisation with respect to silicification has been identified based on cross cutting relationship (megascopic field observations).

1. Fluorite mineralisation prior to silicification (Figure 7.9)
2. Fluorite mineralisation cogenetic with silicification (Figure 7.10)
3. Post silicification fluorite mineralisation (Figure 7.11)

Although association of fluorite with U mineralisation couldn't be located in field during radiometric survey around Chiwarakuta area but it is noteworthy that a significant hydro U anomaly (54ppb U and 4 ppm F) is located by the water sample collected just 100 m NNW of fluorite mineralized faults in the same trend continuation (Figure 7.1).

7.1.1 Petrological studies on fluorite hosted sheared pebbly feldspathic arenite.

Rock samples are medium grained in shades of grey-white. These samples are hard, compact and massive in nature. Fracturing is visible and fluorite smears are observed on the rock surface.

The rock contains clast supported framework. It is moderately sorted contains sub rounded to rounded clasts of medium to coarse sand, granules and pebbles bound by matrix and cement. The clasts are mainly composed of quartz with subordinate feldspar.

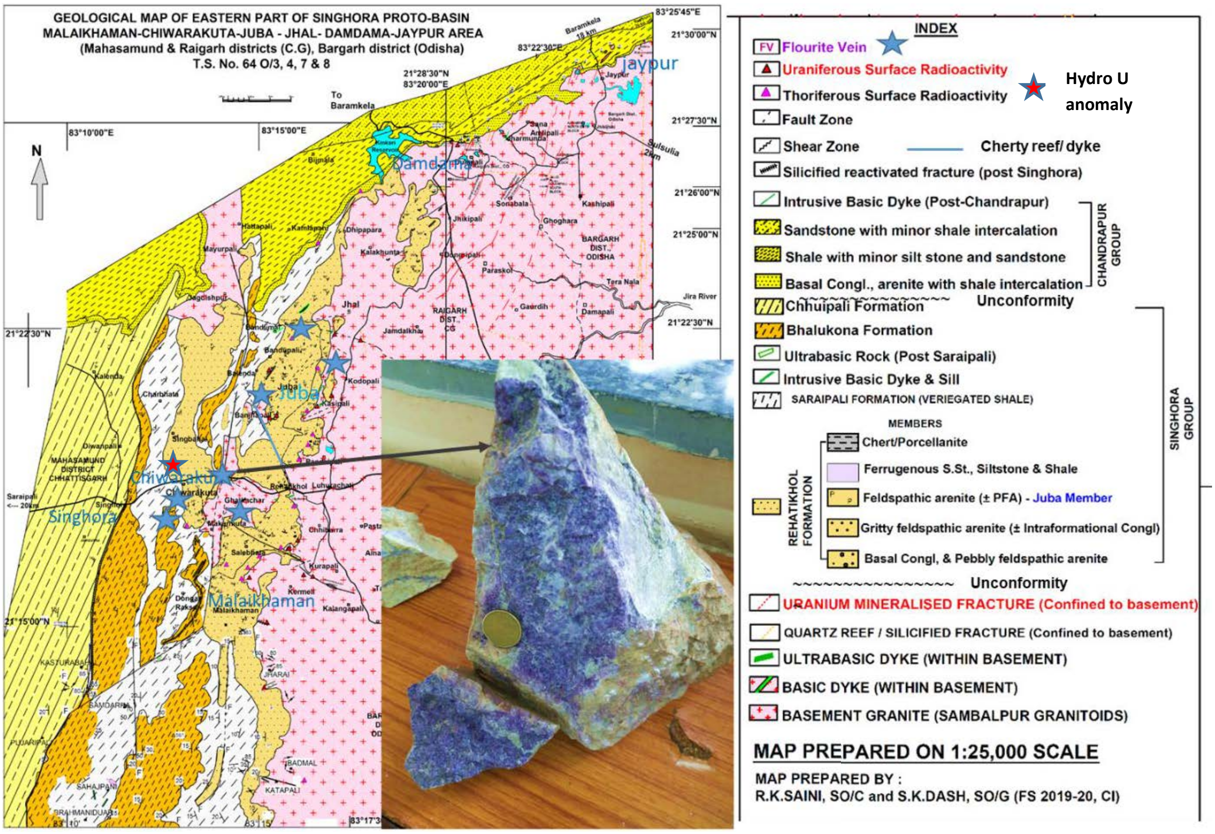

Figure 7.1 Regional geological map of eastern part of Singhora protobasin showing various fluorite occurrences in and around project area.

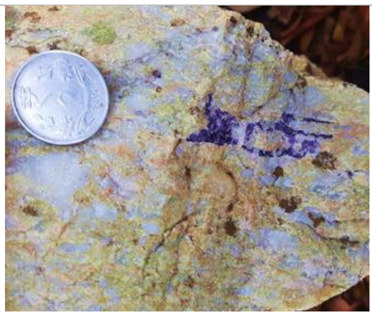		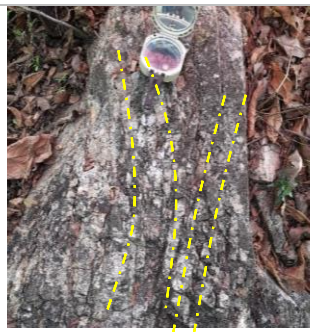
Figure 7.2 Deep navy blue fluorite mineralisation in fracture filling in strained and silicified conglomerate, N of Makarmuta.	Figure 7.3 Highly stretched clast in conglomerate in N350^0 trending shear zone, N of Makarmuta.	Figure 7.4 Shear cleavage in conglomerate having contact with deformed granite Makarmuta.

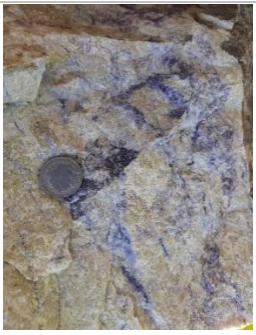

Figure 7.5 Coating of translucent fluorite and purple colour fluorite vein in silicified gritty feldspathic arenite, N of Makarmuta.

Figure 7.6 Violet fluorite mineralisation at N of Makarmuta in silicified gritty feld. arenite.

Figure 7.7 Cross cutting veins (navy blue cutting purple) of fluorite indicating different generation's fluorite, S of Chiwarakuta.

Figure 7.8 Fluorite mineralisation in basement rock near Gatkachhar.

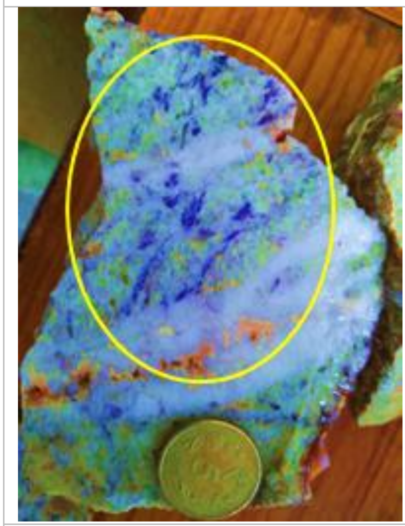

Figure 7.9 Violet Fluorite stringes/ veins cutting across by silica veins. Prior to silicification generation of fluorite.

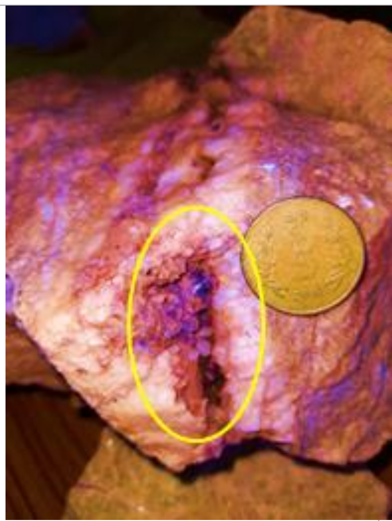

Figure 7.10 Cogenetic purple fluorite in silica vein forming comb and vug structure. Cogenetic generation of fluorite.

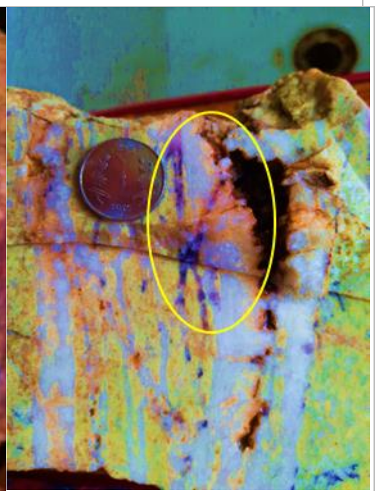

Figure 7.11 Thick silica vein cutting across by violet fluorite. Post silicification generation of fluorite.

Quartz is represented by both mono-crystalline and poly-crystalline grains, whereas feldspar is represented by clasts of perthite and microcline (Figure 7.12). The pebbles are constituted by quartzite and vein quartz. Fine quartz, feldspar, clay and sericite constitute matrix whereas secondary overgrown silica in optical continuity with detrital quartz constitute the binding cement. Zircon is the heavy mineral present. The clast composition indicates mainly a granite

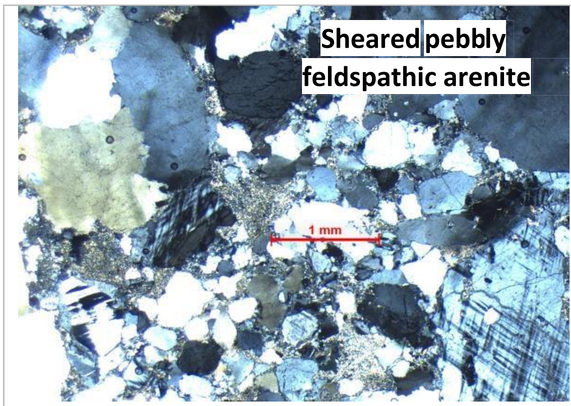

Figure 7.12 General texture of deformed pebbly/ Gritty feldspathic arenite of Chiwarakuta, TL, Air, 2N.

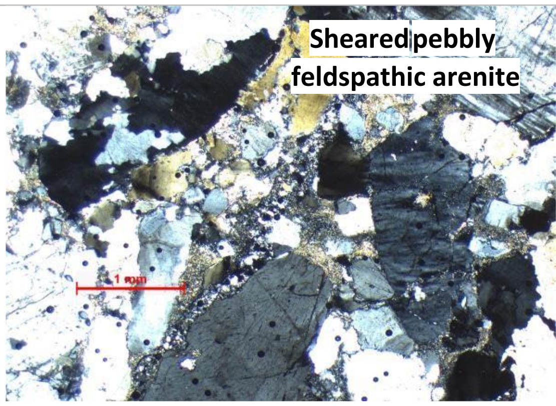

Figure 7.13 Intense microfracturing and generation of epimatrix in deformed pebbly feldspathic arenite at Chiwarakuta, TL, Air, 2N.

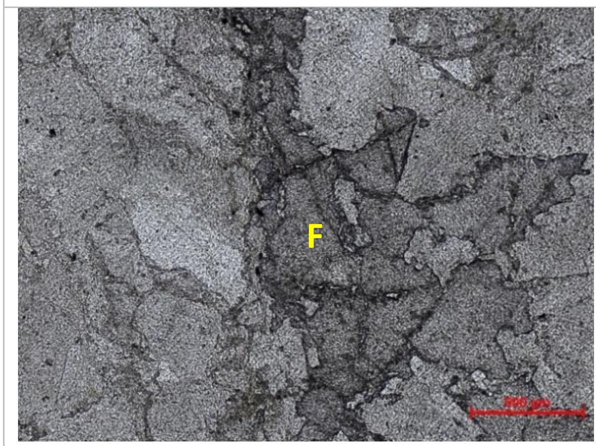

Figure 7.14 Cogentic fluorite and quartz vein in deformed feldspathic arenite, TL, 1N, Air.

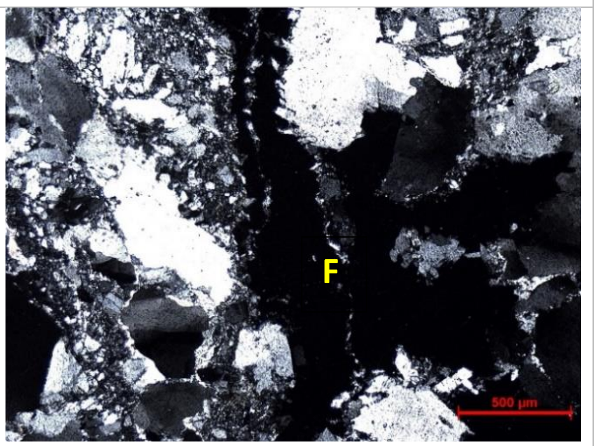

Figure 7.15 Cogentic fluorite and quartz vein in deformed feldspathic arenite, TL, 1N, Air.

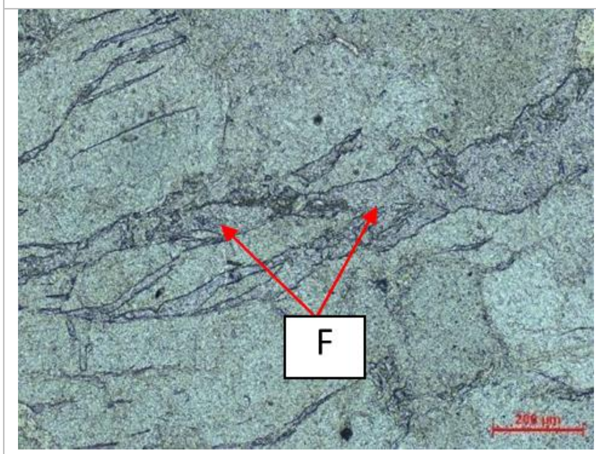

Figure 7.16 Violet colour fluorite in Feldspathic sandstone, Chiwarakuta, TL, air, 1N.

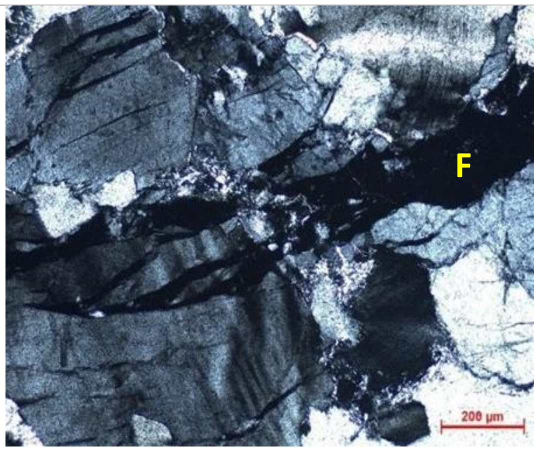

Figure 7.17 Deformation in feldspar in fluorite hosted Sheared sandstone, Chiwarakuta, TL, air, 2N.

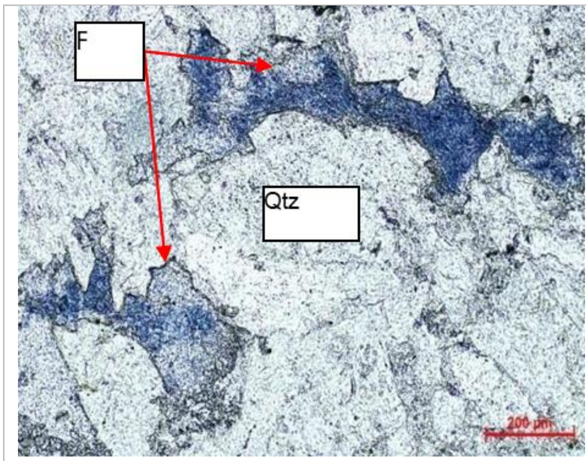

Figure 7.18 Sheared sandstone cut across by ink blue fluorite vein (F), Chiwarakuta.

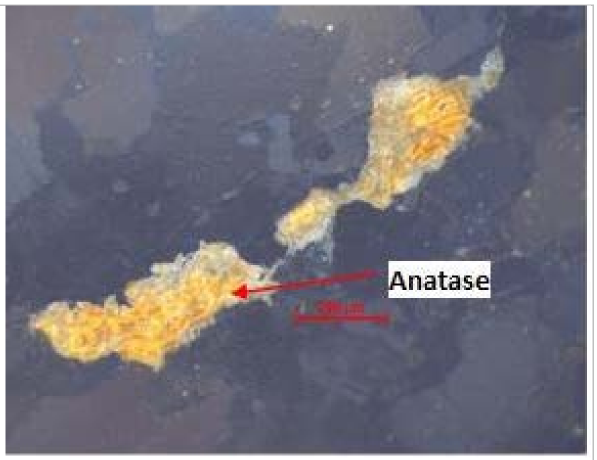

Figure 7.19 Anatase segregation in matrix of pebbly feldspathic arenite, RL, air, 2N.

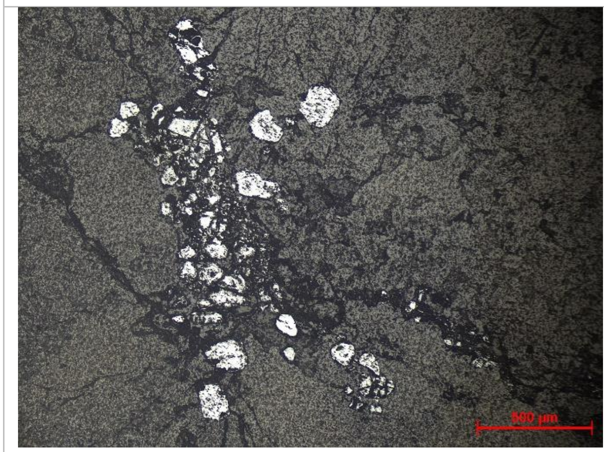

Figure 7.20 Opaques as subhedral subrounded pyrite grains in deformed pebbly feldspathic arenite RL, air, 1N.

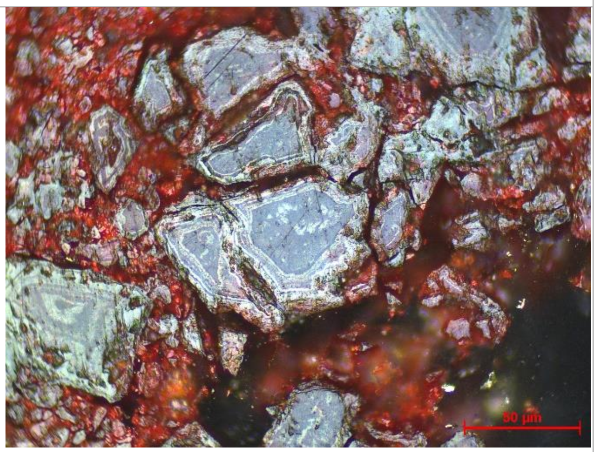

Figure 7.21 Altered magnetite in deformed feldspathic sandstone, E of Chiwrakuta, RL, oil, 1N.

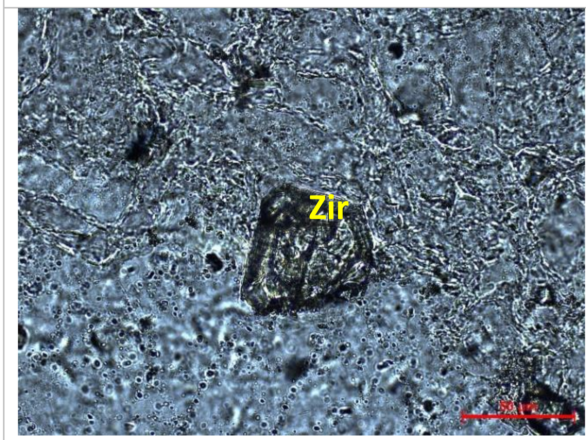

Figure 7.22 Light yellow fine sized zoned zircon in quartz in sheared feldspathic sandstone, SE of Chiwarakuta, TL, oil, 1N.

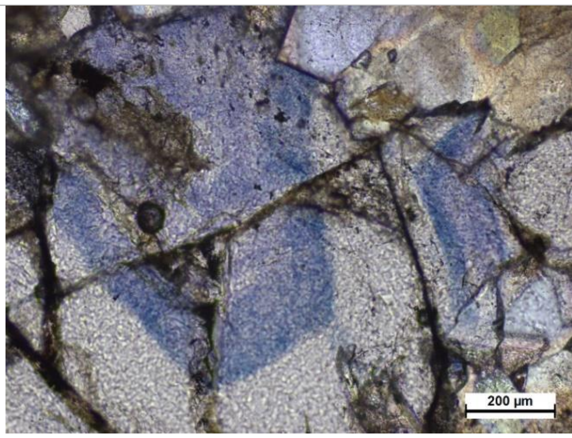

Figure 7.23 Zoned fluorite in basement rock near to the basic dyke, Gatkachhar, TL, air, 1N.

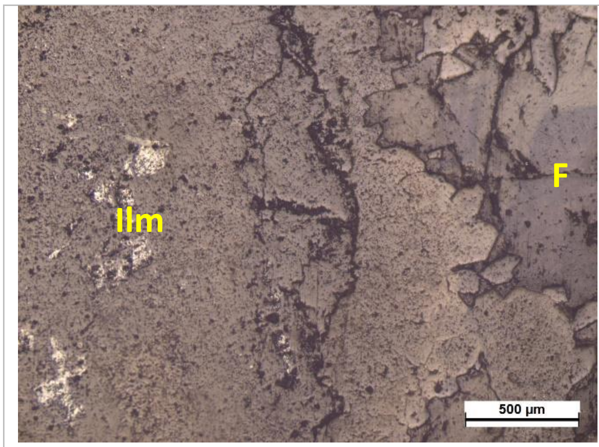

Figure 7.24 Fluorite and opaques (ilmenite) as diseminations in fluorite bearing basement rock, Gatkachhar, RL,air, 1N.

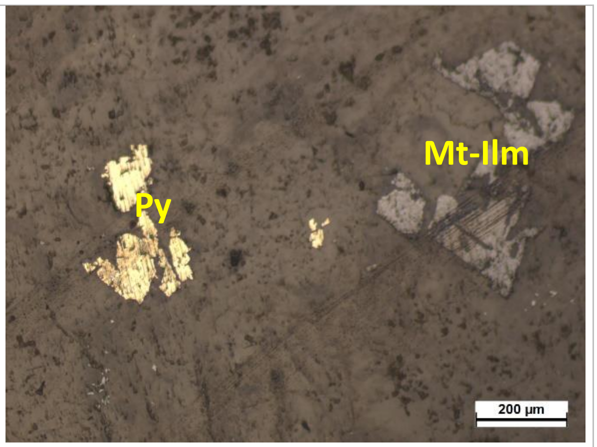

Figure 7.25 Pyrite and magnetite-ilmenite in fluorite bearing basement rock, Gatkachhar, RL, air, 1N.

source rock with minor contribution from sedimentary litho-units. These rocks display shearing effects (Figure 7.12) as displayed by micro-fracturing of the rock mosaic (Figure 7.13-7.16) and variable degree granulation of the clast component. Epimatrix of quartzo feldspathic material also observed as result of shearing and granulation (Figure 7.13). The fractures are often filled with crushed quartzo-feldspathic material and fluorite. Flourite mineralisation occurs as irregular segregation along the weak planes and as smears (Figure 7.14- 7.18). Weak planes and microfracture host the hyderothermal fluorite along with silica.

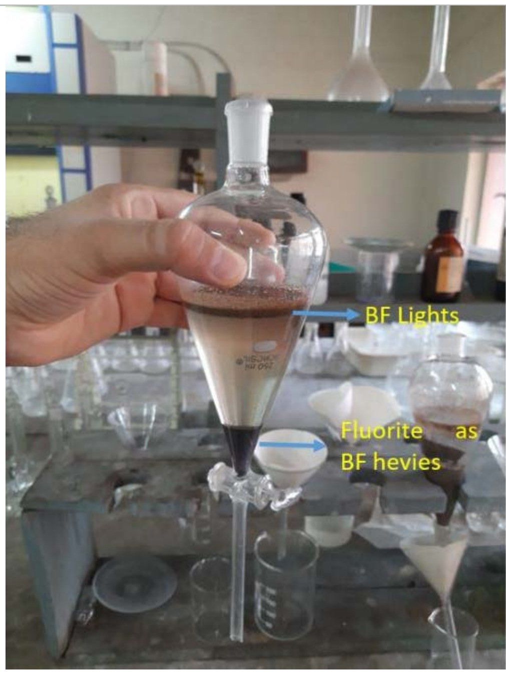

Figure 7.26 Separated fluorite in bromoform as heavy concentrate and quartz feldspar in light fraction. Heavy mineral separation setup.

Mode of occurrence of fluorite is either in vein form or as a fracture filling. It indicates its epigenetic hydrothermal origin. There is close association of fluorite with secondary silica. Cogentic silica veins with fluorite are also evident by petrography (Figure 7.14 & 7.15). Fluorite veins are found to be cutting across deformed quartz and feldspar grain (Figure 7.16 & 7.17). Fluorites of mainly 3 colours are observed in different samples that is violet colour (Figure 7.16), ink blue/ navy blue fluorite (Figure 7.18) and nearly colourless transparent variety with bluish tinge. Anatase is found as irregular segregations, occurring in association with matrix (Figure 7.19). Opaque minerals are pyrite and altered magnetite (Figure 7.20 & 7.21). Pyrite occurs as subhedral / subrounded grains in epimatrix and microfractures. Altered magnetite with goethitisation also observed in this pebbly deformed feldspathic arenite. Fine zircon as inclusion in quartz is noted that indicate granitic provenance of this lithounit (Figure 7.22). Intense deformation in all fluorite bearing lithounits in petrography, field observation and associated of fluorite with silicified zone indicates its structural control bearing i.e. along NNW and NE faults/ fractures.

7.1.2 Fluorite mineralisation hosted by basement rock in Gatkachhar

Mineralisation of fluorite is also reported from Gatkachhar in basement rock that have high specific gravity and consist of pink and dark coloured fine mineral (Figure 7.8). Mineralisation occurs as transparent, navy blue and purple colour fluorite variety as veins and fracture filling and localised in the contact zone of a mafic/ ultramafic rock.

Petrological studies over one sample of this rock has shown role and affinity of basic/ magmatism in fluorite mineralisation in basement rocks of Sambalapur granitoids at Gatkachhar. Rock is medium grained under microscope, consisting secondary quartz and feldspar, doleritic relicts and fluorites as veins with vugs and comb structure. Fluorite is found to be zoned indicating very slow crystallisation in different stages in fracture cavities (Figure 7.23). Pyrite, ilmenite and magnetite- ilmenite intergrowth constitute opaque mineral assemblage (Figure 7.24 & 7.25).

7.1.3 Fluorite separation as bromoform heavies

Average specific gravity of fluorite ranges between 3.175- 3.184 and goes upto 3.56 if high REE and trace elements are present in its lattice. It can be acquired in bromform (sp gr. -

2.89) heavies hence crushed and grounded samples of fluorite vein bearing gritty feldspathic arenite and granitoid has been sieved and -80 to +100 # size is selected for the separation to avoid coagulation. Beaker, separating funnel, filter papers, watch glass plate, stirer, infrared lamp, sieve setup and bromoform liquid is used in entire operation. Fluorite has been acquired >98 % concentration after multiple cycle of operation. Pictorial representation of entire setup is given in Figure 7.26.

During bromo-separation it was observed that deep/navy blue fluorites settled first indicating having higher specific gravity and the white/ translucent ones settled last indicating lower specific gravity with purple having intermediate one. This variation is due to variable distribution of REE and trace elements in fluorite. Average specific gravity of fluorite as measured walker steelyard method after grain separation of bromo-heavies revealed that whitish/ translucent variety possesses average 3.014 (n=4), purple/ violet 3.076 (n=6) and navy blue variety 3.095 (n=3).

7.1.4 Geochemistry of Fluorite mineralisation

Chemical analysis of granite with fluorite vein, near NE-SW basic dyke contact, Gatkachhar basement inlier (n=1) is given in table Table 7.1. Major, minor and trace elements are chemically analysed using ICP-AES while analysis of fluoride has been carried by Ion Selective Electrode method at chemistry lab, CR, Nagpur.

Table 7.1 Major (wt %), trace elements and REE (ppm) data of basement rock with fluorite.

Sample No	SiO_2	Al_2O_3	Fe_2O_3	FeO	MnO	MgO	CaO	K_2O	Na_2O	TiO_2	P_2O_5	LOI	F	Y
GTK/GRF/01	67.80	7.20	1.10	1.00	0.01	0.17	**9.92**	5.80	2.05	0.58	0.10	3.20	**6.80**	**32**
	U_3O_8	Zn	V	Ni	Cr	Co	Cu	Pb	Zr	Hf	Rb	Ba	Sr	
GTK/GRF/01	2	20	51	18	22	47	**60**	14	54	<5	200	1510	19	
	La	Ce	Pr	Nd	Sm	Eu	Gd	Tb	Dy	Ho	Er	Tm	Yb	Lu
GTK/GRF/01	10	22	<5	10	<5	<0.5	5	<2	4	<2	2.5	<2	2.0	0.5

Table 7.2 Chemical Analysis of Fluorite Samples (bromoheavy with Flourite concentrate & Vein Fluorite), Chiwarakuta (n=3).

	CKT/SSTF/11	CKT/SSTF/11A	CKT/SSTF/11B		CKT/SSTF/11	CKT/SSTF/11A	CKT/SSTF/11B
Concentration in Wt %					**REE Concentration in ppm**		
Ca	**46.3**	**46.9**	**46.2**	La	<5	**8**	<5
F	**39.2**	**38.3**	**39.3**	Ce	**7**	**13**	**9**
SiO_2	8.11	8.96	8.10	Pr	<5	<5	<5
TiO_2	0.01	0.01	0.01	Nd	<5	<5	<5
Al_2O_3	1.30	1.16	1.21	Sm	<0.5	<0.5	<0.5
Fe_2O_3	0.20	0.10	0.10	Eu	<2	<2	<2
FeO	<0.01	<0.01	<0.01	Gd	<2	<2	<2
MgO	0.03	0.04	0.03	Tb	<2	<2	<2
MnO	<0.01	<0.01	<0.01	Dy	<2	<2	<2
Na_2O	2.18	2.28	2.25	Ho	<2	<2	<2
K_2O	0.49	0.38	0.42	Er	<2	<2	<2
P_2O_5	<0.01	<0.01	<0.01	Tm	<2	<2	<2
LOI	0.03	0.02	0.02	Yb	<0.5	<0.5	<0.5
Concentration in ppm				Lu	<0.5	<0.5	<0.5
U_3O_8	<1	<1	<1	Y	**8**	**8**	**7**
Sr	14	17	13	Sc	<10	<10	<10
Zr	95	90	98	Th, V, As, Se, Cs, Ni, Cr, Co, Cu, Pb, Hf analysed <10ppm			

Sample analysed higher Cao and F due to fluorite and moderately higher Cu and Y values. Some of REE are analysed below detection limit of ICP- OES hence proper inferences cannot be made. Although, enriched LREE can be inferred from available data indicating crystallisation from more fractionated and evolved melt/ fluid. One sample of separated fluorite from basement rock has been sent for INAA analysis of REE.

Chemical analysis of fluorite vein (n=3) occurring within Rehatikhol arenite at Chiwarakuta area indicate presence of co-genetic silica (SiO2 8.10-8.96% in fluorite vein) with some impurities (?). Though REE content is low, but some significant content of La, Ce, Y are observed (Table 7.2).

7.2 SULPHIDE MINERALISATION

At Juba area, Pyrite (diagenetic, epigenetic and remobilized), pyrrhotite, galena, chalcopyrite, covellite, bornite, luzonite, enargite, argentite, argentopyrite and sternbergite are the reported sulphide minerals associated with Uranium minerals like pitchblende/uraninite & coffinite. Syn/diagenetic sulphide mineralisation in feldspathic arenite observed at Salhebhata-Malaikhaman (Figure4.27) akin to Juba area besides epigenetic sulphide along veinlets/sulphide bleeding near fractures/faults (NW-SE & N-S). PFA is widespread around Salhebhata village where clusters of pyrites from outcrop has been observed (Figure 7.28). Rehatikhol Formation is significantly pyritiferous in PFA unit but occasional pyrite also observed in other units like pebbly/ gritty feldspathic arenite near Chiwarakuta and Singbhal dam, in pebbly arenite horizon of basal conglomerate near Rehatikhol and in pyritiferous pebbly feldspathic arenite other than PFA. At Chhibarra anomaly, diagenetic and epigenetic sulphides (dominantly pyrite and Galena) observed (Figure 7.29). In the upper portion of Rehatikhol Formation, porcellanite layers comprise pyrites as disseminations and at fissility plane on outcrop scale (Figure 7.30). Some basement fractures also contain sulphides. Pyrite-Chalcopyrite- Sphalerite- Secondary uranium association was seen in WNW-ESE silicified basement fracture near Malaikhaman (Malaikhaman anomaly).

	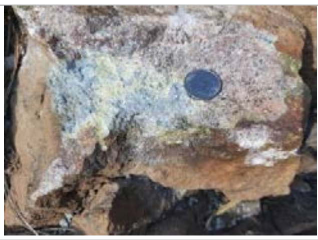		
Figure 7.27 Sulphide bleeding and spheroidal weathering in PFA near Salhebhata.	Figure 7.28 Clusters of syn/ diagenetic pyrite in feldspathic arenite from SE of Salhebhata.	Figure 7.29 Pyrite and galena in PFA at Chhibarra anomaly.	Figure 7.30 Sulphide mineralisation in Porcellanite near Chiwarakuta.

CHAPTER 8
DISCUSSION

This project is an attempt of detailed study of rocks in Chiwarakuta- Rehatikhol- Malaikhaman- Dongar Raksha sector that lies south of earlier studied Juba area, considering it similar potential area for U mineralisation. It encompasses characterisation of Rehatikhol Formation and basement rocks for understanding of uranium, sulphide and fluorite mineralisation. Focus of present study mainly remained on the Rehatikhol Formation to give interpretation about provenance, tectonic setting, paleoweathering and paleoclimatic conditions, and possible controls of U and fluorite mineralisation. Earlier explored adjacent Juba area for unconformity related mineralisation by previous workers, has been is taken into consideration for geochemical comparison.

The area under study has been mapped in detail first time by author on 1:10000 scale (55 sq km area) attributing lithostructural disposition and mineralisation in the area. The present study contributed identification and description of various variants of basement Sambalapur Granitoids i.e. Pink porphyritic granite, biotite granite, biotite muscovite granite (two mica granite?), gneisses and feldspathic injections. Basement Sambalpur granitoids of Chhibarra, Murmuri and Muchbahl- Banabira are characterised as biotite tonalite and biotite granodiorite composition by petromineralogical studies. Deformation imprints, saussuritisation, chloritisation as alteration has been noted in these granitoids.

Geochemical characterisation of Sambalpur Granitoids has been carried out that shows geochemical variation in pink porphyritic granite and biotite granite of different sector in study area. In the classical AFM diagram after Irvine and Baragar, 1971, all the studied samples fall in a typical calc alkaline Al enrichment field indicating composition of source of magma. The Sambalpur Granitoids has been classed under peraluminous to metaaluminous, tonalitic to granodiorite composition based on various binary and ternary diagram like A/CNK vs A/NK plot (Shand, 1943), Ab-Or-An triangular plot of O`connor (1965) for feldspar and SiO_2 vs Na_2O+K_2O plot for plutonites (Middlemost 1994). R1 vs R2 plot of Batchelor and Bowden 1985 for tectonic setting of granitoids indicate syn collision to pre plate collision tectonic setting for emplacement that shows granite rock is basement type not an intrusive phase. These are also characterised as syn-collisional granite based on Nb vs Y and Rb vs (Y+Nb) plot of Pearce et al. (1984). Granitoids are normal to anomalous granite type and follow differentiation trend in Rb-Ba-Sr ternary diagram of EI Bouseily, 1975. Low Rb/ Sr ratio (1.03), less differentiation index (82.80), major oxide data and K_2O vs Na_2O diagram of Chapell and white, 2001 indicates I type granite nature of granitoids. These show moderate abundance and distribution pattern of REE (ΣREE 65-251 ppm). The granitoids of Murmuri, Chhibarra and Kashipali (Pink porphyritic biotite granite) are more differentiated as these possess more total REE (average 217 ppm) than the Clark values of granites. These shows LREE enriched chondrite normalised plot with steep slope.

During the detailed mapping, basic rock near Gatkachhar and garnet bearing ultrabasic rock near Rehatikhol also located intruding the basement (Pre Singhora age deduced based on field relationships). Basic intrusive in basement at Gatkachhar has been identified as altered dolerite by petromineralogical studies. Presence of titanomagnetite and glomeroporphyritic texture has been observed. Inliers of basement rock and capping of Rehatikhol sediments as outlier also has been mapped. These inliers are found to be faulted inliers and attributed by various cross section. The rocks of Singhora group and basement rocks has been found to be structurally disturbed by numerous faults/ fractures. Faulted contact as well normal stratigraphic contact has been located between Rehatikhol Formation and basement granitoids. Major structural grain in Salhebhata- Makarmuta- Chhibarra- Rehatikhol area is ~N-S and NNE trending dominant fractures along with NW-SE, NE-SW joints/silicified fractures. During study it has been noted that U mineralisation is mostly associated NNE-SSW and NE-

SW trending structures (U with sulphides), although association of U mineralisation cannot be ruled out for NW-SE fractures that are mostly associated with silicification. Various important shear zone has been identified like NW trending Kermeli- Salhebhata shear zone that shows sinistral sense of movement with development of S-C fabric. Feldspathic injection in sheared granite also located along this zone. Evidences of strong reactivation of this shear in Rehatikhol sediments has been identified around Salhebhata. Spotty uraniferous anomaly also reported along this shear zone indicating role of structure in U mobilisation and concentration. Present study shown elevated U concentration in samples along this zone.

Fracture and joint analysis has shown NNE and NE trending structural grain is prevailing in study area. The inter relationship of reactivation of fractures has been identified as N-S is oldest, affected by NE-SW (younger) and NW-SE, often silicified is youngest. Although NW fracture are found to be oldest affected by N- S followed by youngest NE and NNE fractures.

Rehatikhol Formation has been divided into 5 lithounit by present study based on grain size variation, mineralogical composition and sedimentological aspects. Mapping of these units has been carried out over 55 sq. km area in detail (on 1:10000 scale). Paleocurrent analysis deducted from asymmetric mega ripples and cross beds indicate NNW to NW paleocurrent direction with an average NNW paleocurrent direction (N328º) in Juba sector, NW (avg direction N 314º) in Salhebhata- Malaikhaman sector with overall unidirectional NW paleocurrent direction (average N323º) of Rehatikhol arenites. Dispersion in data is in the range of ~50º angle and it is more in Salhebhata- Malaikhaman sector than Juba sector indicating more fluctuation in paleocurrent direction/ shift in the channels. Field based sedimentological studies revealed fluviatile origin of basal sediments (basal polymictic conglomerate and gritty feldspathic arenite), and these are found to be deposited in alluvial fan environment as debris flows. Sediments of Juba Member also deposited in fluvial system. Present study suggests lithounits of upper Rehatikhol Formation deposited in near shore marginal marine environment. The total thickness of Rehatikhol sediments vary between 60-120m in study area.

Detailed characterisation of Rehatikhol Formation has been carried out for all defined lithounits. Study suggest distinct petrographic characteristics for all these lithounits. Significant variation has been established in grain size, roundness, sorting and overall feldspar content in sandstones of different lithounits. It is depicted by schematic litholog of Rehatikhol Formation which shows that overall grain size and feldspar content of Rehatikhol sediments decreases from bottom to top (i.e. from basal polymictic conglomerate to porcellanite). The roundness and sorting of grains in Rehatikhol sediments improve from bottom to top (i.e. from basal polymictic conglomerate to ferrugenous sandstone) (Figure 8.1). These suggest textural and compositional maturity of Rehatikhol sediments increases with the time. It also indicate increased chemical weathering, more transportation of sediments, and decrease in gradient of source area and semi-arid to semi humid cold paleoclimatic conditions. Presence of thin micaceous siltstone and shale intercalations are not taken into consideration for this interpretation. These interpretations are also corroborated by geochemical studies.

Overall two reduced facies assemblage and one oxidised facies assemblage has been identified in Rehatikhol Formation (Fig 8.1). Sandstones of Rehatikhol Formation overall consist of quartz (mono and polycrystalline both), Microcline, perthite and antiperthite, minor muscovite occasional granitic rock fragments with zircon, monazite, rutile, xenotime as accessory minerals. Matrix is of siliceous, sericitic and clayey composition which content is found to be very less (< 15%) in all sandstones except ferrugenous sandstone. Sericitic matrix is slightly higher side in this sandstone and it can be classified under wacke. PFA characterised siliceous, sericitic and pyritiferous matrix, plane and sutured contact between grains, significant silica overgrowth as a result of pressure solution, presence of diagenetic, epigenetic and remobilised pyrite. It is characterised by significant pyrite content (upto 7.33% in

Chhibarra) along with presence of epigenetic galena. Some bipyramydal and euhedral quartz grains has been observed in feldspathic arenite and ferrugenous sandstone indicating acidic volcanic origin. It also infers that localised acidic volcanic activity has been started in provenance during the sedimentation of Rehatikhol Formation with the introduction of feldspathic arenite. Modal analysis of Rehatikhol sandstones after Pettijohn and Folk indicate that PFA of study area is subfeldspathic arenite while samples of feldspathic arenite samples falls in subfeldspathic to feldspathic arenite clan of Pettijohn classification. Hence all the sandstones of Rehatikhol Formation has been classified to be feldspathic in nature.

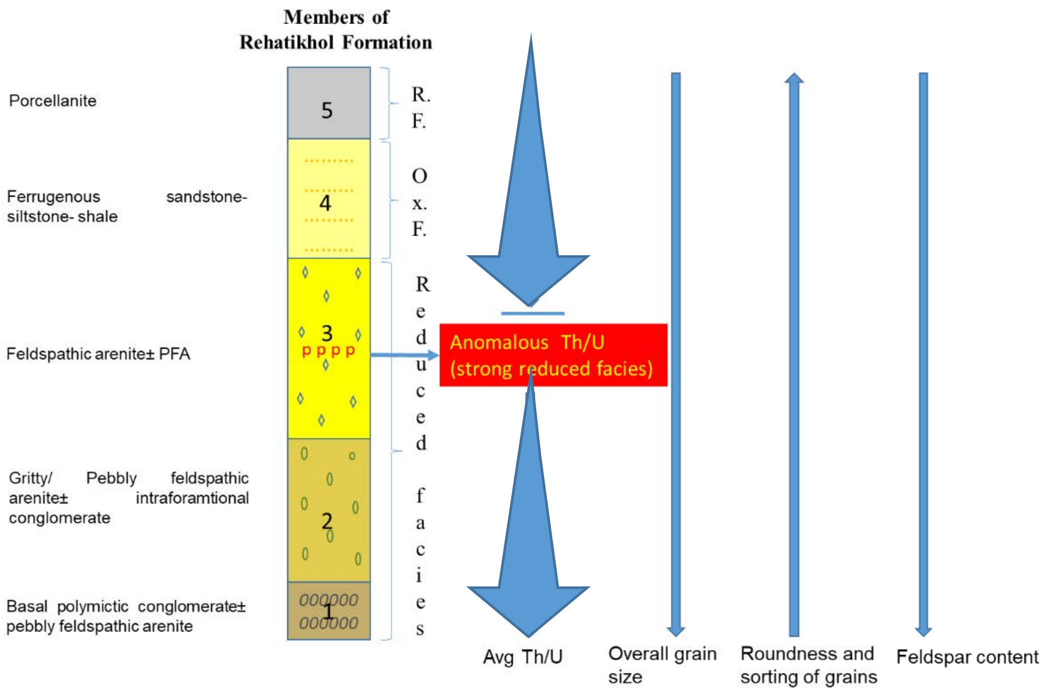

Figure 8.1 Schematic litholog of Rehatikhol Formation depicting comparative characteristics of different lithounits.

Porcellanite at top of Rehatikhol Formation are characterised by presence of fine cryptocrystalline laminated shards of chert, subhedral to euhedral quartz, minor sericite and plagioclase laths, globular calcite and significant fine pyrite, altered magnetite and ilmenite. This unit represent volcanoclastic sedimentation in Singhora protobasin. Provenance discriminant diagram of sandstones of Rehatikhol Formation after Dickinson and Suczek

(1979) suggest presence of source area at craton interior at continental block. Mineralogical composition and textural attributes of sandstones indicate mainly acidic plutonic rock as provenance (i.e. Sambalpur Granitoids) with negligible contribution from acidic volcanoclast and recycled sediments in upper portion of Formation. Present study suggest very proximal source area with high gradient for Rehatikhol Formation. Significant amount of microcline and perthites in sandstone indicates semi-arid to semi humid cold climatic conditions prevailing at source rock area at the time of Rehatikhol sedimentation.

Average Upper Continental Crust (UCC) and post Archean Australian Average Shale (PAAS) spider plots (values after Taylor and McLennan, 1985) for major oxide of Rehatikhol sediments revealed that all lithounits show SiO_2 enrichment except in shale that show depletion due to Al_2O_3 and K_2O dilution. Porcellanites are found to be enriched P_2O_5 content that is conspicuous. Porcellanite and ferrugenous sandstone are less depleted in Fe_2O_3 content in UCC normalised plot due to presence of pyrite in porcellanite and iron oxide staining in sericitic matrix in ferrugenous sandstone. All the geochemical characteristics are corroborated by petromineralogical studies. Shale shows significant enrichment of TiO_2 and slight enrichment of Fe_2O_3 with respect to UCC that infers minor presence of fine Fe- Ti oxide bearing heavies derived from basic igneous source. It indicate supply of sediments also have minor basic influx during the deposition of shale.

K_2O vs Na_2O bivariate plot (after Pettijohn (1963) and Log (SiO_2/Al_2O_3) vs Log (Fe_2O_3/K_2O) classification Diagram (After Herron, 1988) indicate that most of the Rehatikhol sandstone are of arkosic and sub-arkosic composition while some samples got clustered along lithicarenite- sublithic arenite boundary. Felsic igneous source, passive margin tectonic setting, semi humid to semi-arid cold climatic condition has been attributed by the various binary and ternary geochemical plots.

Various alteration index has been calculated that shows average CIA values (62.73 %), CIW (average = 86.56%), PIA values (average =78.08%) and ICV (0.73) of gritty feldspathic arenite correspond to the moderate source weathering similarly PFA characterised average CIA (63.14 %), average CIW (80.84 %), PIA (72.63 %) and ICV (0.89) also representing moderate to slightly higher source weathering. Low average CIA value (59.68 %) in feldspathic arenite of Rehatikhol Formation indicate incipient source weathering under cold, semi-arid climatic conditions. The A–CN–K ternary diagram for Rehatikhol sediments has been plotted that define an intermediate trend over which majority of the samples are plotted above the feldspar tie line , that indicates moderately weathered Al_2O_3-rich source.

Highly radioactive PFA sample of Juba with high U content characterised relatively very high total REE (average 134.54 ppm) followed by high total REE content in Chhibarra PFA with U (average 31.56 ppm). Unmineralised PFA and feldspathic arenite characterised very less total REE content (average 23.55). Positive correlation of U content with total REE indicates REE might be associated U bearing phases. Chondrite normalised spider plot (Boynton, 1984) shows nearly similar pattern between mineralised PFA of Chhibarra and Juba that indicate similar mineralising processes. Mineralised samples characterised high Pr, Gd, Tb, Ho and Tm values. LREE/ HREE ratio indicate that uraniferous PFA of Juba are relatively highly enriched in HREE. Similar inferences also noted in uraniferous PFA of Chhibarra that could be due to presence of HREE rich coffinite/ xenotime. Y also shows very strong positive correlation with HREE indicating contribution from suspected xenotime (may be of hydrothermal origin?) though only mineralised PFA have high Y. U also shows good positive correlation with Y that support these inferences. Comparative study of U mineralised PFA of Juba, Chhibarra (study area) and unmineralised PFA of study shows that uraniferous Juba PFA is slightly more siliceous, depleted in K_2O and Al_2O_3 in comparison to other PFA, possibly because of introduction of U bearing siliceous hydrothermal fluid infiltration that caused rise in silica at the expense of K_2O and Al_2O_3 by alteration of K feldspar to clay. Average Cu, Zn, Rb, Cr and Pb contents are higher side in mineralised PFA that is due to epigenetic polymetallic sulphide mineralisation associated with U mineralisation. Similar PAAS and UCC normalised major oxides and trace elements plots represent similar signature in these PFA. UCC normalised plots show that K, Rb, Ba and Ti are more depleted in U mineralised PFA than unmineralised PFA. Mineralised PFA shows enrichment of Y and Yb.

Detailed radiometric survey carried out in study area has brought up encouraging result in terms of identification of mineralised zones, relationship with host rock and structures, association and possible controls of mineralisation. Distribution of U and Th in Rehatikhol Formation has been attributed by Th/ U ratio in Fig 8.1 that shows enrichment of U in PFA and a trend of increasing Th in basal portion. Highest average radioelemental concentration in basement is observed in biotite- muscovite granite of Jaypur- Damdama area that are more evolved and younger phases of Sambalpur Granitoids. Basal conglomerate, upper horizon conglomerate and some gritty layers show anomalous radioactivity but all are thoriferous in nature. . Low value of U/ Th in sandstones and conglomerate is due to detrital monazite/ zircon that concentrated by mechanical processes. High anomalous value (U/Th>0.35) observed in some granitoid samples (U/Th= 0.32- 10.5, n = 4) of Kermeli- Kurapali area along shear zone showing remobilisation of U and structural controls in NW shear zone. NE trending quartzo-feldspathic injections along in basement rocks around Kermeli- Kurapali also have high intrinsic U content (3-18 ppm) and higher average U/Th ratio (5.56) showing enrichment of U. All these coupled with Malaikhaman anomaly indicate structural controls of U mineralisation in basement rock.

PFA shows enrichment of U and elevated average U/Th ratio (1.48) indicating concentration of U due to sulphides reduction. High anomalous value (U/Th>2) observed in some PFA samples (U/Th= 2- 17, n = 5) collected along shear / fracture zones of Chhibarra, Salhebhata and Gatkachhar area. Significant uranium mineralisation in PFA is located near Chhibarra associated along N30ºE shear zone. Mineralisation is limited to PFA unit (due to pyrite as a strong reducing species) in Rehatikhol Formation and have some structural bearing (only found to be associated with NNE and NE trending fractures) that indicate lithostructural controls of mineralisation in Rehatikhol Formation.

Malaikhaman anomaly has been studied in detail that brought following contribution in understanding the mineralisation. This includes, (i) identification of secondary uranium minerals, apatite, fluorite, chalcopyrite, py with anomalous Zn and Pb in polymetallic vein (ii) presence of NNE trending ferrugenised fracture/ fault very near basin margin which has sinistrally displaced the quartz reef (iii) establishing the reef to be pre-Singhora in age, confined to basement only, as no evidences of reactivation of this shear zone was observed in sediments in same continuity, except some joints in same trend (iv) attributing the U-mineralisation to be structurally controlled, hydrothermal type with U-Cu-Zn-F association. The quartz reef is characterised by minor depletion of LREE ((La/Yb) N = 0.53-1.56) and nearly flat pattern of HREE. The positive Eu anomaly coupled with LREE depletion in these productive quartz veins suggests a source which is enriched in Eu and depleted in LREE due to crystal fractionation.

Similarity of REE pattern with Hutti gold field, Karnataka and Archean Basement-Hosted Gold Deposit in Pinglidian, Jiaodong Peninsula, Eastern China indicate possibility of Au association also with Malaikhaman quartz reef. Presence of polymetallic sulphides, ferrugenised breccia (in near vicinity), hydrothermal fluorite and apatite mineralisation coupled with U mineralisation indicate a possibility of IOCG system in study area.

Fluorite mineralisation has been located at 6 localities in basement rock as well as Rehatikhol Formation. Fluorite is hosted by deformed conglomerate and gritty feldspathic arenite in Rehatikhol Formation while it is hosted in basement granite at the contact of basic intrusive. There is no significant role in controlling fluorite mineralisation but role of structures is clear by present study in the mineralisation of fluorite. Fluorite of multiple generations and 4 colours occurs along NNW and NE trending shear zone/ faults and closely associated with silicification. Structural control of fluorite mineralisation has been established by present study and evidences has been presented.

Fluorite of 3 different colours (colourless/translucent to white, purple/ violet and deep navy blue) are present as veins. It is established that navy blue/ ink colour fluorite is youngest since its veins cuts other existing coloured fluorite. At least 3 generations of fluorite mineralisation with respect to silicification has been identified based on cross cutting relationship (cogenetic with silicification, prior to silicification and post silicification). Petrological studies has established fluorite occurs as fracture filling, veins and coating over larger grains that indicate its hydrothermal origin. Intense deformation in fluorite hosted gritty feldspathic has been attributed in petrography by granulation, crushing, stretching of grains, generation of quartzo feldspathic epimatrix.

During the span of this project, only structural controls of fluorite mineralisation could be identified. To locate more controlling factor, sample has been sent for fluid inclusion study, Oxygen isotope study of cogenetic silica, REE analysis by INAA for detailed geochemical interpretation to understand fluid chemistry, source, association any mineralisation, different generations and their relationships to U mineralisation. In summary, present study is an integrated comprehensive approach for better understanding the lithostructural setup and mineralisation in the area.

CHAPTER 9
CONCLUSION

Based on field studies, petromineralogical and geochemical studies integrated with previous work, following conclusions can be derived-

1. Lithostructural disposition of study area has been described by detailed map of 55 square km area on 1:10000 scale, various cross sections, litholog and field description. The study area has been identified as favourable potential zone to host fracture controlled/ unconformity related uranium mineralisation in association with fluorite and polymetallic sulphide mineralisation.
2. Variation in composition of basement Sambalpur Granitoids has been found and these has been characterised as granodiorite to tonalite in composition, peraluminous to metaluminous with calc alkaline Al rich magma source, syncollisional I type granitoids.
3. Present study incorporate classification of Rehatikhol Formation into various lithounits and their petromineralogical and geochemical characterisation. Sedimentological, petromineralogical, geochemical distinction and field relationships has been well established between all these lithounits.
4. Present study revealed NW paleocurrent direction and alluvial fan to marginal marine depositional environment for Rehatikhol sediments.
5. Petromineralogical and geochemical studies revealed feldspathic to subfeldspathic arenite composition of Rehatikhol sandstone, acidic plutonic source with minor intermediate felsic, recycled sediment and basic influx, passive margin tectonic setting, semi humid to semi-arid cold climatic condition.
6. The pyritiferous feldspathic arenite of study area has been found to have similar petromineralogical and geochemical characteristics to PFA of Juba area, hence it is favourable to host Juba type of mineralisation.

7. Structural controls of U mineralisation has been found in basement rocks as U mineralisation and enrichment of U (in comparison to Th) has been observed along NE / NNE and WNW shear zones.
8. Lithostructural controls of U enrichment has been attributed in Rehatikhol Formation by present study as strong reduced facies (PFA) shows high U/ Th ratio and anomalous values in samples of PFA collected from NE /NNE trending shears/ faults.
9. Structural controls and hydrothermal origin as far established for fluorite mineralisation based on field studies, petromineralogy and geochemistry.
10. Association of fluorite with U and sulphides of Cu- Zn- Pb has been established in basement rocks at Malaikhaman anomaly and this zone can be further explored in detail for subsurface exploration.
11. Although surficial association of U with fluorite couldn't be located during span of this project but hydro uranium anomaly with high F content (54 ppb U and 4 ppm F) indicates their subsurface association in Chiwarakuta area, hence can be tested by sub surface exploration after more detailed work.
12. The geological set-up, by and large, might emerge as a possible target area to look for probable concealed polymetallic (U+ Cu+ Zn+ Pb+ F) mineralisation.

Future scope of work

Present work open new avenue of scope of study in Singhora protobasin i.e. EPMA study of mineralised and unmineralised PFA to determine Co/ Ni ratio to look for volcanogenic sulphides if any, EPMA study of polymetallic sulphide bearing uraniferous vein in quartz reef of Malaikhaman for genetic aspects, detailed REE geochemistry and fluid inclusion study of different fluorites to understand hydrothermal fluid chemistry and relation with U mineralisation.

REFERENCES

Ahmad, T., Longjam, K.C., Fouzdar, B., Bickle, M.J., and Chapman, H.J. (2009). Petrogenesis and tectonic setting of bimodal volcanism in the Sakoli Mobile Belt, Central Indian shield. Island Arc, v.18, pp.155–174.

Amarasinghe, U., Chaudhuri, A., Collins, A.S., Deb, G., and Patranabis-Deb, S. (2015). Evolving provenance in the Proterozoic Pranhita-Godavari Basin, India. Geosc. Front., v.6, pp.453–463.

Batcher, R.A., Bowden, P. (1985). Petrogenetic Interpretation of Granitoid Rock Series Using Multicrationic Parameters. Chem. Geol., v.48, pp.43-55.

Bhatia, M. R. (1983). Plate tectonics and geochemical composition of sandstones. Jour. of Geol. v.91, pp.611–27.

Bhatia, M. R. (1985). Rare earth element geochemistry of Australian Palaeozoic graywackes and mudrocks: provenance and tectonic controls. Sed. Geol., v.45, pp.97-113.

Bhatia, M. R. and Crook, K.A.W., (1986). Trace element characteristics of graywackes and tectonic setting discrimination of sedimentary basins. Contributions to mineralogy and petrology, v.92, pp.181-193.

Bhowmik, S.K., Wilde, S.A., and Bhandari, A. (2011). Zircon U-Pb/ Lu-Hf and monazite chemical dating of the Tirodi biotite gneiss: Implication for latest Palaeoproterozoic to Early Mesoproterozoic orogenesis in the Central Indian Tectonic Zone. Geol. Jour., v. 46, pp.574–596.

Bickford, M.E., Basu, A., Mukherjee, A., Hietpas, J., Schieber, J., Patranabis-Deb, S., Kumar Ray, R., Guhey, R., Bhattacharya, P.,and Dhang, P.C., (2011a). New U-Pb SHRIMP Zircon Ages of the Dhamda Tuff in the Mesoproterozoic Chhattisgarh Basin, Peninsular India: Stratigraphic implications and significance of a 1-Ga thermal-magmatic event. The Jour. of Geol., v.119, pp.535–548.

Bickford, M.E., Basu, A., Patranabis-Deb, S., Dhang, P.C., and Schieber, J., (2011b). Depositional History of the Chhattisgarh Basin, Central India: Constraints from New SHRIMP Zircon Ages: The Jour. of Geol., v.119, pp.33–50.

Blatt, H. (1967). Provenance determinations and recycling of sediments. J. Sedim. Petrol. v.37 pp.1031-1044.

Bora, S., Kumar, S., Yi, K., Kim, N., and Lee, T.H. (2013). Geochemistry and U-Pb SHRIMP zircon chronology of granitoids and microgranular enclaves from Jhirgadandi Pluton of Mahakoshal Belt, Central India Tectonic Zone, India. Jour. of Asian Earth Scie., v. 70–71, pp.99–114.

Boynton, W.V. (1984). Cosmochemistry of the rare earth elements: meteorite studies. In Developm. in geochem. v.2, pp.63-114.

Chakraborty, P.P., Das, K., Tsutsumi, Y., and Horie, K., (2011). Depositional history of the Chhattisgarh Basin, Central India: Constraints from new SHRIMP zircon ages: A discussion. The Jour. of Geol., v.119, pp.549–552.

Chakraborty, P.P., Saha, S., Das, P., (2015). Geology of Mesoproterozoic Chhattisgarh basin central India: current status and future goals. Mazumdar, R., Eriksson, P.G.(Eds.), Precambrian Basins of India, Stratigraphic and Tectonic Context. Geol. Soc. Mem. Lond. v.43, pp.185–205.

Chakraborty, P.P., Sarkar, A., Das, K., Das, P. (2009). Alluvial fan to storm-dominated shelf transition in the Mesoproterozoic Singhora group, Chhattisgarh Supergroup, Central India. Precamb Res v.170, pp.88-106.

Chappell, B.W., White, A.J. (2001). Two contrasting granite types: 25 years later. Austral. Jour. of earth sci., v.48(4), pp.489-499.

Chaudhuri, A.K., Saha, D., Deb, G.K., Deb, S.P., Mukherjee, M.K., and Ghosh, G. (2002). The Purana basins of Southern Cratonic province of India - A case for mesoproterozoic fossil rifts. Intern. Geol. Revi. 13 Gond. Res., v. 5, pp.23–33.

Choudhary, A.K., Naik, A., Mukhopadyay, D., and Gopaldas, K. (1996). Rb-Sr dating of Sambalpur granodiorite, western Orissa. Jour. Geol. Soc. India. v.47 (4), pp.503-506.

Clarke, F.W., Washington, H.S., (1924). The composition of the earth's crust. US Gov Printing Office, v.127.

Cox, R., Lower, D.R., Cullers, R.L. (1995). The influence of sediment recycling and basement composition on evolution of mud rock chemistry in the southwestern United States. Geochemical et Cosmochimica Acta, v.59, pp.2919–2940.

Cullers, R.L. (2000). The geochemistry of shales, siltstones and sandstones of Pennsylvanian–Permian age, Colorado, USA: implications for provenance and metamorphic studies. Lithos, v.51, pp.181–203.

Das, D. P., Dutta, N. K., Dutta, D. R., Thanavellu, C., Babu Rao, K. (2003). Singhora Group: the oldest Proterozoic lithopackage of eastern Bastar Craton and its significance. Ind. Min., v.57, pp.127–138.

Das, D.P., Kundu , A., Das, N., Dutta, D. R., Kumaran, K., Ramamurthy, S., Thangavelu, C., Rajaya, V. (1992). Lithostratigraphy and sedimentation of Chhattisgarh Basin. Ind. Min. v.46 pp.271–288.

Das, K., Chakraborty, P.P., Horie, K., Tsutsumi, Y., Saha, S., and Balakrishnan, S. (2017) Detrital zircon U-Pb geochronology, Nd isotope mapping, and sediment geochemistry from the Singhora Group, Central India, in Mazumder, R., ed., Sedim. Proven: Elsevier, pp.403–451.

Das, K., Yokoyama, K., Chakraborty, P.P., Sarkar, A. (2009). Basal tuffs and contemporaneity of the Chattisgarh and Khariar Basins based on new dates and geochemistry. Jour. Geol. v.117 pp. 88–102.

Das, P., Das, K., Chakraborty, P.P., and Balakrishnan, S. (2011). 1420 Ma diabasic intrusives from the Mesoproterozoic Singhora Group, Chhattisgarh Supergroup, India: Implications towards non-plume intrusive activity. Journal of Earth System Science, v. 120, pp.223–236.

Dasgupta, S., Bose, S., and Das, K. (2013), Tectonic evolution of the Eastern Ghats Belt, India. Prec. Res., v. 227, pp.247–258.

Datta, B. (1998) Stratigraphic and sedimentologic evolution of the Proterozoic siliciclastics in the southern part of the Chhattisgarh and Khariar, central India. Jour. Geol. Soc. Ind., v.51, pp.345-360.

Dey, A., Mukherjee, S., Sanyal, S., Ibanez-Mejia, M., and Sengupta, P. (2017). Deciphering sedimentary provenance and timing of sedimentation from a suite of metapelites from the Chotanagpur granite gneissic complex, India, in Mazumdar, R., ed., Sediment provenance: Influences on compositional change from source to sink. Elsevier. pp.453–486.

Dhang, P. C., Patranabis-Deb, S. (2012). Lithostratigraphy of the basal part of the Chhattisgarh Supergroup around Singhora–Saraipali area and its tectonic implication. In: Tiwari, R. P. (ed.) Cenozoic Tectonics, Seismology and Palaebiology of the Eastern Himalayas and Indo-Myanmar Range. Geol. Soc. of Ind., Bangalore, Mem., v.77, pp.493–515.

Dickinson, W. R. (1985). Interpreting provenance relations from detrital modes of sandstones. Provenance of Arenites (ed.) G G Zuffa (Dordrecht: D. Reidel Pub. Co.), pp.333–362.

Dickinson, W. R., Suczek, (1979). Plate tectonics and sandstone composition: AAPG Bulletin, v.63, pp.2164-2182.

Dutt, N. V. B. S. (1964) A suggested succession of the Purana Formations of the southern part of Chhattisgarh, M.P. Rec. Geol. Surv. Of Ind., v. 93(2), pp.143-148.

Dutt, N. V. B. S. (1964). A suggested succession of the Purana Formations of the southern part of Chhattisgarh, M.P. Records of the Geol. Surv. of Ind., 93-II, pp.143–148.

Ehrenberg, S.N. (1982). Rare earth element geochemistry of garnet lherzolite and megacrystalline nodules from minette of the Colorado Plateau province. Earth und Plan. Sci. Let, Elsev. Scient. Publ. Comp., Amsterdam, v. 51, pp.191-210.

EI, Bouseily, A.M., EI, Sokkary, A.A. (1975). The relation between Rb, Ba and Sr in granitic rocks. Chem. Geol., v.16, pp.207-219.

Fedo, C.M., Nesbitt, H.W., Young, G.M., (1995). Unraveling the effects of potassium metasomatism in sedimentary rocks and paleosols, with implications for paleoweathering conditions and provenance. Geology 23, pp.921–924.

Folk, R. L. (1980). Petrology of Sedimentary Rocks. Hemphill, Austin.

George, B.G., Ray, J.S., Shukla, A.D., Chatterjee, A., Awasthi, N., and Laskar, A.H. (2018). Stratigraphy and geochemistry of the Balwan Limestone, Vindhyan Supergroup, India: Evidence for the bitter springs δ13C anomaly. Precam. Res., v. 313, pp.18–30.

Gopalan, K., Kumar, A., Kumar, S., and Vijayagopal, B. (2013). Depositional history of the Upper Vindhyan succession, central India: Time constraints from Pb–Pb isochron ages of its carbonate components. Precam. Res., v. 233, pp.108–117.

Hayashi K.I., Fujisawa H., Holland H.D., and Ohmoto H. (1997). Geochemistry of ∼1.9 Ga sedimentary rocks from northeastern Labrador, Canada. Geochimica et Cosmochimica Acta, v. 61, pp.4115–4137.

Hayashi, K.I., Fujisawa, H., Holland, H.D. and Ohmoto, H., (1997). Geochemistry of∼ 1.9 Ga sedimentary rocks from northeastern Labrador, Canada. Geochimica et Cosmochimica Acta, v.61(19), pp.4115-4137.

Herron, M.M. (1988). Geochemical classification of terrigenous sands and shales from core or log data. Jour. of Sed. Res, v.58 (5), pp.820.-829.

Ingersoll, R. V., T. F., Bullard, R. L., Ford, J. P., Grimm, J. D., Pickle, and S. W. Sares (2010). "The Effect of Grain Size on Detrital Modes: A Test of the Gazzi-Dickinson Point Counting Method," Implications for Provenance and Source Area Weathering," Int. Geol. Rev, v.54(1), pp. 111-129. Jour. of Sedi. Res., v. 54 (1), 1984, pp. 103-106.

Irvine, T.N.J., Baragar, W.R.A. (1971). A guide to the chemical classification of the common volcanic rocks. Canadian jour. of earth sci., v.8(5), pp.523-548.

Jain, S. K., Sinha, D.K., Verma, S. C. and Singh, Rajendra (1998). Ore mineragraphy of uraniferous polymetallic sulphides at Juba, Chhattisgarh Basin, Raipur District, central India. Exp & Res Atm. Min. (EARFAM), AMD, Hyderabad, v.11, 1998, pp.25-36.

Johnsson, M. J. (1993). The system controlling the composition of clastic sediments, in Johnsson, M. J., and Basu, A., eds., processes controlling the composition of clastic sediments: Boulder, Colorado, Geol. Soc. of America Sp. Paper v..284, pp.1-19.

Khanna, T.C., Bizimis, M., Barbeau, D.L., Keshav Krishna, A., and Sesha Sai, V.V. (2019). Evolution of ca. 2.5 Ga Dongargarh volcano-sedimentary Supergroup, Bastar craton, Central India: Constraints from zircon U-Pb geochronology, bulk-rock geochemistry and Hf-Nd isotope systematics. Earth-Scie. Rev., v. 190, pp.273–309.

Kruzer, H., Harse, W., Kursten, M., Schnitzer, W.A., Murthy, K.S., Srivastava, N.K. (1977). K/Ar dates of two glauconites from the Chandarpur series (Chhattisgarh/India): On the Stratigraphic status of the Late Precambrian basins in Central India. Geol Jb B v.28, pp.23–36

Manikyamba, C., Santosh, M., Kumar, B.C., Rambabu, S., Tang, L., Saha, A., Khelen, A.C., Ganguly, S., Singh, T.D., and Rao, D.V.S. (2016). Zircon U-Pb geochronology, Lu-Hf isotope systematics, and geochemistry of bimodal volcanic rocks and associated granitoids from Kotri Belt, Central India: Implications for Neoarchean–Paleoproterozoic crustal growth. Gond. Res., v.38, pp.313–333.

Maurya A.K., Sridhar. M. (2018). Annual report on Integrated Interpretation, Constrained Modeling and Target Delineation of Heliborne Geophysical Data: Singhora Block I & II, ASRS Group, Unpubl. AMD report.

McLennan, S.M. (1993). Weathering and global denudation. Journal of Geology, v.101, pp. 295–303.

McLennan, S.M., Taylor, S.R., (1991) Sedimentary rocks and crustal evolution: Tectonic setting and secular trends. J. Geol., v.99, pp.1-21.

Middlemost, E.A.K. (1994). Magmas, Rocks and Planetary Development: A Survey of Magmas/Igneous Rock Systems. Addison Wesley Longman Ltd., Singapore, pp.299.

Misra, K.S, Rao, M.K. (1995). Annual report for field season 1994- 95 Unpubl. AMD report. AMD, Hyderabad.

Mohanty, S.P. (2015). Palaeoproterozoic supracrustals of the Bastar Craton: Dongargarh Supergroup and Sausar Group. Geol. Soc., London, Mem., v.43, pp.151–164.

Mukherjee, A., Ray, R.K. (2010). An Alternate View on the Stratigraphic Position of the ∼1-Ga Sukhda Tuff vis-à-vis Chronostratigraphy of the Precambrians of the Central Indian Craton. Jour. Geol., v.118, pp.325–332.

Mukherjee, S., Dey, A., Sanyal, S., Ibanez-Mejia, M., Dutta, U., and Sengupta, P. (2017). Petrology and U–Pb geochronology of zircon in a suite of charnockitic gneisses from parts of the Chotanagpur Granite Gneiss Complex (CGGC): Evidence for the reworking of a Mesoproterozoic basement during the formation of the Rodinia supercontinent: Geological Society. London, Special Publications, v. 457, pp.197–231.

Mukhopadhyay, G., Mukhopadhyay, S.K., Roychowdhury, M., and Parui, P.K. (2010). Stratigraphic correlation between different Gondwana Basins of India. Jour. of Geol. Soc. of Ind., v.76, pp.251–266.

Mukundan, A.R. (1997). Unpubl. AMD annual report, F.S. 1996-97.

Murti, K. S., (1987). Stratigraphy and sedimentation in Chhattisgarh Basin. In. Radhakrishna, B.P. (Ed.), Purana Basins of Peninsular India (Middle to Late Proterozoic). Mem. Geol. Soc. Ind., v.6, pp.239-260.

Murti, K.S. (1987). Stratigraphy and sedimentation in Chhattisgarh Basin. In Purana Basins of Peninsular India, Geol. Soc. Ind. Mem, v.6, pp.239-260.

Murti, K.S. (1996). Geology, sedimentation and economic mineral potential of the southcentral part of Chhattisgarh Basin. Geol. Surv. Ind. Mem., v.125, pp.139.

Nesbitt, H. W., Young, G. M. (1984). Prediction of some weathering trends of plutonic and volcanic rocks based on thermodynamic and kinetic considerations; Geochim. Cosmochim. Acta, v.48 (7), pp.1523–1534.

Nesbitt, H.W., Fedo, C.M., Young, G.M., (1997). Quartz and feldspar stability, steady and non-steady-state weathering, and petrogenesis of siliciclastic sands and muds. Jour. of Geol., v.105, pp.173-191.

Nesbitt, H.W., Young, G.M., (1982). Early Proterozoic climates and plate motions inferred from major element chemistry of lutites. Nature (London), v.299, pp.715-717.

O'Connor, J.T. (1965). A classification of quartz rich igneous rocks based on feldspar ratios. U.S. Geol. Surv. Prof. Paper, v.525-b, pp.79-84.

Pandey, B.K., Chabria, T., Gupta, J.N. (1995). Geochronological characteristic of the Proterozoic terrains of Peninsular India: Relevance to the first order target selection for uranium exploration. Expl Res Atom Min, v.8, pp.182–213.

Pandey, U. K., Sastry, D. V. L. N., Pandey, B. K., Roy, M., Rawat, T. P. S., Ranjan, R. & Shrivastava, V. K. (2012). Geochronological (Rb–Sr and Sm–Nd) studies on intrusive gabbros and dolerite dykes from parts of northern and central Indian cratons: implications for the age and onset of sedimentation in the Bijawar and Chhattisgarh basins and uranium mineralogy. Jour. of the Geol. Soc. of Ind., v.79, pp.30–40.

Pant and Chaturvedi (1999). Unpub. AMD report, F.S. 1998-1999, AMD, Hyderabad.

Patnaik, S.K. (1989) Regional prospecting for base metal mineralization in parts of Chhattisgarh Supergroup, Raipur district, Madhya Pradesh. Rec. Geol. Surv. Ind., v.122 (6), pp.87.

Patranabis-Deb S, Bickford ME, Hill B, Chaudhuri AK, Basu A (2007) SHRIMP ages of zircon in the uppermost tuff in Chhattisgarh basin in central India require ~500-Ma adjustment in Indian Proterozoic stratigraphy. Jour. Geol., v.115, pp.407–415.

Patranabis-Deb, S., Bickford, M.E., Hill, B., Chaudhuri, A.K., Basu, A. (2008). SHRIMP ages of zircon in the uppermost Tuff in Chhattisgarh Basin in central India require ∼500 Ma adjustment in Indian Proterozoic stratigraphy: A reply. Jour. Geol., v,116, pp.540–542.

Pearce, J.A., Harris, N.B.W., Tindle, A.G. (1984). Trace Element Discrimination Diagrams for the Tectonic Interpretation of Granitic Rocks. Jour. Petrol., v.25 (4), pp. 956-983.

Pettijohn, F.J. (1963). Chemical composition of sandstones-excluding carbonate and volcanic sands. Data of geochemistry, sixth ed., US Geol. Surv. Prof. Paper 440-S, pp.19.

Pettijohn, F.J., Potter, P.E., Siever, R., (1987.) Sand and Sandstone. Spri.-Verl., Berlin. pp.306.

Ramakrishnan, M. & Vaidyanadhan, R. (2010). Geology of India, v.5. Geol. Surv. of Ind., Hyderabad.

Rao, D.V., Balaram, V., Sangurmath, Prabhakar, Satyanarayanan, Manavalan. (2015). Major, Trace and REE Characteristics of the High Grade Gold Geochemical Reference Material from Middle Reef, Hutti Gold Mines, Karnataka. Jour. of the Geol. Soc. of Ind, v.85 (3), pp.313- 321.

Roser, B.P., Korsch, R.J. (1986). Determination of tectonic setting of sandstone mudstone suites using SiO_2 content and K_2O/Na_2O ratio. J. Geol. 94, pp.635–650.

Roser, B.P., Korsch, R.J., (1988). Provenance signatures of sandstone-mudstone suites determined using discriminant function analysis of major-element data. Chem. Geol., v.67, pp.119-139.

Ruihong, Li, Albert, Ntwali, Yun, Menghe, Meng, Yinsheng, Du, Hao. (2019). Geological and Geochemical Characteristics of the Archean Basement-Hosted Gold Deposit in Pinglidian, Jiaodong Peninsula, Eastern China: Constraints on Auriferous Quartz-Vein Expl. Min. v.9. pp.62.

Saha, D., and Patranabis-Deb, S. (2014). Proterozoic evolution of Eastern Dharwar and Bastar cratons, India – An overview of the intracratonic basins, craton margins and mobile belts. Journal of Asian Earth Sciences, v. 91, pp.230–251.

Sarangi, S., Gopalan, K., and Kumar, S. (2004). Pb–Pb age of earliest megascopic, eukaryotic alga bearing Rohtas Formation, Vindhyan Supergroup, India: Implications for Precambrian atmospheric oxygen evolution. Prec. Res., v.132, pp.107–121.

Schnitzer, W. A. (1969). Die jung-algonkischen sedimentation straume Peninsular lndiens. Neues Jahrbuch fu¨r Geologie und Pala¨ontologie, Abhandlungen, v.133, pp.191–198.

Schnitzer, W. A. (1969). Zur Stratigraphie und Lithologie des nördlichen Chattisgarh-Beckens (zentral- Indien) under besonderer berucksichtigung von Algenriff- Komplexen. Zeits. der deutsch. Geol. Gesellsch., pp.290- 295.

Schnitzer, W. A. (1971). Das Jungpräkambrium Indiens ("Purana system"). Erlanger, Geologische, v.85, p.44.

Shand, S. J. (1943). Eruptive Rocks. Their Genesis, Composition, Classification, and Their Relation to Ore-Deposits with a Chapter on Meteorite New York. John Wiley & Sons (No. 552.1 S43 1943).

Sinha, D.K. (1995). Unpub. AMD annual report, F.S. 1994- 96, AMD, Hyderabad.

Sinha, D.K. (1996). Chrono-stratigraphy of the Khairagarh Basin, Central India: A reappraisal. Gond. Geol. Mag., v.11, pp.1-15.

Sinha, D.K. (1997). Porcellanite from the Singhora Group – An example of valcaniclastic sedimentation in the Chhattisgarh Supergroup Central India. In abstract volume of XIV Conv Ind Ass Sediment Madras: 9.

Sinha, D.K., Hansoti, S.K. (1995). U and polymetallic sulphides bearing Juba member of Singhora Protobasin of Chhattisgarh Supergroup, Raipur district, Madhya Pradesh. A new horizon. Jour Atom Min Sci, v.3, pp.1-10.

Sinha, D.K., Jain S.K., Choudhury, D.K., Veera Bhasker, D. (2002). Conophyton from Rehatikhol Formation, Chhattisgarh Basin, Central India. In: Guhey R, Thakur P, Sridhar Rao R, (eds) Proceedings volume on Recent Researches on the Proterozoic Basins of India, Pub by Govt Sci College Raipur, pp.27-34.

Sinha, D.K., Jain, S.K., Naganath, K. P. (2011). Tectonic significance and age of Doleritic Sill near Bandhalimal in the Singhora Protobasin of Chhattisgarh Basin, Central India. In: Srivastava, R. K. (eds) Dyke Swarms: Keys for Geod. Inter. Spr, Berlin, pp.167–187.

Sinha, D.K., Raju, K.A., Veera Bhaskar, D., Asha, K. (2001). Sulphur Isotopic Characteristics of pyrite and galena from the Singhora Group, Chhattisgarh Supergroup, India: Genetic implications. Jour Geol Soc India, v.57, pp.171-177.

Sinha, D.K., Tiwary, A., Verma, S.C., Singh, R. (1998). Geology, sedimentary environment and geochemistry of uraniferous arenite of Singhora group, Chhattisgarh Basin, Raipur district, Central India. In: Tiwari RN, (ed) Proc Nat Symp Recent Res Sed Basin, Hindustan Pub Co Dehra-Dun, pp.150-171.

Suttner, L.J., Dutta, P.K. (1986). Alluvial sandstone composition and paleoclimate; I, Framework mineralogy. Jour. of Sedi. Res., v. 56(3), pp.329-345.

Taylor, S.R., S.M., McLennan (1985). The Continental Crust: Its Composition and Evolution. Blackwell, Oxford, UK. pp.312.

Tobias U. Schlegel, Thomas, Wagner, Tobias, Fusswinkel (2020). Fluorite as indicator mineral in iron oxide-copper-gold systems: explaining the IOCG deposit diversity, Chem. Geol., v.548, 119674.

Verma, R.K., Samadder, A.K., Murti, K.S. (1977). Palaeomagnetic study of Gunderdehi shale of Raipur Group from Chhattisgarh basin in India. Indian Jour. Earth Sci.,v.4, pp.183-191.

Yadava, R.S., Agarwal, Mayank (1999). Unpub. AMD annual report, F.S. 1998-1999, AMD, Hyderabad.

Yadava, R.S., Rajeev Ranjan, Shrivastava, V.K., Sachan, A.S. and Rangnath, N. (2007). Occurrences of polymetallic mineralisation in Sambalpur Granitoids, Bastar Craton, Central India, Gondwana Geological Magazine, Special Volume No. 10, pp. 235-242.

Yadava, R.S., Rajeeva Ranjan (2000). Unpub. AMD annual report, F.S. 1999-2000, AMD, Hyderabad.